CHARACTERIZATION OF SEDIMENTS OF THE ALAKNANDA RIVER, GARHWAL HIMALAYA, INDIA

Ph.D THESIS

by

SUGANDHA PANWAR

DEPARTMENT OF EARTH SCIENCES
INDIAN INSTITUTE OF TECHNOLOGY ROORKEE
ROORKEE- 247667, INDIA
FEBRUARY, 2016

CHARACTERIZATION OF SEDIMENTS OF THE ALAKNANDA RIVER, GARHWAL HIMALAYA, INDIA

A THESIS

Submitted in partial fulfilment of the requirements for the award of the degree

of

DOCTOR OF PHILOSOPHY

in

EARTH SCIENCES

by

SUGANDHA PANWAR

DEPARTMENT OF EARTH SCIENCES
INDIAN INSTITUTE OF TECHNOLOGY, ROORKEE
ROORKEE- 247667, INDIA
FEBRUARY, 2016

INDIAN INSTITUTE OF TECHNOLOGY ROORKEE
ROORKEE

CANDIDATE'S DECLARATION

I hereby certify that the work which is being presented in the thesis entitled "**Characterization of Sediments of the Alaknanda River, Garhwal Himalaya, India**", in partial fulfilment of the requirements for the award of the Degree of Doctor of Philosophy and submitted in the Department of Earth Sciences of the Indian Institute of Technology Roorkee is an authentic record of my own work carried out during a period from December, 2011 to February, 2016 under the supervision of Dr. G.J. Chakrapani, Professor, Department of Earth Sciences, Indian Institute of Technology Roorkee, Roorkee.

The matter presented in the thesis has not been submitted by me for the award of any other degree of this or any other Institute.

(Sugandha Panwar)

This is to certify that the above statement made by the candidate is correct to the best of my knowledge.

(G.J. Chakrapani)
Supervisor

The Ph. D. Viva-Voce Examination of **Ms Sugandha Panwar**, Research Scholar, has been held on .....

Chairman, SRC **Signature of External Examiner**

This is to certify that the student has made all the corrections in the thesis.

Signature of Supervisor (s) **Head of the Department**

ABSTRACT

The transportation and transformation of sediments by the fluvial system is an important process which influences the continental landscape, global climate, river water quality and flow dynamics. The Himalayan Rivers viz. Ganga and Brahmaputra transport ~25% of the global sediment flux and are considered to have a large influence on the global climate and vice versa. The previous studies showed that the Ganga River transports ~72.9×10^7 tons of sediments dominantly sourced from the Higher Himalayas. Therefore, it is essential that the sediments from the Upper Ganga basin should be characterized for their physical and chemical characteristics. The Alaknanda River is a headwater stream of the Ganga River flowing in the Garhwal Himalayas in India. The Alaknanda River basin is a unique sub-basin of the Ganga River due to the high rate of physical weathering processes governed by the extreme seasonal rainfall and characteristic bedrock lithology. The sediment erosion rate in the Alaknanda basin is ~863 ton/km^2/year, which is five times higher than the average global physical denudation rate. The Alaknanda River transports an enormous amount of sediments downstream which are responsible for the formation of Ganga alluvial plains. In recent years, owing to the large hydropower potential and projects in the Alaknanda basin, erosion processes and fluvial transport of sediments have become a focus of attention.

The study of sediment load and its size and composition is important in understanding the river processes related to hydraulics, geomorphology, flow dynamics, heavy metal pollutants, siltation in reservoirs and contamination by pathogens. The major factors responsible for grain size characteristics and load vary widely including climatic conditions, lithology, discharge, relief, basin area, river energy and anthropogenic activities. Grain size exerts a strong control on the chemical composition of sediments leading to preferential enrichment of specific nutrients, contaminants, pathogens and heavy metals in certain grain-size fractions. Identification of sediment source holds importance for understanding the sediment dynamics and sediment budgeting of a catchment. Previous studies on the Alaknanda River basin dealt with major, trace, rare earth elements (REEs) and isotopic composition of sediments in the middle and lower Ganga River Basin. However, comprehensive studies on the characteristics of the Alaknanda River sediments were lacking.

With the objective of characterizing the sediments of the Alaknanda River and its tributaries, water and channel sediment samples were collected during three seasons: pre-monsoon, monsoon, and post-monsoon. The biggest advantage of studying recent sediments is

that the sediment composition and its characteristics can be unambiguously correlated with the real-time physiographic and climatic conditions. Quantitative analysis of the sediment load, grain size distribution, major oxide composition, rare earth elements, clay mineralogy and magnetic minerals of the Alaknanda River were conducted. The thesis mostly discusses the spatial and temporal variation of sediment load, grain size distribution, weathering intensity in the basin and the provenance of sediments. In addition, since transportation of carbon by the Himalayan Rivers is a major factor in the biogeochemical cycle of carbon, therefore, a preliminary database of recent total organic carbon (TOC) transported by the Ganga River in its upstream region was also generated; the organic carbon was estimated in the form of the dissolved and particulate load.

The present study on the climatic, hydrological, topographic, geological and anthropogenic activities on a temporal scale showed precipitation as a major factor controlling the amount of sediment load carried by the Alaknanda River. During the monsoon months of June-September, >85% of the annual sediment load is transported by the Alaknanda River. The sediment yield during the non-monsoon and monsoon season at Srinagar and Devprayag varied from 0.61-55.19 tons/km^2/day and 0.52-38.06 tons/km^2/day respectively.

The results showed that sediment load and grain size distribution in the Alaknanda River are influenced by a combination of factors that include topography, hydrology, lithology, confluence with tributaries and anthropogenic activities (dams and reservoirs). The suspended sediments were found to be poorly sorted and the mean grain size (Ms) varied from 8.9-56.3 µm to 25.3-87.3 µm during the post-monsoon and monsoon season respectively, whereas the channel sediments were found to be mostly unimodal, medium to coarse sand (56.4-930 µm) and fine to symmetrically skewed in distribution.

The clay mineral and major oxide indices such as illite crystallinity index, kaolinite/illite ratio, chemical index of alteration (CIA) and weathering index of parker (WIP) provided crucial insights to understand the physical and chemical weathering rate in the basin. A similar CIA value and clay mineral assemblages (illite followed by kaolinite and chlorites) in all the three seasons showed that high physical weathering during the monsoon does not correspond to high chemical weathering. The low amount of Al_2O_3, P_2O_5, CaO present in the channel sediments and the ratios SiO_2/Al_2O_3 and K_2O/Al_2O_3 varying from 1.0-3.1 and 0.9-1.4 respectively showed the immature nature of river sediments.

The provenance of sediments (suspended and channel) was determined by applying multiple geochemical and mineralogical indices. Application of multiple parameters and indices are considered crucially important for the basin having a complex lithology, such as the

Alaknanda River basin. The source of suspended sediment was determined by analyzing the concentration of rare earth elements (REEs). The suspended sediments showed high HREE and inconsistent europium anomaly. The ratios La/Lu and La/Yb >1 and negative Europium anomaly indicated a felsic source of the sediment, whereas the presence of positive Europium and negative Cerium anomaly was attributed to the carbonate and mafic weathering.

The principal component analysis (PCA) on the major oxide composition of channel sediments revealed that weathering of felsic, mafic, and carbonate rocks are responsible for the high sediment load carried by the Alaknanda River. The values of low magnetic field susceptibility (χ_{lf}) highlighted the role of local lithology and sediment mixing. Magnetic parameters and ratios, e.g., χ_{lf}, χ_{ARM}, $B_{(0)CR}$, SIRM, HIRM, S-ratio and the heavy mineral assemblages indicated a predominance of ferrimagnetic minerals in all the samples derived from the low to high grade metamorphic rocks, igneous intrusions, and volcanics of the Alaknanda valley. The results of REEs, major oxides, clay mineral assemblages, magnetic mineral parameters and heavy mineral assemblages were all in accordance with each other and revealed that Inner Lesser Himalayas (Garhwal Group) enriched in carbonates does not only dominantly source the dissolved load but also a large part of the sediment load carried by the Alaknanda River.

The variation in the organic carbon content in the Alaknanda River showed that seasonal erosivity and physiography of the basin are the key parameters which control the mode of transport, residence time, and oxidation of the organic matter. During the monsoon season, at Devprayag, the Alaknanda River contributes ~66% of the total dissolved organic carbon (DOC) flux to the Ganga River.

The present thesis has been organized into six chapters. Chapter 1 outlines a brief introduction and motivation to carry out the study in the Alaknanda basin and the aim and objectives. Chapter 2 summarizes the literature review on global rivers and studies on the Alaknanda River. Chapter 3 deals with the details of the study area (Alaknanda basin) including geographic location, climate, geology, etc. Chapter 4 deals with the methodology formulated to achieve the aims and objectives of the thesis. Chapter 5 includes results and discussion section and Chapter 6 listed the major conclusions of the present study and future scope.

PUBLICATIONS OF THE AUTHOR

International Journals (Peer-Reviewed)

- **Panwar, S.**, Chakrapani, G.J. (2013). Climate Change and Its Influence on Groundwater Resources. Current Science, 105 (1), 37-46. Springer Publ. (Impact factor: 0.926) *(Published)*
- Khan, M.Y.A., Hasan, F., **Panwar, S.**, Chakrapani, G.J. (2015). Neural Network Model for Discharge and Water Level Prediction for Ramganga River Catchment of Ganga Basin, India. Hydrological Sciences Journal. **DOI:** 10.1080/02626667.2015.1083650. Taylor & Francis Publ. (Impact factor: 1.864) *(Published)*
- **Panwar, S.**, Khan, M.Y.A., Chakrapani, G.J. (2016). Grain Size Characteristics and Provenance Determination of Sediment and Dissolved Load of Alaknanda River, Garhwal Himalayas, India. Environmental Earth Sciences 75, 91. Springer Publ. (Impact factor: 1.765) *(Published)*
- **Panwar, S.**, Chakrapani, G.J. (2016). Seasonal Variability of Grain Size, Weathering Intensity and Provenance of Channel Sediments in the Alaknanda River Basin, an Upstream of River Ganga, India. Environmental Earth Sciences 75, 998. Springer Publ. (Impact factor: 1.765) *(Published)*
- **Panwar, S.**, Chakrapani, G.J., Sangode, S.J. (2015)**.** Mineral Magnetic Characterization of Alaknanda River Sediments, Garhwal Himalayas, India. Journal of the Geological Society of India. Springer Publ. (Impact factor: 0.596) *(Under Review)*
- **Panwar, S.**, Chakrapani, G.J. (2015). Quantitative Analysis of Factors Controlling Sediment Yield in the Upper Ganga Basin, Western Himalayas, India. Arabian Journal of Geosciences. Springer Publ. (Impact factor: 1.224) *(Under Review)*
- **Panwar, S.**, Chakrapani, G.J. (2016). Erosion Risk Estimation, Weathering Intensity and Provenance of Sediment Load of the Alaknanda River Basin, Headwaters of River Ganga, India. Natural Hazards. Springer Publ. (Impact factor: 1.719) *(Under Review)*
- **Panwar, S.**, Gaur, D.G., Chakrapani, G.J. (2015). Total Organic Carbon Transport by the Alaknanda River, Garhwal Himalayas, India. Arabian Journal of Geosciences. Springer Publ. (Impact factor: 1.224) *(Under Review)*

Book Chapter

- **Panwar, S.**, Chakrapani, G. J. (2016). Spatial and Temporal Variability in Grain Sizes of Alaknanda River. In Geostatistical and Geospatial Approaches for the Characterization of Natural Resources in the Environment (pp. 313-319). Springer International Publishing. DOI 10.1007/978-3-319-18663-4

ACKNOWLEDGEMENT

The journey of success begins with a will, and there are many souls that inspire and stood with my will. Here, I proudly mention about all the people who supported me throughout my research period. Thank you all for being a part of my life. Without you all, accomplishment and achievements would not have been attained with serenity.

My supervisor: **Prof. G.J. Chakrapani** is an admirable teacher. It was a pleasant experience working with him. During the entire research period, he continuously motivated me. I truly acknowledge his patience during my early days, while checking and correcting my manuscripts several times. During the tough times, he supported me with good appreciation and never allowed me to lose my confidence. I feel blessed, being his student.

Prof. S.J. Sangode, Department of Geology, Pune University, I express my sincere gratitude for helping me with the lab facilities in the Pune University.

IIT Roorkee: I am delighted to be a part of one of the most prestigious educational institute in the country. It's an ease when all the best analytical, literature and boarding facilities are available at the institute.

I extend my sincere thank to the HoD, Department of Earth Sciences, **Prof. D.C. Shrivastava** for providing the research environment and maintaining the friendly administrative support. Thanks to the members of the **Student Research Committee** for the valuable suggestions and motivation. Regard to **Dr. Pitambar Pati** for his inspiring words.

A special thanks to the office staff and especially for **Mr. Nair**. Thanks to **Mrs. Kamala**, Warden, Sarojini Bhawan, for the comfortable lodging in the hostel.

My Labmates: The friendly and open discussion among all lab members (Geochemistry Lab, Department of Earth Sciences, IIT Roorkee) helped in improving my manuscripts and thesis. Field work would not have been excited and unchallenging without the help of **Mr. Yawar Ali Khan, Vijay, Praveen, Dhruv, and Shaumik.** Thank you guys.

Special thanks to **Nandita Singh, KJ Resmy, Anjali Singh, Nazia Khan, Ajit, Rudra, Stephy, Archana, Puspita** and **Anand** for their support throughout the journey. Sincere appreciation goes to my Pune University labmates **Mr. Priyeshu Shrivastava** and **Dr. Swapnil Gudadhe**.

My family: Thanks to the God, for giving me the family where everyone feels and raise strong girls. My papa (Late **Mr. Anand Panwar**) and mumma (**Mrs. Sunita Panwar**) always feed me with the dosage of confidence, independence, and freedom. I am grateful to both. Thanks to

Siddhant, Apurv, Kirti, **Shivangi, Massi (Mrs. Sudhesh Chauhan) and Chahi (Mrs. Poonam)** for the encouragement and love.

My Friends: It is a pleasure to thank you, my besties **Nirupama** and **Shailza**. The best memories of IITR stand with both of you. Special thanks to **Akash Rishishwar**, I admire your helpfulness attitude. Gratitude to **Mr. Chitiz Joshi**, Research Fellow, IIRS, Dehradun, **Mrs. Anju Panwar** and **Mr. Saurabh Purohit** Research Fellows, USAC, Dehradun for minimizing my struggle and always clearing my doubts. I am grateful to **Pooja Khuswaha and Devasari Fuloria** for their helping hand. Thanks to **Priyanka, Neethu, Harjot, Shermi, Tapasi mam, Rupali, Ritu, Rimpi, Pallavi, Anita, Mousumi, Neha, Mayank, Rahul, Manukant** and **Vivek** for making IITR a memorable part of my life.

Thank you God for the endless love and support

SUGANDHA PANWAR

TABLE OF CONTENTS

LIST OF FIGURES

LIST OF TABLES

ABBREVIATIONS AND SYMBOLS

A	Catchment Area
AF	Alaknanda Fault
ARM	Anhysteretic Remanent Magnetism
$B_{0(CR)}$	Coercivity of Isothermal Remanent Magnetization
Bl	Total Barren Land
CIA	Chemical Index of Alteration
COC	Channel Organic Carbon
CR	Carbonate Rock Exposure
Cul	Total Cultivation
CV	Coefficient of Variance
CWC	Central Water Commission
D_{50}	Median Particle Size
Dd	Drainage Density
DEM	Digital Elevation Model
DOC	Dissolved Organic Carbon
Dt	Drainage Texture
E	Basin Relief
Emax	Maximum Elevation
Emean	Mean Elevation
Emin	Minimum Elevation
Epk	Relief Peakedness
Er	Relief Ratio
Fl	Total Fallow Land
FWHM	Full Width at Half Maximum
GIS	Geographic Information System

HI	Hypsometric Integral
HIRM	Hard Isothermal Remanent Magnetization
HREE	Heavy Rare Earth Elements
IC	Inorganic Carbon
ICDD	International Centre for Diffraction Data
ICPMS	Inductively Coupled Plasma Mass Spectrometry
IDW	Inverse Distance Weight
IMD	Indian Meteorological Department
IRM	Isothermal Remanent Magnetization
IRSL	Infra Red Stimulated Luminescence
JPHP	JP Hydroelectric Project, Joshimath
K	Volume Susceptibility
K	Kurtosis
Lb	Basin Length
Lc	Channel Length
LD	Average Lineament Density
LREE	Light Rare Earth Elements
LULC	Land Use Land Cover
MBT	Main Boundary Thrust
Mc	Mean Size of Channel Sediment
MCT	Main Central Thrust
MD	Multi Domain
Ms	Mean Size of Suspended Sediment
Mya	Million Year
NAT	North Almora Thrust
NPOC	Non-Purgeable Organic Carbon
NRSC	National Remote Sensing Centre
OC	Organic Carbon

PC	Principal Component
PCA	Principal Component Analysis
PDF2	Powder Diffraction File 2
Pg	Pentagram
Pmax	Maximum Monthly Precipitation
Pmean	Mean Annual Precipitation
POC	Particulate Organic Carbon
PAHs	Polycyclic Hydrocarbons
PCBs	Polychlorinated Biphenyls
Ppk	Precipitation Peakedness
Ppm	Parts Per Million
PSA	Particle Size Analyzer
PSD	Pseudo-Single Domain
PSD	Particle Size Distribution
Q	Discharge
Qb	Discharge fraction from precipitation
Qd	Discharge fraction from groundwater
Qmax	Maximum Water Discharge
Qmean	Mean Water Discharge
Qpk	Discharge peakedness
REEs/REE	Rare Earth Elements
RMS	Root Mean Square
S	Sorting
SANDRP	South Asian Network on Dams, River and People
ST	Saknidhar Thrust
SAT	South Almora Thrust
SD	Single Domian
SI	Total Snow and Ice Cover

SIRM	Saturation Isothermal Remanent Magnetisation
Sk	Skewness
SL	Sediment Load
SR	Silicate Rocks Exposure
SRTM	Shuttle Radar Topography Mission
SSD	Stable Single Domain
SSP	Specific Stream Power
SSY	Specific Sediment Yield
STDS	South Tibetan Detachment System
Tmean	Mean Annual Temperature
TOC	Total Organic Carbon
Trange	Temperature Range
TRMM	Tropical Rainfall Measuring Mission
TSS	Total Suspended Sediments
UCC	Upper Continental Crust
UGB	Upper Ganga Bain
USGS	United State Geological Survey
viz.	Namely
WIP	Weathering Index of Parker
XRD	X-Ray Diffraction
XRF	X-Ray Fluorescence
Φ	Phi size
$\alpha 1$	Slope
αc	Channel Gradient
χ_{ARM}	Anhysteretic Remanent Magnetism Susceptibility
$\chi_{fd\%}$	Frequency Dependent Susceptibility
χ_{hf}	High Frequency Mass Specific Susceptibility
χ_{lf}	Low Frequency Mass Specific Susceptibility

CHAPTER 1

INTRODUCTION

1.1. Global Significance of Studying River Sediments

1.2. Importance of Studying Sediments of the Alaknanda Basin

1.3. Previous Studies on the Alaknanda River Basin

1.4. Aims and Objectives

1.5. Organization of the Thesis

1.6. Research Design

1.1. GLOBAL SIGNIFICANCE OF STUDYING RIVER SEDIMENTS

Rivers are a crucial component of the global water and carbon cycle and act as an important link between the ocean and terrestrial ecosystem (Berner and Berner, 1996). Rivers transport sediments in the form of dissolved, suspended and bed load. Milliman and Fransworth (2011) estimated that globally rivers transport $36*10^3$ km^3 of freshwater and 20×10^9 tons $year^{-1}$ of suspended sediments annually from continents to oceans. Syvitski et al. (2003) stated that approximately 95% of total sediments entering the ocean are transported by the river system (Table 1.1). Transportation of sediment by rivers is an important aspect that influences directly the climate, pedogenesis, landscape evolution, aquatic life, river water quality and dams and reservoirs on the channel (Allen, 2008). Hence, fluvial sedimentology studies have a wide application in the field of hydraulics, water resource management, climate change and engineering.

Catchment specific factors such as physical and chemical weathering rate, basin area, basin slope, relief, climate, geology, and anthropogenic activities control the form and mode of transportation of sediments carried by the river and its characteristics (size, shape, and composition). Berner and Berner (1987, 1996) have elaborated all these factors. Out of 20×10^9 tons $year^{-1}$ of global suspended sediments transported by the rivers, Asian rivers constitute ~80% of the flux and the Himalayan rivers viz. the Ganga and the Brahmaputra constitute ~25% (Berner and Berner, 1987) (Fig. 1.1). Table 1.2 shows the sediment load carried by the world's rivers. The largest rivers of the world such as the Amazon, Mississippi, Nile and Huanghe do not transport significant amounts of sediment flux to the oceans as compared to the Himalayan Rivers.

The Ganga River that flows through the Himalayan sequence transport 72.9×10^7 tons of sediments to the Bay of Bengal, of which 95% is transported during the monsoon season (Singh et al., 2006). Heavy monsoon and high tectonic activities erode the mountains and the Ganga plains and generate a high amount of sediment load. Previous studies of Galy and France-Lanord (2001); Singh et al. (2008); Garzanti et al. (2011) have established that Higher Himalayan Crystallines are the main supplier of sediments in the Ganga basin. The physical erosion rate in the headwater region of the Ganga River i.e. the Bhagirathi and the Alaknanda sub-basin is 907 tons km^2 $year^{-1}$ and 863 tons km^2 $year^{-1}$ respectively (Chakrapani and Saini, 2009). The amount of sediments in the river decides the incision and aggradation of the channel. The high sediment load carried by the Ganga River from the Upper Ganga Basin is responsible for the formation of Ganga alluvial plains, which is considered to be the most fertile land and supports the livelihood of a large population in India.

Raymo and Ruddiman (1992) correlated the Cenozoic climate change with the upliftment of the Himalayas and higher silicate weathering rates. Annually, fluvial network transport, transform and store ~2 Pg of terrigenous organic carbon (Battin, 2008). Galy et al. (2007b) observed that over the past 15 Mya, the Ganga-Brahmaputra river system deposited $0.6*10^{12}$ mol organic carbon (15% of the global burial flux) in the Bay of Bengal. This sequestration of organic carbon since the Cenozoic Era has forced a cooling trend on the global climate (Raymo and Ruddiman, 1992; Berner and Berner, 1996; Gaillardet et al., 1999; Galy and France-Lanord, 2001). The study of Frings et al. (2015) stated that the Si mobilization is quite high in the Himalayan Rivers and chemical weathering of Si in the Ganga plains since Neogene has been affecting the silicate weathering efficiency in the Ganga Basin.

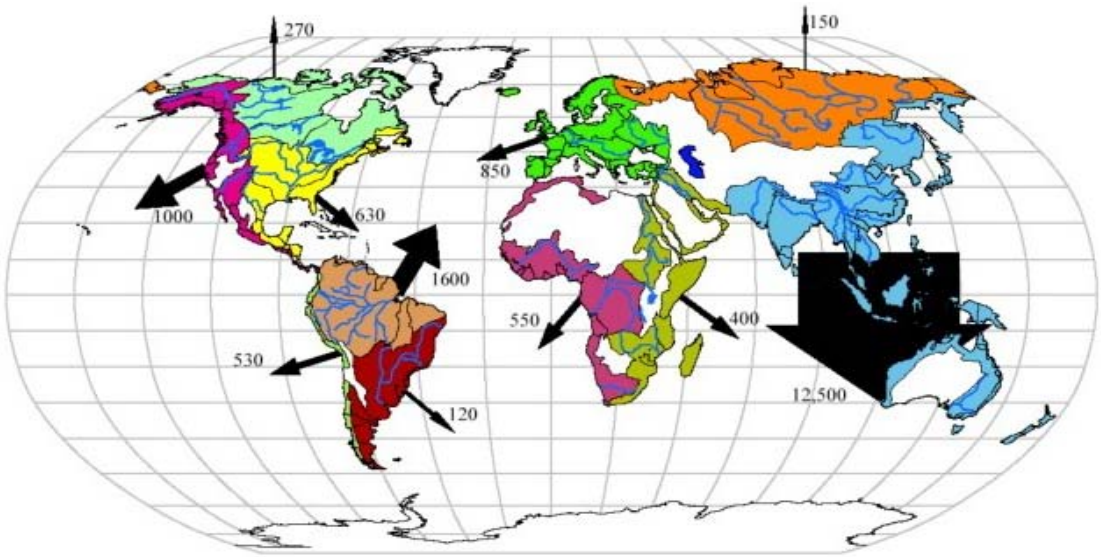

Figure1.1 Annual fluvial sediment discharge to the world's oceans (Milliman and Fransworth, 2011) (Unit in $*10^6$ ton/year)

Table 1.1 Amount of sediment transported by different weathering agents to the oceans (Adapted from Syvitski et al., 2003)

Sediment Load	**Amount ($*10^9$ ton/year)**
Suspended load	18
Bed load	2
Dissolved load	5
Glaciers sea ice, icebergs	2
Wind	0.7
Coastal erosion	0.4

Apart from regulating the physiography and global climate, sediment load also control the water quality and its utilization. The sediments in the river are considered as a pollutant and act

as a source for inorganic and organic constituents (USEPA, 2007). Some major and trace elements (Al, Fe, Mn, Cu, Zn, Pb, Hg and As) are hydrophobes and travel on the sediment surface. Nutrients (P, Si, N) and organic compounds such as polycyclic hydrocarbons (PAHs), polychlorinated biphenyls (PCBs) and chlorinated pesticides are also sediment associated and travel as suspended and bed load (USEPA, 2007; Horowitz et al., 2012). Warren et al. (2003); Walling (2005) have described the importance of fine sediment in the transportation of nutrients, contaminants, pathogens and heavy metals. Sediment load also control the biology of the fluvial environment by supplying valuable nutrient and breeding ground for the aquatic life.

Table 1.2 Water and sediment discharge in some of the large rivers of the world (Adapted from McLennan, 1993)

River	Water discharge (km^3/year)	Drainage area (10^6 km^2)	Sediment discharge (10^6 tons/year)	Sediment yield (tons/km^2/year)
Amazon	6300	6.15	1200	195
Colorado	20	0.64	0.01	0.02
Columbia	251	0.67	10	15
Congo (Zaire)	1250	3.72	43	12
Dambe	206	0.81	67	83
Ganga-Brahmaputra	**971**	**1.48**	**1060**	**716**
Huang He	49	0.75	1050	1400
Indus	238	0.97	59	61
Mackenzie	306	1.81	42	23
Mekong	470	0.79	160	202
Mississippi	580	3.27	210	64
Niger	192	1.21	40	33
Nile	30	3.03	0	0
Orinoco	1100	0.99	150	152
St. Lawrence	447	1.03	4	4

The life span of dams, reservoirs and canals are associated with the sediment yield of the basin. The understanding of the sediment characteristics, its transportation mechanism, and source bedrock help in regulating the infield mitigation techniques and methods to reduce diffuse pollution and in combating the siltation problem in the dammed rivers. Studies of Walling and Moorehead (1989); Galy and France-Lanord (2001); Walling (2005); Singh (2009); Yan et al. (2012); Li et al. (2013) observed that trapping of sediments in reservoirs

influence global sediment budget and suggest to study the sediment budget, sediment dynamics and sediment provenance in the dammed rivers on a regular basis.

1.2. IMPORTANCE OF STUDYING SEDIMENTS OF THE ALAKNANDA BASIN

Since 25% of the total global sediment flux is carried by the Ganga-Brahmaputra River system, it becomes important to study the headwater of these rivers; Alaknanda River is one of the two headwaters of the Ganga River in the Himalayan region. The carbon isotopic ($\delta^{13}C$) studies of Bay of Bengal sediments suggest that due to intense physical weathering, >65% of the Ganga mainstream sediments are derived from the Higher Himalayan Crystallines (France-Lanord et al., 1993; France-Lanord and Derry, 1997; Singh et al., 1998; Galy and France-Lanord, 2001; Singh et al., 2008; Garzanti et al., 2011).

The Alaknanda River, which flows in the Garhwal Himalayan region of India, is a headwater stream of the Ganga River. Alaknanda is a major supplier of sediment load to the Ganga River, which is responsible for the formation of Ganga alluvial plains. The key features of the Alaknanda watershed are active tectonics, high physical weathering, heavy monsoon, diverse lithology, mountainous morphology and maximum natural land cover (Valdiya, 1980; Singh and Hasnain, 1998; Chakrapani and Saini, 2009; Chakrapani et al., 2009; Shukla et al., 2014). Chakrapani and Saini (2009) calculated the physical weathering rate in the Alaknanda watershed to be 3.25 mm $year^{-1}$, which is far in excess of the global average of 0.58 mm $year^{-1}$ and chemical weathering rate of 153 tons km^{-2} $year^{-1}$ which is six times higher than the global average of 24 tons km^{-2} $year^{-1}$ (Chakrapani et al., 2009).

Due to its steep topography and immense perennial supply of water, Alaknanda River basin offers huge hydroelectric power potential. According to South Asian Network on Dams, River and Public (SANDRP), ~130 dams are under a proposal to fetch hydropower from Alaknanda-Bhagirathi river systems. The important factors that affect the hydropower structure are the sediment load and the sediment size. Chakrapani (2005) and Panwar et al. (2016) mentioned that the composition of Upper Ganga River sediments is enriched in quartz (>60%). The sediment load enriched in quartz can be quite a challenge to tackle the hydropower management. Till date, no study has been reported that discusses the grain size variability and source characterization of sediments of the Alaknanda River. This offers an opportunity to carry the sedimentological and geochemical studies in the Alaknanda basin. Moreover, after the devastating floods in the year 2013 in the Alaknanda valley, environmental concerns have been raised among the researchers to evaluate the natural and anthropogenic influence in the basin.

1.3. PREVIOUS STUDIES ON THE ALAKNANDA RIVER BASIN

The pioneer study of Sarin and Krishnaswami (1984) showed that chemical denudation rate in the Ganga-Brahmaputra drainage basin is 2-3 times higher than the global average. Later, Sarin et al. (1989) stated that dissolved load of the Himalayan tributaries are dominated by carbonate weathering while silicate weathering plays a subordinate role. Following these studies, numbers of research have been concentrated on the Himalayan Rivers. Table 1.3 gives an overview of all the published studies conducted on the Upper Ganga Basin.

In the Alaknanda basin, most of the previously published studies were concentrated on the dissolved load of the river. The first comprehensive study with a focus on the Alaknanda River was carried by Singh and Hasnain (1998). They calculated the chemical and physical denudation rate in the Alaknanda basin to be 133 tons km^2/year and 356 tons km^2/year respectively and attributed high erosion processes to factors such as high relief, intense monsoon rainfall, landslides and glacial erosion. Singh et al. (1998) studied the $^{87}Sr/^{86}Sr$, $\delta^{18}O$ and $\delta^{13}C$ isotopic composition of the dissolved load and quantified that silicate weathering contributes 33-89% of Sr in the waters of Bhagirathi, Bhilangna, Alaknanda and Ganga Rivers. The study of Bickle et al. (2003, 2005) discussed the seasonal variation in the composition of the dissolved load due to high monsoon rains and glacial melt down. Bickle (2005) observed that both silicate and carbonate weathering controls the Sr concentration of the dissolved load. However, based on one year daily sampling of the dissolved load of the Rivers Alaknanda, Bhagirathi and Ganga at Devprayag, Chakrapani (2005) studied the major ion chemistry, Sr concentration and REEs composition of the water and revealed the dominance of carbonate rock weathering in the Upper Ganga basin. The Sr isotopic composition and Sr/Ca ratio indicate that the weathering of silicate, carbonate and sulfur rich rocks found in the Lesser Himalayas source the dissolved load of the River Ganga at Devprayag. Later, Tripathy and Singh (2010) applied the forward and inverse models to find out the different pools of the major ion composition and inferred that carbonate>silicate>evaporite weathering controls the water composition. Their study also confirms that at Devprayag after the confluence, Alaknanda River exerts a strong control on the $^{87}Sr/^{86}Sr$ of the Ganga River. Yadav and Chakrapani (2011) studied the dissolution kinetics of various lithologies in the Alaknanda-Bhagirathi basin and confirmed that though carbonate formations constitute <10% of the basin area, it controls 61-85% of the water composition.

Chakrapani and Veizer (2005) using the $\delta^{13}C_{DIC}$ values in the Alaknanda and Bhagirathi rivers, found carbonate weathering and bacterial respiration as the dominant source of dissolved inorganic carbon (DIC) while the dissolution of gypsum and oxidation of pyrite

(present in the Lesser Himalayas) as the major source of sulphide (Chakrapani and Veizer, 2006). Chakrapani et al. (2009) quantified the physical and the chemical weathering rate in the Alaknanda basin using the major ion composition of dissolved load and attributed low values of the chemical saturation index (CSI) to factors such as high relief and flow. The study of Frings et al. (2015) highlighted the role of mountainous topography in the mobilization of Si and supplying the sediments to the alluvial plains where 75% of the total decomposition of silicate minerals take place.

The few studies that deal with the sediment load in the UGB include Pandey et al. (1999, 2002), Chakrapani (2005), Mukherjee et al. (2007), Chakrapani and Saini (2009) and Chakrapani et al. (2009) and Frings et al. (2015). Pandey et al. (1999) studied the suspended sediment concentration of the Bhagirathi River and mentioned about the dissolution of suspended sediments during the monsoon season. They observed that annual suspended sediment transported by the Bhagirathi River (1010 tons/km^2/year) is two times higher than the Alaknanda River (365 tons/km^2/year). Singh et al. (2008) observed that there exists a spatial variability in the physical erosion rates in the Alaknanda and Bhagirathi sub-basins. Chakrapani and Saini (2009) presented in detail the factors that control the sediment yield of the Alaknanda and Bhagirathi River. The spatial and temporal relationship of sediment load with discharge, relief and lithology were highlights of their study. The study of Dosseto et al. (2015) shows that in the Alaknanda basin, runoff and physical erosion controls the silicate weathering rates.

The study of Pandey et al. (2002) is the only published study related to the particle size distribution in the Alaknanda basin. Pandey et al. (2002) discussed the grain size distribution of the melt waters of the Pindari glacier. In the melt water of the Pindari glacier, the sizes of sediments were medium to coarse silt. Chakrapani (2005) studied the mineral composition of the suspended sediments of the Alaknanda, Bhagirathi and Ganga rivers at Devprayag. High physical weathering in the basin is revealed by the presence of the minerals such as quartz and mica/illite. Mukherjee et al. (2007) conducted a geochemical survey in rivers Bhilangana, Alaknanda, Mandakini, and Bhagirathi and observed the enrichment of U and Th in the river sediments.

Anthropogenic and natural disturbances promoting high erosion in the UGB have been studied by Barnard et al. (2001), Wasson (2003) and Sati et al. (2011). Apart from natural factors, landslides due to unscientific road construction were cited as a major factor promoting erosion in the Alaknanda-Bhagirathi basin. Shulka et al. (2014) prepared the landslide intensity map of the Alaknanda basin and observed that most of the landslides are concentrated in the

middle part of the basin (the region between Vaikrita and Ramgarh Thrust) that receives the highest rainfall in the area.

Through previous works (discussed above and in Table 1.3), weathering regime and geochemistry of major ions in the Alaknanda basin is well known (Singh and Hasnain, 1998; Pandey et al., 1999; Chakrapani and Veizer, 2005; Chakrapani and Veizer, 2006; Chakrapani et al., 2009; Yadav and Chakrapani, 2011). However, no comprehensive study related to suspended and channel sediment size, composition, and the provenance have been reported. As Alaknanda River is a major contributor of the dissolved and sediment load to the Ganga River, a detailed study of sediment transported by the river is essential for a comprehensive global data concerning the Himalayan Rivers.

1.4. AIMS AND OBJECTIVES

The thesis work aimed at the following objectives:

- Estimation of seasonal and spatial variations in the sediment load of the Alaknanda River and its tributaries and identification of the factors responsible for the variation
- Characterizing the sediments for grain size, mineral, environmental magnetism and chemical composition
- To understand the provenance of the suspended and channel sediments using mineral and chemical composition (major oxides, REEs, mineral magnetism and heavy minerals)
- To make preliminary assessment of total organic carbon (TOC) flux of the Alaknanda River

Table 1.3 Previous studies conducted in the Alaknanda-Bhagirathi basin

Area of Research	River/Tributary	Method/Approach	Previous studies
Dissolved load	Ganga Basin	Major ions	Sarin and Krishnaswami (1984)
	Ganga Basin	Major ions	Sarin et al. (1992)
	Alaknanda River	Major ions	Singh and Hasnian (1998)
	Upper Ganga Basin	$^{87}Sr/^{86}Sr$, $\delta^{18}O$ and $\delta^{13}C$ isotope	Singh et al. (1998)
	Ganga, Alaknanda Bhagirathi and Dhauli Ganga	Major ions and $^{87}Sr/^{86}Sr$ isotope	Bickle et al. (2003, 2005)
	Alaknanda, Bhagirathi and Ganga River at Devprayag	Major and trace elements	Chakrapani (2005)
	Alaknanda-Bhagirathi River and major tributaries	$\delta^{13}C_{DIC}$	Chakrapani and Veizer (2005)
	Alaknanda-Bhagirathi River and major tributaries	$\delta^{34}S$	Chakrapani and Veizer (2006)
	Alaknanda and Bhagirathi Rivers	Major ions	Chakrapani et al. (2009)
	Ganga Basin	Major ions and Sr isotopes	Tripathy and Singh (2010)
	Alaknanda and Bhagirathi Rivers	Dissolved load and bed-rock composition	Yadav and Chakrapani (2011)
	Ganga Basin	Si isotope	Frings et al. (2015)
Suspended sediments	Bhagirathi River	Sediment load and mineral composition	Pandey et al. (1999)
	Pindari glacier sediments	Sediment load, particle size distribution, and textural analysis through SEM images	Pandey et al. (2002)
	Alaknanda, Bhagirathi and Ganga River at Devprayag	Mineral Composition	Chakrapani (2005)
	Alaknanda-Bhagirathi basin	Sediment load and controlling variables	Chakrapani and Saini (2009)

Bank Sediments	Ganga Basin	Sr and Nd isotopes	Singh et al. (2008)
Fluvial terraces	Alaknanda River basin	δ^7Li	Dosseto et al. (2015)
	Alaknanda River basin	Morphometic indicators	Sati et al. (2007)
Bed-rock and soil samples	Alaknanda-Bhagirathi basin	Trace elements	Mukherjee et al. (2007)
Landslide and erosion activities	Chamoli region of the Alaknanda Basin	Landslide mapping and cosmogenic radionuclide dating ^{10}Be and ^{26}Al	Barnard et al. (2001)
Sediment budget	Chamoli district of the Alaknanda Basin	Suspended sediment, IRSL dates, and land cover data	Wasson (2003)
Natural hazard vulnerability	Alaknanda basin	GIS-based morpho-tectonic studies	Shukla et al. (2014)

1.5. ORGANIZATION OF THE THESIS

The thesis is synthesized and organized into the following chapters:

Chapter 1 gives the general introduction and mentions the purpose and motivation to carry out the study in the Alaknanda basin. It highlights the importance of the Alaknanda River, the formulation of objectives and research design.

Chapter 2 summarizes the literature review on sedimentological studies dealing with the physical, chemical and mineral composition of global river sediments.

Chapter 3 presents the details about the Alaknanda River basin, its location, physiography, climate, geology, anthropogenic, socio-economic and environmental issues.

Chapter 4 describes the methodology for the present research including sample collection, laboratory analysis, and the statistical approach. As per the methodology, following analytical database was generated:

i. Total suspended sediments load
ii. Particle size distribution
iii. Rare earth element (REEs) composition of suspended sediments
iv. Major oxide and magnetic mineral composition of channel sediments
v. Clay minerals in sediments
vi. Total organic carbon (TOC) in the dissolved, suspended and channel sediments

Chapter 5 presents the results generated in this study along with a detailed discussion, interpretation, and possible explanations.

Chapter 6 lists the major conclusions from the study and future scope.

1.6. RESEARCH DESIGN

1.6.1. Estimation of the Sediment Load and Identification of Controlling Factors

Alaknanda River is a major contributor of sediment load to the Ganga River. Landslides, glaciers, channel erosion, sheet and rill erosion, glacial lake outburst and landslide lake burst are the most common natural source of sediments (Wasson, 2003). The recent anthropogenic activity in the form of dams and road constructions is altering the natural mechanism of erosion (Barnard et al., 2001; Wasson, 2003; Machiwal et al., 2010; Sati et al., 2011). The sediment load variations were studied for:

- Estimation of the pre-monsoon, monsoon and post-monsoon variability in the sediment load.

- Quantification of twenty nine variables that control the sediment load carried by the river using the geographic information system (GIS) and the previously published data of the Indian Meteorological Department (IMD), Pune and the Central Water Commission (CWC), Lucknow.
- Establishing five prominent factors for sediment load variations - *hydrological* (discharge, TSS, etc.), *topographic* (area of the basin, elevation, slope and channel length), *Climatic* (temperature, rainfall and atmospheric pressure), *Geological* (rock types and structural control) and *Anthropogenic* (land use land cover alterations).

1.6.2. Variability in Particle Size Distribution

Particle size distribution (PSD) controls the mobilization, transport, deposition and mineral and chemical composition of sediment. Apart from hydraulics, particle size is an important parameter that controls the siltation in reservoirs, wearing of turbine blades, contamination of water by pathogens and heavy metals and provides breeding ground for the aquatic life forms (Lindholm, 1987; Horowitz and Elrick, 1987; Walling and Moorehead, 1989; Slattery and Burt, 1997; Xu, 1999; Pandey et al., 2002; Zhang et al., 2006). Particle size distribution was studied as:

- Laser diffraction technique based instrument was used for estimating the PSD of the suspended and channel sediments.
- Statistical grain size parameters such as mean size, sorting, skewness and kurtosis were determined by following Folk and Ward (1957) and Garzanti et al. (2011).
- Relating PSD with factors such as climate, discharge, slope, stream power, lithology, and anthropogenic modifications.

1.6.3. Estimating Weathering Intensity in the Basin

Physical and chemical weathering rates in the basin are quite high in comparison to the global average (Singh and Hasnain, 1998; Galy and France-Lanord, 2001; Bickle et al., 2003; Krishnaswami and Singh, 2005; Chakrapani and Saini, 2009; Garzanti et al., 2011). But all the previous studies were based on samples from Devprayag (the exit point of the watershed). In this study, samples were collected from the upstream of Devprayag and weathering intensity of the Alaknanda basin was estimated using multiple indices such as:

- Clay mineralogy (kaolinite/illite ratio, illite chemistry index and illite crystallinity index)
- Major oxide composition (chemical index of alteration, weathering index of parker and molar ratio of Al/Si)

1.6.4. Sediment Source Characterization

Sediment composition is specific to the lithology of the basin. Therefore, the composition of sediment can be employed to find out the source bedrock. Mineral and chemical composition of suspended and channel sediment were applied to identify the source bedrocks. In this study, the following fingerprinting techniques were used:

- Rare earth elements (REEs)
- Major oxide composition
- Mineral magnetism and heavy minerals

1.6.5. Assessment of Total Organic Carbon Flux

A preliminary assessment of the organic carbon flux by the Alaknanda River was carried out by analyzing the dissolved organic carbon (DOC), particulate organic carbon (POC) and channel organic carbon (COC) in samples by an Organic Carbon Analyzer.

CHAPTER 2

LITERATURE REVIEW

2.1. Sediment Load and Particle Size Distribution

2.2. Major Oxides Composition

2.3. Rare Earth Elements (REEs)

2.4. Clay Mineralogy

2.5. Environmental Magnetism and Heavy Minerals

2.6. Total Organic Carbon (TOC) flux

2.1. SEDIMENT LOAD AND PARTICLE SIZE DISTRIBUTION

Horowitz and Elrick (1987) observed that the mineral and element composition of sediments depend on two general properties- physical (e.g. grain size, surface area, and surface charge) and chemical (e.g. composition and ion exchange capacity). There exist an inter-relationship between these properties. With a decrease in particle size, the surface area of sediment, its surface chemistry, adsorption property and cation-exchange ability increases (Horowitz and Elrick, 1987; Walling and Moorehead, 1989; Horowitz, 1991; Walling et al., 2000). Studying the sediment size and its composition has wide application in understanding the river processes related to hydraulics, geomorphology, flow dynamics, heavy metal pollutants, siltation in reservoirs and contamination by pathogens (Slattery and Burt, 1997; Xu, 1999; Pandey et al., 2002; Zhang et al., 2006). Bainbridge et al. (2012) highlighted the importance of grain size in controlling the niche and ecosystem of a river.

Particle Size Distribution (PSD) is the percentage of mass, volume, or number of particles in a range of particular sizes. Lindholm (1987); Meyers and Eadie (1993); Xu (1999); Walling et al. (2000) and Weltje and von Eynatten (2004) observed that due to the grain size effect, preferential enrichment of specific mineral in certain grain-size fraction occurs. As an example <2µm grain size is composed of secondary silicate minerals while the coarse particles are quartz enriched. It is seen that fine particles are enriched in clay minerals, organic carbon, and trace elements. Warren et al. (2003) and Walling (2005) observed the importance of fine sediments in the transportation of nutrients, contaminants, pathogens and heavy metals through the fluvial system.

The grain size distribution of sediments varies along the course of the river. Generally, the major factors responsible for sediment load and grain size characteristics vary widely, including climatic conditions, lithology, discharge, relief, basin area, river energy and anthropogenic activities (Milliman and Meade, 1983; Lindholm, 1987; Gaillardet et al., 1999; Xu, 1999; Chakrapani, 2005; Goni et al., 2006; Feng et al., 2011; Xu et al., 2012). In the mountainous terrains, river power is a leading factor that varies both spatially and temporally depending on the discharge, slope, and other related factors.

Most of the researchers working on the fluvial system have focused on the seasonal and spatial variations in the total suspended sediments concentration, but till date the grain size distribution of sediments has not been studied in detail. Church and Kellerhals (1978) and Rice and Church (1998) observed that due to the process of abrasion and preferential grain size transportation, the percentage of fine particles in the bed sediment increases downstream. Passega (1977) studied the grain size distribution of the Mississippi River and noticed a vertical

variation in the deposition of coarse to fine sediments which were influenced by the shear stress and turbulence during floods. During the floods, due to increasing in discharge, the coarsening of sediment size was noticed (Lenzi et al., 2006). A diverse range of hydrological and geological conditions may influence the effective and absolute particle size distribution of suspended sediments carried by the river (Walling, 1996). Phillips and Walling (1999) discussed the particle size characteristics of the fine grained bed sediments, taking into consideration the difference between effective and absolute particle size, the river carries. They inferred that the effective particle size precisely represents the true particle size and deposition process can be conferred by enrichment/depletion ratio of the suspended sediments. Thill et al. (2001) studied the influence of salt flocculation in the evolution of particle size in the Rhone River. They inferred that the presence of coarse sediment fraction in the river (>5mm) can be explained by the process of settling and dilution, whereas a complex process of the break-up, resuspension, and primary productivity controlled the amount of finer fraction (2-5mm). Bouchez et al. (2011) sampled the suspended sediments of the Amazon River and established a relation between the distribution of elements and grain size. Their multi-approach study concluded that the composition of river sediment is a result of the interplay between weathering, hydrodynamic sorting, and crustal composition. The effect of anthropogenic activities on the sediment size was studied by Diplas and Parker (1992). Human activities such as agriculture, urbanization and mining can result in the enrichment of fine sediments in the gravel-bedded streams. Lin et al. (2002) studied the distribution of heavy metals in the Yangtze River sediment and East China Sea continental shelf sediments and inferred that heavy metals linearly increase with an increase in the amount of fine-grained sediments and decreased rapidly away from land. Xu (2007) observed that the sedimentation processes in the reservoir are dependent on the grain size carried by the river and the construction of reservoirs should be designed differently for the gravel and sand-bedded rivers. Bravard et al. (2014) studied the process of sand transportation in the Lower Mekong channel, China and highlight the influence of dam construction on the grain size distribution. After the dam construction, the river was found to carry coarser bed sediments.

The study of Garzanti et al. (2011) is the only published study that presents the grain size distribution of the suspended sediments carried by the Ganga River. The Ganga River sediments comprise of a poorly sorted admixture of clay, medium silt and fine sand. In recent years, owing to the large hydropower potential in the Alaknanda basin, knowledge on the amount of sediment load and particle size distribution is essential for combating sedimentation in the reservoirs and preventing turbine destruction. The purpose of this research was to

understand the trend in the spatial and temporal variation in the sediment load and PSD of the Alaknanda River and its major tributaries and the controlling factors.

2.2. MAJOR OXIDES COMPOSITION

River sediments are considered as a true representative of the bedrock geology. The bedrock is transformed into soil/sediment by the combined effect of climate, tectonics and lithology (Berner and Berner, 1987; Raymo et al., 1988; Raymo and Ruddiman, 1992; McLennan, 1993; Berner and Berner, 1996; Gaillardet et al., 1999). Every mineral produces distinct weathering products and, therefore, the composition of sediments can be used to trace the source of river sediments. McLennan (1993) observed that the chemical composition of sediment resulted from the interplay of various processes such as weathering, transportation, sorting, and diagenesis. The composition of recent river sediment depends on both the natural and anthropogenic processes. Natural processes that determine the composition of sediment include erosion and weathering. Physical weathering processes generate sediments that are compositionally similar to the source rock, whereas, chemical weathering generates sediments that are compositionally distinct. The study by Li and Yang (2010) showed that regional factors such as topography, tectonics, soil cover, temperature, and precipitation dominantly determine the intensity of chemical weathering. In terms of lithology, Meybeck (1987) observed that carbonate and evaporites weather twelve and forty to eighty times respectively, faster than the silicate rocks.

Major elements form a major proportion of the sediments and include O, Si, Al, Fe, Ca, Na, Mg, K and Ti, and generally measured as weight percent. Trace elements are accessory elements and form <0.1% of the sediment composition. X-ray Fluorescence (XRF) is a widely popular technique used to estimate the percentage of major and trace elements. Major oxides include SiO_2, TiO_2, Al_2O_3, Na_2O, K_2O, CaO, MgO, MnO, Fe_2O_3, P_2O_5. The work of Martin and Maybeck (1979); Berner and Berner (1996); White and Blum (1995); Gaillardet et al. (1995); Gaillardet et al. (1999); Ramesh et al. (1999, 2000); Dalai et al. (2004); Singh (2009, 2010) and Shao et al. (2012) showed the large array of implication of sediment composition data.

Classical studies on river geochemistry include the work of Russell (1937) on the sediments of the Mississippi River, Franzinelli and Potter (1983) on the sediments of the Amazon River and Gaillardet et al. (1999) on the global rivers. Vital and Stattegger (2000) studied the major and trace element composition of sediments of the lower reaches of the Amazon River and observed that few of the trace elements have a strong tendency to associate

with the silt fraction. Dalai et al. (2004); Singh (2010) studied the correlation between the major oxide composition of sediment and its mean size to infer the chemical immaturity of river sediments.

Sarin and Krishnaswami (1984); Chakrapani and Subramanian (1990); Singh et al. (1999); Ramesh et al. (2000); Chakrapani (2005); Singh et al. (2006); Tripathy and Singh (2010); Singh (2010); Garzanti et al. (2011) carried out significant research work on the sediment geochemistry of the Indian rivers. In the Ganga-Brahmaputra basin, Ramesh et al. (2000) observed high Si concentration in sediments. Singh (2010) studied the major and trace element geochemistry and the provenance of the Ganga River sediments. Various indices such as K_2O/Na_2O, SiO_2/Al_2O_3 and positive correlation of SiO_2 with Na_2O, Al_2O_3 and TiO_2 indicate the silicate source whereas, a strong positive correlation between CaO and MgO point to the carbonate rocks as a source of the sediments carried by the Ganga River (Das and Haake, 2003; Das et al., 2008; Wu et al., 2012; Gupta et al., 2012).

Nesbitt et al. (1980) during their research on chemical weathering of granodiorites observed that the cation exchange process plays a vital role in the removal of the elements from the rock and observed that alkali and alkaline earth elements are easily removed during the early stages of chemical weathering. Nesbitt and Wilson (1992) characterized the nature of element mobility and stability and found Ti, Fe, and Al to be conservative during the weathering. Gaillardet et al. (1999) studied the major and trace element geochemistry of the suspended load of the world's major rivers and proposed a systematic weathering index for the highly mobile Na, K and Ba elements. An inverse relation was noted between the sediment load and the weathering intensity. The process of dilution leads to the leaching of Na, K, Ca and Mg cations and enrichment of immobile element in the river sediment such as Ti and Al. Since Al is considered as immobile, the element ratios such as K/Al and Na/Al are used as weathering indices (Limmer et al., 2012).

Nesbitt and Young (1982) observed that feldspars are the most abundant reactive (labile) mineral; chemical weathering process involves the degradation of feldspars and concomitant formation of clay minerals. Ca, Na and K are generally removed from the feldspars by aggressive soil solutions resulting in an increase proportion of alumina to alkalis in the weathered product. Nesbitt and Young (1982) proposed Chemical Index of Alteration (CIA) as an index to quantify the extent of chemical weathering:

$$CIA = [Al_2O_3/(Al_2O_3 + Na_2O + K_2O + CaO^*)] \times 100$$

Another widely used index is the Weathering Index of Parker (WIP), formulated by Parker (1970) and developed by (Hamdan and Burnham, 1996). WIP is calculated as the ratio of alkali and alkaline earth elements present in the weathered product (Shao et al., 2012).

$$WIP = (2Na_2O/0.35 + MgO/0.9 + 2K_2O/0.25 + CaO/0.7)^* \times 100$$

Garzanti et al. (2011) and Shao et al. (2012) mentions that the CIA is appropriate for the silicate terrain and WIP for the metamorphic rocks (Borges and Huh, 2007; Price and Velbel, 2003). McLennan (1993) calculated the CIA values for global river systems and found that there exist a negative correlation between sediment yield and weathering history. Li and Yang (2010) pointed that the CIA is sensitive to the surface temperature, topography and soil depth. In context to the Ganga River, Singh (2010) found low CIA value that indicates the low intensity of silicate weathering prevails in the Ganga basin.

In the present research, major oxides composition of channel sediments was applied to quantify the weathering intensity of the Alaknanda River basin (using CIA and WIP values) and to find out the prominent lithology contributing to the sediment load.

2.3. RARE EARTH ELEMENTS (REEs)

In a fluvial system, sediment load can have various sources, varying from hillslope erosion to channel processes. Identification of the sediment source ensures sediment budgeting and is an in-field mitigation approach for watershed management practices. The most common sediment fingerprinting methods include radiogenic and stable isotopes, total nitrogen, phosphorus and carbon isotopes, clay mineralogy, and trace elements especially the rare earth elements (Pande et al., 1994; Walling et al., 1998; Nigel et al., 1998; Galy et al., 2007b; Davis et al., 2009; Choudhary et al., 2009a,b; Deasy and Quinton., 2010; Garzanti et al., 2011; Sahoo et al., 2012, 2014; Walling et al., 2013; Li et al., 2013; Girmay et al., 2015). To find out the source of suspended sediments in this study, rare earth elements (REEs) were used as a tracer.

As defined by IUPAC, REEs are a collection of seventeen elements placed in group 3rd and period 6th and 7th of the periodic table specially the lanthanide series, from lanthanum (La) to lutetium (Lu), plus scandium (Sc) and yttrium (Y) characterized by similar chemical properties. Based on the electronic configuration, REEs from La to Eu are referred as Light Rare Earth Elements (LREE) and from Gd to Lu as Heavy Rare Earth Elements (HREE). Deasy and Quinton (2010) and Walling et al. (2013) remark that an ideal tracer should possess four important characteristics, (i) adequately represent the physical and chemical properties of sediment, (ii) easy to detect at a very low concentration, (iii) have multiple signatures that would all behave same when used as a tracer, and (iv) non-toxic. REEs fulfill most of the

characteristics of ideal tracers as they behave conservatively during sediment formation and transportation and within different grain sizes also, they resemble their source rock's REEs pattern (Taylor and McLennan, 1985; Goldstein and Jacobson, 1988; Singh and Rajamani, 2001; Xu et al., 2012). Studies of Tripathi et al. (2007) and Ramesh et al. (2000) discuss the fractionation of REE on a local scale and considered that episode of fluvial processes leads to the homogenization of REE and enhance its use as a provenance indicator.

Goldstein and Jacobsen (1988); Sholkovitz (1992); Dupre et al. (1996); Gaillardet et al. (1999); Ramesh et al. (2000); Singh and Rajamani (2001); Rengarajan and Sarin (2004); Tripathi et al. (2007); Xu et al. (2012) have applied REEs to determine the source of the fluvial sediments in different river systems such as the Amazon, the Mekong and the Ganges. Normalization to the UCC (Upper Continental Crust) or NASC (Normalized American Shale Composites) is a widely accepted method of comparing the REEs content of various geological materials (Taylor and McLennan, 1985). The concentration of REEs varies markedly with rock type and source area. As shown by many studies, the river sediments are generally enriched in normalized LREE than the HREE (Byrne and Kim, 1990; Yang et al., 2002; Yang et al., 2004; Xu et al., 2012; Li et al., 2013).

Goldstein and Jacobson (1988) measured REE flux of the Amazon, Indus, Mississippi, Murray-Darling, and Ohio rivers and suggest that pH is a major factor controlling the concentration of REEs in a dissolved load. The dissolved load was found to be mostly enriched in HREE and suspended sediment flux was found to be LREE enriched. Yang et al. (2002) characterized the sediments of the Changjiang and Huanghe Rivers and observed that REEs are enriched in heavy minerals and Fe-Mn oxide phase account for the major fraction of leachable REEs. Shouye et al. (2003) based on the fractionation indices $(La/Yb)_{UCC}$ and $(Gd/Yb)_{UCC}$, $(La/Sc)_{UCC}$ and $(Th/Sc)_{UCC}$ distinguished the provenance of suspended sediments of the Chinese and Korean river at the mouth of the Yellow sea. Xu et al. (2009) studied the bottom sediments of the Korean and Chinese rivers along the Yellow sea. REE proxies were calculated and marked differently for both the river systems. Compared to the Korean rivers, Chinese rivers showed positive Eu anomaly. REEs proxies such as ΣLREE/ΣHREE ratios, $(La/Yb)_{UCC}$ and $(Gd/Yb)_{UCC}$ proved as a useful tool for diagnosing the provenance of sediment at the mouth of the basin. Before these comparative studies, it was considered that Chinese rivers (Changjiang, Huanghe) are the major supplier of sediment depositing in the Yellow sea. But the importance of the Korean river in supplying the sediment was only highlighted by the employment of REEs as a tracer (Liu et al., 2009). Yan et al. (2012) studied the REEs concentration of different Bays situated along the South East China Sea, the REE concentration

was found to be quite similar in a particular Bay but vary considerably along the Bays. The negative Eu anomaly and LREE/HREE >1 indicated the terrigenous source of the sediment, pointing that the sediment along the South China Sea is basically derived from the river system rather than the marine erosion. Li et al. (2013) found that in comparison to the Chinese rivers, the Taiwanese river systems are enriched in REEs concentration. The ratios $(La/Lu)_{UCC}$, $(Gd/Lu)_{UCC}$, $(La/Yb)_{UCC}$ and $(Gd/Yb)_{UCC}$ indicate the fractionation within LREE and HREE and aided in distinguishing the source of the Chinese and Taiwanese rivers.

REEs have also been applied for inferring the source of Himalayan river sediments such as the Ganga, Brahmaputra, Indus, and the Yamuna. Tripathi and Rajamani (1999) and Tripathi et al. (2007) studied the Upper Ganga Plain sediments and found REEs enrichment in the heavy minerals fraction of the sediments. They inferred that Ganga alluvial sediments are predominantly derived from the Higher Himalayan Crystalline and the Tertiary Sub-Himalayan sediments. Rengarajan and Sarin (2004) studied the distribution of REEs in the Yamuna and Chambal River sediments and spot the enrichment of HREE and positive Eu anomaly in the sediments of the Yamuna River. The plagioclase feldspar and its weathering products were considered as a cause of positive Eu anomaly in the dissolved and sediment load. Ramesh et al. (2000) traced the source of surface sediments of the Yamuna, Brahmaputra, Jamuna, Padma and Meghna River and inferred that composition of sediment is influenced by the change in lithology and the confluence with tributaries as pointed by the large fluctuation in the La/Yb ratio. The LREE enrichment and Eu anomaly >1 in the sediments reflect the prevalence of intense silicate weathering in the Himalayan terrain. Though most of the provenance based studies were carried out on the Ganga sediments, but none of them mentions about the provenance of sediments transported by the headwater streams (upstream of Devprayag, the Alaknanda, and Bhagirathi Rivers). Therefore, the aim of this study is to estimate the concentration of REEs, studying the fractionation pattern and identification of the source rock of the suspended sediments carried by the Alaknanda River and its tributaries.

2.4. CLAY MINERALOGY

The composition of river sediments result from the weathering activities and thus shed light on geochemical processes, energy conditions, weathering regime, physical conditions, and source bedrock. The bedrock of the basin exerts a strong control on the leaching rate of sediments. To attain chemical equilibrium, most of the unstable minerals (on the earth's surface) break down involving chemical weathering processes (Nesbitt and Young, 1984, 1996). Goldich (1938) explained the weathering stability of minerals, whereby minerals formed

at high temperatures such as olivine and pyroxenes are susceptible to chemical weathering than those formed at lower temperatures such as quartz. Thus, due to chemical weathering reaction, unstable minerals are leached out of the sediment and in the process of transportation sediment becomes enriched with the stable minerals such as quartz. Nesbitt and Young (1984) predicted the weathering trends of volcanic and plutonic rocks and suggested that clay minerals are specific to rock type, e.g. kaolinite is formed by the weathering of feldspar while smectite by the weathering of ferromagnesium minerals. Thus, depending on the basin geology, topography and climate, clay mineral assemblages become specific to the river basin (Hillier, 1995; Huyghe et al., 2011).

Hillier (1995) specified the origin of authigenic clay minerals to in-situ precipitation out of pore fluids, reactions of amorphous material, or to the transformation of precursor minerals such as feldspars and mica or other clay minerals or to the diagenetic processes. Gibbs (1967); Irion (1983); Martinelli et al. (1993) and Guyot et al. (2007) observed changes in the clay mineral assemblage during the course of transportation of sediments downstream. Irion (1983) observed that in the Amazon River, the amount of chlorite decreases and the amount of smectite and kaolinite increases as the river moves downstream. Griffin et al. (1968) established that geography and climate have an impact on the distribution of clay minerals; chlorite is a dominant mineral reported from the polar region where mechanical weathering is high, the presence of illite reflects continental input, smectite points to the weathering of volcanic regions and kaolinite is a dominant clay mineral reported in a region of intense chemical weathering. Gibbs (1967) while studying the river sediments of the Amazon River and its tributaries found that tropical rivers generally, carry high kaolinite and low smectite and chlorite+illite content. Gibbs (1967); Johnsson and Meade (1990); Stanley and Wingerath (1996); Hemming et al. (1998) and Guyot et al. (2007) observed that kaolinite forms in the region characterized by intense chemical weathering (in a tropical environment with high precipitation), whereas smectite attributes to the intermediate weathering intensity in the badly drained area. Based on the clay mineral assemblages and value of illite indices of the detrital sediment, He et al. (2013) classified the Yangtze River basin into three parts, upper stream where the rate of physical weathering is quite high and low and middle stream where chemical weathering rates are low.

Clay mineralogy study of Indian rivers was first attempted by Subramanian (1980). He studied the clay mineralogy of major Indian River systems such as Mahanadi, Krishna, Godavari, Kaveri, Narmada, Tapti and the Himalayan Rivers such as the Ganga and the Brahmaputra. The important finding was that the Himalayan Rivers are characterized by the

presence of high amount of illite followed by kaolinite, chlorite, and absence of mixed clays or montmorillonites, whereas, peninsular rivers are characterized by ample of montmorillonite. Chakrapani (2005) observed that mica dominates along the entire stretch of the Ganga River. Dalai et al. (2004) observed that similar to the Ganga River, Yamuna River sediments (a major tributary of the Ganga River) are also enriched in illite and kaolinite and along with low Al concentration affirms that low intensity of chemical weathering prevails in the Yamuna River basin. Singh et al. (2006) observed that vermiculite is a dominant clay mineral present in the Brahmaputra River and inferred that less intense chemical erosion rate prevails in the Brahmaputra River in comparison to the Ganga River.

The most popular technique for phase identification of clay minerals is the X-Ray Powder Diffraction (Powder-XRD). XRD works on the principle of diffraction and Bragg's Law. XRD is considered as the most accurate technique in terms of phase identification and quantification of clay minerals. Due to changes in the composition of sediments during erosion and weathering, Martinelli et al. (1993); Datta and Subramanian (1997); Dalai et al. (2004); Singh (2010); Liu et al. (2007); Garzanti et al. (2011) recommended the use of multiple indices such as major oxides, trace elements and clay mineral composition of sediments for the quantification of weathering intensity in the river basin. In the present work, clay mineral assemblages were identified and quantified in the channel sediment samples of the pre-monsoon and post-monsoon season. However, apart from clay minerals, the major oxide composition of the channel sediments was also employed for quantifying the chemical weathering rates in the Alaknanda River basin.

2.5. ENVIRONMENTAL MAGNETISM AND HEAVY MINERALS

Environmental Magnetism: Mineral magnetism offers an opportunity to detect the presence of ferromagnetic, ferrimagnetic, diamagnetic and paramagnetic minerals in soil and sediments (Thompson and Oldfield, 1986; Maher et al. 1994; Dearing et al., 1996, Maher and Thompson., 1999; Maher et al., 2002; Booth et al., 2005; Sangode et al., 2007; Hatfield and Maher, 2009; Porate et al., 2012). Studies of Oldfield et al. (1979); Thompson and Oldfied (1986); Maher et al. (1994); Maher and Thompson (1999); Walden et al. (1997); Maher et al. (2002); Booth et al. (2005); Sangode et al. (2007); Hatfield and Maher (2009); Porate et al. (2012) show that mineral magnetism can be applied to determine the provenance, sediment mixing, and paleo-environment conditions in the river basin. As magnetic properties of anthropogenically produced materials are distinct, mineral magnetism also offers an opportunity to study the pollution assessment and environmental degradation (Oldfield et al.,

1985; Dekkers, 1997; Liu et al., 1995; and Dearing et al., 1996). Working with mineral magnetic techniques is quite advantageous, as it's a fast and non-destructive method of analysis that requires minimum sample preparation

The magnetic parameters that can reveal the information regarding the magnetic mineralogy, its concentration and grain size include the magnetic susceptibility (χ), anhysteretic remanent magnetisation (ARM), and induced remanent magnetisation (IRM) (Oldfield et al., 1979; Thompson and Oldfied, 1986; Caitcheon, 1993; Dekkers, 1997; Maher and Thompson, 1999; Jenkins et al., 2002; Evan and Heller, 2003; Booth et al., 2005; Sangode et al., 2007; Franke et al., 2009; Horng and Huh, 2011; Sherriff, 2014; Kulkarni et al., 2014).

In the fluvial system, magnetic properties of sediments are conserved within a spatial and temporal scale (Maher et al., 1994; Catitcheon, 1998; Hatfield and Maher, 2009). Previous studies reveal that even if magnetic minerals are <2% of the sediment composition, they show their signatures, and hence magnetic characterization of sediments can be carried out. In the quaternary sediments, magnetite, titanomagnetite, maghemite, hematite, and goethite occur commonly along with a high proportion of diamagnetic and paramagnetic minerals (Sangode et al., 2007). The magnetic susceptibility (χ) is considered as an important parameter that traces the concentration of ferrimagnetic minerals present in a sample. In the absence of ferrimagnetic minerals, χ is also sensitive to anti-ferromagnetic and paramagnetic minerals (Oldfield et al., 1985; Thompson and Oldfield, 1986; Dekkers, 1997; Walden et al., 1997; Jenkins et al., 2002; Robertson et al., 2003).

Magnetic characterization helps in matching the source and sink. Walling et al. (1979) and Peart and Walling (1986) were among the first ones who applied mineral magnetic proxies as a potential technique for determining the source of fluvial sediments by relating the magnetic properties of suspended sediments and soil. Based on their contribution, the quantitative mineral magnetism technique has evolved as a cost and time effective tool for the mineral characterization (Hatfield and Maher, 2009). Caitcheon (1993); Walling and Woodward (1995); Collins et al. (1998) stated that the spatial variation of magnetic parameters is controlled by the change in lithology or soil and remobilization and change in hydrological parameters. Walling et al. (1999) applied mineral magnetic properties for provenance determination of the River Ouse, Yorkshire, UK along with radionuclide ^{137}Cs, ^{226}Ra, and ^{210}Pb, their results were able to quantify the contribution from tributaries and the local lithology. Robertson et al. (2003) characterized urban sediment samples around the roads of Manchester, U.K. A combined approach of calculating the magnetic parameters and estimating heavy metal concentration was successful in determining the sediment source and pollution

level. Sangode et al. (2001, 2007) studied the Western Bengal fan sediments and found that weathering of the Deccan Plateau by the Godavari and Krishna river system is a major source of Western Bengal fan sediments. Kulkarni et al. (2014) characterized the magnetic mineral assemblage of bed load and flood plain sediments of River Godavari (based on magnetic indices such as $\chi_{fd\%}$, χ_{ARM}, SIRM, S-ratio and $B_{0(CR)}$ and clay mineralogy) and inferred Deccan basalt to be the appropriate source.

Environmental magnetism has not been widely applied for the Himalayan Rivers. In the present study, the magnetic mineral assemblages of the Alaknanda River and its tributaries using environmental magnetic parameters were characterized.

Heavy Minerals: Heavy minerals (minerals having a specific gravity >2.9 g/cm^3) have been successfully used as a provenance indicator for both the consolidated and unconsolidated sediments. Based on optical studies, on the basis of transparency, heavy minerals have been classified as, opaque and non-opaque. Based on the resistance to weathering, non-opaque minerals are divided into ultra-stable (e.g. zircon, rutile, and tourmaline) and metastable minerals (e.g., epidote, garnet, hornblende, and olivine). The high specific gravity provides mechanical resistance to the heavy minerals from weathering. Heavy minerals get deposited and sorted according to specific gravity, size, and shape and thus form heavy mineral suites in the sediments that are specific from the source to the depositional environment (Fletcher and Loh, 1996). Morton and Hallsworth (1999) rank heavy mineral according to their physical stability. According to Morton et al. (1992) and Morton and Hallsworth (1994, 1999), a list of factors may affect the heavy mineral assemblages in river transportation and include weathering intensity, climatic conditions, sediment supply, mechanical abrasion during the transport, physical sorting and the diagenetic processes during burial. X-ray Diffraction is the most precise and rapid tool to identify the heavy minerals present in sediments. Since the dissolution rate in the mountainous region is quite high, interpreting provenance based on just the heavy minerals can be vague. The present study identified heavy minerals in the channel sediments of the Alaknanda River along with other fingerprinting indices (major oxides and environmental magnetism) to identify the source bedrocks.

2.6. TOTAL ORGANIC CARBON (TOC) FLUX

The carbon biogeochemical cycle involves interaction between the living thing and the abiotic environment. Photosynthesis is a major process that consumes atmospheric CO_2. After silicate weathering process, the transportation and deposition of the organic carbon (OC) by the fluvial system represent the second largest atmospheric CO_2 sink (Galy et al., 2007b).

Total organic carbon (TOC) carried by the river comprises of dissolved organic carbon (DOC) and particulate organic carbon (POC) (i.e. TOC = DOC+POC). Sources of OC in a river channel can be autochthonous (generated within the channel) or allochthonous (within the watershed). Decomposition of living beings (plants, animals, and microbes) is a natural source of organic carbon (OC) but in most of the urban river basins, anthropogenic waste can have a much bigger share (Demlie and Wohnlich, 2006). In terms of origin, OC is of two types, recent and the fossilized. C_3 and C_4 plants are the major sources of recent OC, whereas, fossilized carbon (stored in rocks) range from many thousands to millions of years in age. C_3 and C_4 vegetation reflects the dissimilarity in the contribution of organic matter to the fluvial system. $\delta^{13}C$ is used to evaluate the source of recent OC (whether it is derived from the C_3 or C_4 plants), while, $\Delta^{14}C$ tell the age of the fossilized carbon and help in localizing the geological formation. Using the global data, Raymond et al. (2007) and Evans et al. (2007) proved that DOC carried by the river systems is mostly recent in origin, and thus more than the fossilized carbon it's the recent OC that exhibits control on the carbon cycle.

Battin (2008) observed the role of the fluvial network in the transportation, transformation and outgassing of organic carbon (OC) to the atmosphere. Annually, fluvial network transport, transform and store ~2 Pg of terrigenous organic carbon. The study of Hayes et al. (1999); Burdige (2005) and Galy et al. (2008) stated that due to the continuous metabolism of OC in the fluvial networks, ~70% of riverine organic carbon is returned to the atmosphere. The outgassing from the Amazon basin itself is ~0.3 Pg C $year^{-1}$ (Cole et al., 2007 and Battin, 2008). But the 'Upliftment-Weathering Hypothesis' of Raymo et al. (1988), Raymo and Ruddiman (1992) and supported by Berner and Berner (1996); Gaillardet et al. (1999); Galy and France-Lanord (2001) stated that the higher rate of mechanical as well as chemical weathering of the Himalayan terrain during the Cenozoic period, burial of large masses of OC and its sequestration forces a cooling trend on the global climate. Over the past 15 Mya, the Ganga-Brahmaputra River system has deposited $0.6*10^{12}$ mol organic carbon in the Bay of Bengal that accounts for 15% of the global carbon burial flux. The deposition of OC exerts a negative feedback on the global climate change (France-Lanord and Derry, 1997; Galy et al., 2007b). Ittekkot et al. (1985); Safiullah et al. (1985); Aucour et al. (2006) have documented the concentration and composition of organic matter carried by the Ganga River. Apart from being an important part of the global carbon cycle, OC has a significant role in controlling the chemistry and biology of the river system (Sachse et al., 2005). Wu et al. (2007); Ni et al. (2008) mentioned that DOC in water can increase the solubility of minerals and compounds while POC acts as a carrier of organic chemicals.

Fluvial processes during the course of transportation influence the flux and composition of terrestrial OC. Ittekkot et al. (1985); Keil et al. (1997); Aller et al. (2004) and Wheatcroft et al. (2010) suggest that large amount of terrigenous POC is degraded during transportation and little is preserved in the ocean margins. Meade et al. (1985); Keil et al. (1997); Aucour et al. (2003, 2006) observed that fluvial processes that influence the OC flux of the river include photosynthesis, oxidation, sedimentation-resuspension of particles and desorption-sorption of organic compounds on mineral surfaces. The particle size of sediment also plays an important role in transferring and transportation of OC (Galy et al., 2007b). Warren et al. (2003) and Walling (2005) observed the importance of fine sediments in the transportation of nutrients, contaminants, and pathogens through the fluvial systems. The amount of adsorbed organic matter increases with an increase in the mineral surface area (i.e. directly depending on the concentration of finer sediments) (Keil et al., 1997). Dahm et al. (1981) and Moreira-Turcq et al. (2003) highlighted that discharge is an important parameter that governs both the grain size distribution and the carbon concentration carried by the river.

The $\delta^{13}C$ and $\Delta^{14}C$ studies in the Ganga-Brahmaputra river system by Galy et al. (2007b) highlighted that Himalayan Rivers transport 70-85% of the recent organic matter. Using the $^{13}C/^{12}C$ ratio of OC in modern soils and river sediments, it has been proved that C_3 vegetation is the major source of the recent OC carried by the river Ganga (Aucour et al., 2006; Galy et al., 2007b). Aucour et al. (2006) and Galy et al. (2008) reported low POC from the mountainous tributaries of the Ganga River, namely, Kosi and Narayani (flowing from the Nepal Himalayas) and high POC from the Ganga plains. In the absence of data from the headwater streams, there is a huge gap regarding the source of OC in the Ganga River. The Alaknanda River contributes a high amount of sediment load to the Ganga River. In this study, the focus was on the transport of OC in the mountains (Alaknanda watershed) and flux to the Ganga River. Using temporal data, the study dealt with the role of physical weathering, seasonal changes and hydrodynamics on the OC flux.

CHAPTER 3

STUDY AREA

3.1. Physiography

3.2. Climate

3.3. Geology

3.4. Anthropogenic Impact and Land Use Land Cover Changes

3.5. Socio-Economic Importance

3.6. Environmental Concerns

The Ganga River in its headwater region consists of two perennial streams, the Alaknanda and the Bhagirathi rivers, which confluence at Devprayag to formally initiate the Ganga River. Hydrologically, due to high discharge and large catchment area in comparison to the Bhagirathi River, Alaknanda is considered as a significant upstream of the Ganga River.

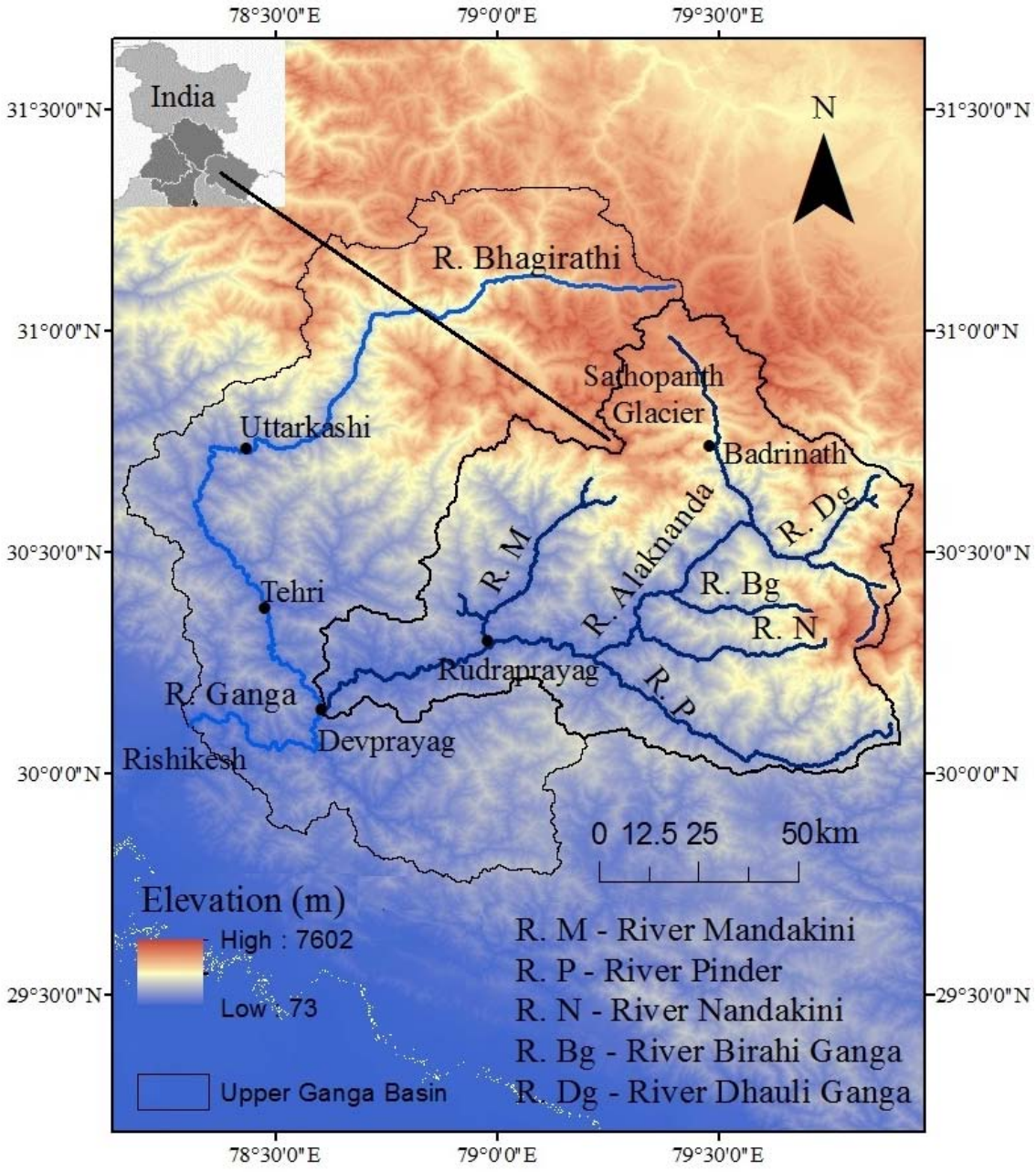

Figure 3.1 Location of the Alaknanda River basin

Alaknanda River flows in the North Western Himalayan region, particularly the Garhwal Himalayas in the state of Uttarakhand, India. The major source of Alaknanda River are the twin glaciers viz. the Bhagirath Kharak and the Sathopanth. After flowing ~200 km from its source to its outlet, at Devprayag, the Alaknanda River confluences with the Bhagirathi River to form

a mega stream known as the Ganga River. Figure 3.1 shows the location of the Alaknanda River with respect to the Upper Ganga Basin (UGB).

3.1 PHYSIOGRAPHY

The geomorphology of the Alaknanda basin is characterized by glaciers, structural hills, gorges, narrow valleys, and terraces. The total catchment area of the Alaknanda basin is 8716.1 km^2 with a high drainage density of 1.1. At Devprayag, the Alaknanda River is of 10^{th} order (calculated according to the Strahler number using spatial analyst tool in the software ARCMAP 10.2). Important tributaries of the Alaknanda River are Dhauli Ganga, Nandakini, Pinder and Mandakini (Fig. 3.1). These tributaries are all perennial and contribute a large amount of sediment and water load to the Alaknanda River. Figure 3.2 shows the sub-catchment areas of the Alaknanda River. Table 3.1 displays the characteristic features of the Alaknanda River and its major tributaries.

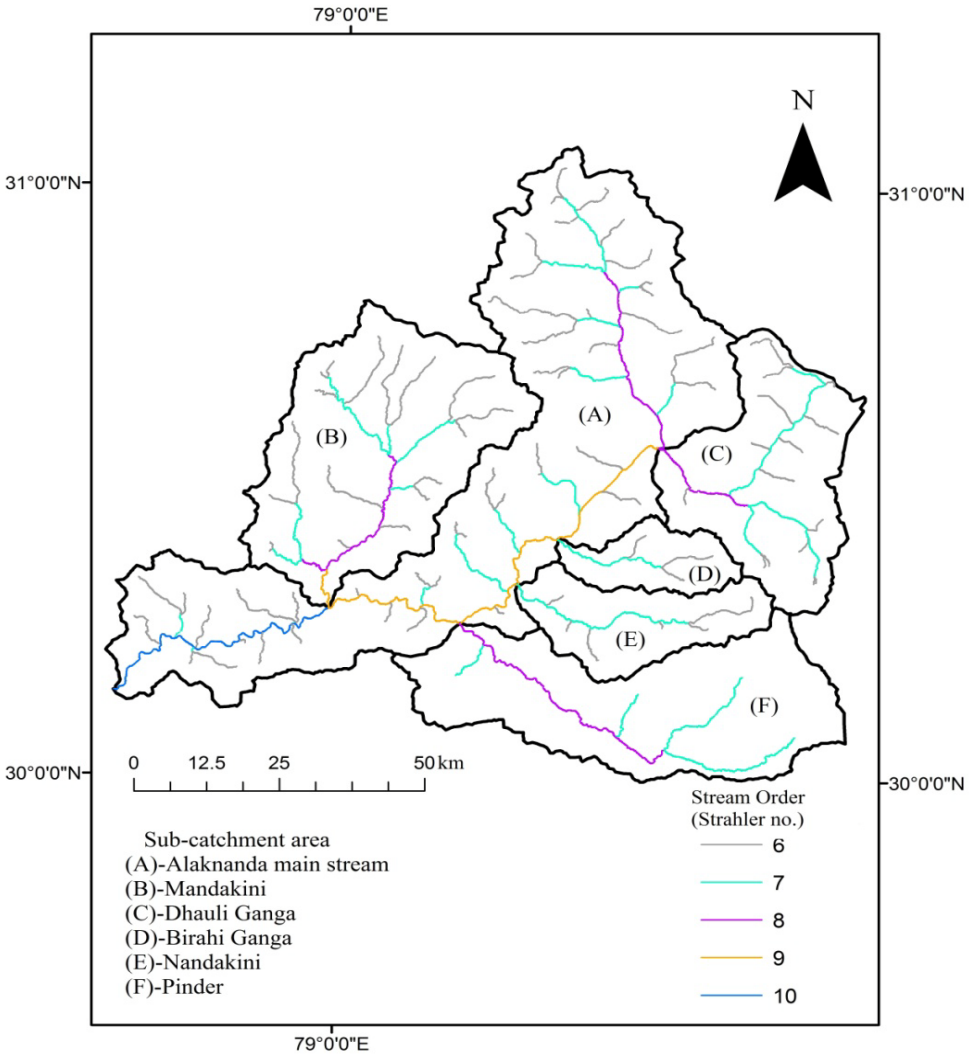

Figure 3.2 Sub-catchment areas of the Alaknanda River basin

Table 3.1 Physiographic characteristics of the Alaknanda River basin estimated using GIS

Basin	Area (km^2)	Basin Relief (m)	Mean Slope (in degrees)	Drainage Density (km^3)
Alaknanda (at Devprayag)	8716	7005	30.8	1.11
Sub-basins				
Dhauli Ganga	1082	5704	33.0	0.87
Birahi Ganga	297	5022	33.6	0.62
Nandakini	547	6034	30.5	0.88
Pinder	1489	5664	29.4	0.88
Mandakini	1645	6121	29.4	0.76

The channel gradient of the Alaknanda River is steep in the upper part of the basin (generally 20 m/km), and become gentler southwards (AHEC, 2011). The unconsolidated quaternary sediments, rock fall, periglacial, glacial and hill slope scree form the part of the river valley slopes. The thickness of these sediments varies from 2-15 m depending on the slope, aspect and bedding planes (AHEC, 2011).

Due to high tectonic activities and heavy monsoon, geomorphology of the basin is quite complex. To better understand the physiography of the basin, it has been divided into two regions:

3.1.1. Higher Himalayas

The mean elevation of the Higher Himalayas is ~6000 m. Some of the highest mountain peaks of the Himalayan Ranges namely, Nanda Devi, Kamet, Trisuli, and Chaukhamba are located in the Alaknanda River basin. According to the climate and geological conditions, the Higher Himalaya is divided into two zones: Inner Himalayas or Tethyan Himalayas or Trans-Himalayas and Outer Himalayas or Higher Himalayan Crystallines.

Tethyan Himalayas/ Trans Himalayan region is a leeward region and is devoid of vegetation. Saraswati, Dhauli Ganga, and Girthi Ganga sub-basins fall in this category. Being a glacial terrain, the Higher Himalayas has a predominant glacial morphology characterized by cirques, moraines, hanging valley and glacial lakes. The Satopanth and the Bhagirath Kharak glaciers which are the source of the Alaknanda River are covered with very thick supraglacial moraine and follow a curvy-linear course. The equilibrium line altitude (ELA) for the Satopanth glacier is located at 4677 m and for the Bhagirath glacier at 4942 m (AHEC, 2011). Outer Himalayas being a part of the windward side receives high monsoon rains and thus has high vegetation in comparison to the Trans Himalayan region.

3.1.2. Lesser Himalayas

The average altitude of the Lesser Himalayas varies from 2000-3500 m. Physiographically, the zone comprises of high to moderate dissected structural hills, steep slopes, deep cut gorges and narrow valleys. Main Central thrust (MCT) and Main Boundary Thrust (MBT) defines the northern and southern limit of this zone. The entrenched meandering, deep gorges and elevated aggradational and degradational terraces report the tectonic upliftment in this part of the basin (Valdiya, 1980; Sati et al., 2007). Sati et al. (2007) observed six levels of aggradational terraces around the Srinagar town. In comparison to the Higher Himalayas, this region supports a sizeable number of population and agricultural activities.

3.2. CLIMATE

The climate in the Alaknanda basin varies from Sub-tropical to Alpine (Sati et al., 2007). Due to the mountainous terrain (characterized by valley and ridge topography), microclimatic conditions prevail in the basin. The temperature in the basin varies both spatially and temporally (season to season and from valley to higher elevated regions). The highest temperature recorded in the Srinagar town is 30° C (in the month of June) and lowest is 0.5° at Tungnath in the month of January (CWC, 2007).

Table 3.2 Mean monthly variation in temperature and rainfall in the Alaknanda basin

Mean monthly temperature (degree) in the Alaknanda basin													
Place	**Altitude (ft)**	**Jan**	**Feb**	**Mar**	**Apr**	**May**	**Jun**	**Jul**	**Aug**	**Sep**	**Oct**	**Nov**	**Dec**
Tungnath	11382	0.5	1	3	6	7	12	12	11	5	4	2	1
Joshimath	6731	2	3	7	11	14	17	18	17	16	10	7	4
Chamoli	4244	8	10	14	19	22	23	21	22	20	17	13	10
Rudraprayag	2276	8	10	14	20	23	24	22	22	21	18	14	10
Srinagar	1939	14	18	20	25	25	30	29	28	25	27	17	5
Mean annual rainfall (mm) in the Alaknanda basin													
Place	**Altitude (ft)**	**Jan**	**Feb**	**Mar**	**Apr**	**May**	**Jun**	**Jul**	**Aug**	**Sep**	**Oct**	**Nov**	**Dec**
Chamoli	4244	58	78	82	43	69	103	290	329	132	44	10	25
Rudraprayag	2276	76	73	85	55	94	218	578	639	236	53	14	30
Pauri-Garhwal	3733	43	33	36	19	38	124	453	444	194	56	7	18

(Compiled based on the data for the year 1901-2002, 2008-2013, provided by the Indian Meteorological Department, IMD)

Table 3.2 and Figure 3.3(a-b) show the variation in mean temperature and rainfall in the Alaknanda basin. Higher ranges are snow covered throughout the year, whereas lower reaches experience severe winter. During the months of June to September, ~75% of rainfall occurs which increase the discharge of the river proportionally (Chakrapani, 2005; CWC, 2007; Singh

and Hasnain, 1998). Basically, during the two months (July and August), rainfall >400 cm occurs. Leeward and windward directions of slope influence the spatial variability of precipitation. Highest rainfall is recorded in Okhimath (1578 mm), whereas lowest rainfall is recorded in the Srinagar town (550 mm) (IMD data). Due to heavy rainfall and narrow valleys, instances of cloud burst, flash floods, riverine floods and landslides are quite common in the Alaknanda basin. The direction of wind flow in the UGB is from North-East to North-West and likewise, the physiography, wind speed in the higher altitudes varies between 120-160 km/hour and decreases to 50-60 km/hour at lower reaches.

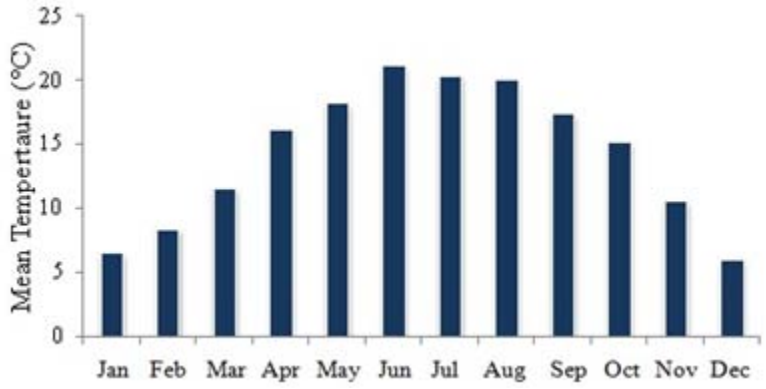

(a)

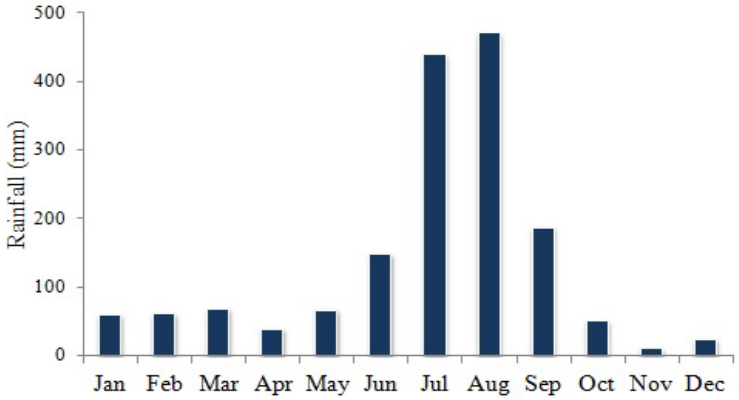

(b)

Figure 3.3 Variation in (a) monthly rainfall, (b) monthly temperature in the Alaknanda basin (based on Indian Meteorological Department data)

3.3. GEOLOGY

The Himalayas are a young and dynamic orogenic belt trending east-west for about 2400 km and having a width span of 325-425 km. The Himalayas from north to south are classified into four distinct geological units viz. Trans-Himalaya or Tethys Himalaya, Greater or Higher Himalaya, Lesser or Lower Himalaya, Sub-Himalaya or Outer Himalaya or Siwaliks. These units are based on tectonic and lithologic discontinuities and are separated by distinct thrust faults (Gansser, 1964, Valdiya, 1980). Figure 3.4 shows Himalayan geological units.

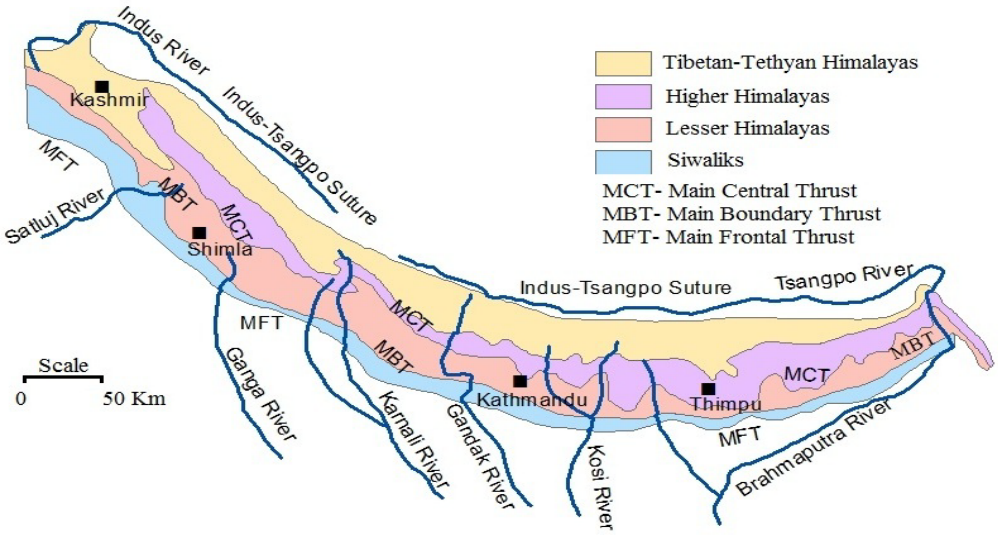

Figure 3.4 Himalayan geological successions (modified Gansser, 1964) (http://www.ranjan.net.np/ranjan/index.php/)

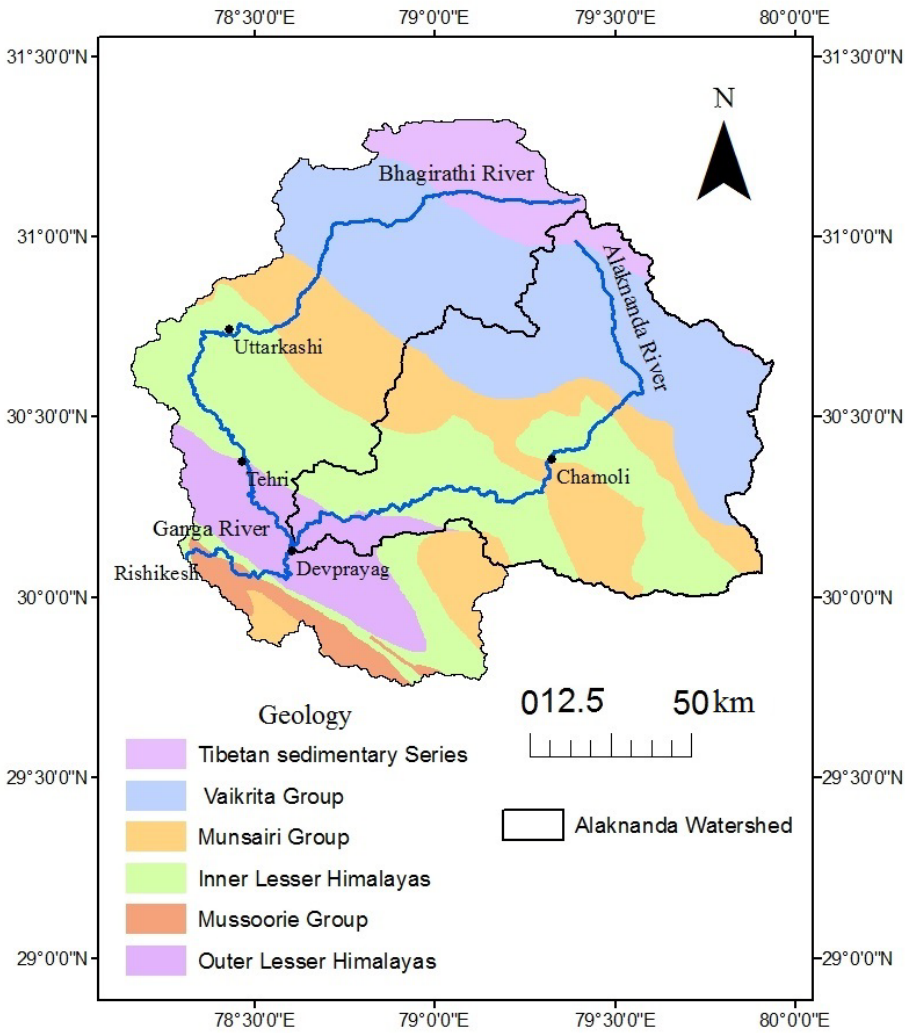

Figure 3.5 Geological map of Upper Ganga Basin, depicting the approximate lithology of Alaknanda basin (modified after Valdiya, 1980; Bickle et al., 2003)

Table 3.3 Lithological succession of the Alaknanda basin (Kumar, 1971, 2005)

Group	Formation	Lithology
Garhwal Group	Granite (1900 Ma and 1600 Ma)	
	Berinag	Quartzites with penecontemporaneous mafic volcanics
	Discontinuity	
	Deoban	Limestone-Dolomite, shale
	Granite (2200-2100 Ma)	
	Uttarkashi	Quartzite with penecontemporaneous mafic volcanic, dolomitic limestone, shale
Higher Himalayan Crystalline Group	Granite (2500 Ma)	
	Badrinath	Garnet-sillimanite-muscovite-kyanite-bearing gneiss, mica schist, migmatite, calc-silicates
	Pandukeshwar	Banded quartzite gneiss, para-amphibolites
	Joshimath	Garnet-mica-schist, sillimanite-kyanite schist
	Bhimgora	White Quartzite
	Ragsi	Kyanite-mica schist, gneiss, para-amphibolite

The Alaknanda River basin comprises of three lithological sequences viz. the Tethyan Sedimentary Sequence in the upper part, the Higher Himalayan Crystallines in the middle and the Lesser Himalayas in the lower part (Valdiya, 1980; Bickle et al., 2003; Kumar, 2005; Shukla et al., 2014). The geological framework of the basin is quite complex. Various names have been given by different geologists to the same succession of rocks at same places. Figure 3.5 shows the geological map of the Upper Ganga Basin (till Rishikesh). Dominantly, the Alaknanda River drains through the Higher Himalayan Crystallines and the Lesser Himalayas.

Heim and Gansser (1939); Valdiya (1980); Gururajan and Choudhuri (1999) divided Higher Himalayan Crystallines into two groups: Munsairi and Vaikrita based on the degree of metamorphism. The Munsairi group comprises of low to medium grade metamorphic rocks mostly dominated by mylonitic gneiss and augen gneiss. The Vaikrita Group is characterized by amphibolite facies (Jain et al., 2013).

In this thesis, the stratigraphic succession proposed by Kumar (2005) has been followed (Table 3.3 and 3.4). The various successions of rocks present throughout the Alaknanda basin are as follows:

3.3.1. Tibetan Sedimentary Sequence

The Tibetan/Tethyan Sedimentary Sequence lies in the north of the Higher Himalayan Crystallines and comprises of a lithological sequence between the late Proterozoic and late Mesozoic age. The sequence of purple shale and limestone, white quartzite with intercalation of purple shale and limestone, sericitic quartzite, grey limestone with intercalation of phyllite comprises the Tibetan Sedimentary Sequence.

3.3.2. Higher Himalayan Crystalline Group

Occurring as a linear zone, Higher Himalayan Crystallines form the oldest crystalline rocks of the Himalayas and comprises of gneisses, schists, amphibolites and migmatites. Following lithological succession constitutes Higher Himalayan Crystallines:

***Ragsi Formation*:** Ragsi schist and gneiss comprises the Ragsi Formation and forms the famous peak of Tungnath (in the Mandakini valleys). In Nagol Gad, it is in contact with the Garhwal Group along the Main Central Thrust (MCT) and is overlain by the Bhimgora Quartzite. In the Helang valley, Ragsi Formation is associated with para-amphibolite/marble and gneisses. In the Pindar River basin, the Ragsi Formation and the overlying Bhimgora Quartzite are cut-off by the MCT.

***Bhimgora Quartzite*:** White coloured, fine grained recrystallized quartzite comprises the Bhimgora Quartzite. The formation occurs along the Chamoli-Okhimath road and near Tapoban in the Dhauliganga sub-catchment area. In the Alaknanda valley, associated with quartzite are chlorite phyllites. In the Mandakini valley, it is exposed as a thin band in the north of Kalimath and continues westward to the south of Sonprayag.

***Joshimath Formation*:** Joshimath Formation comprises of an interbedded sequence of garnet mica schist, staurolite-kyanite schist, sericite quartzite, and amphiobolite associated with coarse-grained biotite augen-gneiss.

***Pandukeshwar Formation*:** Pandukeshwar Formation comprises of regularly bedded quartzite/banded quartzitic gneisses in which sedimentary structures such as cross bedding are preserved. Interbedded with quartzitic gneisses is garnet-biotite schist.

***Badrinath Formation*:** The formation is well exposed between the Hanuman Chatti and Badrinath in the Alaknanda valley. It comprises of garnet, sillimanite, muscovite and kyanite bearing gneiss, mica schist, migmatites, and garnet amphibolites intruded by leucogranite and pegmatite. In Dhauliganga sub-basin, Badrinath Formation is well exposed around Kosa in association with quartzitic gneiss.

3.3.3. Lesser Himalayas

Inner Lesser Himalayas (Garhwal Group)

It comprises of a thick succession of low grade metasediments made up of quartzite with penecontemporaneous metabasics and carbonate rocks lying between MCT in the north and the Main Boundary Fault (MBF-2) in the south. Acid and basic igneous rocks intrude the rocks of the Garhwal Group. The Garhwal group is subdivided into four formations (Table 3.4). The detail description is as follows:

***Uttarkashi Formation*:** It is the oldest group of rocks exposed in anticlinal cores in the Bhagirathi valley around Uttarkashi. The Uttarkashi Formation is divided into three members, viz. the Netala quartzite, Dhanari slate and Khattukhal members, in ascending order. However, this formation is not encountered in the Alaknanda basin.

***Rautgara Formation*:** Rautgara Formation comprises of massive, cream coloured, purplish and brownish fine grained quartzite interbedded with purple green slate and calcareous phyllite. In the Alaknanda valley, it is made up of alternating bands of quartzite and metavolcanic. It is subdivided into five members, namely, Dhari metavolcanics, Haryali quartzite, Karnaprayag metavolcanics, Nagnath quartzite and Bhikuna metavolcanics.

***Deoban Formation*:** It is essentially made up of carbonates, conformably overlying the Rautgara Formation and is overlain by the Berinag Formation. In the Alaknanda basin, it is exposed in the form of an anticline and is known as the Calc-zone of Chamoli. It is subdivided into five members, Simgad member, Tejam dolomite, Naulara phyllite, Balgad dolomite and Patet slate.

***Berinag Formation*:** Lithologically, it is similar to the Rautgara Formation and comprises of a thick succession of quartzite with penecontemporaneous mafic metavolcanics. It distinguishes from Rautgara Formation in having a lower number of interbedded volcanic flows. The Berinag Formation is divided into the Nawagoan member at the base and the Hudoli member at the top.

Outer Lesser Himalayas (Jaunsar Group)

This Group consists of undifferentiated Mandhali-Chandpur-Nagthat Formations characterized by purple grey quartzites, grits, and thinly bedded limestones phyllite along with lenticular greywacke, purple green quartzite, grit and conglomerates (Valdiya, 1980). Downstream of Devprayag (around Rishikesh), rocks of the Mussoorie Group (Blaini, Krol and Tal Formations) comprises of conglomerates, limestone, dolomites, shale and quartzites.

Table 3.4 Lithological succession of the Garhwal group (adapter from Kumar, 2005)

Formation	Member	Lithology
Berinag	Hudoli Nawagaon	Thick bedded massive quartzite, quartzitic phyllites with intraformational conglomerates with phyllitic partings with mafic volcanics
Deoban	Patet Slate	Black carbonaceous slate/phyllite, bluish grey limestone with bands of magnesite and talc-schist
	Balgad Dolomite	Massive dolomite with limestone and talc-chlorite schist
	Naulara Phyllites	Black carbonaceous phyllite and green slate
	Tejam Dolomite	Dolomite, dolomitic limestones with talc-sericite schist
	Simgad Member	Purple quartz predominate siltstone and purple phyllite and calcareous phyllites and dolomites
Rautgara	Bheekuna Metavolcanics	Mafic amygdaloidal lava altered to hornblende-actinolite-chlorite phyllite with veins of epidote and tourmaline
	Nagnath Quartzite	Interbedded fine grained quartzite and phyllite
	Karnaprayag Volcanics	Mafic spilitic lava, intertrappean purple phyllite
	Haryali Quartzite	Quartzites with thin bedded phyllite and lenticular dolomite/limestone
	Dhari Volcanics	Mafic amygdaloidal lava flows with phyllites and bands of quartzites
Uttarkashi	Khattukhal	Grayish black to grayish blue limestone and dolomite with thinly bedded grey slate
	Dhaneri Slate	Banded grey, green purple slate interbedded with quartzites
	Netala Member	Current bedded quartzites and interbedded slate with minor lenses of limestone

3.3.4. Structural Setup

Main Central Thrust (MCT) and the North Almora Thrust (NAT) are the main structural discontinuities running through the Alaknanda Basin.

***Main Central Thrust (MCT)*:** The Lesser Himalayan rocks are separated from the Higher Himalayan rocks by the MCT. On the basis of metamorphic grades, the Higher Himalayan Crystallines are divided into three parts, namely, Lower, Middle and Upper Crystallines (Purohit et al., 1990). The Lower Crystallines lies in close contact with MCT and constitute low grade metamorphic rocks such as chlorite-schist, schistose quartzite, biotite-schist and mylonitic migmatites. The Middle Crystallines comprises of gneissic and banded migmatites. The Upper Crystalline rocks are represented by medium to high grade metamorphic rocks such as kyanite schist, garnetiferous-mica schist and biotite gneisses (Valdiya, 1980).

***North Almora Thrust (NAT)*:** The North Almora Thrust is a high angle 45-70° WNW-ESE to NW-SE trending tectonic plane which separates the Garhwal Group (the Inner Lesser Himalaya) in the north from the Jaunsar and Dudatoli Groups of the Outer Lesser Himalaya in the south. In general, it dips towards the south in the eastern part, but at places, it is vertical to sub-vertical dipping on either side. It is locally referred as the Srinagar Thrust in the Alaknanda valley or as the Dharasu Thrust in the Bhagirathi valley.

***Alaknanda Fault*:** It is a major fault mapped in the Alaknanda valley extending from the south of the Nandprayag in the east to beyond Chirpatiyakhal in the west. It continues northwestward and runs almost parallel to the NAT. However, it appears as the offset MCT in the Bhagirathi valley.

***Cross-faults*:** There are a number of cross faults that trend NS or NNE-SSW. Of these, the Martoli Fault is north-south trending major cross-fault. It is present near Niti Pass and continues beyond into Tibet, in the north. Continuing southwards, it has been mapped in the Girthi valley, near Barmatiya. Further, in the south, it is traceable to the Rishiganga valley and beyond within the Higher Himalayan Crystalline Group.

3.4. ANTHROPOGENIC IMPACT AND LAND USE LAND COVER CHANGES

The land use land cover map of the year 2011 of the Alaknanda basin shows that forest cover ~60% of the total land area, followed by glaciers and agricultural land. The average population density in the catchment area is ~117.5 person/km^2 (calculated using the data of Census, 2011 http://www.census2011.co.in), majorly concentrated in the lower part of the basin. In recent years, the rapid construction and development of roads, dams, and reservoirs in the Alaknanda basin have resulted in the shrinkage of glacial and forest cover and an unusual land cover changes in the basin. Figure 3.6 and Table 3.5 shows the change in the areal extent of land cover classes during the period of 6 years (year 2005-2011).

The unscientific constructions in the basin have resulted in natural disasters such as landslides, rock fall, and floods. The floods in the year 2013 in this part of Uttarakhand state (often called as Himalayan Tsunami) have questioned the anthropogenic modifications going on the river channels (dams and reservoir construction for the hydropower generation and habitation on the river terraces and near the flood plains).

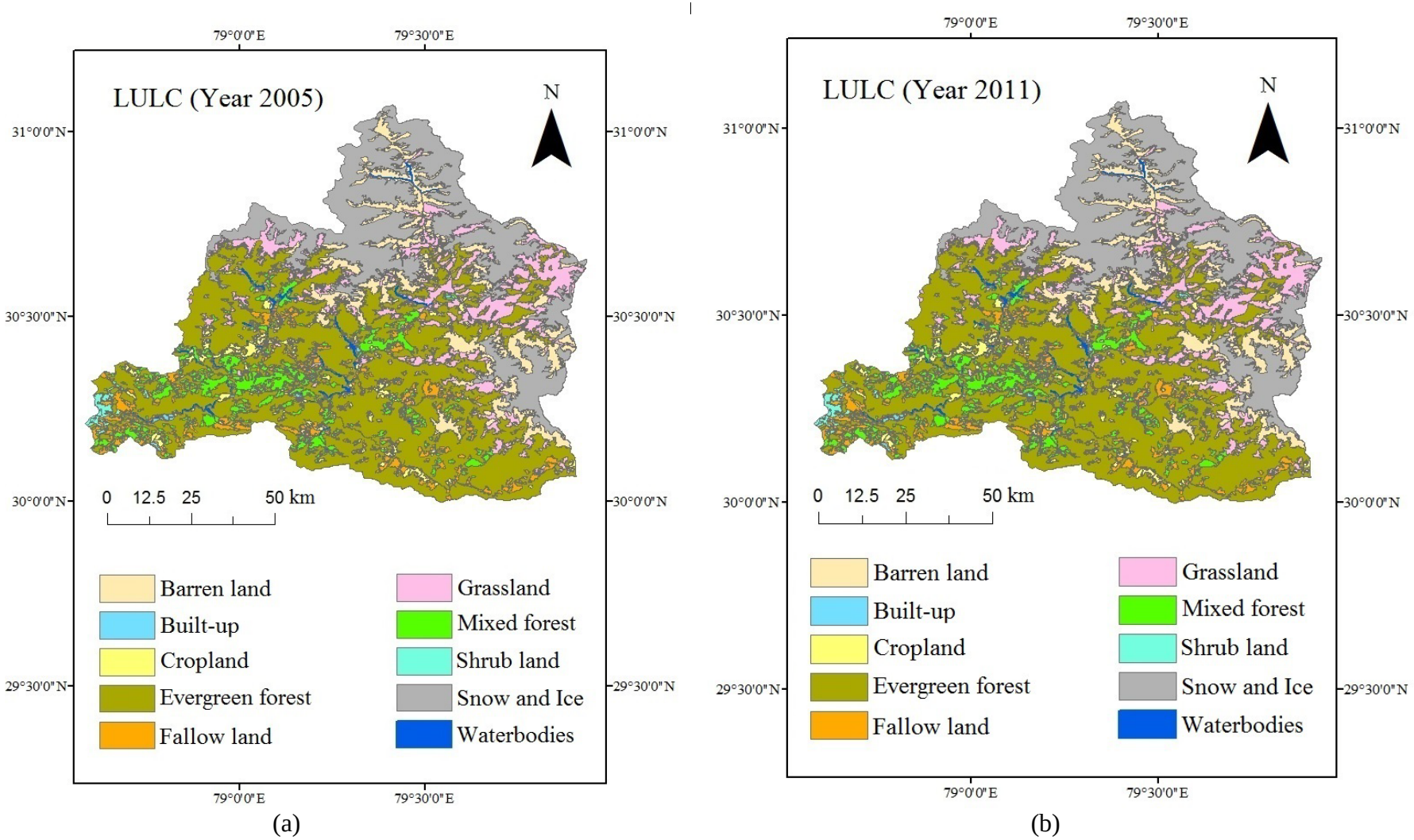

Figure 3.6 Land use land cover changes in the Alaknanda basin (a) LULC map of the year 2005; (b) LULC map of the year 2011 (BHUVAN thematic layers, NRSC, India)

Table 3.5 Change in areal extent of LULC classes in the Alaknanda basin (Year 2005-2011)

LULC class	Year 2005 Area (km^2)	Year 2011 Area (km^2)	% Change in area
Barren land	794.9	829.7	4.4%
Built-up	9.3	16.5	77.9%
Cropland	202.9	214.8	5.9%
Evergreen forest	3843.2	3849.6	0.2%
Fallow land	397.1	373.4	-6.0%
Grassland	899.8	909.1	1.0%
Mixed forest	575.4	565.9	-1.7%
Shrub land	40.4	44.3	9.7%
Snow and Ice	1903.6	1856.2	-2.5%
Water bodies	49.4	56.6	14.5%
Total	8716.1	8716.1	

Studies of Barnard et al. (2001), Wasson (2003) and Sati et al. (2011) discuss the anthropogenic disturbances in the Alaknanda valley. Sati et al. (2011) observed that the majority of landslides in the year 2010 have occurred around the areas where construction and widening of roads was going on without geological consideration. In the future, the changes in land use pattern may affect the landscape processes and dynamics of erosion. Morin et al. (2015) showed that anthropogenic impacts can influence the sediment transportation pathway and modify the sediment transportation equilibrium and primary productivity of the basin.

3.5. SOCIO-ECONOMIC IMPORTANCE

The Alaknanda-Bhagirathi basin has a large potential for hydropower generation. Table 3.6 shows the major hydropower projects engaged in the Alaknanda basin. The estimated hydroelectric power potential of the UGB is ~20,711 MW. According to SANDRP (South Asian Network on Dams, Rivers and People), upto Devprayag, more than 130 major hydropower projects are proposed to be built in the Alaknanda-Bhagirathi basin. Since, Himalayas are tectonically active (simulated by the frequent occurrence of earthquakes and massive landslides) and receives heavy monsoon each year, the sustainability of hydropower projects in this part of the Himalayas are highly questionable and disputed among the scientific community.

In terms of tourism, many Hindu and Sikh ancient temples are located in the basin. Every year, millions of Hindus travel to pilgrims such as Badrinath, Kedarnath, Hemkund Sahib, Nanda Devi and Devprayag during the so called ‘Chardham Yatra’ season. This Yatra is a major source of income for the local people. The Alaknanda basin is also known for its

beautiful Himalayan scenery. Two UNESCO World Heritage sites are present in the Alaknanda basin viz. the Nanda Devi Wildlife Sanctuary and the Valley of Flower National Park.

Table 3.6 Major hydropower projects in the Alaknanda basin (Source: Sati, 2009)

Hydropower Projects	River Valley	Capacity (MW)	Current Status
Tapovan-Vishnugad	Dhauli Ganga	520	Under Construction
Singoli-Batwadi	Mandakini	90	Under Construction
Srinagar	Alaknanda	300	Under Construction
Vishnuprayag	Alaknanda	400	Existing
Lata-Tapowan	Dhauli Ganga	162	Under Construction
Kotli Bhel IB	Alaknanda	320	Under Construction
Total Hydropower Generation		**455.45**	

3.6. ENVIRONMENTAL CONCERNS

Globally, it is observed that intense land use changes occurred due to human activities rather than natural processes (Lunetta et al. 2002). After the disastrous floods in the year 2010 and 2013 in the Upper Ganga basin, the construction of dams, reservoirs, and roads in the fragile environment of the Himalayas became the controversial topic in India. With this regard, in the year 2013, due to environmental concerns, the Supreme Court of India ordered to stop the constructions of all dams in the Alaknanda basin until the scientific community assurance.

During the present research, only two dams were operating on the Alaknanda River, one is Vishnuprayag Hydropower at Lambagad and other in the construction phase (a 300MW Srinagar Hydropower project) at Srinagar. However, in future the Government plans to build >130 dams in the Upper Ganga Basin (Alaknanda and Bhagirathi basin).

Studies of Barnard et al. (2001); Wasson (2003) and Sati et al. (2011) mentioned that anthropogenic activities are disturbing the stability of slopes in the Alaknanda-Bhagirathi basin through road, tunnels, dams and reservoir constructions. Sati et al. (2011) observed that the maximum number of landslides in the year 2010 was witnessed along the National Highway-58 where road widening work was in progress, mostly concentrated between the Alaknanda Fault (AF) and Saknidhar Thrust (ST). The muck generated from the construction and excavation, generally increases the turbidity of the river water and influences the natural flow and geochemistry of the river Alaknanda (Valdiya, 2014).

CHAPTER 4

METHODOLOGY

4.1. Sampling and Field Work

4.2. Laboratory Analysis

4.2.1. Sediment Yield and Controlling Factors

4.2.2. Particle Size Distribution

4.2.3. Major Oxides Composition

4.2.4. Rare Earth Elements (REEs)

4.2.5. Clay Mineralogy

4.2.6. Environmental Magnetism and Heavy Minerals

4.2.7. Total Organic Carbon (TOC)

4.2.8. Principal Component Analysis (PCA)

4.1.SAMPLING AND FIELD WORK

Climate has a huge impact on the geochemistry of the river. Three prominent seasons namely Pre-monsoon (February to May), Monsoon (June-September) and Post-monsoon (October to January) prevails in the Ganga basin. According to Chakrapani and Saini (2009), there exists a huge temporal variability and the Alaknanda River carries ~75% of its total annual sediment load during the monsoon months. Therefore, for better representation of samples of the Alaknanda River, seasonal sampling was conducted during the months of October, 2012 (during the last week of October), March, 2014 (during the second week of March) and August, 2014 (during the second week of August). The location of sampling sites is shown in Figure 4.1 and Table 4.1. In all the three seasons, sampling sites were approximately the same; though in sampling-I (Post-monsoon season, October 2012) number of sample collected were less.

Samples were collected from Govindghat (~42 km from the Sathopanth Glacier) to Devprayag (the mouth of the watershed). In addition to the Alaknanda River, samples were also collected from the major tributaries. One representative sample was collected each from the Dhauli Ganga, Birahi Ganga, Nandakini, Pinder and Mandakini River at the exit of their respective watersheds, approximately 1-3 km before their confluence with the Alaknanda River. To find the influence of geochemistry of the Alaknanda River on the Ganga River, an additional sample was collected from the Bhagirathi River and two samples were collected from the Ganga River, one at Devprayag and another at the Rishikesh.

During the sampling, 5 liters of water samples from the banks of the flowing river part and ~3-4 kg freshly deposited channel sediment samples were collected. Efforts were made to collect the samples from 1-2 m depth and where the flow was good. Water samples were collected in poly-propylene bottles, which were rinsed with 5% HCl and distilled water, 24 hours prior to the sampling. At the sampling site, before the sample collection, bottles were again repeatedly rinsed with the river water. Channel sediment samples were collected along the banks of the river at T0 active flood plain part, and care was taken to remove ~8-10 cm top layer of sediment with the stainless steel spatula. Samples were collected in clean polythene bags which were sealed instantly to prevent contamination. Suspended sediments were separated from the water, by settling, decantation and filtration processes. Although it is advisable to collect the samples from the middle of the river at mid-depth to reduce the effect of hydrodynamic sorting (Lupker et al. 2011; 2012b); in the present study, it was not possible to collect samples from the middle of the river because of lack of boat facility. However, all the samples were collected from sites where there was sufficient flow of water.

For total organic carbon (TOC) analysis, water samples were collected in dark colored tinted glass bottles and 5-10 mg of $HgCl_2$ was added to prevent direct sunlight penetration to prevent microbial growth (Tamooh et al., 2012). All the water and sediment samples were collected in glass jars and stored in a cold refrigerated temperature before the analysis commenced.

Table 4.1 Sample collection sites with geographic locations

Sample	Sample Location	Latitude	Longitude	River
A1	Govindghat	30° 37’ 16.6’’	79° 33’ 43.1’’	Alaknanda
A2	Vishnuprayag	30° 33’ 53.2’’	79° 33’ 45.4’’	Alaknanda
A3	Chamoli	30° 24’ 04.8’’	79° 19’ 45.2’’	Alaknanda
A4	Nandprayag	30° 19’ 54.4’’	79° 18’ 36.7’’	Alaknanda
A5	Karnaprayag	30° 17’ 11.6’’	79° 10’ 03.0’’	Alaknanda
A6	Rudraprayag	30° 16’ 29.5’’	78° 57’ 51.9’’	Alaknanda
A7	Kalyasaur	30° 14’ 31.6’’	78° 15’ 22.2’’	Alaknanda
A8	Srinagar	30° 14’ 14.1’’	78° 49’ 11.7’’	Alaknanda
A9	Bagwan	30° 13’ 23.9’’	78° 40’ 52.7’’	Alaknanda
A10	Devprayag	30° 08’ 37.3’’	78° 36’ 11.4’’	Alaknanda
Dg	Vishnuprayag	30° 33’ 44.0’’	79° 34’ 34.6’’	Dhauli Ganga
Bg	Birahi	30° 24’ 25.4’’	79° 23’ 26.0’’	Birahi Ganga
N	Nandprayag	30° 19’ 51.8’’	79° 19’ 0.04’’	Nandakini
P	Karnaprayag	30° 15’ 31.6’’	79° 13’ 05.9’’	Pinder
M	Rudraprayag	30° 17’ 18.9’’	78° 58’ 46.4’’	Mandakini
B	Devprayag	30° 09’ 17.3’’	78° 36’ 07.0’’	Bhagirathi
G1	Devprayag	30° 08’ 21.1’’	78° 35’ 49.1’’	Ganga
G2	Rishikesh	30° 07’ 19.3’’	78° 18’ 36.9’’	Ganga

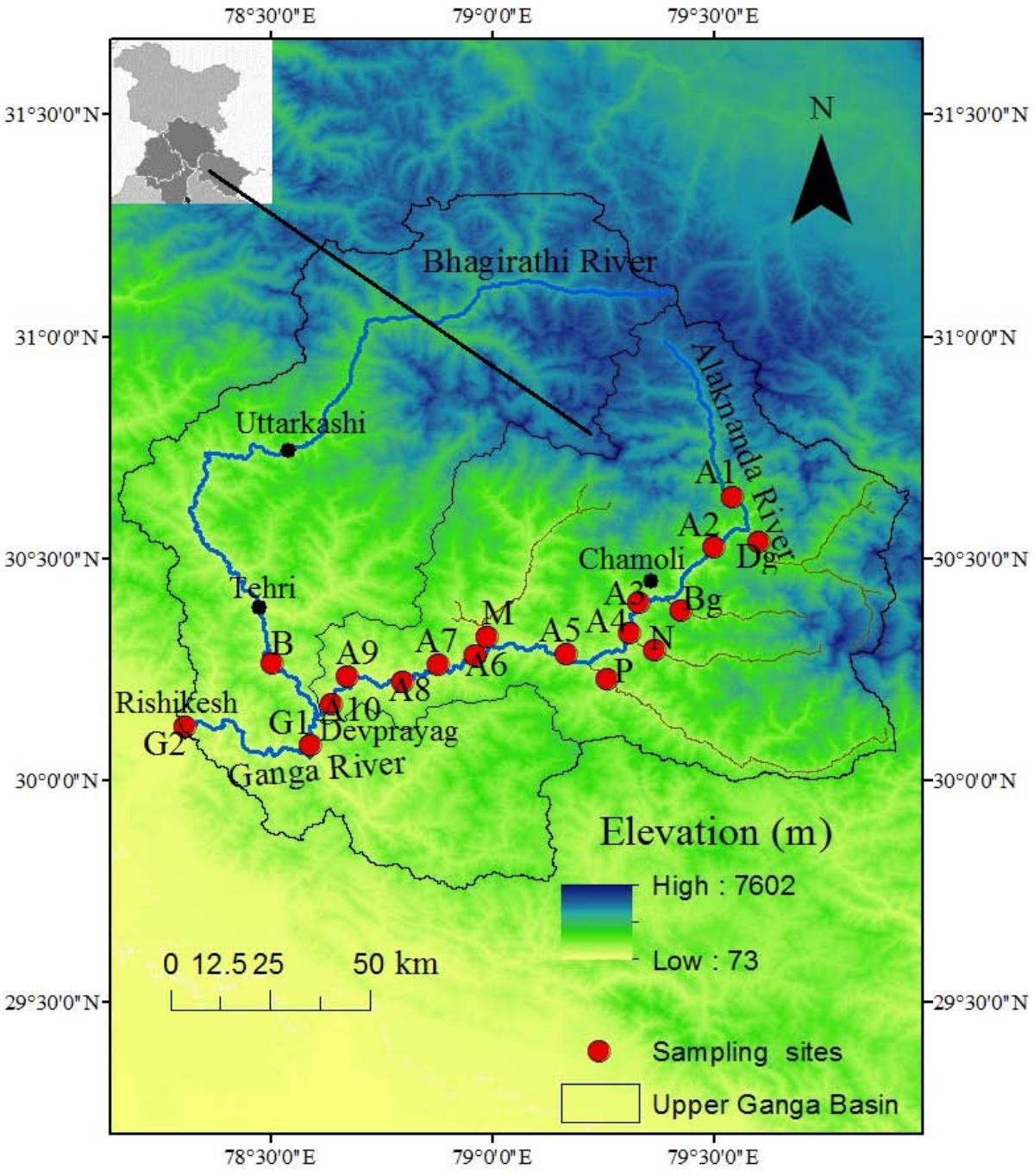

Figure 4.1 Sample collection sites

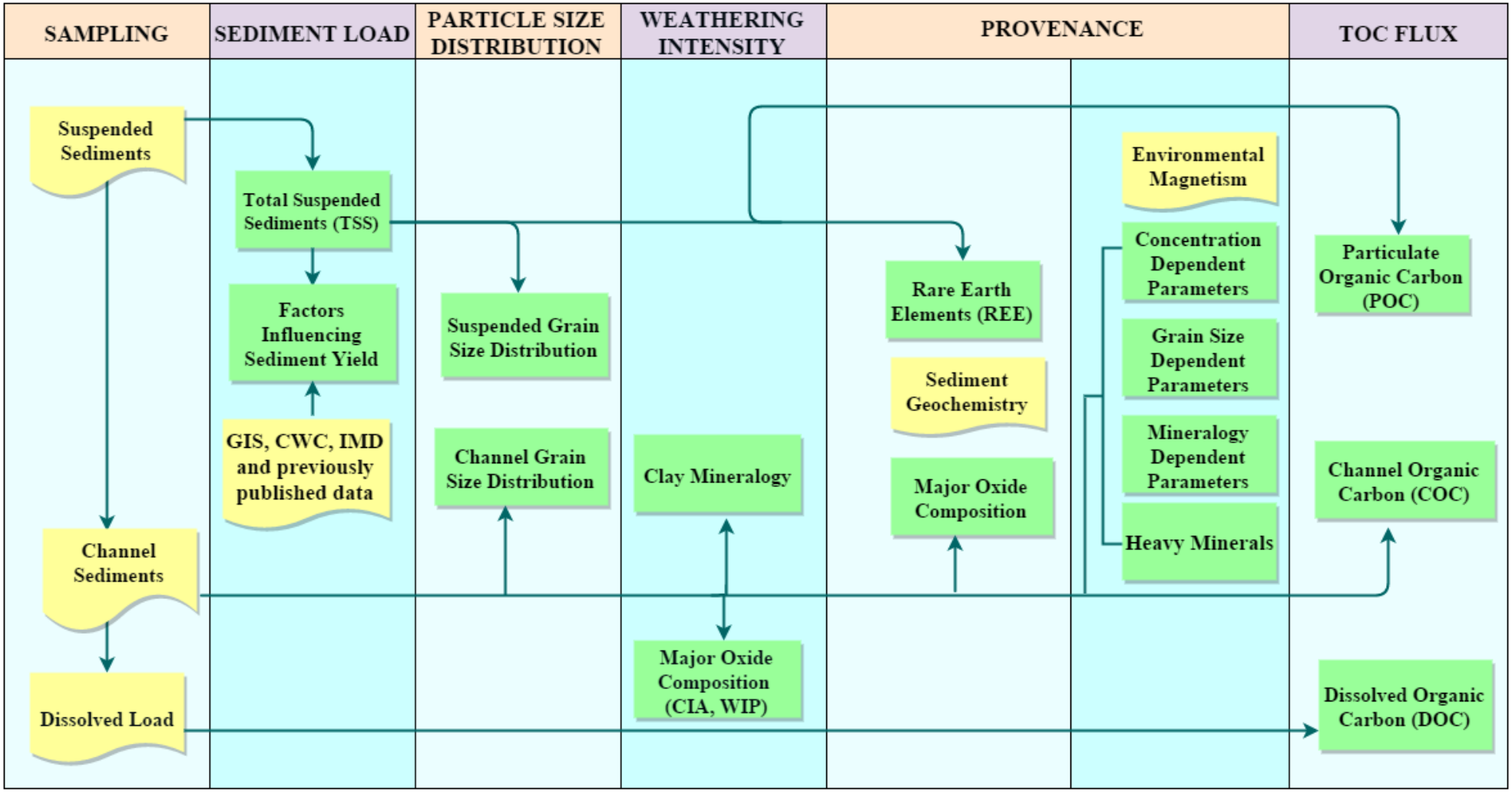

Figure 4.2 Methodology designed and adopted during the research work

Table 4.2 Analytical instruments employed for sediment characterization (D_{50} = median particle size; CV = coefficient of variance)

Analysis	Sample Type	Instrument	Standard/ Reference material	Accuracy/Detection Limit
Grain Size Analysis	Suspended sediments/ Channel sediments (Bulk)	Microtrac S3500 Particle Size Analyzer	Glass beads 1: D_{50} = 1.0-1.4 µ; Glass beads 2: D_{50} = 57.17-61.17 µ; Glass beads 3: D_{50} = 620-665 µ	Glass beads 1: CV = 0.4%; Glass beads 2: CV = 1.0%; Glass bead 3: CV = 0.7%
Major Oxides	Channel sediments (Bulk)	Bruker S-8 Tiger X-Ray Fluorescence	GSD-9 (Standard sample of shale produced by IGGE, China)	CV <5%
Rare Earth Elements	Suspended sediments	PerkinElmer SCIEX ELAN DRC-e ICP-MS	SGR (Standard sample of shale produced by USGS)	CV <10%
Clay Minerals	Channel sediments (<2µm size)	Bruker D8 X-Ray Diffractometer	Instrument is positioned at 2-40° theta using CuK-alpha radiations	Preferred orientation leads to accurate peak intensities
Magnetic Susceptibility	Channel sediments (Bulk)	Bartington MS2B sensor	$10cm^3$ containing small ferrite bead	At 0.1 range, precision is ±0.1
Anhysteretic Remanent magnetism (ARM)	Channel sediments (Bulk)	Magnon AFD 300 Magnetizer	Manually adjusting peak fields in a µ-metal shield	Peak field are up to 160 mT
Isothermal Remanent Magnetisation (IRM)	Channel sediments (Bulk)	ASC Scientific Impulse Magnetizer (IM-10) and	Manually adjusting the voltage and output signal	Generates magnetic field up to 2T
		Minispin Spinner Magnetometer	Specimens are spun at 6 Hz inside a triple shielded annular fluxgate	Better than 1 x 10^{-7} emu/cc at 24 sec
Heavy Minerals	Channel sediments (63-125 µm)	Bruker D8 X-Ray Diffractometer	Instrument is positioned at 20-80° theta using CuK-alpha radiations	Preferred orientation leads to accurate peak intensities
TOC	Dissolved, Suspended, Channel sediments	Analytik Jena TOC Analyzer Multi N/C 3100	Solid Module (POC and COC)- Calcium Carbonte ($CaCO_3$)	Solid Module (POC and COC)- Detection range 0-500 mg C
			Liquid Module (DOC)- Potassium	Liquid Module (DOC)- Detection

	Hydrogen Phthalate (KHP)	limit of 4 µg/l

4.2.LABORATORY ANALYSIS

Figure 4.2 shows the methodology designed for the present study. On returning to the laboratory, water samples were filtered (within 4-5 days) to collect suspended sediments. Filtrates collected were covered and kept in the refrigerator for freeze drying. Channel sediment samples for the geochemical and TOC analysis were also kept in the refrigerator maintained at a temperature <4°C, till analyzed. For TOC analysis, samples were analyzed within a week. For grain size analysis, samples were air dried in a closed room. The following sections, explain in detail the procedure/technique involved in processing, evaluating, estimating and generating the data for each parameter and objective. Table 4.2 shows the specification of particular instrument used in this research.

4.2.1. Sediment Yield And Controlling Factors

4.2.1.1.Sediment Yield

Sediment load was estimated for the post-monsoon, pre-monsoon and monsoon season. Approximately, 5 litre water samples collected during the field work were filtered through 0.45 µm cellulose nitrate membrane filter paper to collect the total suspended sediments (TSS). The filter papers were weighed before and after filtering for the determination of TSS. TSS was calculated by using the following formula:

$$\mathbf{TSS = (A-B)/C}$$

Where, TSS = Total suspended sediments (gram/litre)

A = End weight of filter paper (gram)

B = Initial weight of filter paper (gram)

C = Volume of water filter (litre)

Sediment load (SL) was calculated following the Milliman and Meade (1983); Gaillardet et al. (1999) and Syvitski et al. (2003):

$$\mathbf{SL = Q*TSS}$$

Where, SL = Sediment load (mass/time)

Q = Discharge (volume/time)

TSS = Total suspended sediments (mass/volume of water)

Specific sediment yield (SSY) which is defined as a mean annual sediment yield averaged over the drainage area was calculated as:

$$\mathbf{SSY = SL/A}$$

Where, SSY = Specific sediment yield (mass/area/time)

SL = Sediment load (mass/time)

A = Area of the watershed (length^2)

4.2.1.2.Factors Influencing Sediment Yield

The sediment load in any basin can be broadly attributed to five factors viz. climatic, hydrologic, topographic, geological and anthropogenic. Table 4.3 elaborate all these factors. Five factors were further divided into 29 variables, which were quantified based on the spatial and temporal data. In view of the limitation of data for the watersheds of the tributaries, we carved the sub-catchment areas according to data availability points (gauging sites). The discharge and sediment load for five locations were available - Lambagad (year 2002-2005), Rudraprayag (year 1991-2005), Srinagar (year 2004-2005), Maneri (year 2004-2005) and Rishikesh (year 2004-2005). Figure 4.3 gives the overview of the different sub-catchment areas extracted based on the discharging sites. Table 4.3 describes the approach followed to estimate all the twenty nine variables and Table 4.4 show the source of the data used in this study.

The remote sensing and GIS techniques hold an advantage of providing the synoptic detail of the morphometric data of the watershed and river channels (Legleiter et al., 2004). For estimating climatic variables, mean monthly, maximum monthly and minimum monthly temperature data of the years 1901-2002 provided by the Indian Meteorological Department (IMD), India was used. In the absence of temperature data for the upper part of the basin, a freely available WORLDCLIM 10-sec ESRI data was used. Figure 4.4(a) shows the Inverse Distance Weighted (IDW) interpolated mean temperature map of the UGB.

Monthly precipitation data from the gauge stations - Tehri, Dehradun, Haridwar, Chamoli and Rudraprayag provided by the IMD for the years 1901-2002 and 2008-2013 was used, whereas, in the absence of data for the upper part of the basin, Tropical Rainfall Measuring Mission (TRMM) data was used. TRMM data for the years 1998-2009 was used in this study. Figure 4.4(b) shows the IDW interpolated mean precipitation map of the UGB. The spatial analyst tool available in the ARCMAP 10.2 was used for the interpolation of temperature and rainfall point data.

Topographical factors such as elevation, slope, basin, and channel length were estimated using the SRTM 90 m DEM and Google Earth imagery. Drainage density (Dd) and stream

order maps were generated using the spatial analyst tool function in the ARCMAP 10.2. Figure 4.5(a-d) shows the elevation, slope, drainage density and stream order map generated for the UGB.

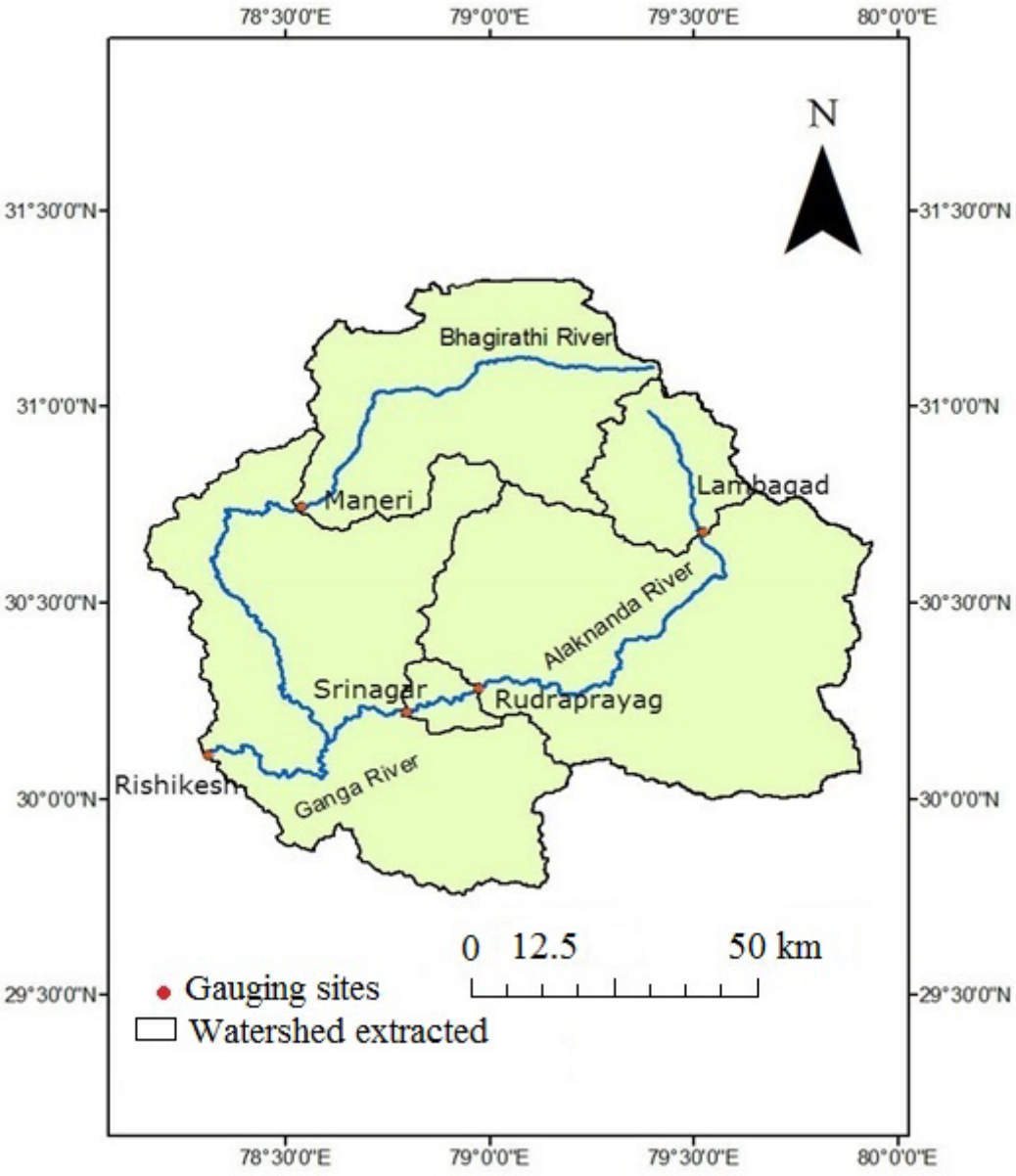

Figure 4.3 Gauging sites and extracted watersheds

Table 4.3 Variables affecting sediment load in the Upper Ganga Basin (UGB), methodology followed and source of the data

Factors/ Variables	Symbol	Description	Data Source
Sediment load (ton/year)	SL	Clastic material that moves through the channel	CWC and previously published data
Specific sediment yield (ton km^{-2} $year^{-1}$)	SSY	Mean annual sediment load averaged over the drainage area	Calculated
		Climatic	
Mean annual precipitation (mm $year^{-1}$)	Pmean	Mean annual precipitation in the drainage basin	IMD data
Maximum monthly precipitation (mm/month)	Pmax	Long term mean monthly precipitation for the wettest month of the year	IMD data
Precipitation peakedness	Ppk	Ratio of the mean annual precipitation and the maximum monthly precipitation of the basin	IMD data
Mean annual temperature (°C)	Tmean	Long term mean annual temperature in the drainage basin	IMD data
Temperature range (°C)	Trange	Difference between the mean monthly temperature of the hottest and coldest month	Calculated
		Hydrologic	
Mean water discharge (m^3s^{-1})	Qmean	Long term mean discharge at the basin outlet	CWC and previously published data
Maximum monthly water discharge (m^3s^{-1})	Qmax	Long term maximum monthly discharge at the basin outlet	CWC and previously published data
Discharge peakedness	Qpk	Ratio of mean discharge over maximum discharge	Calculated
		Topographic	
Catchment area (km^2)	A	Basin area above gauging station	Calculated through GIS
Mean elevation (m)	Emean	Arithmetic mean of the elevation of all cells in the sub-basin	Calculated through GIS
Maximum elevation (m)	Emax	Elevation of the highest cell in the basin	Calculated through GIS
Minimum elevation (m)	Emin	Elevation of the lowest cell in the basin	Calculated through GIS

Basin relief (m)	E	Difference between the maximum and the minimum cell value in the basin	Calculated through GIS
Relief peakedness	Epk	Ratio of the mean elevation and the maximum elevation of the basin	Calculated through GIS
Relief ratio	Er	Ratio of basin relief and basin length	Calculated through GIS
Hypsometric integral	HI	Given by: (Emean-Emin*)/(*Emax-Emin*)*	Calculated
Basin length (km)	Lb	Straight line distance from the most remote point on water divide to the gauging station	Calculated through GIS
Channel length (km)	Lc	Length of the main channel of the drainage basin from its headwater to the outlet	Calculated through GIS
Slope (m km^{-1})	α1	Ratio of mean elevation of the basin and the square root of the basin area	Calculated through GIS
Channel gradient (m km^{-1})	Ac	Average slope of the main river channel	Calculated through GIS
		Geological	
Carbonate rock exposure	CR	Percentage of carbonate rock present in the basin	Calculated through GIS using map of Valdiya (1980) and Bickle (2003)
Silicate rock exposure	SR	Percentage of silicate rocks present in the basin	Calculated through GIS using map of Valdiya (1980) and Bickle (2003)
Average lineament density	LD	Total length of all the lineaments divided by the total area of the drainage basin	Calculated using the lineament thematic layer of NRSC (Bhuwan data)
Drainage density	Dd	Total length of all the streams divided by the total area of the drainage basin	Calculated through GIS
Drainage texture	Dt	Total number of streams divided by the perimeter of the drainage basin	Calculated through GIS
		Anthropogenic	
Total snow and ice cover (%)	SI	Percentage of snow and ice covered in the basin	Calculated using LULC map of the year 2005
Total cultivation (%)	Cul	Percentage of cultivated area in the basin	Calculated using LULC map of the year 2005
Total fallow land (%)	Fl	Percentage of fallow land area in the basin	Calculated using LULC map of the year 2005
Total barren land (%)	Bl	Percentage of barren land area in the basin	Calculated using LULC map of the year 2005

Table 4.4 Source of total suspended sediment (TSS), discharge and rainfall data

Gauging sites	Year	Data Type/ Source
Maneri	2004-2005	TSS: Chakrapani and Saini (2009)
	2004-2005	Discharge: Chakrapani and Saini (2009)
	1901-2002	Temperature: Indian Meteorological Department (IMD)
	1901-2002	Rainfall: IMD
Lambagad	2002-2005	TSS: JP Hydro-electric Project, Joshimath (JPHP)
	2002-2005	Discharge: JPHP
	1950-2000	Temperature: WORLDCLIM 10 Arc-sec Grid
	1998-2009	Rainfall: Tropical Rainfall Measuring Mission (TRMM)
Rudraprayag	1991-2005	TSS: Central Water Commission (CWC)
	1991-2005	Discharge: CWC
	1901-2002	Temperature: IMD
	1901-2002	Rainfall: IMD
Srinagar	2004-2005	TSS: Chakrapani and Saini (2009)
	2004-2005	Discharge: Chakrapani and Saini (2009)
	1950-2000	Temperature: WORLDCLIM 10 Arc-sec Grid
	1998-2009	Rainfall: TRMM
Rishikesh	2004-2005	TSS: Chakrapani and Saini (2009)
	2004-2005	Discharge: Chakrapani and Saini (2009)
	1950-2000	Temperature: WORLDCLIM 10 Arc-sec Grid
	1998-2009	Rainfall: TRMM

The land use land cover (LULC) map of the year 2005-2006 at 1:50,000 scale was downloaded from the BHUVAN, NRSC Portal, India. A small part of the watershed area that comes under the Republic of China was classified using the Google Earth imagery of August 2005. Figure 4.6 shows the LULC map of the UGB.

Geological factors are difficult to quantify in the complex lithology basin such as the UGB. Following the approach of Tripathy and Singh (2010), we digitized the geological map of the UGB composed by Valdiya (1980) and Bickle et al. (2003). Silicate rocks are dominantly present throughout the UGB and carbonates and some mafic intrusions are present in the Inner Lesser Himalayas. In this case, only dominant lithology (carbonate) is considered to represent the particular formation. The lineament map of the year 2005-2006 was obtained from the free database of BHUVAN NRSC, India at 1:50,000 scale. Figure 4.7(a-b) shows the geological and lineament map of the UGB.

For identifying and analyzing the controls of sediment yield, the pair wise correlation between the different variables were performed by calculating the Pearson Correlation Coefficients (Table 5.3).

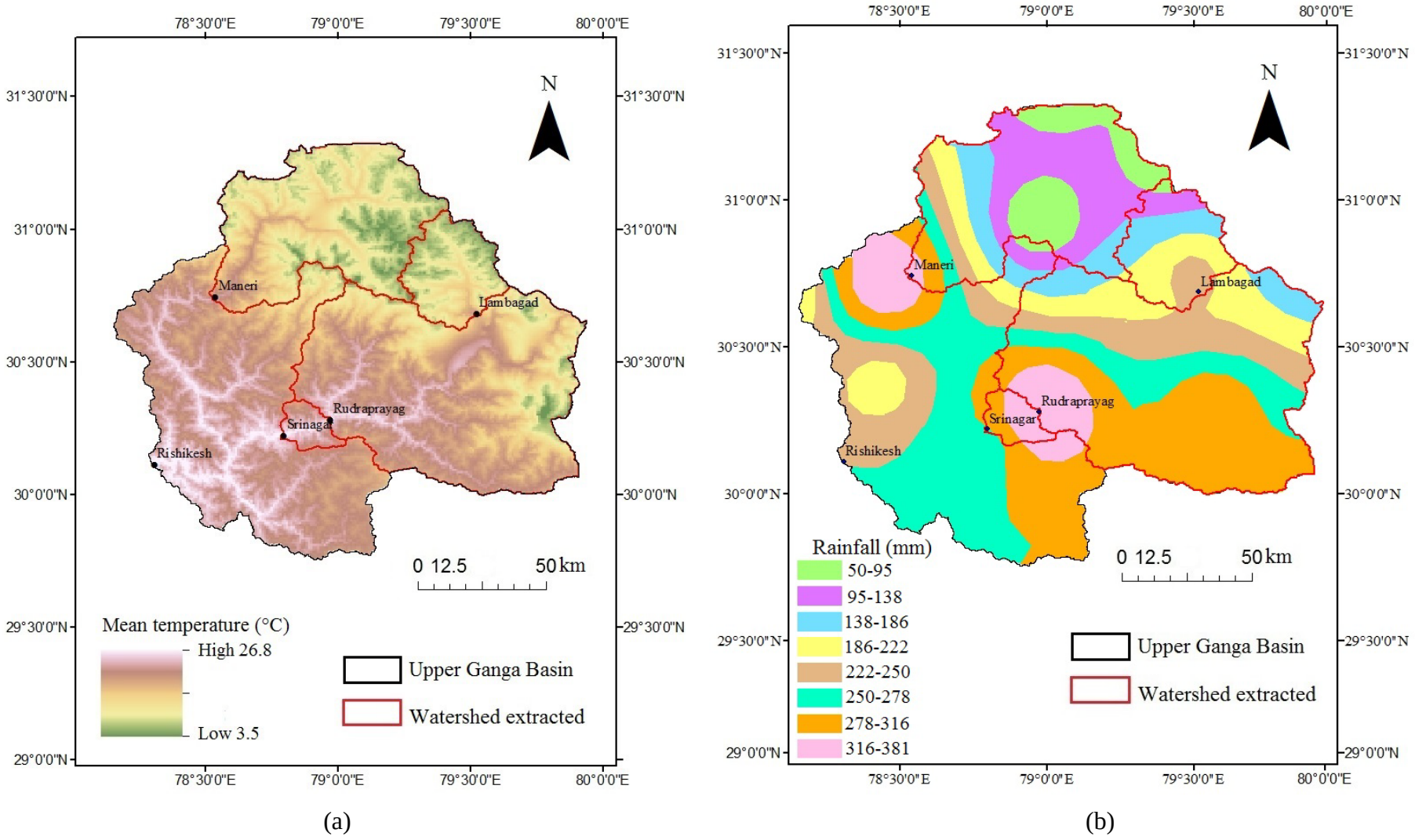

(a) (b)

Figure 4.4 (a) Inverse Distance Weighted (IDW) interpolated mean temperature map; (b) IDW interpolated mean precipitation map of the UGB

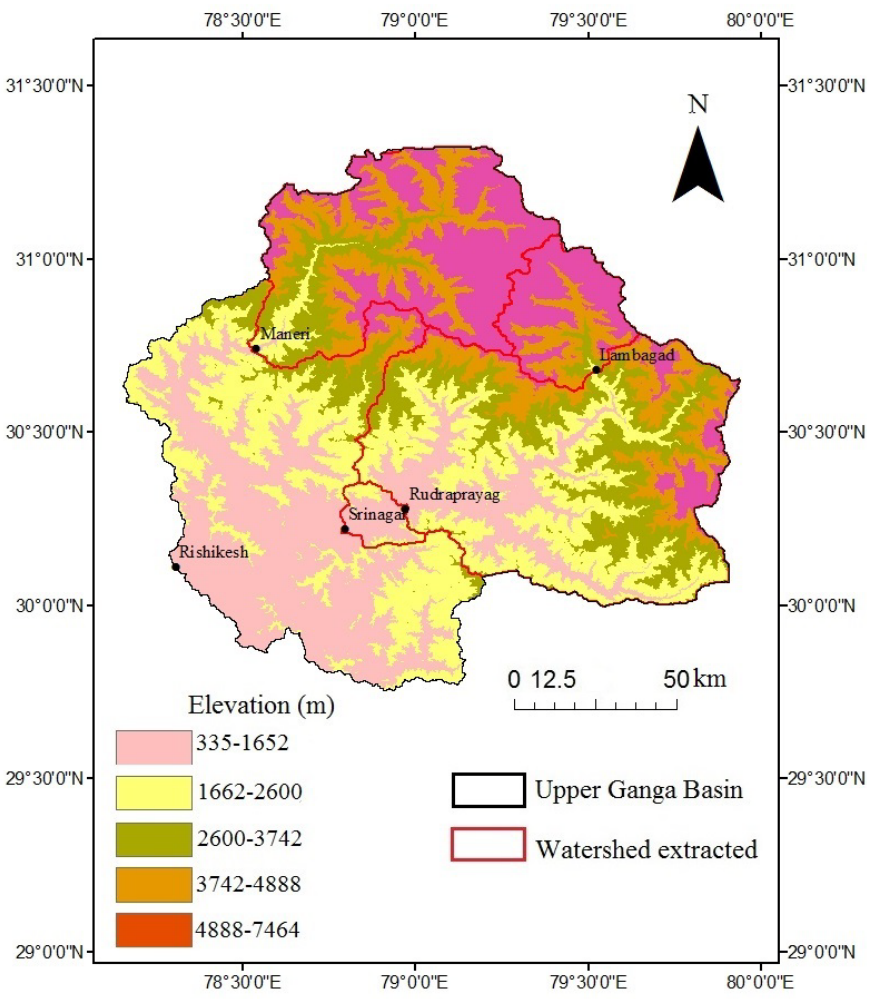
78°30'0"E
79°0'0"E
79°30'0"E
80°0'0"E
31°30'0"N
31°0'0"N
30°30'0"N
30°0'0"N
29°30'0"N
29°0'0"N
N
Maneri
Lambagad
Rudraprayag
Srinagar
Rishikesh
0 12.5 50 km
Elevation (m)
335-1652
1662-2600
2600-3742
3742-4888
4888-7464
Upper Ganga Basin
Watershed extracted

(a)

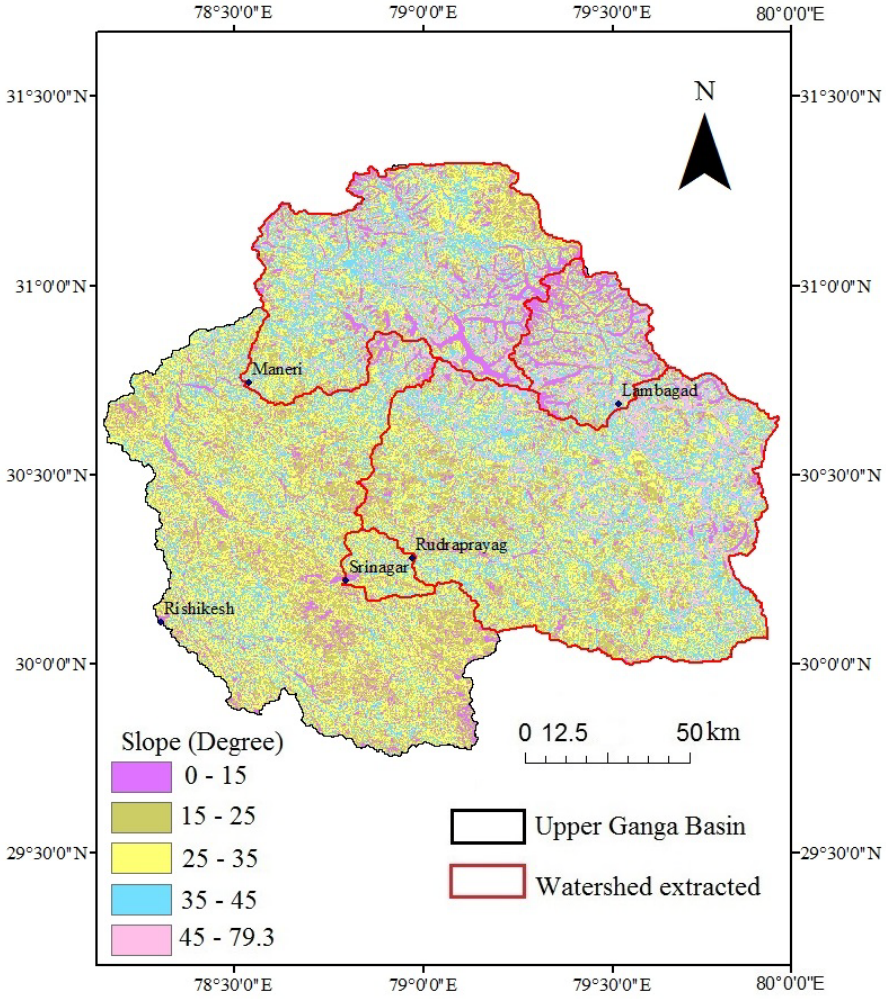
78°30'0"E
79°0'0"E
79°30'0"E
80°0'0"E
31°30'0"N
31°0'0"N
30°30'0"N
30°0'0"N
29°30'0"N
N
Maneri
Lambagad
Rudraprayag
Srinagar
Rishikesh
0 12.5 50 km
Slope (Degree)
0 - 15
15 - 25
25 - 35
35 - 45
45 - 79.3
Upper Ganga Basin
Watershed extracted

(b)

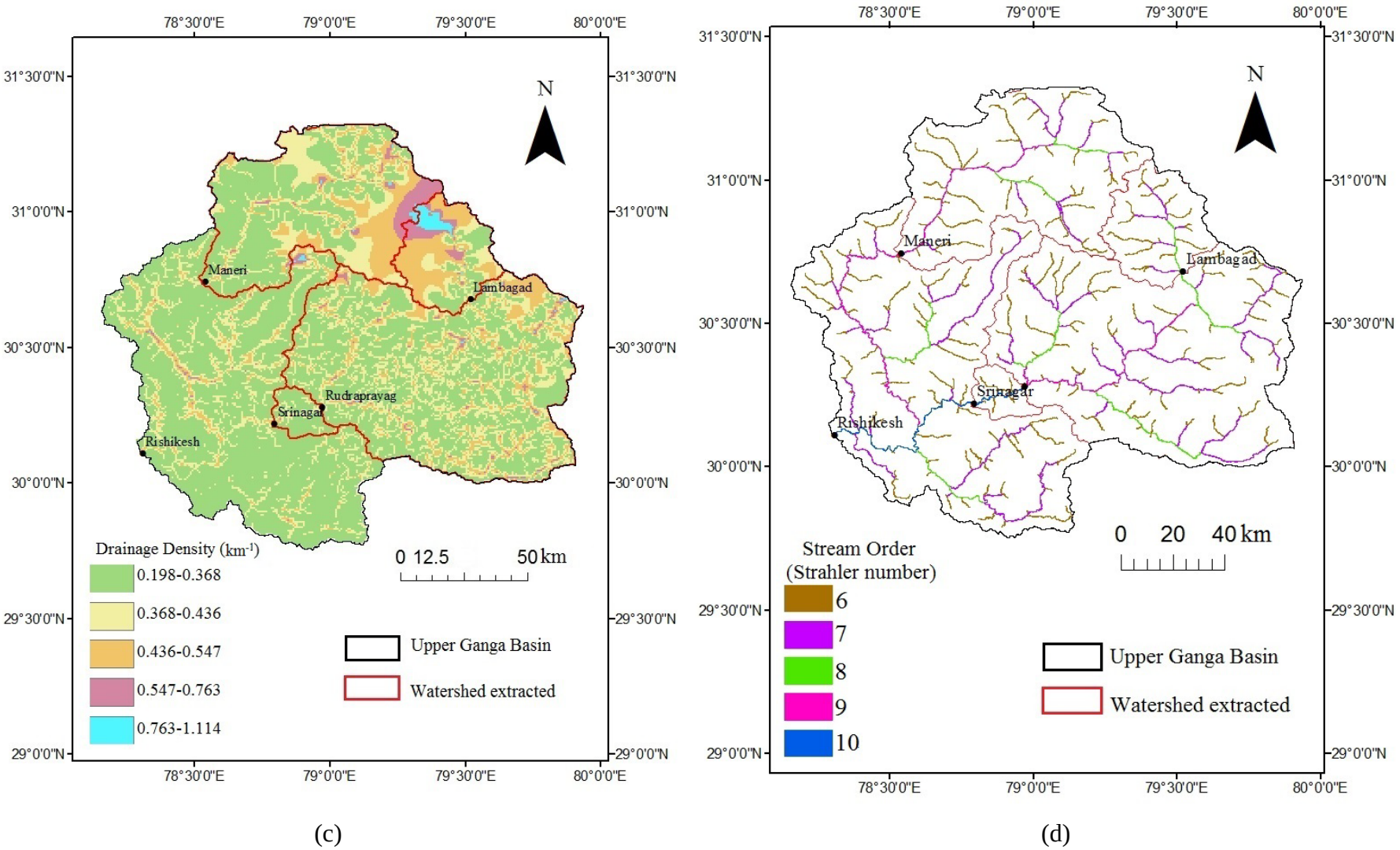

(c) (d)

Figure 4.5 (a) Mean elevation map; (b) Slope map (c) Drainage density map; (d) Stream order map of the UGB

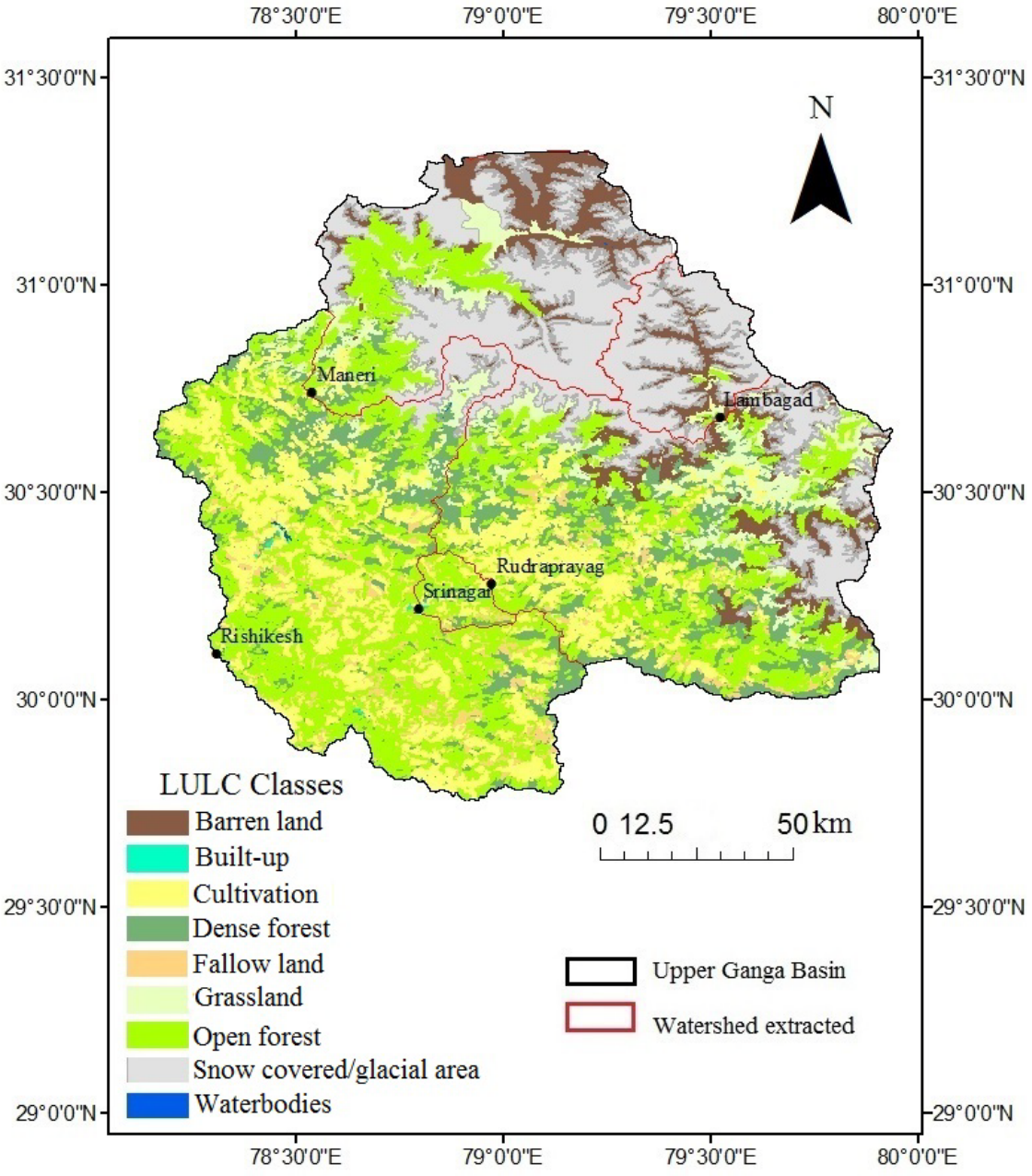

Figure 4.6 Land Use Land Cover (LULC) map of the UGB of the year 2005 (Source: BHUVAN NRSC Portal)

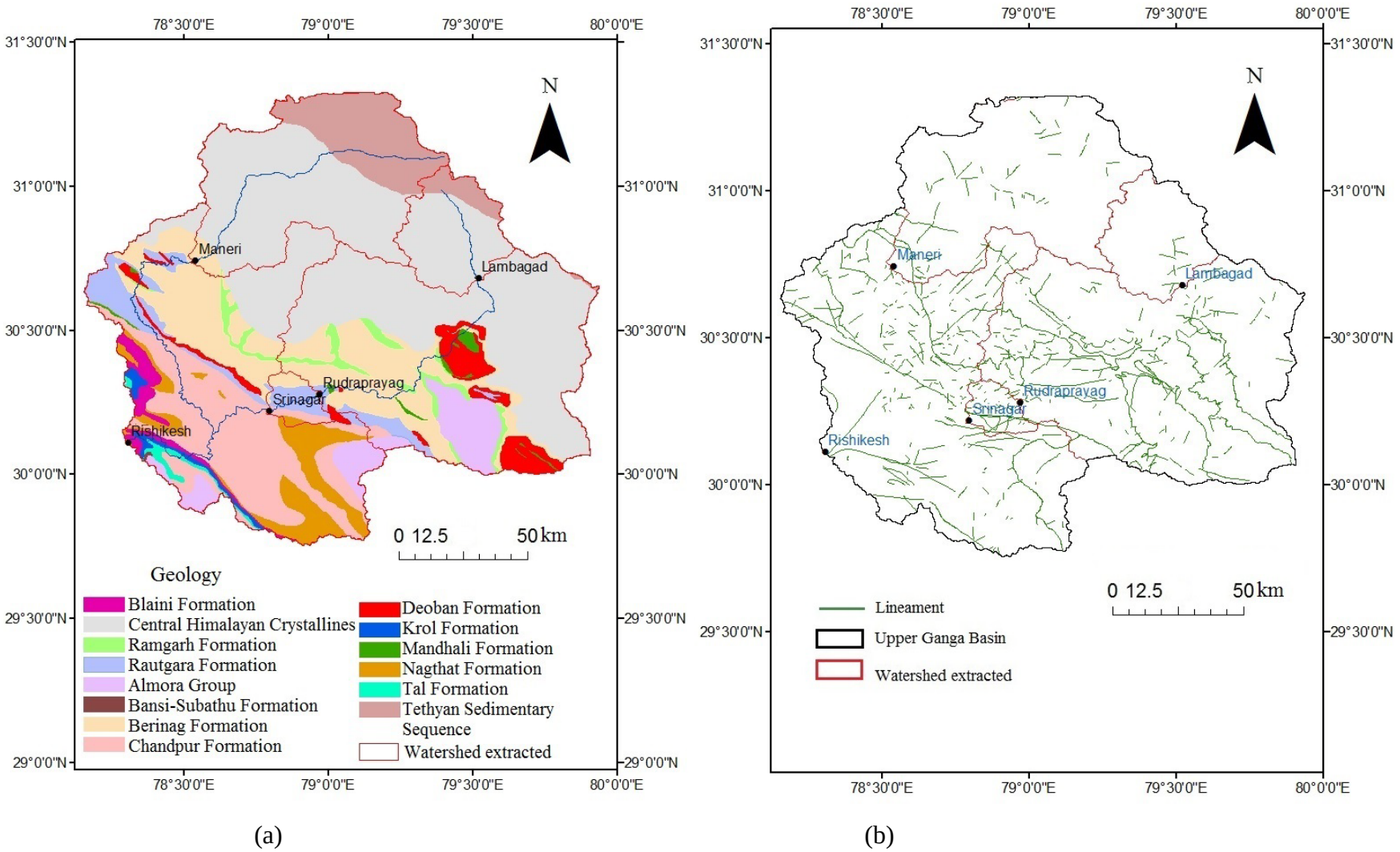

(a) (b)

Figure 4.7 (a) Geology of the UGB (modified after Valdiya, 1980 and Bickle et al., 2003); (b) Lineament map of UGB (Source: BHUVAN NRSC Portal, India)

4.2.2. Particle Size Distribution

The effective sediment size (i.e. without organic carbon removal) of suspended and channel sediment was estimated using the Microtrac S3500 Particle Size Analyzer. The instrument operates on the principle of Laser Diffraction and every particle was measured as a 'sphere-equivalent diameter'. At a specific size, particles diffract light at a specific angle and generate a stable diffraction pattern. The lower and upper limit of measurement of Microtrac S3500 Particle Size Analyzer is 0.289 µm-1.4 mm. The wavelength of the laser used in the Particle Size Analyzer (PSA) is 780 nm.

Table 4.5 Statistical equations used for quantifying grain size distribution parameters (Folk and Ward, 1957; Lindohlm, 1987; Boggs, 2010)

Grain size parameters	**Statistical equations**
Graphic Mean (M)	$M = \frac{\phi 16 + \phi 50 + \phi 84}{3}$
Inclusive graphic standard deviation (Sorting, S)	$S = \frac{\phi 84 - \phi 16}{4} + \frac{\phi 95 - \phi 5}{6.6}$
Inclusive graphic skewness (Sk)	$Sk = \frac{\phi 84 + \phi 16 - 2\phi 50}{2(\phi 84 - \phi 16)} + \frac{\phi 95 + \phi 5 - 2\phi 50}{2(\phi 95 + \phi 5)}$
Graphic kurtosis (K)	$K = \frac{\phi 95 - \phi 5}{2.44(\phi 75 - \phi 25)}$

The samples were collected along the banks of the river, at T0 active flood plain part. Due to reduced energy at the banks, channel sediments were mostly of sand grade size. Following the approach of Waznah et al. (2010) and Kamaruzzaman et al. (2010), samples comprising of >90% of the coarse sands were analyzed by dry sieving methods, using Automatic Sieving Machine. The samples having <90% of coarse sand were analyzed using Particle Size Analyzer (PSA). Particle size distribution of channel sediments were performed for all the three seasons, (post-monsoon, pre-monsoon and monsoon), whereas in the case of suspended sediments, post-monsoon and monsoon season samples were analyzed. Sample analysis was performed in the dry mode and each sample was run three times to get an average result. The RMS residual error for the samples varies from 0.343-0.502%. Statistical grain size parameters, such as mean size, sorting, skewness and kurtosis were determined by following Folk and Ward (1957) and Garzanti et al. (2011). Table 4.5 shows the statistical equations for determining all the grain size distribution parameters.

4.2.3. Major Oxides Composition

Major oxide composition of the sediments (SiO_2, Al_2O_3, Fe_2O_3, CaO, MgO, Na_2O, K_2O, P_2O_5, TiO_2 and MnO) was estimated using the X-Ray Fluorescence (XRF) spectrometry technique. XRF analysis was carried out using the Bruker S-8 Tiger X-Ray Fluorescence at the Wadia Institute of Himalayan Geology, Dehradun, India.

XRF spectrometry works on the principle of excitation of an individual atom with primary X-ray radiation. Exited atoms emit X-ray photons that are unique for a particular element. These photons are scanned by the detector and individual elements in the sample are identified and quantified.

Following the approach mentioned by Saini et al. (2000), bulk sediment samples were powdered <75 µm in size. Approximately, 5 gm of powdered sample was used for making the pellet. Polyvinyl acid was used as an adhesive; 2-3 drops of saturated polyvinyl acid diluted in ultrapure water were added to the powder sediment for making the pellets compact and stable. The pressure of ~2000 kg/cm^2 was applied for palletizing the sample as a top layer with the boric acid used as a backing material (for increasing the thickness of the pellet). Approximately, 3.5 mm thick pellets were prepared, which are considered quite good for X-ray analysis. Pellets prepared were kept in the hot box overnight to drive off the excess water present in it. All the elements in the XRF were exited at 12 kV vacuum paths without any primary beam filter. Reference material GSD-9 stream sediments prepared by the Institute of Geophysical and Geochemical Exploration (IGGE) China was used as a standard for the calibration of the instrument and all the results were obtained in percentage.

To aid the interpretation of the results, the major oxide data generated in the study was geochemically normalized with the major oxide content of the Upper Continental Crust (UCC) mentioned in Taylor and McLennan (1985).

4.2.3.1. Weathering Indices

During the chemical weathering, degradation of feldspars and the formation of clay minerals take place that results in the leaching of the alkalis (Na^+, K^+) and Ca^{+2} and concentration of Al and Si in the residue. In the present study, three indices were used to estimate the degree of chemical weathering:

The Chemical Index of Alteration (CIA) developed by Nesbitt and Young (1982) quantifies the conversion of feldspar minerals into aluminous clay minerals. Following equation formulated by Nesbitt and Young (1982) was used to estimate the extent of chemical weathering:

$$CIA = [Al_2O_3/(Al_2O_3 + Na_2O + K_2O + CaO^*)] \times 100$$

The Weathering Index of Parker (WIP) developed by Parker (1970) and (Hamdan and Burnham, 1996) was used to quantify the mass transfer of labile elements during the chemical weathering reactions. WIP was calculated as the ratio of the amount of alkali and alkaline elements using the following equation:

$$WIP = (2Na_2O/0.35 + MgO/0.9 + 2K_2O/0.25 + CaO^*/0.7) \times 100$$

The molar concentrations of oxides were used to calculate the CIA and WIP values. CaO* being the concentration derived only from the silicate fraction of the sample. McLennan (1993) was followed for CaO* correction.

Al/Si ratio is considered to yield better results in the heterogenous lithology basin, as the Ganga basin. Following Lupkar et al. (2011, 2012b) Al/Si molar ratio and its relationships with K/Si, Na/Si and Fe/Si was calculated to estimate the degree of chemical weathering and the role of the lithology.

4.2.4. Rare Earth Elements (REEs)

The Alaknanda River carries ~85% of the annual sediment load during the monsoon season, as a result, a good amount of suspended sediments were obtained during the monsoon sampling (August, 2014) which were used for REEs analysis. REEs in the suspended sediments were analyzed using the Inductively Coupled Plasma Mass Spectrometry (ICP-MS) at the Wadia Institute of Himalayan Geology, Dehradun, India. ICP-MS has higher and accurate detection limit for the REEs. ICP-MS (PerkinElmer SCIEX ELAN DRCe) integrates high temperature ICP (Inductively Coupled Plasma) with a mass spectrometer. The plasma in the instrument convert atoms into ions; and then ions in the mass spectrometer are separated and transformed into electrical signals. The electrical signals generated are then converted into an analyte concentration. The detection limit of the instrument for the REE is <1 ppm (µg/ml).

The samples were analyzed following the methodology described by Khanna et al. (2009). 100 mg of suspended sediment sample was digested with 10 ml of HF-HNO_3 mixture (2:1) in a Teflon crucible on a hot plate maintained at a temperature of 50-60 °C and heated to dryness. This step was repeated 2-3 times until the samples achieved a completely dry state. Then ~2-3 ml of $HClO_4$ was added and the samples were again heated to dryness. Further, 10 ml of 10% HNO_3 was added and the samples were heated for additional 10 minutes for achieving a clear solution. With the addition of distilled water, the final volume was diluted to 100 ml. ICP-MS used for analyzing the sample aliquot was calibrated with reference sample MAG-1, an international geo-standard by the United State Geological Survey (USGS). All the results were reported in ppm. To aid interpretation of the results, the REEs data generated in the study was

geochemically normalized with the rare earth element content of the Upper Continental Crust (UCC) mentioned in Taylor and McLennan (1985) and McLennan (2001).

4.2.5. Clay Mineralogy

The clay size fraction (<2 μm) was separated from the channel sediment samples (Pre-monsoon, 2014 and Monsoon, 2014) by sedimentation method using Atterberg cylinders (Muller, 1967). Prior to clay mineral analysis by the X-ray Diffraction, samples were treated with 10% ultrapure hydrogen peroxide (H_2O_2) to remove the organic carbon and 1% HCl to remove carbonate components. Mineral phases were identified on the air-dried and glycolated samples using Bruker D8 Powdered X-Ray Diffractometer (Powder-XRD) at the Institute Instrumentation Centre, IIT Roorkee. The approach mentioned by Biscaye (1965) was followed for the slide preparation and mineral identification.

Powder-XRD is based on the principle of diffraction and Bragg's Law. The cathode ray tube installed in the instrument produces monochromatic radiation. These radiations when strike the mineral present in the sample, following Bragg's Law produces a constructive interference. By scanning the sample through 2θ angle, all the possible diffraction peaks are attained which are converted to d-spacing. Each mineral has a characteristic d-spacing and when compared with a standard reference pattern gives an accurate identification of mineral.

Air-dried and ethylene-glycol solvation slides were prepared and run on (001) plane. The powder XRD with target CuKα radiation was operated at an angle range of 2-40° at an interval of 1° per minute. Identification of minerals was done on the ethylene-glycol solvation diffractograms. The semi-quantitative clay mineral estimation was done following the Rietveld method (Rietveld, 1969). Rietveld refinement was carried out in the X'pert Hiscore Plus software using the ICDD PDF2 database. Illite chemistry index and illite crystallinity index were determined following the method described by Chamley (1989) and Liu et al. (2007). Illite chemistry index, often used for identification of clay minerals is defined as the ratio of the peak area of 5Å/10Å peak. Whereas, illite crystallinity index helps in knowing the hydraulic conditions was measured as a width of 10Å Illite peak (FWHM = full width at half maximum) (Petschick et al., 1996; Ehrmann, 1998; He et al., 2013).

4.2.6. Environmental Magnetism And Heavy Minerals

Environmental Magnetism: Environmental magnetic studies include estimating three set of parameters as shown in Table 4.6. All the samples were analyzed at the Mineral Magnetic Laboratory at the Department of Geology, Pune University, Pune. Air dried channel sediment samples (of the Pre-monsoon season of the year 2014) were subjected to coning and quartering before commencing the magnetic analysis. Each sample weighing ~8-10 grams was packed into 10 ml plastic container using the cling-film for the immobilization of the sediment. Using the Bartington MS2B sensor low and high frequency (0.45 and 4.65 KHz) mass specific susceptibility (χ_{lf} and χ_{hf} respectively) was measured. Magnetic susceptibility was determined as a mean of six repeated measurements in six different directions for each frequency (Walden et al. 1997; Dekkers 1997; Sangode et al. 2007; Gudadhe et al. 2012).

Anhysteretic remanent magnetization (ARM) and isothermal remanent magnetization (IRM) were induced and measured with the Molspin A.F Demagnetizer and the Molspin Pulse Magnetizer. Normalizing the mass specific ARM by the biasing field strength, anhysteretic susceptibility (χ_{ARM}) was reported in m^3/kg. Using the Minispin Fluxgate Spinner Magnetometer IRM Spectra, forward field was imparted at 50, 100, 200, 300, 500, 800 and 1000 mT and backfield at -10, -30, -50, -70, -100 and -300 mT. For finding the concentration of magnetic minerals, parameters such as χ, SIRM and χ_{ARM} were estimated, whereas, parameters such as χfd, χ_{ARM}/χ, χ_{ARM}/SIRM were estimated to determine the magnetic grain size.

***Heavy Mineral Analysis*:** Five channel sediment samples namely, A1, A3, A6, A8 and A10 (sampled during the pre-monsoon, 2014) were selected for heavy mineral analysis. The sieved fraction of sediment ranging from 63-125 µm was used for heavy mineral separation. Heavy mineral assemblages from specific grain size fraction (63-125 µm) reduce the effect of hydrodynamic size sorting (Morton and Hallsworth, 1994; Hounslow and Morton, 2004). Heavy minerals were separated from the lighter fraction using a bromoform. Bromoform of density 2.84 g/cc was used to separate the sediment fraction of density >2.84 g/cc from the lighter fraction. The separated minerals were dried and after removing organic matter using 10% ultrapure Hydrogen Peroxide (H_2O_2) were subjected to heavy minerals analysis using the Bruker D8 X-Ray Diffractometer (XRD) at the Institute Instrumentation Centre, IIT Roorkee, India. Following the approach of Webster et al. (2003), sediment slides were scanned at a 2θ angle range of 20°-80° with a count of 2° per step. Diffraction data was interpreted using the PANalytical X'Pert Highscore Plus software. Database of inorganic minerals (PDF2) published by International Centre for Diffraction Data (ICDD) was used as a reference.

Table 4.6 Magnetic mineral parameters

Parameter	Description	References
Concentration dependent parameters		
Volume susceptibility (K)	The ratio of induced magnetization to applied magnetic field	Oldfield et al., 1985; Thompson and Oldfield (1986); Dekkers (1997)
Low frequency mass specific susceptibility (χ_{lf})	Susceptibility at low frequency application of magnetic field. It's the concentration of bulk magnetic minerals present in the sample	Oldfield et al. (1985); Walden et al. (1997); Dekkers (1997); Jenkins et al. (2002); Robertson et al. (2003); Sangode et al. (2007)
Saturation isothermal remanent magnetization (SIRM)	Highest volume of magnetic remanence in a sample	Oldfield et al. (1985); Dekkers (1997); Booth et al., 2005; Sangode et al. (2007)
Grain Size Dependent Parameters		
Frequency dependent susceptibility ($\chi_{fd\%}$)	The variation of susceptibility between low and high frequency magnetic field	Oldfield et al. (1985); Thompson and Oldfield (1986); Dekkers (1997); Booth et al., 2005; Sangode et al. (2007)
Anhysteretic remanent magnetism susceptibility (χ_{ARM})	Magnetic particles of stable single domain (SD) type	Booth et al., 2005; Sangode et al. (2007); Hatfield and Maher (2009)
Mineralogy dependent parameters		
Coercivity of isothermal remanent magnetization (B_{0CR})	Reverse field strength required to return a magnetized sample from SIRM to zero	Oldfield et al. (1985); Thompson and Oldfield (1986); Walden et al. (1997)
HIRM, S-ratio, SIRM/χ_{lf}, F_{300}	These ratios are calculated using the concentration dependent and grain size dependent parameters	

4.2.7. TOTAL ORGANIC CARBON (TOC)

With an aim to estimate the organic carbon (OC) flux and factors influencing it in the Alaknanda basin, water and channel sediment samples collected during the pre-monsoon and monsoon season were used for dissolved organic carbon (DOC) and channel organic carbon (COC) analysis. However, for estimating the particulate organic carbon (POC) content, monsoon samples were used. For finding out the control of fine sediment in influencing the TOC concentration, channel sediments in the bulk and <63µm size fraction were analyzed.

DOC, POC, and COC content were estimated using the Analytik Jena TOC Analyzer Multi N/C 3100 instrument. For DOC, measurement range of the instrument varied from 0 to 10 g/l with a detection limit of 4 µg/l, whereas, in the case of a solid module (sediment), the detection range of the instrument is 0-500 mg C. Potassium Hydrogen Phthalate (KHP) was used as a standard for liquid module. Calibration was conducted with 500 µg/l to 5 mg/l KHP concentration range. Since inorganic carbon may have been present substantially in the water

sample, NPOC (Non-Purgeable Organic Carbon) method was adopted for DOC estimation. NPOC method is best suited for detection of low TOC content in the samples containing high inorganic dissolved carbon content. Prior to instrumental analysis, all the water samples were acidified with a 2N ultrapure HCl solution. The TOC concentration in the river sediments was determined by the direct method. Suspended and channel sediment samples were leached using 4 weight% HCl at 80°C for 1 hour to remove the traces of inorganic carbonate (IC) (Galy et al., 2007a). Calcium carbonate was used as a standard for solid module analysis. A six-point calibration was performed with 10 mg, 25 mg, 50 mg, 100 mg, 250 mg and 500 mg $CaCO_3$. For analysis, 0.5 grams of the dried sediment sample was placed in a carbon free porcelain boat and combusted at a temperature >950 °C. A continuous calibration check was performed after every 8 samples.

4.2.8. Principal Component Analysis (PCA)

Major oxide composition can be used to semi-quantify the weathering intensity and tracing the source of sediment. For provenance determination, principal component analysis (PCA) was used as a statistical tool. PCA holds an advantage of reducing the dimensionality of the geochemical data and to separate different and large number of variables into a smaller number of components. In the absence of long term data for PCA and in view of the fact that the major composition of the sediment does not alter much annually, we integrated major oxide composition data of our sampling with the unpublished data of the major oxide composition of channel sediments of the year 2007 (Panwar et al., 2016). SPSS statistics version 20 was used to perform PCA. Table 5.6 show the statistics of the data used for performing the PCA. The major oxide data geochemically normalized with Upper Continental Crust (UCC) was used (Taylor and McLennan, 1985) to run the PCA based on the correlation matrix and varimax rotation was applied to aid interpretation of the results. Following the Kaiser Principle, eigen values >1 was used to select significant factors (Liu et al., 2003; Reid and Spencer, 2009). In principal component analysis, a rule of thumb (mentioned in Liu et al., 2003; Reid and Spencer, 2009) is that regardless of whether values are positive or negative, a loading >0.6 is considered to be very high, >0.3 to be high, and <0.3 to be irrelevant. Therefore, in this study, a loading of <0.3 is considered as unimportant and have not been used for the interpretation of the output results.

CHAPTER 5

RESULTS AND DISCUSSION

5.1. Factors Influencing Sediment Yield in the Upper Ganga Basin

5.2. Particle Size Distribution of Suspended and Channel sediments

5.3. Weathering Intensity in the Basin

5.4. Sediment Source Characterization

5.4.1. Rare Earth Elements

5.4.2. Major Oxides

5.4.3. Environmental Magnetism and Heavy Minerals

5.5. Total Organic Carbon (TOC) flux

5.1. FACTORS INFLUENCING SEDIMENT YIELD IN THE UPPER GANGA BASIN

5.1.1. Variation in Sediment Load

Table 5.1 and Figure 5.1(a-b) show the seasonal and spatial variability in the total suspended sediments (TSS) and specific sediment yield (SSY) during the non-monsoon and monsoon season. Apart from an increase in TSS in the monsoon season (>85% in comparison to pre and post-monsoon season), the most important observation was the increase in the TSS concentration in the lower part of the Alaknanda basin.

Table 5.1 Total suspended sediments (TSS) carried by the Alaknanda River, its tributaries and the Ganga River during different seasons

Total Suspended Sediments (TSS) in mg/l			
Samples	**Post-monsoon, 2012**	**Pre-Monsoon, 2014**	**Monsoon, 2014**
A1	-	306.9	1641.2
A2	-	374.4	2226.9
A3	5.8	352.5	2066.4
A4	-	171	1821.8
A5	3.4	163.4	2272
A6	5.6	170.7	2081.8
A7	22.4	1468.1	3467
A8	97.3	147.5	3279.7
A9	195.3	148.5	3118.5
A10	198	170.6	3158.6
Dg	-	169.2	887.4
Bg	2.1	3.8	38.5
N	-	147.1	3393.9
P	3.1	137.8	580.7
M	-	179.6	813.7
B	26.1	167	747.9
G1	120.9	158.5	2377.6
G2	58	356.1	3312

5.1.2. Factors Influencing Sediment Yield

Sediment yield generation in the river basin is a very complex process and can be attributed to five major processes categorized as (i) climatic, (ii) hydrologic, (iii) topographic, (iv) geologic and (v) anthropogenic (Milliman and Syvitski, 1992; Restrepo et al., 2006; Ali and de-Boer, 2008). All these factors are highly influential in the UGB (catchment area of the Ganga River till Rishikesh). Table 4.3 show in detail the five factors divisible into 29 variables. Table 5.2 shows the quantitative value of each variable influencing the sediment load in the UGB. Using the long term previously published data of sediment load, precipitation, discharge and Geographic Information System (GIS) platform; following sections elaborately discuss all

the controlling variables that explain the temporal and spatial variation in sediment load carried by the Alaknanda River.

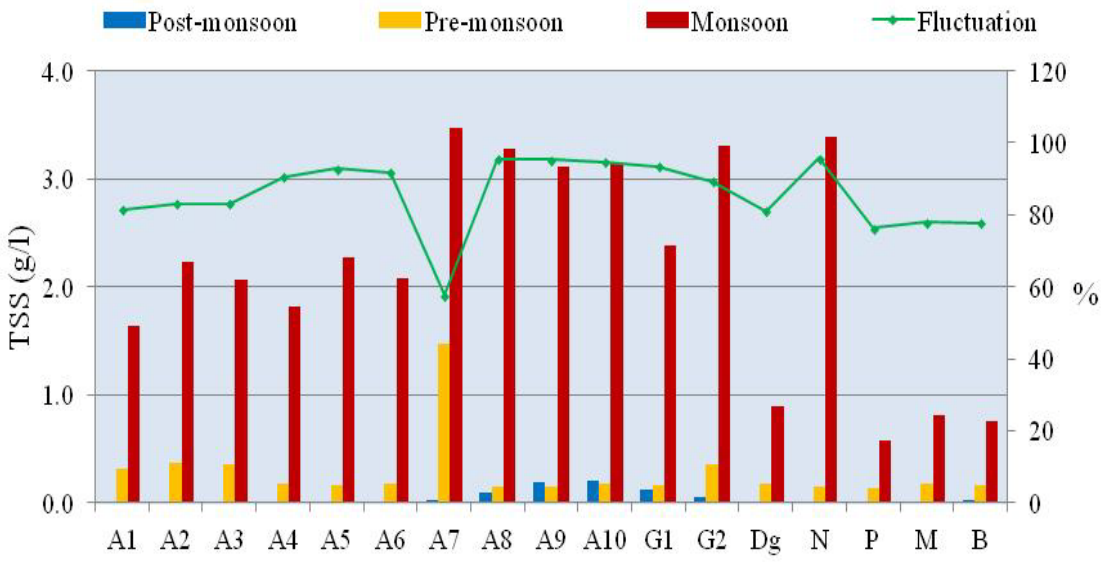

(a)

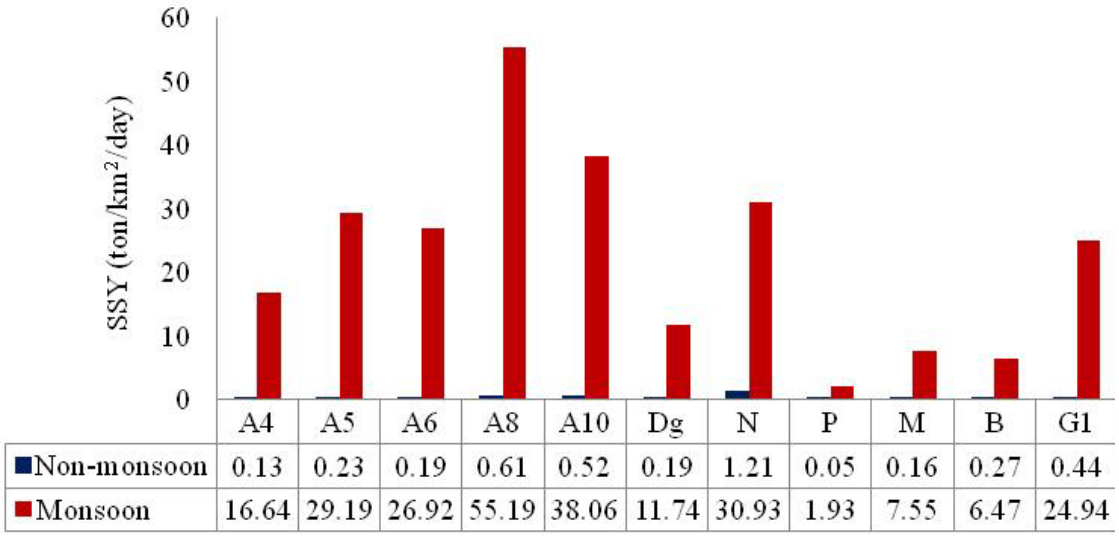

	A4	A5	A6	A8	A10	Dg	N	P	M	B	G1
Non-monsoon	0.13	0.23	0.19	0.61	0.52	0.19	1.21	0.05	0.16	0.27	0.44
Monsoon	16.64	29.19	26.92	55.19	38.06	11.74	30.93	1.93	7.55	6.47	24.94

(b)

Figure 5.1 (a) Seasonal and spatial variability in total suspended sediments (TSS); (b) Seasonal variation in the specific sediment yield (SSY) (Non-monsoon, here refers to minimum value during the post/pre-monsoon season)

Table 5.2 Hydrologic, topographic, climatic, geologic and anthropogenic controlling factors at different discharging sites

Factors/ Variables	**Srinagar** (Year 2004-05)	**Rudraprayag** (Year 1991-2005)	**Lambagarh** (Year 2002-05)	**Maneri** (Year 2004-05)	**Rishikesh** (Year 2004-05)
SL	$1.02*10^7$	$3.34*10^7$	$2.08*10^6$	$1.02*10^7$	$1.09*10^6$
SSY	1234.23	4203.61	1713.59	2562.04	56.77
Climatic					
Pmean	162.00	381.38	116.50	316.00	236.00
Pmax	186.00	502.70	138.00	381.00	250.00
Ppk	0.87	0.76	0.84	0.83	0.94
Tmean	21.76	19.04	11.20	16.63	23.13
Trange	18.09	16.63	6.40	4.90	18.77
Hydrologic					
Qmean	524.19	380.17	86.04	355	751.02
Qmax	1607.10	3279.84	557.63	1030	2471.72
Qpk	0.33	0.12	0.15	0.34	0.30
Geological					
CR	5.40	5.40	0.00	3.33	31.95
SR	94.61	94.61	100.00	96.67	68.05
LD	0.21	0.20	0.04	0.08	0.18
Dd	1.11	1.11	0.91	0.97	1.11
Dt	7.81	7.94	1.54	3.41	7.80
Topographic					
A	8252.11	7939.89	1214.93	3971.80	19124.30
Emean	3053.17	3119.29	4658.10	4040.93	3691.07
Emax	7464.00	7464.00	7464.00	6904.00	7464.00
Emin	529.00	608.00	2177.00	1278.00	335.00
E	6935.00	6856.00	5287.00	5626.00	7129.00
Epk	0.41	0.42	0.62	0.59	0.49
Er	63.03	74.47	187.02	60.36	42.49
HI	0.36	0.37	0.47	0.49	0.47
Lb	110.02	92.06	28.27	93.20	167.77
Lc	174.34	147.00	43.38	104.36	303.70
α1	33.61	35.00	13.36	64.12	26.69
αc	26.25	30.53	67.54	66.16	24.58
Anthropogenic					
SG	21.83	22.69	72.31	20.27	20.25
Cul	6.80	6.69	5.31	8.72	15.40
FL	4.14	3.85	0.00	6.71	6.69
Bl	10.48	10.89	21.30	8.82	8.81

Table 5.3 Correlation matrix showing the relation between specific sediment yield (SSY) and different controlling variables (strong correlations shown in bold)

	SSY	*Qmean*	*Qmax*	*Qpk*	*A*	*Emean*	*Emax*	*Emin*	*E*	*Epk*	*Er*	*HI*	*Lb*	*Lc*	*α1*	*αc*	*Pmean*	*Pmax*	*Ppk*	*Tmean*	*Trange*	*SG*	*Cul*	*FL*	*Bl*	*CR*	*SR*	*LD*	*Dd*	*Dt*
SSY	1.0																													
Qmean	-0.5	1																												
Qmax	0.4	0.6	1																											
Qpk	**-0.6**	0.6	-0.3	1																										
A	-0.5	0.9	0.6	0.3	1																									
Emean	-0.2	-0.6	-0.7	-0.1	-0.4	1																								
Emax	-0.2	0.1	0.4	-0.5	0.3	-0.3	1																							
Emin	0.1	-0.9	-0.8	-0.3	-0.8	0.9	-0.2	1																						
E	-0.2	0.9	0.8	0.1	0.8	-0.9	0.5	-1.0	1																					
Epk	-0.1	-0.6	-0.8	0.0	-0.5	1.0	-0.5	0.9	-0.9	1																				
Er	0.1	-0.9	-0.6	-0.6	-0.7	0.7	0.2	0.9	-0.7	0.6	1																			
HI	-0.4	-0.1	-0.6	0.3	0.0	0.8	-0.5	0.5	-0.6	0.9	0.2	1																		
Lb	-0.4	1.0	0.6	0.6	0.9	-0.6	0.1	-0.9	0.8	-0.5	-0.9	0.0	1																	
Lc	-0.5	1.0	0.6	0.4	1.0	-0.5	0.3	-0.9	0.8	-0.5	-0.7	-0.1	1.0	1																
α1	0.3	0.1	0.0	0.5	-0.1	-0.2	-0.9	-0.2	-0.1	0.0	-0.6	0.1	0.2	0.0	1															
αc	0.2	-0.8	-0.8	-0.1	-0.8	0.8	-0.6	0.9	-1.0	0.9	0.6	0.7	-0.7	-0.8	0.2	1														
Pmean	**0.7**	0.2	**0.7**	-0.1	0.2	-0.4	-0.4	-0.4	0.3	-0.3	-0.6	-0.2	0.3	0.2	0.6	-0.2	1													
Pmax	**0.8**	0.1	**0.7**	-0.2	0.0	-0.4	-0.3	-0.4	0.2	-0.3	-0.5	-0.2	0.2	0.0	0.6	-0.1	1.0	1												
Ppk	**-0.9**	0.6	-0.2	**0.6**	0.6	0.1	0.2	-0.2	0.3	0.1	-0.2	0.4	0.6	0.6	-0.3	-0.3	-0.5	-0.7	1											
Tmean	-0.3	1.0	0.7	0.5	0.9	-0.8	0.2	-1.0	0.9	-0.8	-0.9	-0.4	0.9	0.9	0.2	-0.9	0.3	0.2	0.4	1										
Trange	-0.2	0.8	0.8	0.0	0.8	-0.8	0.7	-0.9	1.0	-0.9	-0.6	-0.7	0.7	0.8	-0.3	-1.0	0.1	0.1	0.3	0.9	1									
SG	-0.1	-0.8	-0.6	-0.5	-0.6	0.8	0.3	0.9	-0.7	0.7	1.0	0.3	-0.8	-0.7	-0.6	0.6	-0.6	-0.6	-0.1	-0.8	-0.5	1								
Cul	-0.4	0.8	0.3	0.5	0.9	-0.1	0.0	-0.6	0.5	-0.1	-0.6	0.4	0.9	0.9	0.1	-0.4	0.1	0.0	0.7	0.6	0.4	-0.5	1							
FL	-0.2	0.8	0.4	0.7	0.6	-0.4	-0.5	-0.7	0.5	-0.3	-0.9	0.2	0.8	0.7	0.7	-0.4	0.5	0.4	0.3	0.7	0.3	-0.9	0.7	1						
Bl	0.0	-0.8	-0.5	-0.6	-0.6	0.7	0.3	0.8	-0.6	0.6	1.0	0.2	-0.8	-0.7	-0.7	0.5	-0.6	-0.5	-0.2	-0.8	-0.5	1.0	-0.6	-0.9	1					
CR	**-0.6**	0.9	0.5	0.3	1.0	-0.2	0.3	-0.6	0.6	-0.2	-0.5	0.2	0.9	0.9	-0.2	-0.6	0.1	-0.1	0.7	0.7	0.6	-0.4	1.0	0.6	-0.5	1				
SR	**0.6**	-0.9	-0.5	-0.3	-1.0	0.2	-0.3	0.6	-0.6	0.2	0.5	-0.2	-0.9	-0.9	0.2	0.6	-0.1	0.1	-0.7	-0.7	-0.6	0.4	-1.0	-0.6	0.5	-1.0	1			
LD	0.0	0.7	0.8	0.1	0.7	-1.0	0.4	-0.9	1.0	-1.0	-0.7	-0.8	0.7	0.7	0.0	-1.0	0.3	0.3	0.1	0.9	0.9	-0.7	0.3	0.4	-0.6	0.4	-0.4	1		
Dd	-0.1	0.8	0.8	0.1	0.8	-0.9	0.4	-1.0	1.0	-0.9	-0.7	-0.7	0.8	0.8	0.0	-1.0	0.3	0.3	0.2	0.9	1.0	-0.7	0.4	0.5	-0.7	0.5	-0.5	1.0	1	
Dt	0.0	0.8	0.8	0.1	0.7	-0.9	0.4	-1.0	1.0	-0.9	-0.8	-0.7	0.8	0.8	0.0	-1.0	0.4	0.3	0.1	0.9	0.9	-0.8	0.4	0.5	-0.7	0.5	-0.5	1.0	1.0	1

5.1.2.1. Climatic Factors

Precipitation and temperature are the active forces that directly control the erosion activities in the river basin. In the UGB, there exists a climatic variability. The temperature in the upper part of the basin is mostly cold during the entire year but during the months of June-September, heavy rainfall, and high temperature results in a high glacial melt that increases the discharge of the river (Singh and Hasnain, 1998; Chakrapani and Saini, 2009).

The presence of high amount of quartz and illite in the suspended load indicates the dominance of physical weathering processes in the UGB (Chakrapani, 2005 and Section 5.3.1). Due to fragile topography, heavy rains and high discharge, mass wasting events are quite common throughout the basin and Alaknanda-Bhagirathi River delivers >85% of the sediment load during the monsoon season (Fig. 5.1 and 5.2). The sediment yield during the non-monsoon and monsoon season of the year 2014 at Srinagar and Devprayag varied from 0.61 to 55.19 ton/km^2/day and 0.52 to 38.06 ton/km^2/day respectively (Fig. 5.1b). Figure 5.3 show the landslide intensity map prepared by Shukla et al. (2014). The map shows that most of the landslides are concentrated in the middle part of the basin (the region between Vaikrita and Ramgarh Thrust) that receives the highest rainfall in the catchment area (Fig. 4.4b shows rainfall map of the UGB).

The amount and intensity of rainfall may resist or advance the erosion rate in the basin. Figure 5.1 and 5.2 shows that during the high rainfall months of June-September, the maximum amount of sediment is transported by the Alaknanda, Bhagirathi, and the Ganga River. Table 5.3 shows a strong correlation of R^2= ~0.8 exist between the maximum rainfall (Pmax) and SSY. Figure 5.4(a-d) shows the correlation between mean monthly precipitation (Pmean) and total suspended sediments (TSS) at different discharging sites. However, precipitation peakedness (Ppk) that indicates the high intensity of rainfall varies from 0.20 to 1.02. Rainfall is highly variable in the Alaknanda basin, not only seasonally but day-to-day also. Ppk showed the negative correlation (R^2= -0.9) with TSS (Table 5.3). This may be attributed to the lag time between the high intensity rainfall event and erosion intensity of the basin. The large occurrence of the rocky outcrop (mostly silicate rocks), shallower mountainous soil and spatial erodibility of the basin (due to diverse lithology) may restrict the sediment peakedness during the intense rainfall events.

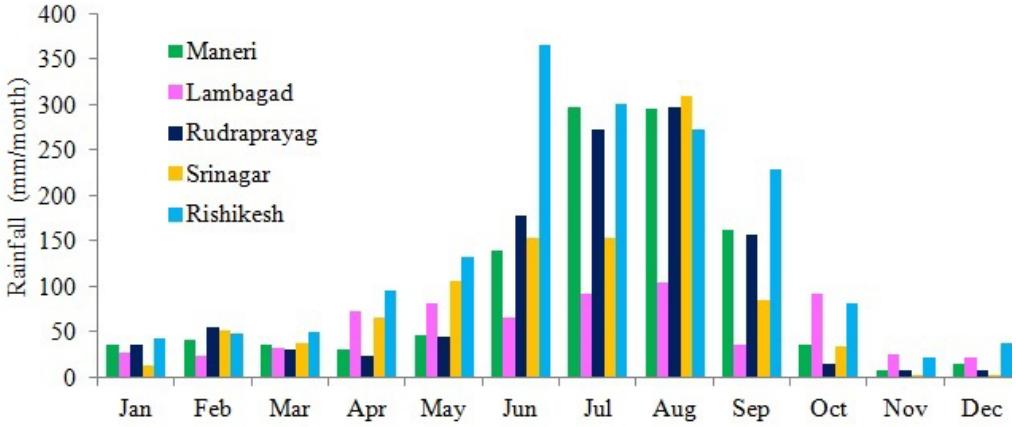

(a)

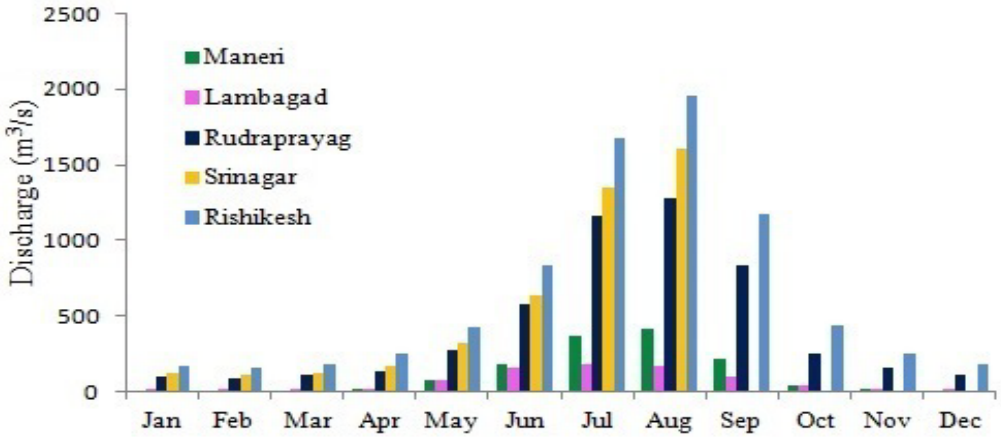

(b)

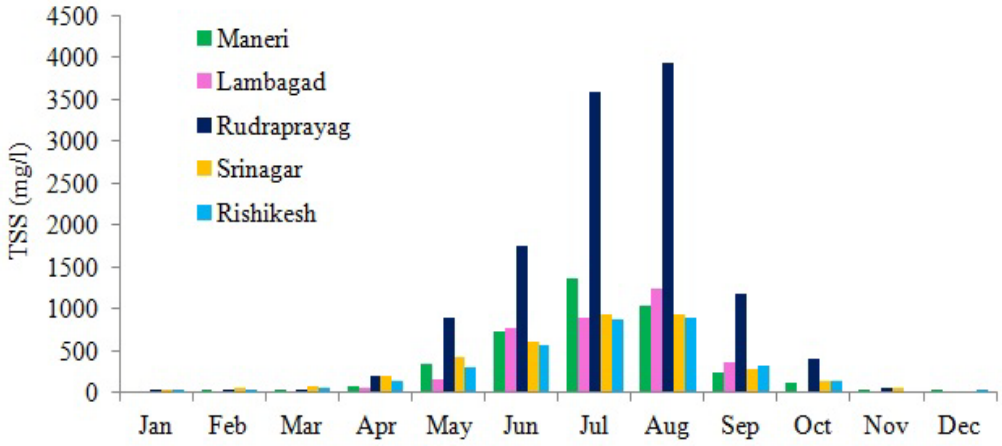

(c)

Figure 5.2 (a) Monthly rainfall variation in the UGB (IMD and TRMM data); (b) Monthly variation of discharge in the UGB (AHEC, 2011); (c) Monthly variation of total suspended sediments (TSS) in the UGB (CWC India, Chakrapani and Saini, 2009 and JPHP, Joshimath)

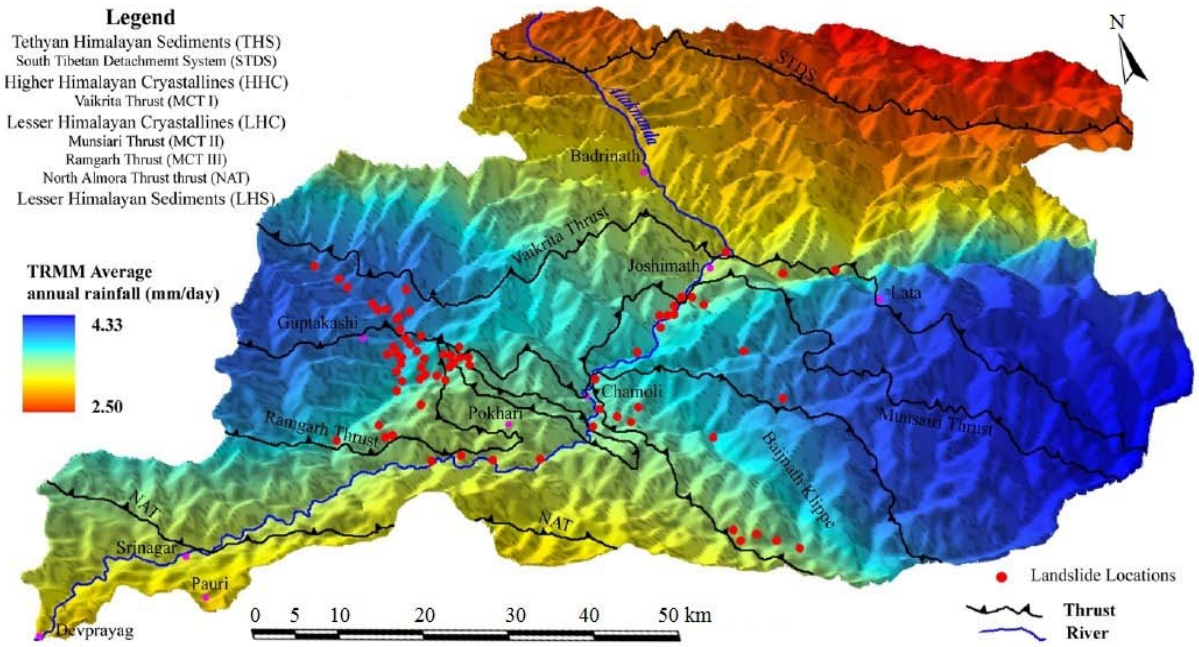

Figure 5.3 3D Tilted average annual rainfall map of Alaknanda River basin showing landslides concentrated along the region of high rainfall (adapted from Shulka et al., 2014)

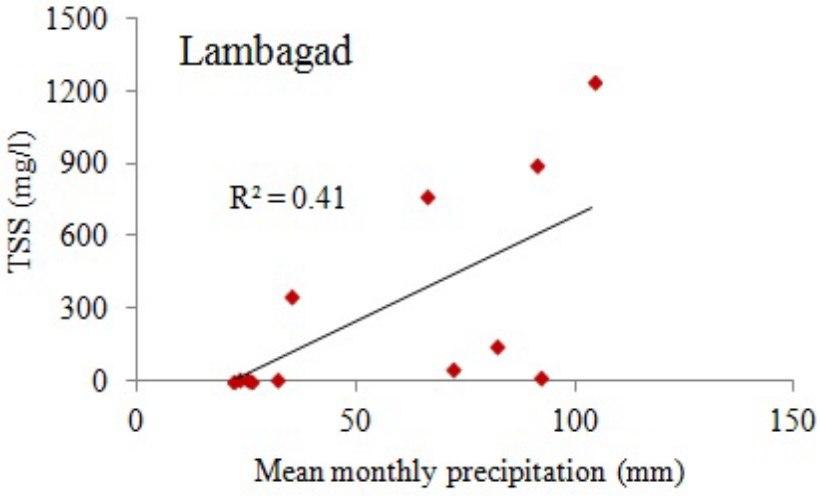

(a)

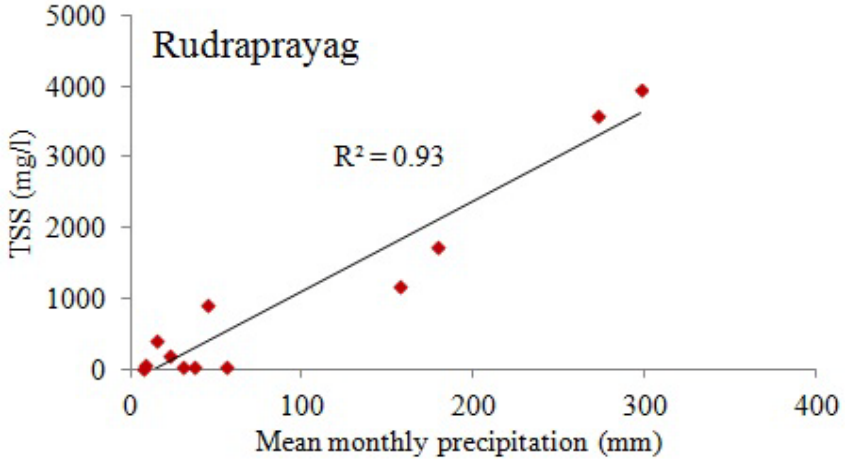

(b)

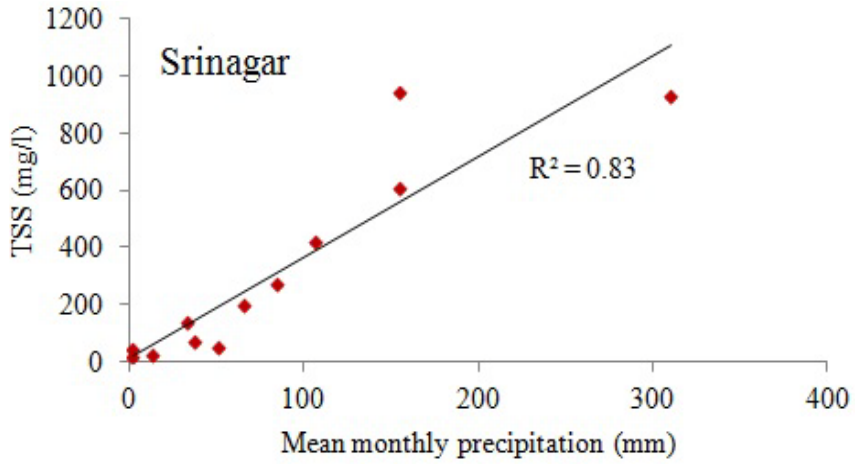

(c)

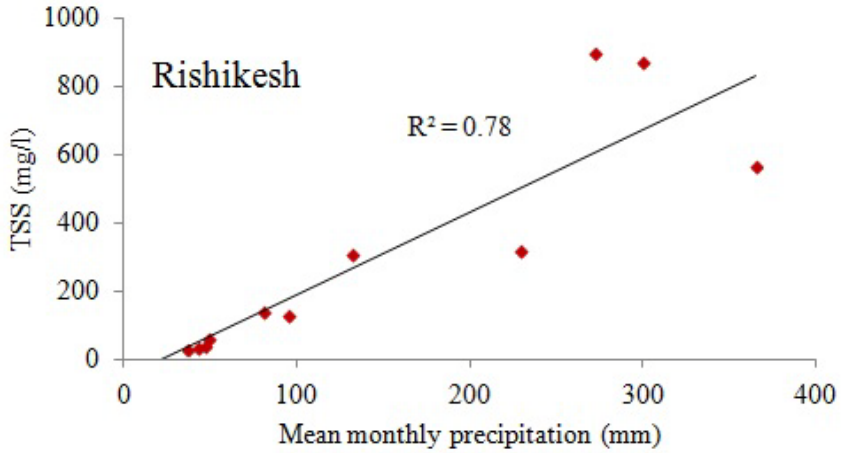

(d)

Figure 5.4 Correlation of monthly rainfall with TSS carried by the (a) Alaknanda River at Lambagad (source: TRMM data and JPHP, Joshimath); (b) Alaknanda River at Rudraprayag (source: IMD and CWC, India); (c) Alaknanda River at Srinagar (source: TRMM data and Chakrapani and Saini, 2009); (d) Ganga River at Rishikesh (source: TRMM data and Chakrapani and Saini, 2009)

5.1.2.2.Hydrologic Factors

The foremost hydrologic factor that directly influences the sediment yield in the river basin includes discharge (Q). Table 5.3 shows that after precipitation, discharge of the river shows the strongest relation with the sediment load. In the Himalayan Rivers, discharge is contributed by monsoon rainfall, snow and glacier melt and deep groundwater (Andermann et al. 2012a). Precipitation and discharge have a close association in the UGB (Fig. 5.2a-b). The study of Andermann et al. (2012a, b) highlights that total discharge (Q) of the river can be separated into direct discharge (Qd, river discharge fraction from all precipitation events) and baseflow discharge (Qb, river discharge fraction from groundwater). The relationship between Qd and TSS revealed that Qd is a better proxy to estimate suspended sediment fluxes and TSS in the Himalayan Rivers is dependent on the amount of water draining from the near surface/slopes. During the monsoon season, Hasnain and Chauhan (1993) and Hasnain and Thayyen (1999) observed permafrost and rainfall as an important source of sediment; near the proglacial source Alaknanda River carried 2.16 gram/litre of TSS. The long term discharge and TSS data of Rudraprayag and Lambagad proved that discharge is the key factor that controls the amount of sediment carried by the river. Figure 5.5(a-b) and 5.6(a-b) display three distinct regimes exist in the UGB: low discharge-low TSS, high discharge-high TSS and the discharge peakedness that does not correspond to sediment peakedness at Rudraprayag and Lambagad. This indicates that the effective sediment discharge of the river does not occur during the highest flow and during peak discharge event dilution of sediment may happen (Figure 5.5b and 5.6b). Since, monsoon contribute significantly to the river discharge (Qd) which is important to evacuate the erosional mass fluxes, the Alaknanda-Bhagirathi River system is supply-limited and hillslopes as contributing source are transport-limited. The Upper Continental Crust (UCC) normalized SiO_2>1 and the low amount of Al_2O_3, P_2O_5, CaO present in the channel sediments suggest that dilution effect predominates during the transportation of sediments in the Alaknanda River (Section 5.4.2). A moderately good correlation between TSS and dissolved organic carbon (DOC) in the Alaknanda and Ganga River at Devprayag also suggest that as the concentration of TSS increases the dilution effect predominates resulting in high DOC concentration (Section 5.5.1). Thus, due to a high energy environment prevailing in the UGB (because of steep terrain and high discharge), fresh and labile TSS is consumed quickly and locally without significant transport downstream and may restrict sediment peakedness during the precipitation and discharge peakedness (Ppk and Qpk) events.

It can also be interpreted that during the storm events, the Alaknanda-Bhagirathi Rivers remain sediment deficient and may incise the channel. Singh et al. (2012) mentioned that if

discharge increases and sediment supply decreases, the Alaknanda River incises the channel. Juyal et al. (2010) mentioned that strengthened monsoon supported by tectonic activities enhance the erosion rate and thus incision occurs in the Alaknanda valley. Singh et al. (2012) observed valley fill deposits (around the Srinagar area) to be a significant source of sediments having an erosion rate ~3350 ton/km^2/year^{-1}. During the mega floods in the year 2013, incision was noticed around Srinagar and Bhainswara towns by Rana et al. (2013). These studies were all concentrated on a local scale but give a glimpse of the fluvial erosion potential of the Alaknanda-Bhagirathi Rivers; however, this demands detailed field work in the Alaknanda-Bhagirathi valley.

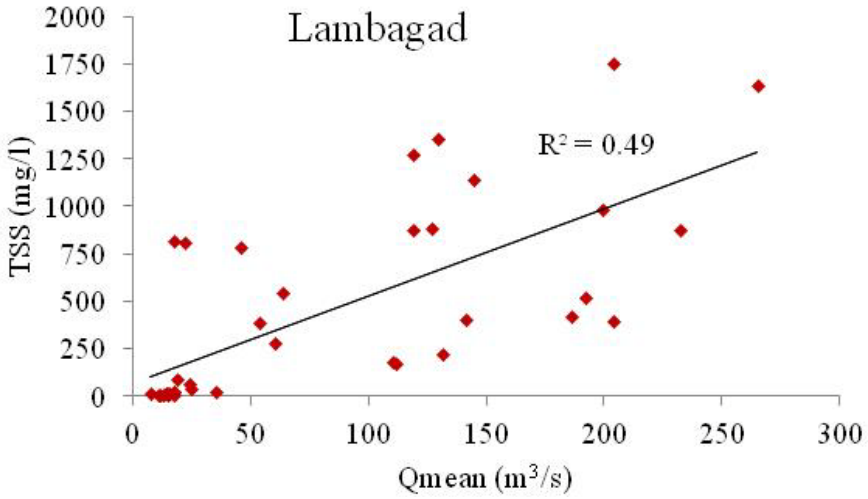

(a)

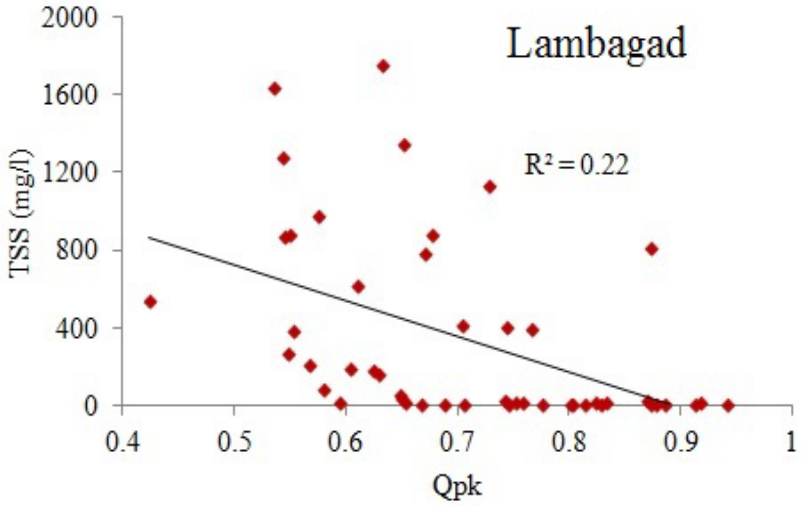

(b)

Figure 5.5 (a) Correlation between the monthy Qmean and TSS at Lambagad (year 2002-2005); (b) Correlation between the monthly Qpk and TSS at Lambagad (year 2002-2005)

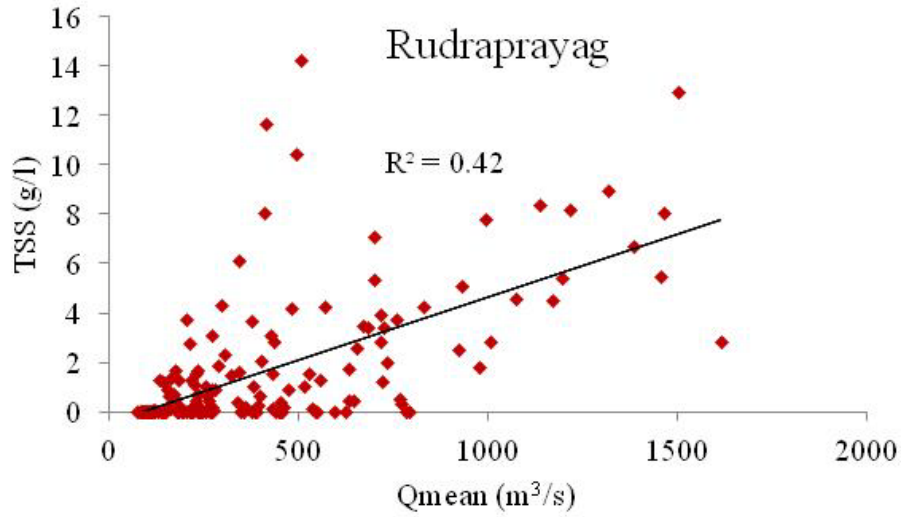

(a)

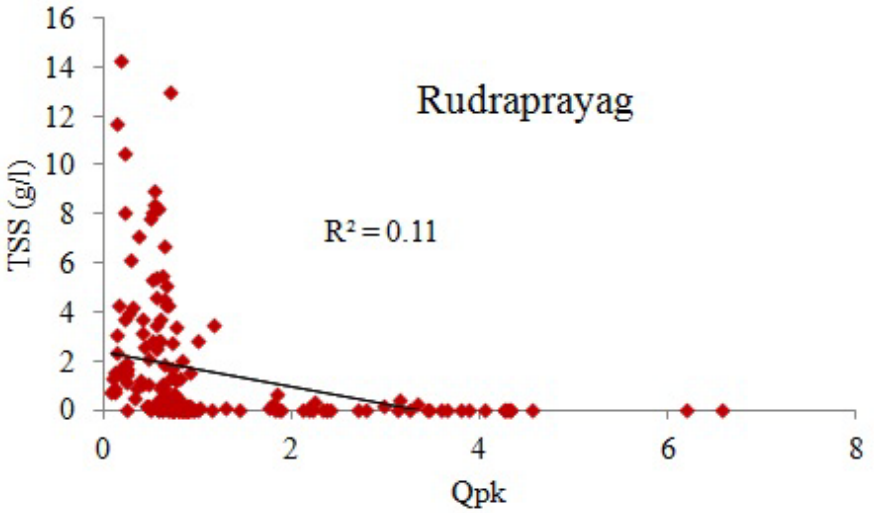

(b)

Figure 5.6 (a) Correlation between the monthly Qmean and TSS at Rudraprayag (year 1991-2005); (b) Correlation between the monthly Qpk and TSS at Rudraprayag (year 1991-2005)

5.1.2.3.Geological Factors

Geology exerts a control over stream flow primarily by controlling the basin permeability (e.g. granite versus limestone). Lithological control on permeability is affected by porosity, joints and fractures present in the rocks.

***Lithology of the basin*:** Lithology of the basin has a huge influence on the mechanical erosion within the river channel (Chakrapani and Saini, 2009). Table 5.3 points the role of lithology in controlling sediment yield in the basin. A moderate positive relation (R^2= 0.6) was found between the percentage of silicate rocks (SR) and SSY (Table 5.3). The role of geology can be better understood by understanding the sediment load variation. The high sediment load in the lower part of the basin (Fig. 5.1a) is due to the presence of low-grade metamorphic rocks such as phyllite and quartzite, comparatively low slope and the high anthropogenic activities (Fig. 4.5b, 4.6 and 4.7a). At Karnaprayag (sample A5) and Srinagar (sample A7 and A8) where the river plain is quite wide, no decrease in sediment load was observed (Fig. 5.1a). The presence of easily erodible rocks (the presence of basic rock intrusions at Karnaprayag and fractured phyllites at Srinagar) enable the river to carry high sediment load. During the non-monsoon season, clasts of phyllites are seen in the river channel and around banks at Srinagar. However, the additional discharge from the Pinder River to the Alaknanda River can also increase the capacity of the river to carry high sediment load as reported at sampling site A5.

The role of lithology in controlling sediment yield can be accurately determined by using the geochemical indices. Previous studies of Chakrapani (2005), Chakrapani et al. (2009) and Garzanti et al. (2011) show that felsic rocks dominantly supply sediment load and carbonate rocks supply dissolved load to the Ganga River. A moderately weak relation (R^2= -0.6) was found between the percentage of carbonate rocks (CR) and SSY (Table 5.3). Sections 5.4.1, 5.4.2 and 5.4.3, elaborate on the control of different rock formations supporting high sediment load in the UGB based on the geochemical and mineralogical composition of sediment.

***Lineament density*:** Lineaments are the zones of weakness or the expression of faults controlling hydrogeological settings of the basin (Hung et al., 2005; Rao et al., 2011). Active thrust zones- Main Central Thrust (MCT) and STDS (South Tibetan Detachment System) pass through this zone that influences the structural stability of the area promoting landslides and earthquakes. Due to active neo-tectonics in the UGB, lineaments are considered to be of structural origin (BHUVAN NRSC, map of lineaments, Fig. 4.7b). Lineament Density (LD) in the sub-basins varies from 0.04-0.21 km^{-1} (Table 5.2). High structural activities in the Srinagar and Rudraprayag drainage areas result in high LD. River flowing through the fractured terrain can generate high sediment load. Shukla et al. (2014) observed that 50% of landslides in the

Alaknanda valley are concentrated near the zones of high to very high tectonic activities (Fig. 5.3). But it's the high intensity monsoon rains during the months of June-September which induce maximum landslides (Section 5.1.2.1 and 5.1.2.2 and Table 5.3).

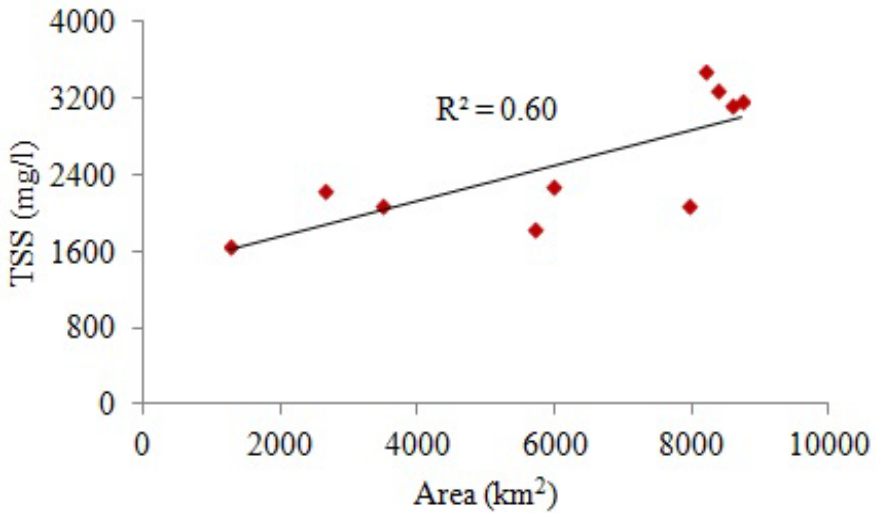

Figure 5.7 Correlation between TSS carried by the Alaknanda River and drainage area of each sampling point (catchment area extracted using the spatial analyst tool in ARCMAP 10.2 software)

5.1.2.4.Topographic Factors

The topography of the basin has a huge influence on the discharge and sediment load of the river. The variables such as elevation (E), relief, basin length (Lb), hypsometric integral (HI) and slope (α) does not strongly seem to influence the sediment yield of the basin (Table 5.3). The basin parameters that moderately influence the sediment load in the basin include the catchment area (A) and the channel length (Lc). The highest R^2= -0.5 value, relates to the catchment area (A) and the channel length (Lc) (Table 5.3). An inverse relation between the sediment load and drainage area has been widely reported for most of the river basins (Milliman and Meade, 1983; McLennan, 1993; Berner and Berner, 1996).

However, in this research, it was noticed that sediment load increases downstream (Fig. 5.1a). Figure 5.7 also shows that there exist a moderately positive relationship between the drainage area and the TSS carried by the Alaknanda River. This explanation indicates that at a small and large scale the results may vary and that apart from the drainage area, the factors such as lithology and anthropogenic disturbance can also impact the result. The lower part of the basin is composed of low grade metamorphic rocks such as phyllites, quartzites and dolomites. Presently, anthropogenic presence in the form of dams, reservoir, habitation and road constructions are quite high in the UGB than the decade ago (year 2005-2006).

5.1.2.5.Anthropogenic Factors

Land use and land cover change (LULCC) acts as an important variable controlling the sediment production and transportation. LULC classes influence the surface roughness, soil structure, soil composition, infiltration rate and hydraulic conductivity of the basin (Wei et al., 2009 and Yan et al., 2013). The LULC map of the year 2005 shows that the forest covered ~45% of the total watershed area, followed by the glacial and snow cover that accounts for ~20% of the total area. Agricultural land in the UGB covered ~15% and built-up covered only 0.1% of the total area (Fig. 4.6 and Table 3.5). Table 5.3 shows the absence of any strong relation between the sediment yield and land cover classes of the watersheds. In the absence of data (or just based on the LULC map), anthropogenic involvement in promoting erosion and high sediment yield cannot be accurately determined as built-up covers only 0.1% of the total land area. However, previous studies shed some lights on the relation between anthropogenic disturbances and the sediment erosion. The studies of Barnard et al. (2001) and Wasson (2003) mentioned that the majority of landslides in the UGB occurred due to road construction. Wasson (2003) observed that in the year 1999, two-third of the landslides occurred due to human activities; in the year 2010, ~300 landslides of various dimensions were found to be riddled around the National Highway-58 (Sati et al., 2011). Tourism in the UGB is quite high and road construction activities in the mountainous terrain can disturb the natural balance. In the year 2005-2006, major hydropower projects at Tehri, Maneri and Vishnuprayag were operating in the UGB that may influence erosion processes. But disagreeing to all these studies, Lupkar et al. (2012) using ^{10}Be calculated the denudation rate in the Ganga Basin to be 1.0-1.1 mm year^{-1}. This calculated denudation rate is found to be equilvalent to the gauged fluxes and thus, contradict the common view that landuse changes in the Himalayas have promoted erosion. Takata et al. (2009) showed that due to anthropization in Asia, the intensity of monsoon has decreased over the few last centuries (Takata et al. (2009). Section 5.1.2.1 explains rainfall as a dominant controlling factor promoting sediment erosion in the UGB.

5.2. PARTICLE SIZE DISTRIBUTION OF SUSPENDED AND CHANNEL SEDIMENTS

5.2.1 Particle Size Distribution of Suspended Sediments

A good amount of suspended sediments obtained during the post-monsoon and monsoon season were used for grain size analysis. Figure 5.8(a) shows that the mean grain size (Ms) of the TSS in the Alaknanda basin is dominantly coarse silt. Both the temporal and spatial

variability was noticed in all the samples. The mean grain size (Ms) varied from 8.9-56.3 µm and 25.3-87.3 µm in the post-monsoon and monsoon season respectively (Fig. 5.8a and 5.9).

During the monsoon season, >85% of the annual sediment load is transported, of which <63µm (silt+clay) constituted ~47-89% and only 0-2.5% constituted of clay grade size, whereas in the post-monsoon season river dominantly supplied finer sediments (Fig. 5.8a and Fig. 5.9). Supported by high discharge, high TSS in the river increases the erosivity of the channel and strengthens the shear flow, thereby increasing the capacity of the river to carry large sediments enriched in sand grade size (Xu, 2002). However, Fig. 5.10(a) depicts that the relationship between discharge and Ms is not so strong in the Alaknanda basin. Xu (2002) remarked that allochthonous input of sediments from gully erosion are mostly unsorted. In the Alaknanda basin, most of the landslides dump debris directly into the river (field observation) and may obstruct the relation between discharge and mean grain size and also the downstream fining pattern of grain size distribution. The specific stream power (SSP) which is a function of slope and discharge (Bagnold, 1960, 1977) also shows poor correlation with Ms, however, a moderately positive relation was found between TSS and Ms (Fig. 5.10b,c). The study of Whipple et al. (2000) and Sklar and Dietrich (2001) highlighted that the sediment supply control the bedrock incision more than stream power. During the monsoon season in the Alaknanda basin, high TSS caused the strong abrasion of bedrock and resulted in larger grains carried by the river.

Spatial factors such as lithology, frequent change in slope and sediment load contribution from the tributaries seemed to influence the grain size distribution. The steep slope and high elevation in the Higher Himalayas do not support large grain size in the river channel and the largest sediment size was found at the sampling site A10 and G1. Whipple and Meade (2004) observed that the critical joint spacing in the rock and high discharge aided the abrasion and plucking processes. At Devprayag, a large outcrop of highly jointed and fractured phyllites occurs (Valdiya, 1980) and high discharge during both the post-monsoon and monsoon season supports high sediment load with coarse grains (as found in samples A10 and G1) (Fig. 5.1 and 5.8a). Deposition of large sediments in the Srinagar reservoir resulted in finer grain sizes in sample A7.

Figure 5.9 shows sorting (S) varied from 1.2-3.1Φ and 1.2-2.5Φ during the post-monsoon and monsoon season respectively indicating the prevalence of poorly sorted grains with symmetrical to fine skewed and mesokurtic distribution. High gradient, glacial contribution and the lesser distance of transport can be the reason for the enrichment of coarse and poorly sorted nature of suspended sediments (Pandey et al., 2002; Panwar et al., 2016). Most of the

suspended sediment samples showed unimodal distribution as a result of the efficient mixing of water and sediment load due to high river power (resulting from high discharge and steep slopes) and location of sampling sites 2-3 km downstream of confluence (Fig. 4.1). The bimodal distribution in the samples A2 and A6 pointed the role of tributaries (Dhauli Ganga and Mandakini River) in influencing the grain size distribution. In the future, the detailed sampling of Dhauli Ganga and Mandakini Rivers can give a better explanation of the influence of these tributaries on the Alaknanda River. However, based on sample Dg and M, it can be concluded the Dhauli Ganga River carries finer sediments and Mandakini carries larger sediment size than the Alaknanda River and after the confluence exerts their influence on the particle size distribution of the Alaknanda River.

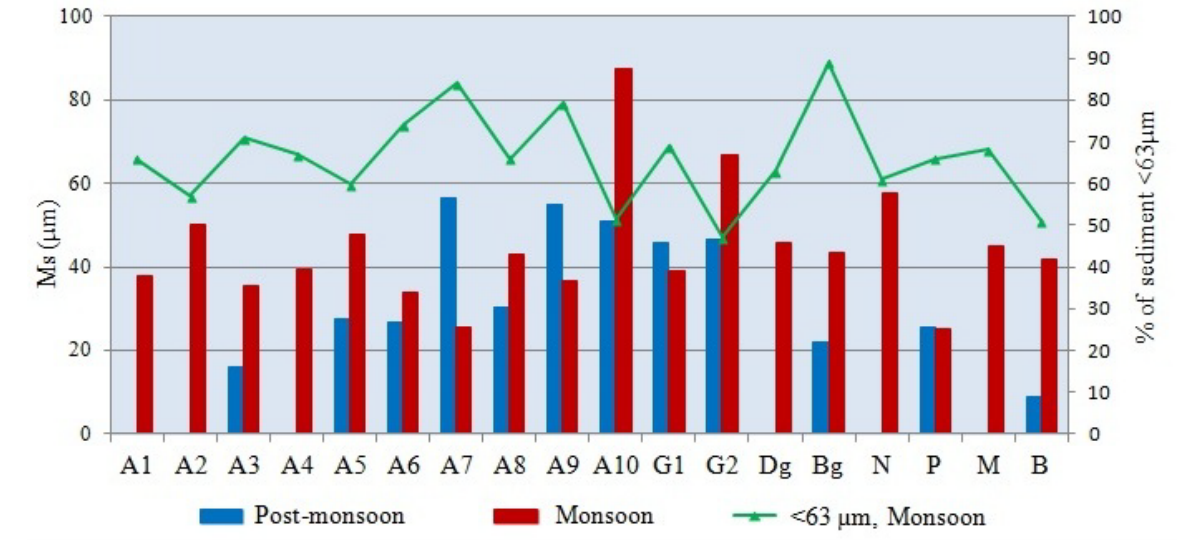

(a)

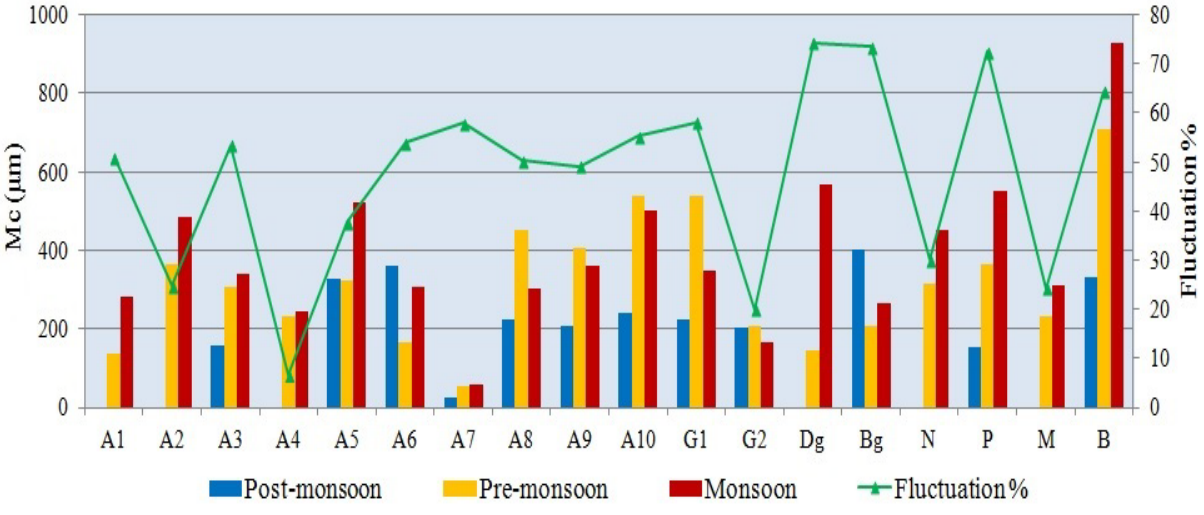

(b)

Figure 5.8 Variation in mean size for (a) suspended sediments; (b) channel sediments

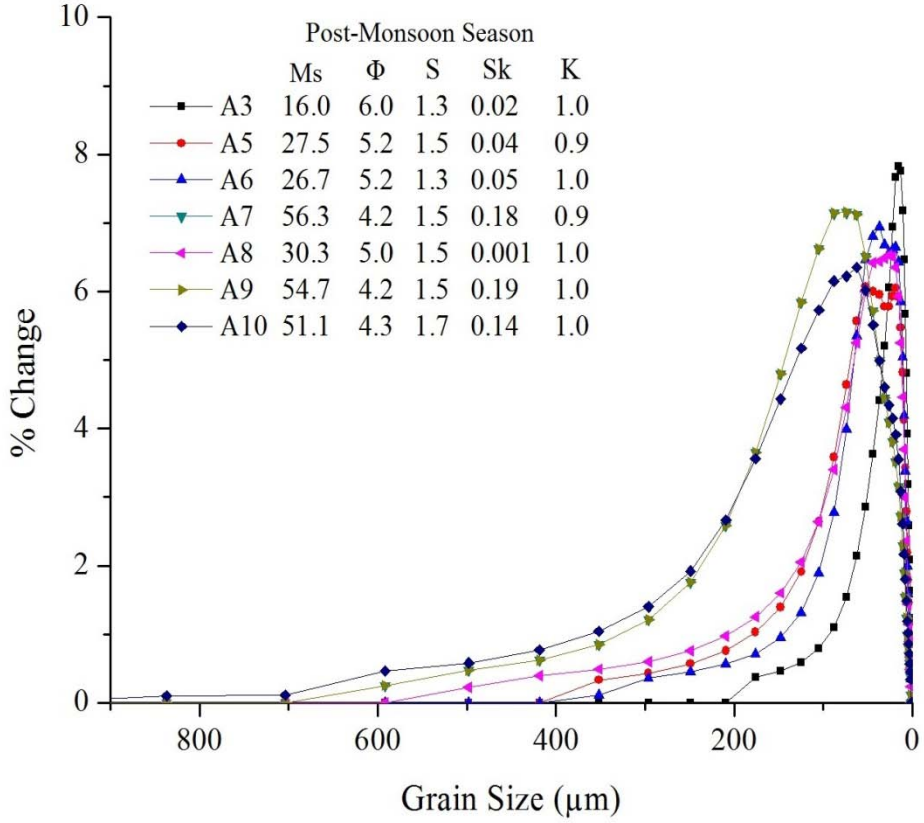
Post-Monsoon Season
Ms Φ S Sk K
A3 16.0 6.0 1.3 0.02 1.0
A5 27.5 5.2 1.5 0.04 0.9
A6 26.7 5.2 1.3 0.05 1.0
A7 56.3 4.2 1.5 0.18 0.9
A8 30.3 5.0 1.5 0.001 1.0
A9 54.7 4.2 1.5 0.19 1.0
A10 51.1 4.3 1.7 0.14 1.0
% Change
Grain Size (µm)
0
2
4
6
8
10
800
600
400
200
0

(a)

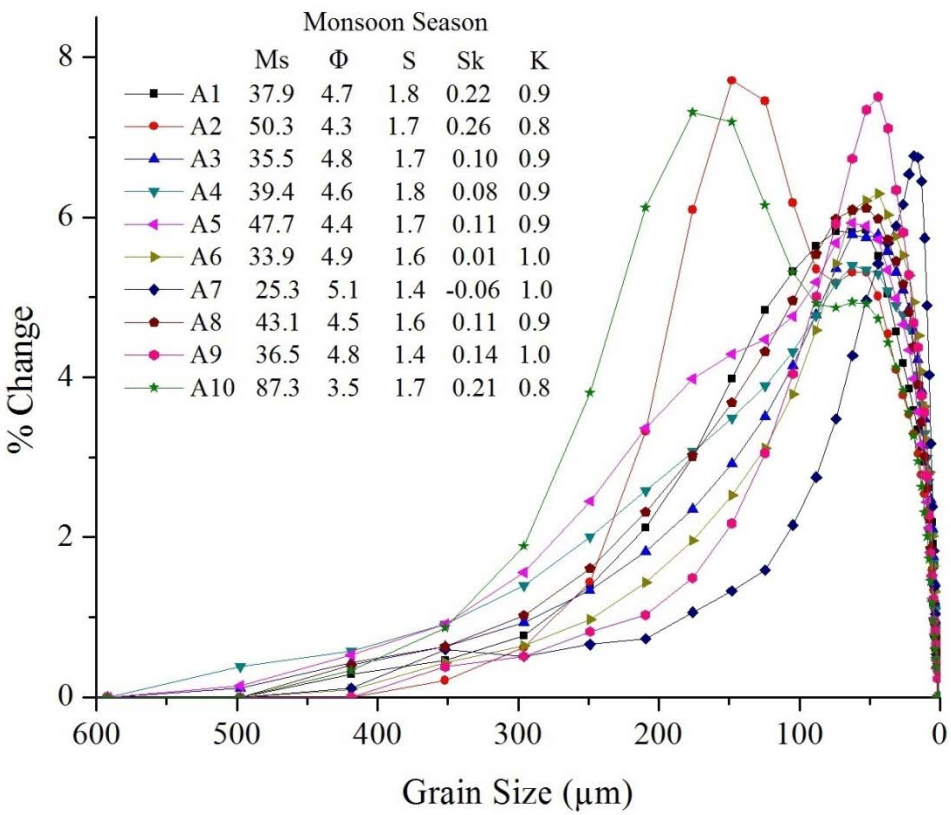
Monsoon Season
Ms Φ S Sk K
A1 37.9 4.7 1.8 0.22 0.9
A2 50.3 4.3 1.7 0.26 0.8
A3 35.5 4.8 1.7 0.10 0.9
A4 39.4 4.6 1.8 0.08 0.9
A5 47.7 4.4 1.7 0.11 0.9
A6 33.9 4.9 1.6 0.01 1.0
A7 25.3 5.1 1.4 -0.06 1.0
A8 43.1 4.5 1.6 0.11 0.9
A9 36.5 4.8 1.4 0.14 1.0
A10 87.3 3.5 1.7 0.21 0.8
% Change
Grain Size (µm)
0
2
4
6
8
600
500
400
300
200
100
0

(b)

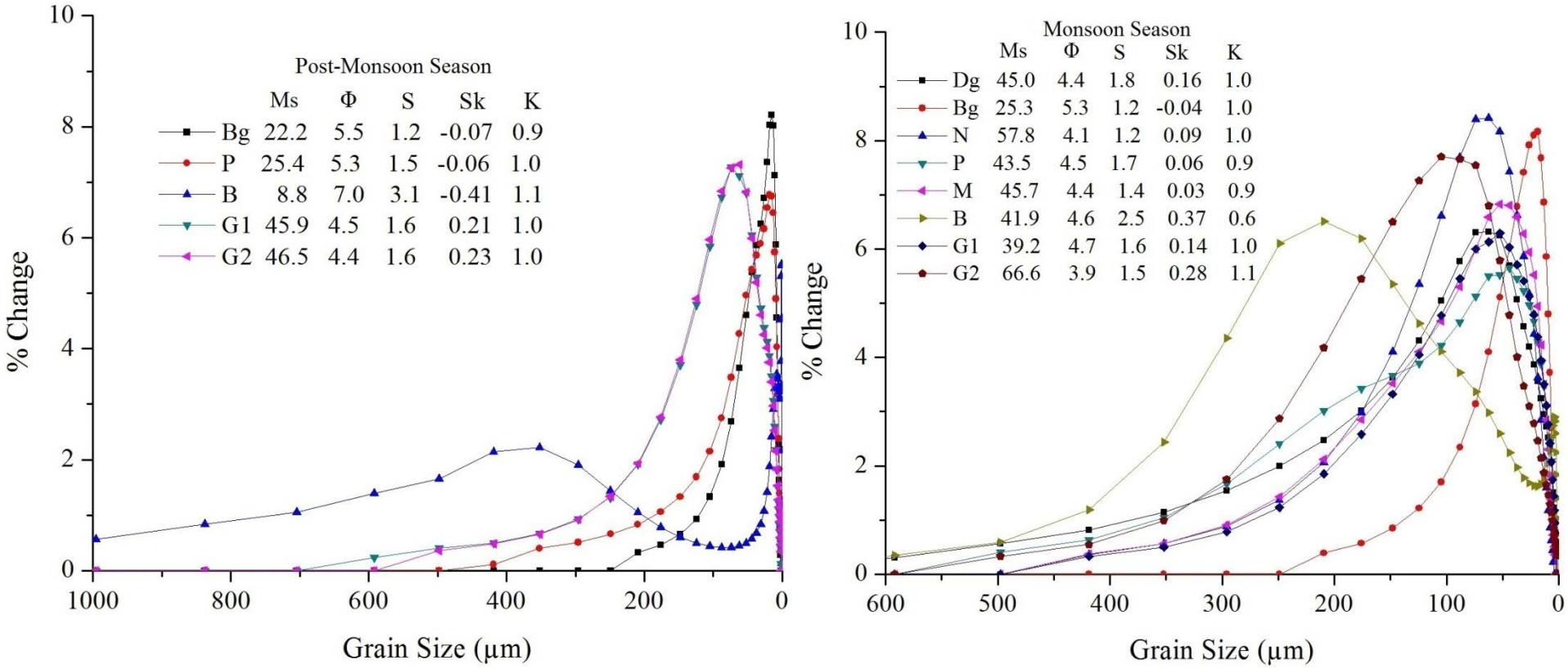

(c) (d)

Figure 5.9 Variation in grain size distribution of suspended sediments and statistical parameter calculated using Folk and Ward (1957) for (a) Post-monsoon suspended sediments of the Alaknanda River; (b) Monsoon suspended sediments of the Alaknanda River; (c) Post-monsoon suspended sediments of the tributaries and the Ganga River; (d) Monsoon suspended sediments of the tributaries and the Ganga River [Ms – suspended sediment mean grain size (in µm), Φ= phi size ($\Phi = -\log_2 d$), S-sorting, Sk-Skewness, K-Kurtosis]

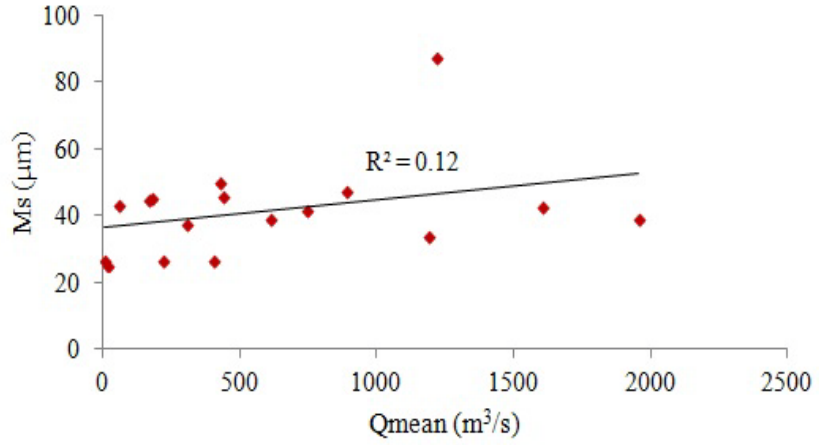

(a)

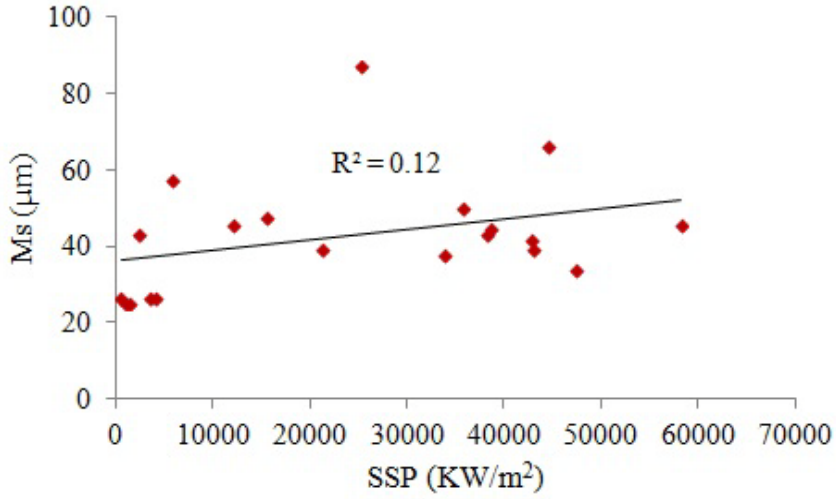

(b)

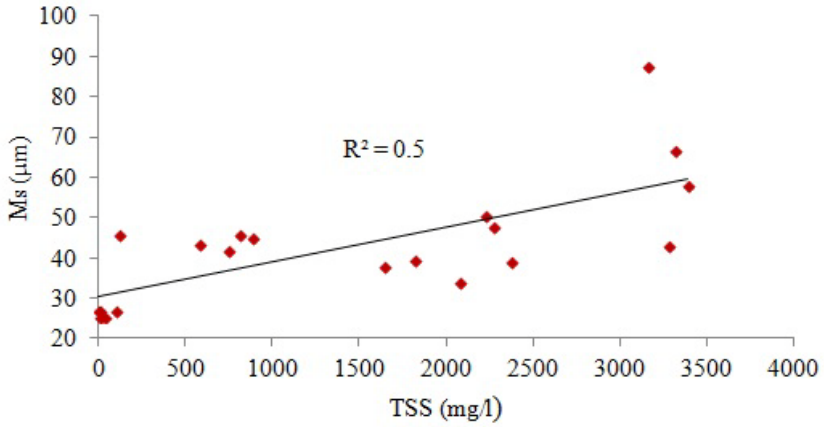

(c)

Figure 5.10 Correlation of suspended mean grain size (Ms) with (a) discharge (Qmean); (b) specific stream power (SSP); (c) total suspended sediments (TSS)

5.2.2. Particle Size Distribution of Channel Sediments

Figure 5.8(b) shows the spatial and temporal variability in the mean size of the channel sediment (Mc) and prevalence of mostly medium to coarse sand in the post-monsoon, pre-monsoon, and monsoon season. In all the three seasons, similar to suspended sediments, there seems no spatial downstream trend for Mc (Fig. 5.8b). The complex geology, additional discharge from tributaries and mountainous topography may have averted the downstream pattern in the Upper Ganga Basin. Figure 5.11(a-f) shows an overview of the seasonal grain size distribution of the Alaknanda River and its tributaries. Smallest grain size was found at Kalyasaur (A7), the sample collected near the reservoir. The largest sediment size was found to be of the Bhagirathi River (Sample B) during the pre-monsoon and monsoon season due to scouring of bed sediment and settlement of fine grains in the Tehri Dam located upstream. Sorting (S) varied from 0.07-0.9Φ, 0.6-2.0Φ and 0.5-2.0Φ during the post-monsoon, pre-monsoon and monsoon season respectively. During the post-monsoon, sediments were found to be moderately sorted, whereas poor to moderate sorted during the pre-monsoon and monsoon season. In terms of skewness, in all the seasons, sediments belonged to fine to symmetrically skewed category. Mesokurtic to platykurtic samples were common in the Alaknanda River and its tributaries (Fig. 5.11).

Similar to the suspended sediments, channel sediments also showed unimodal grain size curves in all the seasons (Fig. 5.11). The somewhat similar lithology in sub-watersheds of the Alaknanda basin and the location of samples ~2-3 km downstream of the confluence (resulted in the better mixing of sediments) may have averted the bimodal distribution in the high energy environment. The bimodal distribution was noticed only in samples Dg, A2, B and G2 collected during the monsoon season. Similar to the suspended sediments, channel sediment samples B and A2 showed the bimodal nature confirming the influence of dam and tributary Dhauli Ganga in influencing the grain size distribution. The selective winnowing of fine sediments downstream of dam and release of finer backfill from the dam during the monsoon may result in the bimodal distribution at the sample site B and A2. Bimodality in the Dhauli Ganga (sample Dg) demands detail study of the tributary. Bimodality in sample G2 indicate sediments are sourced from the anthropogenic activities (sample G2 was collected from Rishikesh, a first major town in the UGB).

A peculiar feature noticed during the monsoon, 2014 sampling was the downstream decrease in grain size after sample location A7 (i.e. Srinagar), the grain size of the samples A8, A9, A10 during the monsoon season was much smaller than that estimated during the pre-monsoon season of the year 2014 (Fig. 5.8b). The discrepancy shown in the grain size of the

river from Srinagar to Devprayag can be attributed to flow conditions. Figure 5.12 show the images of sampling time and the extremely low flow condition of the Alaknanda River at Devprayag during the pre-monsoon, 2014. At the low flow condition, the river is capable of generating small shear stress and thus transports bed fines that result in the enrichment of coarse grained sediment on the channel. Similar results were also observed by Draut et al. (2011), who inferred that after the construction of the dam on River Elwha, coarse sediments increased downstream. Xu (1996); Xu (2007) observed that reservoir construction influenced the grain size distribution downstream of the reservoir on the River Hanjiang, China, first by trapping the upstream sediments and second by scouring the downstream channel. A similar observation was also shown by the Bhagirathi River at Devprayag (low TSS and large channel sediment with bimodal distribution) (Fig.5.1a, 5.8b and 5.11), which gives an idea about the change in the grain size distribution of the Alaknanda River after the operation of the Srinagar dam.

The present study indicates a significant influence of man-made interventions in grain size distribution of the Alaknanda River. Since channel morphology is influenced by the sediment load and grain size, the Alaknanda river channel will change substantially after the damming. The change in sediment size can influence the sediment composition, as it is seen that coarse sediments are characterized by lithic fragments and fine sediments are generally enriched in heavy minerals and contains lesser quartz content. Sediment size distribution is vital for the aquatic ecosystem. Wohl et al. (2015) mentioned that benthic invertebrates are sensitive to excess fine sediment on the channel and thrive best in the coarse sediments. In the future, these observations indicate that damming the Alaknanda basin will affect the fragile ecosystem of the Upper Ganga Basin.

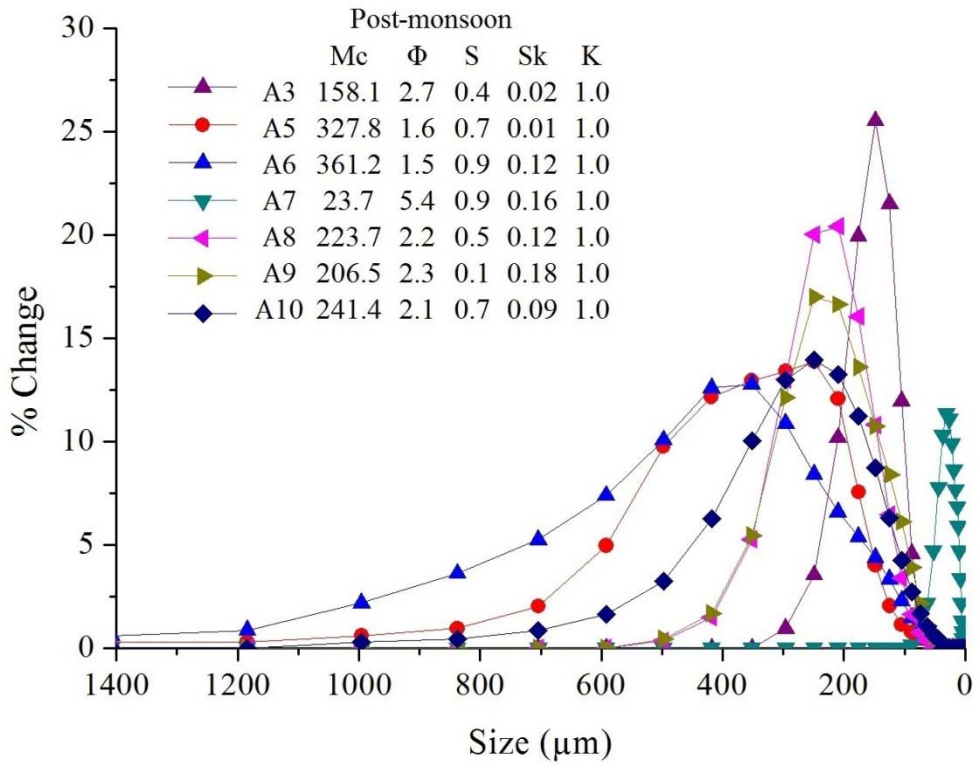
Post-monsoon
Mc Φ S Sk K
A3 158.1 2.7 0.4 0.02 1.0
A5 327.8 1.6 0.7 0.01 1.0
A6 361.2 1.5 0.9 0.12 1.0
A7 23.7 5.4 0.9 0.16 1.0
A8 223.7 2.2 0.5 0.12 1.0
A9 206.5 2.3 0.1 0.18 1.0
A10 241.4 2.1 0.7 0.09 1.0
% Change
Size (µm)
30
25
20
15
10
5
0
1400
1200
1000
800
600
400
200
0

(a)

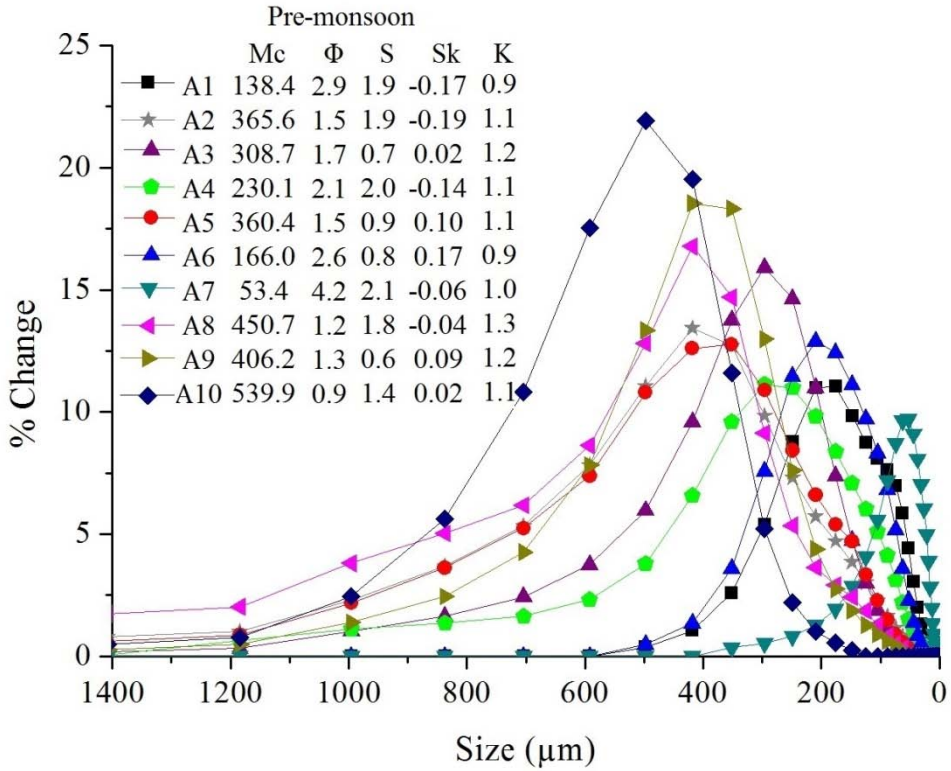
Pre-monsoon
Mc Φ S Sk K
A1 138.4 2.9 1.9 -0.17 0.9
A2 365.6 1.5 1.9 -0.19 1.1
A3 308.7 1.7 0.7 0.02 1.2
A4 230.1 2.1 2.0 -0.14 1.1
A5 360.4 1.5 0.9 0.10 1.1
A6 166.0 2.6 0.8 0.17 0.9
A7 53.4 4.2 2.1 -0.06 1.0
A8 450.7 1.2 1.8 -0.04 1.3
A9 406.2 1.3 0.6 0.09 1.2
A10 539.9 0.9 1.4 0.02 1.1
% Change
Size (µm)
25
20
15
10
5
0
1400
1200
1000
800
600
400
200
0

(b)

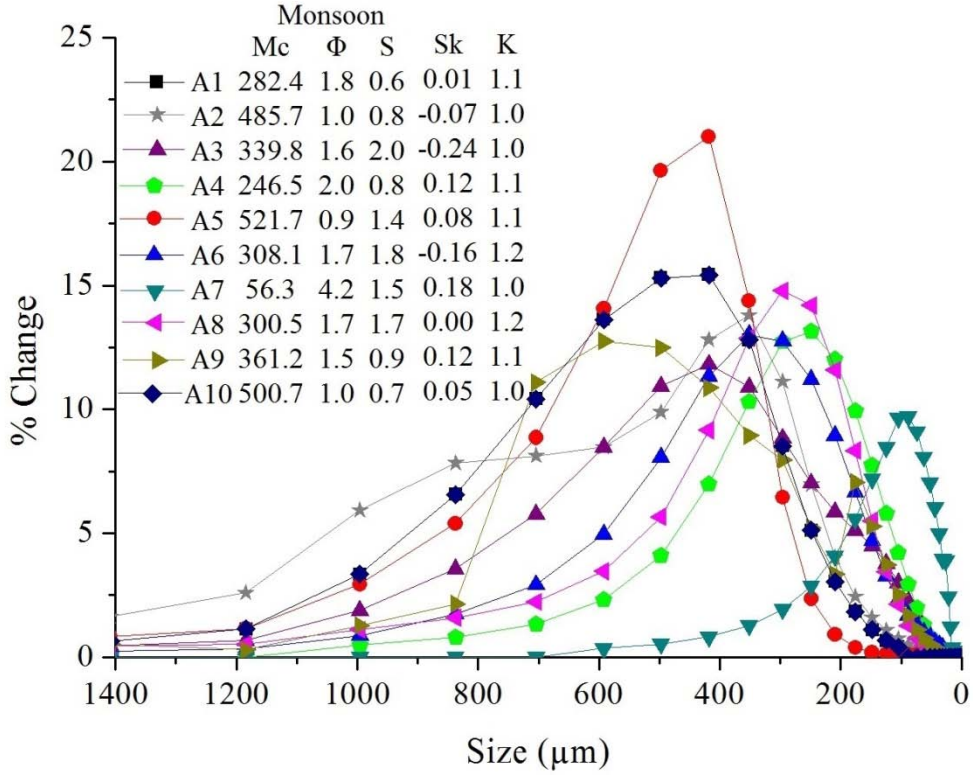
Monsoon
Mc Φ S Sk K
A1 282.4 1.8 0.6 0.01 1.1
A2 485.7 1.0 0.8 -0.07 1.0
A3 339.8 1.6 2.0 -0.24 1.0
A4 246.5 2.0 0.8 0.12 1.1
A5 521.7 0.9 1.4 0.08 1.1
A6 308.1 1.7 1.8 -0.16 1.2
A7 56.3 4.2 1.5 0.18 1.0
A8 300.5 1.7 1.7 0.00 1.2
A9 361.2 1.5 0.9 0.12 1.1
A10 500.7 1.0 0.7 0.05 1.0
% Change
Size (µm)

(c)

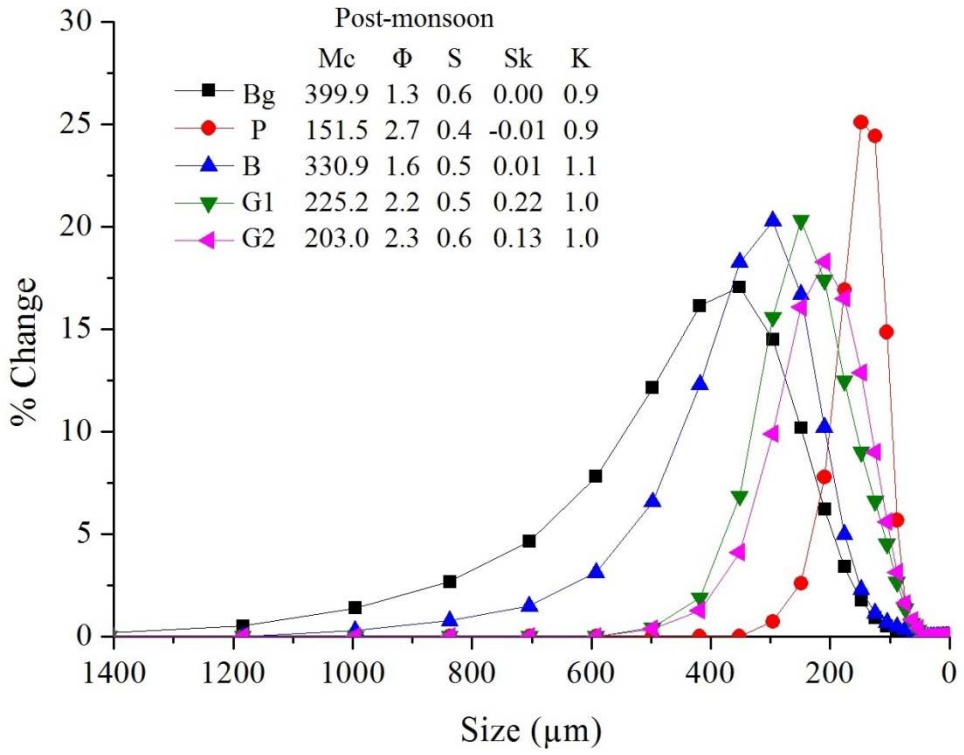
Post-monsoon
Mc Φ S Sk K
Bg 399.9 1.3 0.6 0.00 0.9
P 151.5 2.7 0.4 -0.01 0.9
B 330.9 1.6 0.5 0.01 1.1
G1 225.2 2.2 0.5 0.22 1.0
G2 203.0 2.3 0.6 0.13 1.0
% Change
Size (µm)

(d)

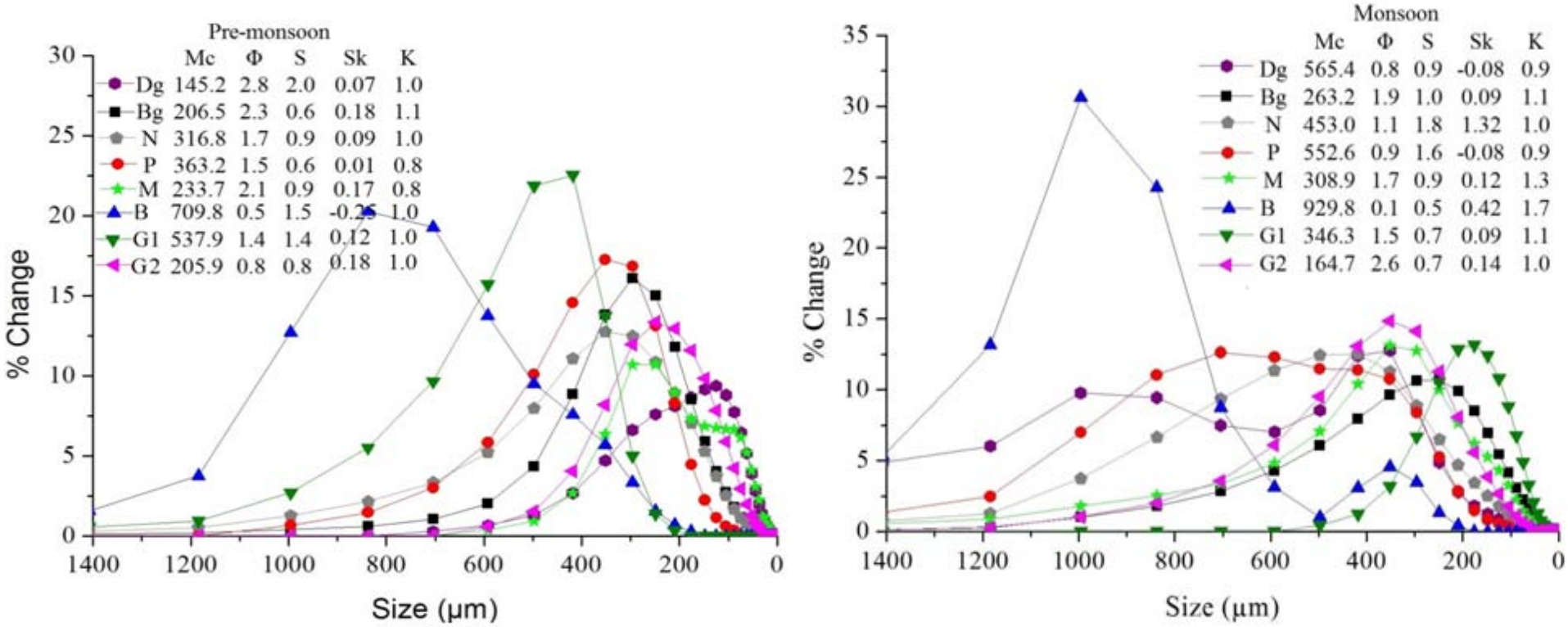

(e) (f)

Figure 5.11 Variation in grain size distribution of channel sediments and statistical parameter calculated using Folk and Ward (1957) for (a) the Alaknanda River during Post-Monsoon, 2012; (b) the Alaknanda River during Pre-monsoon, 2014 (c) the Alaknanda River during Monsoon, 2014; (d) Tributaries and the Ganga River during Post-Monsoon, 2012; (e) Tributaries and the Ganga River during Pre-monsoon, 2014; (f) Tributaries and the Ganga River during Monsoon, 2014 [Mc- channel sediment mean grain size (in µm), Φ= phi size ($\Phi = -\log_2 d$), S-sorting, Sk-Skewness, K-Kurtosis]

Figure 5.12 Flow of Alaknanda River during different time periods at Devprayag

5.3. WEATHERING INTENSITY IN THE BASIN

5.3.1. Clay Mineral Assemblages

Studies on clay mineral assemblages in the river sediments reflect both the weathering intensity and the source bedrock. From the previous studies of Ramesh et al. (2000); Chakrapani (2005); Singh (2010); Garzanti et al. (2011), it is known that Ganga river sediments are enriched in quartz and feldspar and illite and kaolinite are the dominant clay minerals. Table 5.4 show the spatial and temporal changes in the clay mineral assemblages of the Alaknanda River and some of its tributaries.

The clay mineral analysis revealed that illites followed by kaolinite and chlorite are the most common clay minerals present in the Alaknanda River and its tributaries (Table 5.4). In both the season, physical weathering processes (characterized by the presence of illite and chlorite) dominate chemical weathering reactions (inferred by the abundance of kaolinite). The concentration of illite and chlorite in all the samples varied from 52.1 to 89.3%. The average concentration of illite during the pre-monsoon and monsoon season of the year 2014 varied between ~63% and ~61% respectively. The presence of high to low grade metamorphic rocks enriched in mica and feldspar throughout the Alaknanda basin, strong tectonics around the

Main Central Thrust (MCT) and high river energy resulted in the dominance of illite in all the samples from upstream to downstream both spatially and temporally.

Chlorite resulted from the weathering of low grade metamorphic and mafic rocks. The concentration of kaolinite varied from 18.6-42.5% and 7.8-39.4% during the pre-monsoon and monsoon season, whereas the concentration of vermiculites and montmorillonite was found to be insignificant in all the samples. The tributaries also showed the same pattern as present in the Alaknanda mainstream sediments i.e., the dominance of illite, followed by kaolonite and chlorite.

Table 5.4 Spatial and temporal variation in the clay mineral assemblages of the Alaknanda River and its tributaries in <2 μm clay size sediments (%)

Sample	Illite	Kao-linite	Chlorite	Vermi-culite	Montmr-illonite	Illite Chemistry Index	Illite Crystallinity Index	Kaolinite/ Illite Ratio
				Pre-monsoon				
A1	66.6	27.4	4.3	1.4	0.3	0.09	0.09	0.41
A2	68.0	23.0	4.0	2.8	2.2	0.11	0.02	0.34
A3	72.6	20.8	4.4	2.1	0.1	0.23	0.10	0.29
A6	73.5	18.6	6.0	1.8	0.1	0.09	0.04	0.25
A8	52.8	38.7	5.9	3.1	0.3	0.14	0.05	0.73
A10	62.5	31.8	4.0	1.4	0.2	0.11	0.04	0.51
Dg	68.8	26.0	3.8	1.2	0.2	0.14	0.28	0.38
Bg	59.7	32.2	3.9	2.5	0.2	0.07	0.19	0.54
N	63.1	27.0	5.6	4.1	0.2	0.07	0.37	0.43
P	55.1	36.2	5.5	2.8	0.5	0.16	0.06	0.66
M	73.2	20.9	3.6	2.2	0.1	0.09	0.04	0.29
B	68.1	27.0	3.5	1.4	0.1	0.09	0.15	0.40
G1	48.2	42.5	3.9	5.2	0.2	0.09	0.15	0.88
G2	56.9	35.3	4.7	3.0	0.1	0.11	0.15	0.62
				Monsoon				
A2	54.2	38.0	7.1	0.5	0.3	0.07	0.22	0.70
A4	54.4	39.4	4.3	1.8	0.2	0.09	0.06	0.72
A6	62.2	29.6	6.3	1.7	0.2	0.09	0.07	0.48
A10	50.7	38.6	6.4	3.9	0.4	0.33	0.07	0.76
Dg	65.2	29.4	3.2	2.1	0.1	0.09	0.21	0.45
Bg	58.4	32.3	7.0	1.8	0.4	0.07	0.16	0.55
N	79.1	7.8	10.2	2.6	0.3	0.09	0.11	0.10
M	60.6	34.0	5.1	0.4	0.0	0.09	0.11	0.56
G1	66.3	26.2	5.5	1.9	0.1	0.11	0.33	0.40

The intensity of chemical weathering was determined by the illite chemistry index and the illite crystallinity index (Table 5.4). The value of illite chemistry index <0.5 represent weak chemical weathering conditions dominated by Fe-Mg-rich illites (Liu et al., 2007). Moreover, the low value of illite crystallinity index in all the sediment samples (<0.4) represent high crystallinity of clay minerals which indicate the absence of hydrolysis process (a chemical weathering process) (Krumm and Buggisch, 1991; Liu et al., 2007). Thus, based on low values of kaolinite/illite ratio, illite chemistry index and illite crystallinity (Table 5.4), it can be stated that physical weathering processes dominate in the Alaknanda basin.

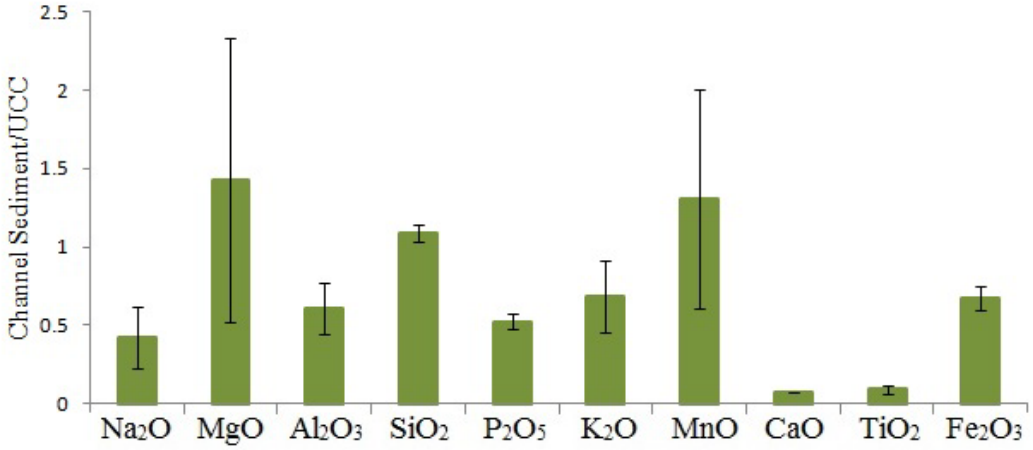

Figure 5.13 UCC normalized major oxide composition of Alaknanda river sediments

5.3.2. Major Oxide and Chemical Weathering Indices

The major oxide composition of the Alaknanda River sediments is shown in Table 5.5. SiO_2 dominantly forms ~60% of the chemical composition, followed by Al_2O_3, CaO, MgO, Fe_2O_3 and K_2O. For assessing the mobility of elements during weathering and transport, the major oxide composition of sediment was normalized with the Upper Continental Crust (UCC) (Taylor and McLennan, 1985). Figure 5.13 shows the normalized pattern of the major oxide composition of channel sediments with reference to the UCC. The UCC normalized SiO_2>1 suggests that dilution effect during the transportation process results in the enrichment of SiO_2. The normalized concentration of MgO and MnO was also >1 (Fig. 5.13) but the large error bars restrict their mobilization estimation during transportation. The presence of high SiO_2 with the low amount of Al_2O_3, P_2O_5, CaO and TiO_2 with respect to UCC suggest that sediments have not been subjected to intense silicate weathering processes.

Based on the dominant reaction, i.e. the enrichment of Al_2O_3 and dilution of major oxides Na_2O, K_2O and CaO during the chemical weathering reactions, Nesbitt and Young (1982)

formulated the equation to estimate the extent of chemical weathering as the Chemical Index of Alteration (CIA):

$$CIA = [Al_2O_3/(Al_2O_3 + Na_2O + K_2O + CaO^*)] \times 100$$

Figure 5.14(a) shows that CIA values are with the reference line of the unweathered granites/granodiorites (Nesbitt and Young, 1989). There's no upstream and downstream variation in the CIA values. The average CIA value in the Alaknanda River basin is ~56, which is far less than the global average of 72.1 (calculated by Li and Yang, 2010) and the average CIA value of Asian rivers (~66). The CIA value is also less than that of the Yamuna River having an average value of ~59 (Dalai et al., 2004) and the Indus River having a CIA value of 63.8 (McLennan, 1993). Figure 5.15 (A-CN-K diagram) shows the graphical representation of the CIA and the prevalence of weak chemical weathering. The results show that the parent rocks from which the major oxides are derived are enriched in feldspar. Plagioclase enrichment was noticeable in the sample A6 collected during the monsoon season. Sample 10 (collected from Govindghat during the monsoon season) plots below the feldspar line suggesting the presence of higher percentage of K_2O. Raymo and Ruddiman (1992); Hren et al. (2007); Li and Yang (2010) observed that high physical erosion in the Himalayas enhances the chemical weathering rates. However, similar to the findings of Yang et al. (2004) in the Changjiang and Huanghe drainage basins, high physical weathering in the Alaknanda basin also does not favor high chemical erosion. The similar CIA value and similar clay mineral assemblages in all the three seasons and low CIA value during the monsoon season at the sample site A1 (Fig. 5.14a) indicates that the high physical weathering during the monsoon does not correspond to high chemical weathering in the Alaknanda basin due to rapid flushing of sediments downstream. The large rocky outcrop, steep topography, high runoff and shallower mountainous soil which cannot retain water for hydrolysis can be cited as a reason for uneven physical and chemical weathering rates. Low values of illite crystallinity in all the sediment samples reaffirm the absence of hydrolysis process in the Alaknanda basin (Section 5.3.1).

Another index which quantifies the chemical weathering based on major oxides includes Weathering Index of Parker (WIP). WIP was formulated by Parker (1970) and Hamdan and Burnham (1996) as the ratio of the amount of alkali and alkaline elements. WIP was calculated as:

$$WIP = (2Na_2O/0.35 + MgO/0.9 + 2K_2O/0.25 + CaO/0.7)^* \times 100$$

The WIP value of sediments varied from 40.8 to 47.6 (Fig. 5.14b) and similar to CIA, it also points to a lesser degree of chemical weathering during the monsoon season.

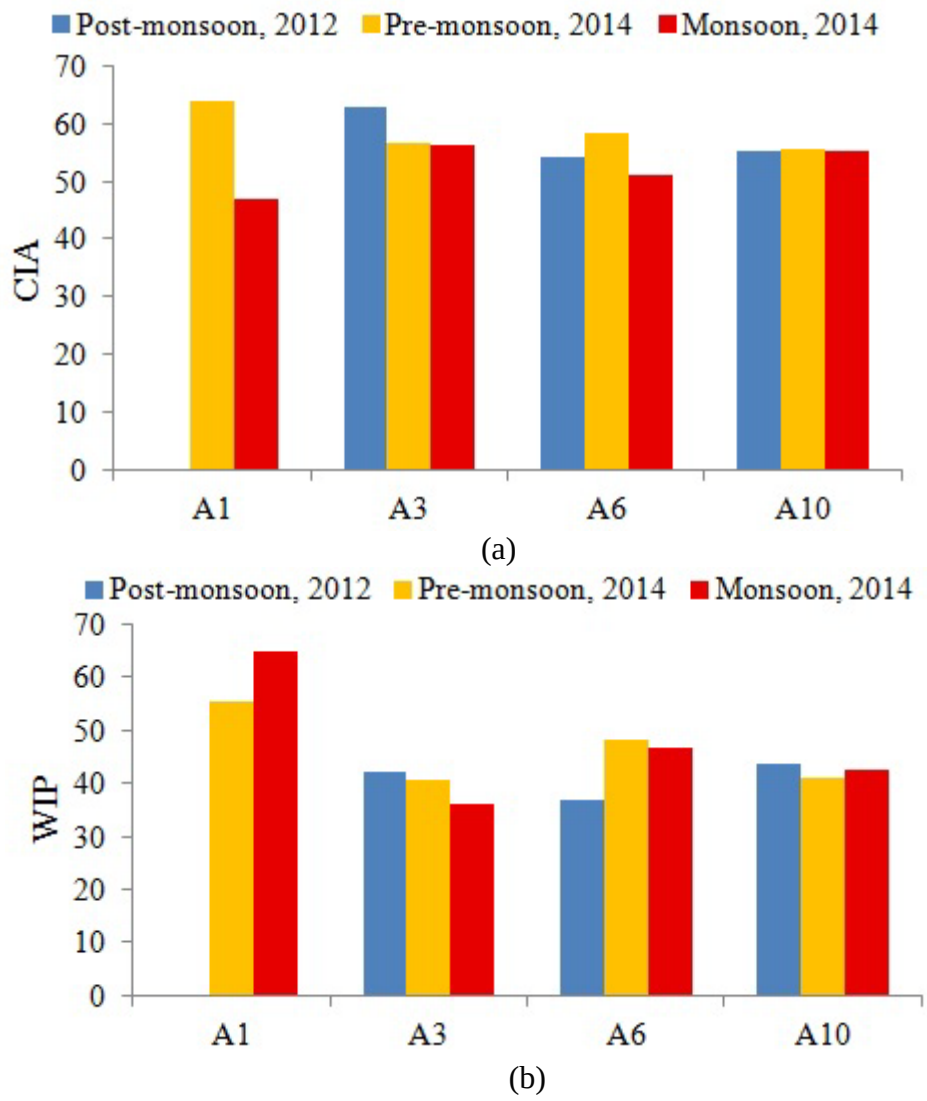

Figure 5.14 (a) CIA value during the year 2012-2014; (b) WIP value during the year 2012-2014

In the heterogeneous Ganga basin, where both the Higher and Lesser Himalayas source the river sediments, Al/Si ratio can be used as weathering proxy. Contrary to CIA and WIP, Al/Si ratio is independent of sediment sorting. In the Alaknanda Basin, Al/Si ratio varied from 0.04-0.13. The low values indicate the presence of coarse grains and weak chemical weathering rate in the basin. Figure 5.16 shows the relation between labile fraction and Al/Si ratio. The strong positive correlation of K/Si with Al/Si suggests the depletion of K with respect to silica and provenance from the same source rock. Whereas, poor correlation between Na/Si and Al/Si, Fe/Si and Al/Si indicate their presence from the heterogeneous source; Na_2O in the Alaknanda River sediments may have their source from the plagioclase (probably albite) and Fe_2O_3 from the biotite and clay minerals (Lupker et al. 2012b). Thus, the weathering of both the Higher

Himalayas and Lesser Himalayas seems to influence the chemical weathering in the Alaknanda River basin and Al/Si ratio can be distinguished as a better proxy than the CIA and WIP in the Upper Ganga Basin.

However, similar to the studies carried by Duzgoren-Aydin and Aydin (2002); Price and Velbel (2003) and Shao et al. (2012), in this study also CIA and WIP indices correlated very well. Li and Yang (2010) in their study dealing with global river basins observed a positive relation between the climatic factors and intensity of chemical weathering. In the Alaknanda basin, similar CIA, WIP, and Al/Si value during the post-, pre- and monsoon season showed that there is no such effect of a change in climatic variables such as temperature, pressure and precipitation on chemical weathering processes. However, a good relation exists between the change in climatic factors and sediment load (in the monsoon ~85% increase in the sediment load was noticed, section 5.1.1).

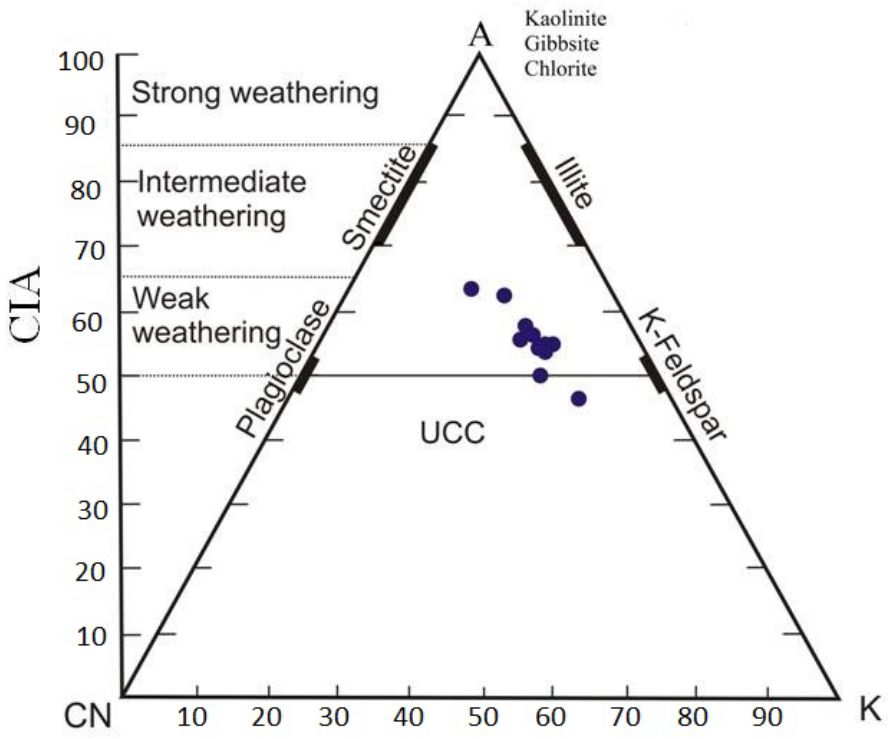

Figure 5.15 A-CN-K diagram showing the weathering trend (molar concentration of Al_2O_3-CaO*+Na_2O-K_2O was plotted)

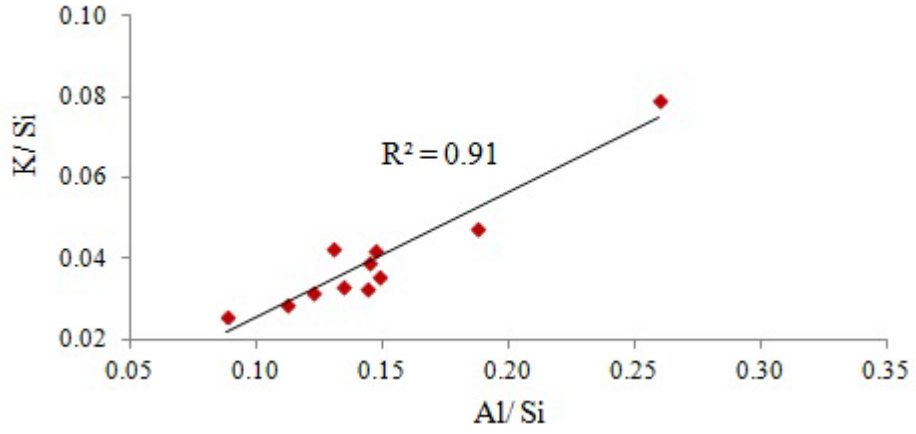

(a)

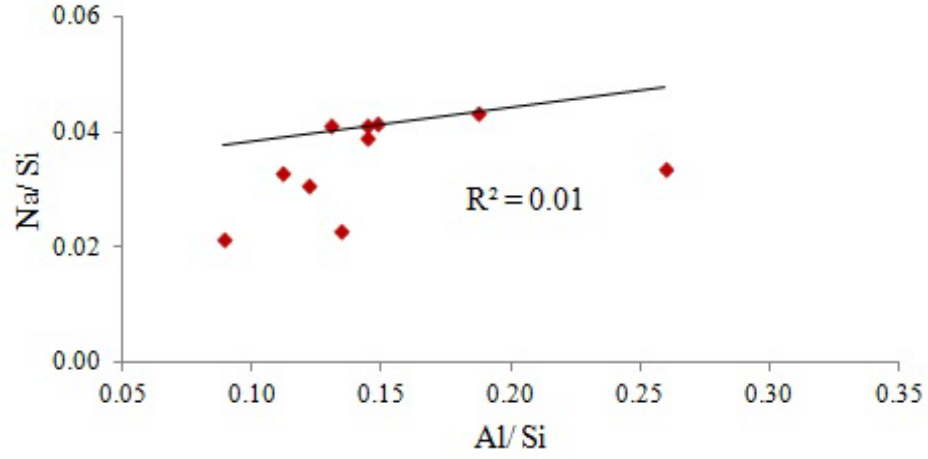

(b)

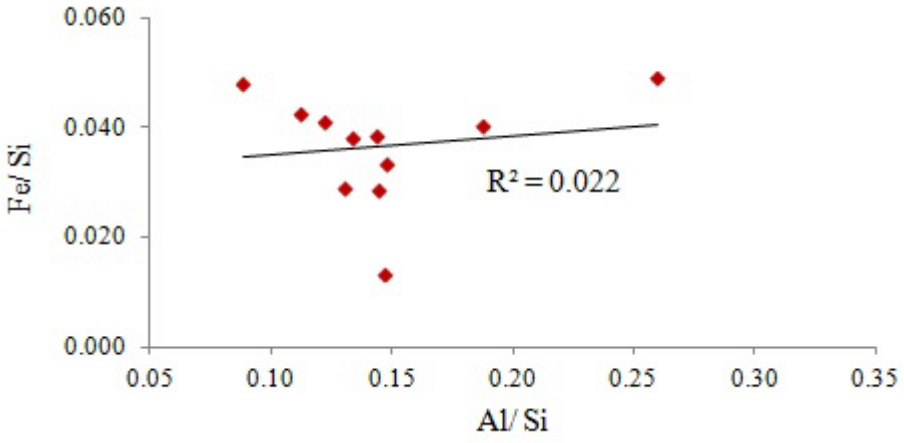

(c)

Figure 5.16 Correlation of Al/Si with (a) K/Si; (b) Na/Si; (c) Fe/Si

Table 5.5 Major oxide composition of channel sediments (normalized by UCC composition mentioned in McLennan, 2001)

	Sample	**Na_2O**	**MgO**	**Al_2O_3**	**SiO_2**	**P_2O_5**	**K_2O**	**MnO**	**CaO**	**TiO_2**	**Fe_2O_3**
					Weight %						
Post-monsoon 2012	A3	0.69	7.67	6.66	58.60	0.05	1.53	5.53	0.18	0.07	2.97
	A6	1.26	2.89	7.03	74.11	0.07	1.69	3.19	0.32	0.11	4.18
	A10	1.48	2.66	9.03	73.64	0.08	2.28	2.72	0.35	0.04	2.81
Pre-monsoon 2014	A1	1.18	2.15	14.98	68.00	0.10	4.22	1.07	0.49	0.05	4.43
	A3	1.10	4.84	7.18	69.34	0.03	1.74	3.65	0.26	0.07	3.78
	A6	1.58	2.70	11.26	70.84	0.07	2.64	2.41	0.37	0.05	3.81
	A10	1.57	2.50	8.98	73.53	0.10	1.89	3.12	0.30	0.09	3.78
Monsoon 2014	A1	4.28	0.51	9.92	79.49	0.07	2.62	0.72	0.10	0.02	1.42
	A3	0.78	5.45	5.33	70.92	0.13	1.44	4.71	0.48	0.09	4.55
	A6	1.58	2.66	8.22	74.42	0.09	2.48	3.65	0.30	0.05	2.88
	A10	1.58	2.44	9.25	73.67	0.07	2.08	2.90	0.33	0.08	3.28
Chakrapani (2007 unpublished)	AS1	4.13	0.44	10.86	78.91	0.17	3.38	0.03	0.89	0.16	1.20
	AS2	3.18	0.90	9.98	75.29	0.30	2.77	0.06	1.42	0.27	4.79
	AS4	0.94	7.16	6.44	56.99	0.21	1.86	0.05	8.09	0.28	10.57
	AS7	1.93	2.27	9.09	75.68	0.31	2.43	0.06	2.65	0.41	4.05
	AS8	1.44	2.71	9.80	73.41	0.21	2.42	0.04	2.40	0.43	2.50
	AS10	1.55	2.81	11.76	69.21	0.20	2.95	0.05	2.25	0.53	5.13
	AS11	1.91	2.03	8.16	74.36	0.28	2.09	0.07	3.13	0.36	3.65
					UCC Normalized Values						
Post-monsoon 2012	Sample	Na_2O	MgO	Al_2O_3	SiO_2	P_2O_5	K_2O	MnO	CaO	TiO_2	Fe_2O_3
	A3	0.18	3.49	0.44	0.89	0.33	0.45	2.51	0.04	0.10	0.59
	A6	0.32	1.31	0.46	1.12	0.47	0.50	1.45	0.08	0.16	0.83
	A10	0.38	1.21	0.59	1.12	0.53	0.67	1.24	0.08	0.06	0.56

Pre-monsoon 2014	A1	0.30	0.98	0.99	1.03	0.67	1.24	0.49	0.12	0.08	0.88
	A3	0.28	2.20	0.47	1.05	0.20	0.51	1.66	0.06	0.10	0.75
	A6	0.41	1.23	0.74	1.07	0.47	0.78	1.10	0.09	0.07	0.76
	A10	0.40	1.14	0.59	1.11	0.67	0.56	1.42	0.07	0.14	0.75
Monsoon 2014	A1	1.10	0.23	0.65	1.20	0.47	0.77	0.33	0.02	0.03	0.28
	A3	0.20	2.48	0.35	1.07	0.87	0.42	2.14	0.11	0.14	0.90
	A6	0.41	1.21	0.54	1.13	0.60	0.73	1.66	0.07	0.07	0.57
	A10	0.41	1.11	0.61	1.12	0.47	0.61	1.32	0.08	0.11	0.65
Chakrapani (2007 unpublished)	AS1	1.06	0.20	0.71	1.20	1.13	0.99	0.01	0.21	0.24	0.24
	AS2	0.82	0.41	0.66	1.14	2.00	0.81	0.03	0.34	0.40	0.95
	AS4	0.24	3.25	0.42	0.86	1.40	0.55	0.02	1.93	0.41	2.10
	AS7	0.49	1.03	0.60	1.15	2.07	0.71	0.03	0.63	0.60	0.80
	AS8	0.37	1.23	0.64	1.11	1.40	0.71	0.02	0.57	0.63	0.50
	AS10	0.40	1.28	0.77	1.05	1.33	0.87	0.02	0.54	0.78	1.02
	AS11	0.49	0.92	0.54	1.13	1.87	0.61	0.03	0.75	0.53	0.73

Table 5.6 Statistics of the major oxide composition of channel sediments of the Alaknanda River (%)

Sample	Minimum	Maximum	Average	Standard Deviation
SiO_2	56.99	79.49	71.69	5.89
Al_2O_3	5.33	14.98	9.11	2.28
K_2O	1.44	4.22	2.36	0.69
Fe_2O_3	1.20	10.57	3.88	1.98
Na_2O	0.69	4.28	1.79	1.03
MgO	0.44	7.67	3.04	2.01
CaO	0.10	8.09	1.35	1.94
P_2O_5	0.03	0.31	0.14	0.09
MnO	0.03	5.53	1.89	1.85
TiO_2	0.02	0.53	0.18	0.16

Table 5.7 REEs composition of suspended sediments (values in ppm; normalized by UCC composition mentioned in McLennan, 2001)

Element	A1	A2	A3	A4	A5	A6	A8	A10	Dg	N	P	M	B	G1	G2
La	32.5	12.3	32.5	35.6	34.0	32.6	32.1	34.0	36.8	49.4	32.2	34.5	31.4	38.0	37.8
Ce	68.3	24.6	66.3	70.7	70.4	66.0	64.6	69.9	74.2	94.5	63.3	74.2	65.1	78.0	75.0
Pr	7.20	2.60	7.00	7.50	7.20	6.80	6.70	7.10	7.60	10.1	6.50	7.90	6.80	8.10	7.90
Nd	27.9	10.0	27.3	29.2	28.3	27.0	26.0	28.0	30.3	39.1	25.8	31.9	26.2	32.4	30.0
Sm	6.63	2.03	5.69	6.07	5.82	5.75	5.59	5.82	6.16	8.37	5.12	7.17	5.89	6.82	6.53
Eu	1.32	0.46	1.06	1.02	1.23	1.00	1.09	1.05	1.65	1.41	1.17	2.01	1.86	1.19	1.12
Gd	5.11	1.59	4.33	4.52	4.40	4.32	4.26	4.53	4.58	6.37	3.94	5.60	4.98	5.20	4.88
Tb	0.89	0.25	0.72	0.74	0.72	0.71	0.72	0.75	0.74	1.13	0.66	0.96	0.88	0.82	0.80
Dy	4.68	1.32	3.56	3.76	3.65	3.60	3.48	3.72	3.71	5.96	3.38	5.38	5.03	4.41	4.07
Ho	0.90	0.24	0.65	0.68	0.65	0.65	0.66	0.69	0.66	1.23	0.65	1.05	1.01	0.78	0.77
Er	2.35	0.65	1.86	1.89	1.81	1.83	1.83	2.01	1.83	3.33	1.84	3.03	2.87	2.24	2.22
Tm	0.32	0.10	0.26	0.25	0.24	0.26	0.26	0.29	0.26	0.46	0.25	0.41	0.40	0.29	0.30
Yb	1.86	0.54	1.46	1.46	1.49	1.49	1.45	1.61	1.45	2.55	1.44	2.33	2.49	1.77	1.65
Lu	0.27	0.08	0.21	0.22	0.20	0.21	0.21	0.24	0.21	0.35	0.22	0.34	0.36	0.26	0.24
UCC normalized indices															
$(\Sigma REE)_N$	16.1	5.09	13.6	14.2	13.9	13.5	13.5	14.3	15.0	21.3	13.2	19.0	17.6	16.1	15.5
$(\Sigma LREE)_N$	5.71	2.00	5.42	5.82	5.63	5.39	5.27	5.60	5.99	7.91	5.11	6.24	5.34	6.39	6.15
$(\Sigma HREE)_N$	10.4	3.09	8.22	8.36	8.35	8.14	8.20	8.72	9.02	13.4	8.08	12.8	12.2	9.71	9.31
$(LREE/HREE)_N$	0.55	0.65	0.66	0.70	0.67	0.66	0.64	0.64	0.66	0.59	0.63	0.49	0.44	0.66	0.66
$(Ce/Yb)_N$	1.26	1.57	1.56	1.66	1.62	1.52	1.53	1.49	1.76	1.27	1.51	1.09	0.90	1.51	1.56
$(Ce/La)_N$	0.99	0.94	0.96	0.93	0.97	0.95	0.94	0.96	0.95	0.90	0.92	1.01	0.97	0.96	0.93
$(Gd/Yb)_N$	1.59	1.70	1.72	1.79	1.71	1.68	1.70	1.63	1.83	1.45	1.58	1.39	1.16	1.70	1.71
$(La/Yb)_N$	1.28	1.67	1.63	1.79	1.67	1.60	1.62	1.55	1.86	1.42	1.64	1.09	0.92	1.57	1.68
$(La/Lu)_N$	1.28	1.64	1.65	1.73	1.81	1.66	1.63	1.51	1.87	1.51	1.56	1.08	0.93	1.56	1.68
Eu anomaly	1.07	1.20	1.00	0.92	1.14	0.94	1.05	0.96	1.46	0.91	1.22	1.49	1.61	0.94	0.93
Ce anomaly	1.02	0.99	1.00	0.99	1.03	1.01	1.00	1.03	1.01	0.96	1.00	1.02	1.02	1.01	0.99

5.4. SEDIMENT SOURCE CHARACTERIZATION

5.4.1. Rare Earth Elements (Fingerprinting Suspended Sediments)

The normalized ratio $(La/Yb)_N$ and $(Ce/Yb)_N$ >1 showed a preferential uptake of LREE. The value of ratio $(La/Lu)_N$, $(La/Yb)_N$, and $(Gd/Yb)_N$ showed that due to the faster rate of transportation, fractionation was less (Table 5.7). Unlike most world rivers such as the Amazon, Mississippi, Huanghe and Indus which show LREE enrichment (Yang et al., 2002), sediments of the Alaknanda River are enriched in HREE and LREE/HREE ratio varied from 0.44-0.70 (Fig. 5.17). Generally, it is seen that HREE are preferentially transported in solution as they form more soluble bicarbonate and organic complexes than the LREE (Singh and Rajamani, 2001; Yang et al., 2002). The presence of calcite/dolomite on the suspended sediment and dilution of calcium during the monsoon in the river water (Chakrapani, 2005; Chakrapani et al., 2009) have resulted in the enrichment of HREE in the suspended sediments. Lupker et al. (2012) mention the presence of carbonate in the order of 10% in the Upper Ganga sediments and that the dissolution of carbonates in the Himalayan Rivers varied from 77% loss for calcite and 30-86% loss for dolomite. Speciation studies carried by Zhang et al. (1998) shows that REEs have a high affinity for the carbonates, organic matter and Fe-Mn oxides that can scavenge REEs from the water. Thus, carbonate weathering source the substantial proportion of carbonate that enriched HREE concentration in the suspended sediments of the Alaknanda River.

The ratios $(La/Lu)_N$ and $(La/Yb)_N$ >1 show the presence of the high silicate fraction in the suspended sediments which was also confirmed by the presence of K-feldspar in the <2 μm sediments. The abundance of feldspar in the sediments was also supported by negative $(Ce/La)_N$ ratio. During monsoon, Eu anomaly varied from slightly positive to a slightly negative within a range of 0.91-1.61 (Fig. 5.17). The negative Eu anomaly indicates a highly differentiated felsic source, whereas the positive Eu anomaly can be attributed to the carbonate and mafic weathering. The weathering of carbonate formations present in the Alaknanda basin can result in the substitution of Eu^{2+} for Ca^{2+} and the positive Eu anomaly in the sediments (Panwar et al., 2016). Bhandari et al. (1992) observed positive Eu anomaly values in the limonitic deposits present in the Spiti Valley section at Lalung, northern Himalayas. Because of the complex lithology of the Alaknanda basin, there was no consistent pattern observed in the Eu anomaly from upstream to downstream regions.

The absence of Ce anomaly in most of the samples was due to the spatial variation in the conditions of discharge and lithology resulting in the oxidation and scavenging of sediments

(Pourret et al., 2008). Ce anomaly varied from 0.96-1.03, the values show that oxidation of cerium was not so pronounced in the sediments (Fig. 5.17). The values of <1 indicate the reduction of Ce(IV) to Ce(III) and enrichment of Ce(III) in the dissolved load (Hannigan et al., 2010; Wiggering and Beukes, 1990). Since Ce(IV) is less soluble, the suspended sediments show negative Ce anomaly. The absence of particulate organic carbon (POC) in all the suspended sediment samples (section 5.5.1) rule out the probability of association of Ce (IV) with organic matter. Studies of Palmer (1985); Nagarajan et al. (2011) mentioned that negative Ce anomaly in the sediments can be due to the weathering of carbonate rocks.

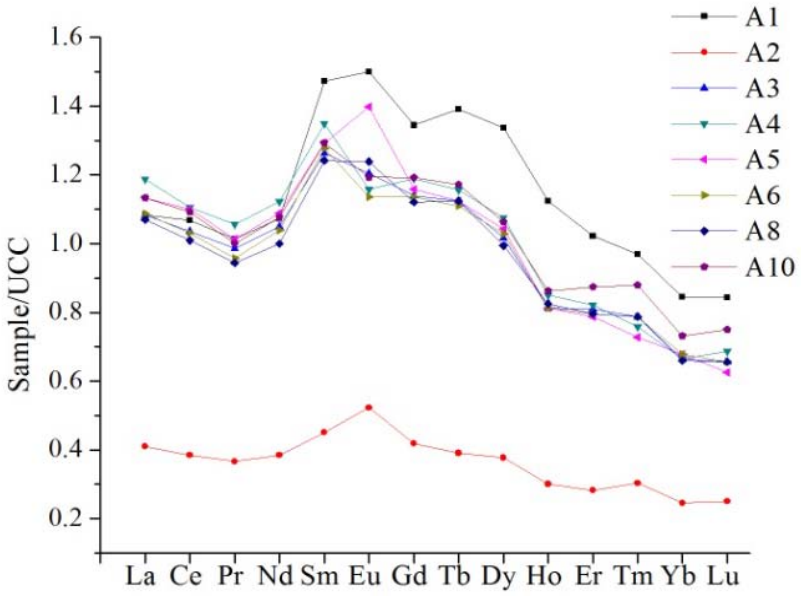

(a)

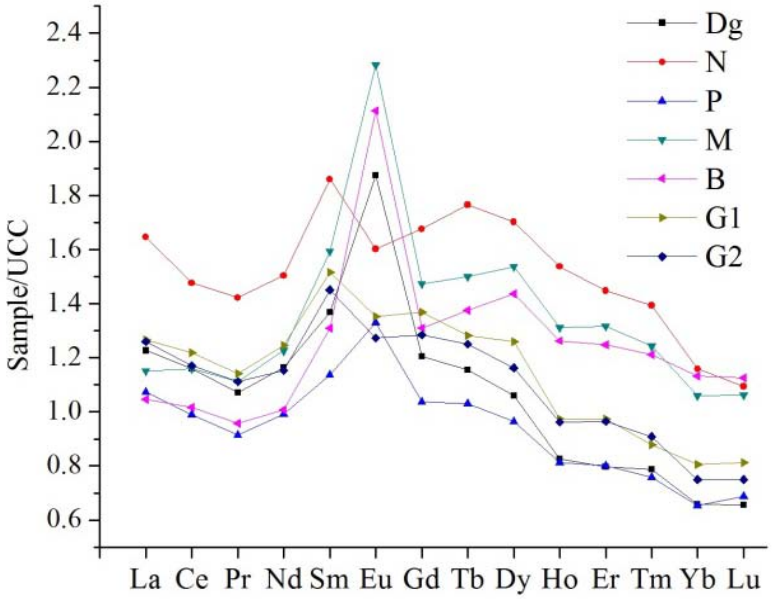

(b)

Figure 5.17 Normalized REEs pattern of suspended sediments (a) Alaknanda River; (b) Tributaries and the Ganga River

The enrichment of HREE, positive Eu anomaly and negative Ce anomaly in some of the samples confirmed that along with the K-feldspar (present in Higher Himalayan Crystalline Formation), the weathering of carbonates (limestone, dolomite, and magnesite of Garhwal Group) also contribute to suspended sediments in the Alaknanda River. Except Nandakini, all the tributaries showed positive Eu anomaly. The Bhagirathi River at Devprayag (sample B) also showed the similar result (high HREE and positive Eu anomaly) due to similar lithology in the Bhagirathi basin.

Similar to Ramesh et al. (2000); Chakrapani (2005), and Panwar et al. (2016), in this study also suspended sediments of the Alaknanda and the Ganga River at Devprayag and Rishikesh (sample A10, G1, and G2) showed high LREEs and negative Eu anomaly. Due to mixing of water and sediments and preferential uptake of LREE and dissolution of HREE, samples from the Ganga River (G1 and G2) showed negative Eu anomaly hinting that Alaknanda is a major contributor of the suspended load to the Ganga River, more than the companion River Bhagirathi.

5.4.2. Major Oxides (Fingerprinting Channel Sediments)

Table 5.5 and 5.6 lists the major oxide composition of channel sediments. SiO_2 and Al_2O_3 are the dominant oxides accounting ~63 to 90% of the total sediment composition. Due to the hydrodynamic sorting of sediments during transportation, channel sediments became enriched in SiO_2 and depleted in Na_2O, Fe_2O_3, K_2O, and H_2O^+ in comparison to surface sediments. The heterogeneities in river sediment chemistry with respect to depth have been discussed in detail by Lupker et al. (2011, 2012b).

In the Alaknanda basin, the ratios SiO_2/Al_2O_3 and K_2O/Al_2O_3 varied from 1.0 to 3.1 and 0.9-1.4 respectively prove the immature nature of river sediments. The ratio K_2O/Na_2O signified the type of feldspar present in the source rock; K_2O/Na_2O >1 clearly points the enrichment of K-feldspar rocks in the terrain (Das et al., 2006; Gupta et al., 2012; Verma et al., 2012). A simplified tool to measure the degree of dependence of one variable on other is the Pearson Correlation matrix. Table 5.8 shows the correlation matrix and some meaningful insights into the relationships among the oxides. A positive correlation was found to exist between SiO_2 and Na_2O (0.68), Al_2O_3 and K_2O (0.93), P_2O_5 and TiO_2 (0.82) and CaO and Fe_2O_3 (0.79), whereas, a strong negative correlation between MgO and SiO_2 (-0.89), MgO and Na_2O (-0.75) was observed. This pattern proves that silicate weathering predominates in the Alaknanda basin. The negative correlation of CaO and MgO with Al_2O_3 shows their derivation from carbonate rocks (Table 5.8).

However, to further reduce the dimensionality of the data without losing its originality and bringing out all the strong and important relationships in a dataset, the Principal Component Analysis (PCA) was employed (Liu et al., 2003). Studies of Yang and Youn (2007); Marques et al. (2008) mentioned the importance of PCA in the field of geochemistry; PCA classifies the geochemical data according to the geochemical affinity and its provenance (source rock characteristics). Table 5.6 shows the statistics of the data used for PCA analysis. Ten principal components (PC) were extracted and rotated using the varimax normalization. Following the Kaiser criterion, components with eigen values >1 were accepted (Liu et al., 2003). First three principal components explained ~88% of the total variance. The loading of different components is shown in Table 5.9. The loading of <0.3 was considered as unimportant and was not used for the interpretation of the output results.

Table 5.8 Pearson correlation matrix showing relation between major oxides of channel sediment

	Na_2O	**MgO**	**Al_2O_3**	**SiO_2**	**P_2O_5**	**K_2O**	**MnO**	**CaO**	**TiO_2**	**Fe_2O_3**
Na_2O	1									
MgO	-0.75	1								
Al_2O_3	0.34	-0.62	1							
SiO2	0.68	-0.89	0.27	1						
P_2O_5	0.24	-0.24	0.08	0.14	1					
K_2O	0.45	-0.62	0.93	0.28	0.19	1				
MnO	-0.53	0.53	-0.51	-0.27	-0.74	-0.57	1			
CaO	-0.14	0.34	-0.19	-0.47	0.60	-0.08	-0.56	1		
TiO_2	0.01	-0.07	0.10	-0.03	0.82	0.10	-0.68	0.60	1	
Fe_2O_3	-0.46	0.55	-0.23	-0.68	0.29	-0.19	-0.17	0.79	0.30	1

The extracted factors constituted a unique source of variance that explains the provenance of the sediments (refer Table 5.9). PC1 explains the largest variance accounting for ~42% of the total variance. PC1 shows a positive loading for MgO, Fe_2O_3 and CaO and negative loading for Na_2O and SiO_2 (which represents the absence of plagioclase weathering) indicates their source from the calcareous formations especially magnesite and dolomite in the Garhwal Himalayas. Garhwal group of rocks are also associated with penecontemporaneous mafic volcanic rocks. PC2 shows a high positive loading for P_2O_5, CaO and TiO_2 along with a negative loading from MnO indicating their origin from the mafic source. The Garhwal and Bowali volcanics in the Garhwal Himalayas are enriched in mafic rocks associated with

Berinag and Nagthat Quartzites (Bhat et al., 1998). PC3 accounts for 12.86% of the total variance in the sediment composition and shows a positive loading for Al_2O_3 and K_2O and points their association with the K-feldspar weathering. In the previous studies, due to a strong correlation between K_2O, Na_2O, SiO_2 and Al_2O_3, sediments of Ganga River were considered to be derived from the K-feldspar rocks of the Higher Himalayan Crystallines (Galy and France-Lanord, 2001; Singh, 2010), but with the employment of PCA in this study, along with the K-feldspar weathering, the weathering of Inner Lesser Himalayan rocks (Garhwal group) enriched in magnesite, dolomites and mafic intrusion are also proved to be a significant source of channel sediments.

Table 5.9 Varimax rotation PCA loading matrix

Rotated Component Matrix			
	PC1	**PC2**	**PC3**
Na_2O	-0.779	0.195	0.262
MgO	0.839	-0.117	-0.469
Al_2O_3	-0.195	0.011	0.962
SiO_2	-0.957	0.002	0.084
P_2O_5	-0.148	0.924	0.034
K_2O	-0.214	0.101	0.951
MnO	0.246	-0.813	-0.48
CaO	0.485	0.808	-0.065
TiO_2	0.022	0.875	0.027
Fe_2O_3	0.767	0.472	-0.063
Eigen Value	3.879	2.410	1.496
Variance (%)	41.819	33.316	12.861
Cumulative variance (%)	41.819	75.135	87.996

5.4.3. Environmental Magnetism and Heavy Minerals

Magnetic properties are interpreted by studying various parameters that are concentration dependent, grain size dependent or qualitative. Table 5.10, 5.11 and 5.12 highlight the magnetic parameters estimated for the Alaknanda River and its tributaries. Following sections draw inferences on such parameters to characterize magnetic minerals:

5.4.3.1.Magnetic Concentration Dependent Parameters

Oldfield et al. (1985) and Thompson and Oldfield (1986) observed magnetic susceptibility (χ) as an important parameter that traces the concentration of ferrimagnetic minerals in a sample. In the absence of ferrimagnetic minerals, χ is sensitive to anti-ferromagnetic and paramagnetic minerals also (Walden et al., 1997; Dekkers, 1997; Jenkins et al., 2002; Robertson et al., 2003). The low field magnetic susceptibility (χ_{lf}) for the Alaknanda River sediments varied from 0.8 to 7.5*10^{-8} m^3kg^{-1}. The continuous presence of diamagnetic mineral quartz and calcite resulted in low values of magnetic susceptibility in all the samples collected from the Alaknanda River. Chakrapani (2005) and results generated in this research (Table 5.5 and 5.6) show the dominance of quartz in the suspended and channel sediments of the Alaknanda River. The presence of quartz was also confirmed in <2 µm sediment fraction. Table 5.9 shows the spatial variation in the low magnetic susceptibility value (χ_{lf}). There seems no downstream trend (Fig. 5.18a) in the susceptibility value which may be due to the variation in geology or river energy that effects the sorting of grains. A comparatively high susceptibility value in sample A3 (Chamoli) can be attributed to the lithology of the region. Magnetite, hematite, and pyrite deposits are found associated with Bowali volcanic rocks in the Chamoli district (Bhat et al., 1998). The presence of magnetite leads to very high magnetic susceptibility values, whereas the oxidative weathering of other minerals can lead to the formation of several iron oxide complexes such as maghemite and hematite (Pant et al., 1998). At Srinagar town (Sample A8), downstream of the dam construction, the high rate of fluvial erosion of phyllites introduces ferrimagnetic minerals with high susceptibility. Among tributaries, the highest susceptibility value was seen in the Pinder River sediments (4.4*10^{-8} m^3 kg^{-1}) (Fig. 5.18a). Before merging with Alaknanda, the Pinder River flows through the Garhwal group of rocks, the weathering of carbonates and basic intrusive rocks resulted in high susceptibility noticed in sample P and A5. Though tributaries, Birahi Ganga, and Nandakini also flow through Garhwal group, only Pinder covers the longest distance flowing through the Berinag Formation intruded with basic volcanic rocks. The other concentration dependent parameter i.e., Saturation Isothermal Remanent Magnetisation (SIRM) show the highest value in sample A8 (unlike χ, SIRM is not affected by the concentration of paramagnetic and diamagnetic minerals, Weiguo and Lizhong, 2003). The individual values of SIRM and χ_{lf} and a weak positive correlation between SIRM and χ_{lf} (Fig. 5.18a-c and Table 5.13) indicate that χ_{lf} is mainly contributed by ferrimagnetic materials with the dominance of paramagnetic and diamagnetic minerals in the sediments of the Alaknanda River and its tributaries.

Table 5.10 Concentration dependent parameters

Sample	χlf (*10^{-8} m^3/kg)	SIRM (*10^{-5} Am^2kg^{-1})
A1	1.12	73.30
A2	0.84	52.32
A3	9.05	86.88
A4	2.39	76.88
A5	7.35	106.21
A6	1.59	73.46
A7	2.27	135.30
A8	7.53	424.87
A9	1.53	66.00
A10	2.96	93.49
Dg1	1.35	83.89
Bg1	1.10	82.50
N1	1.04	48.95
P1	4.42	42.06
M1	1.13	56.52

Table 5.11 Descriptive statistics for magnetic parameters calculated for the Alaknanda River (Sample A1-A10)

Statistics	χlf	χfd	SIRM	S-Ratio$_{300}$	HIRM	SIRM/χlf	B$_{(o)CR}$
Mean	3.66	0.01	98.87	-1.04	2.28	39.42	27.24
Median	2.33	0.00	81.88	-0.96	1.65	37.62	28.44
Minimum	0.84	-0.02	52.32	-1.85	0.20	9.60	19.01
Maximum	9.05	0.08	224.87	-0.91	4.75	65.25	33.42
Standard Deviation	3.07	0.03	49.96	0.28	1.78	19.39	6.61
Skewness	0.97	1.96	2.08	-3.10	0.54	-0.11	-0.45
Kurtosis	-0.90	4.53	4.80	9.70	-1.45	-1.11	0.27

5.4.3.2.Magnetic Grain Size Distribution

The concept of magnetic domain offers quantitative information about the magnetic grain size. Magnetic domain influence the magnetic properties of ferrimagnetic minerals that can be examined by the magnetic grain size dependent parameters such as $\chi_{fd\%}$, χ_{ARM}, χ_{ARM}/χ_{lf} and

χ_{ARM}/SIRM (Thompson and Oldfield, 1986; Dearing et al., 1996; Jenkins et al., 2002; Sherriff, 2014). The low χ_{fd} and low values of χ_{ARM}/χ_{lf} may indicate the predominance of MD, PSD and SSD grains (Hall et al., 1989; Dearing et al., 1996; Weiguo and Lizhong, 2003; Liu et al., 2010; Veerasingam et al., 2014). The χ_{fd} <2% and low value of χ_{ARM}/SIRM confirmed the absence of superparamagnetic (SP) grains and the presence of coarse grains of multi-domain (MD) nature in all the samples. However, Figure 5.18(d-e) shows that SSD (grain size 0.02-0.4 μm) magnetic minerals may significantly contribute to χ_{lf}. The relationship between different magnetic parameters as shown by Pearson's Correlation Coefficient matrix in Table 5.13 highlights negative correlation between χ_{lf} and the grain size dependent parameters χ_{fd}, χ_{ARM}/χ_{lf}, χ_{ARM}/SIRM and SIRM/χ_{lf}, suggesting that as the concentration of magnetic mineral increases, the grain size enhances from SP to SD to MD (similar to Venkatachalapathy et al., 2011; Kulkarni et al., 2014; Veersingham et al., 2014).

Table 5.12 Mineralogy dependent parameters

Sample	χfd	χ_{ARM} (*$10^{-8}m^3$/kg)	S-Ratio $_{300}$	HIRM	$B_{(o)CR}$
A1	0.019	1.43	-0.97	1.24	32.35
A2	-0.019	8.86	-0.93	1.82	33.42
A3	0.004	1.72	-0.98	1.04	19.01
A4	-0.008	1.52	-0.93	2.61	43.16
A5	0.006	1.57	-0.91	4.72	28.75
A6	-0.005	1.29	-1.00	0.39	23.69
A7	0.078	3.35	-0.93	4.75	28.13
A8	-0.003	5.56	-0.98	4.54	24.46
A9	0.027	9.75	-0.96	1.48	25.32
A10	-0.001	1.25	-1.00	0.20	29.18
Dg1	0.014	9.16	-0.93	2.74	33.43
Bg1	-0.078	7.09	-0.86	5.44	23.69
N1	0.007	5.20	-0.88	2.98	28.75
P1	0.008	9.55	-0.82	3.78	38.10
M1	0.083	1.21	-0.93	1.87	3.42

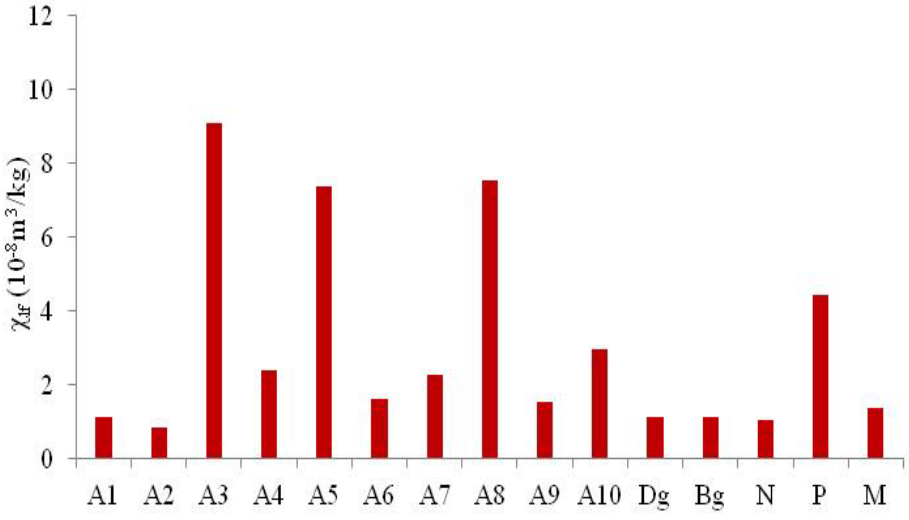
12
10
8
6
4
2
0
χ_{lf} ($10^{-8}m^3/kg$)
A1 A2 A3 A4 A5 A6 A7 A8 A9 A10 Dg Bg N P M

(a)

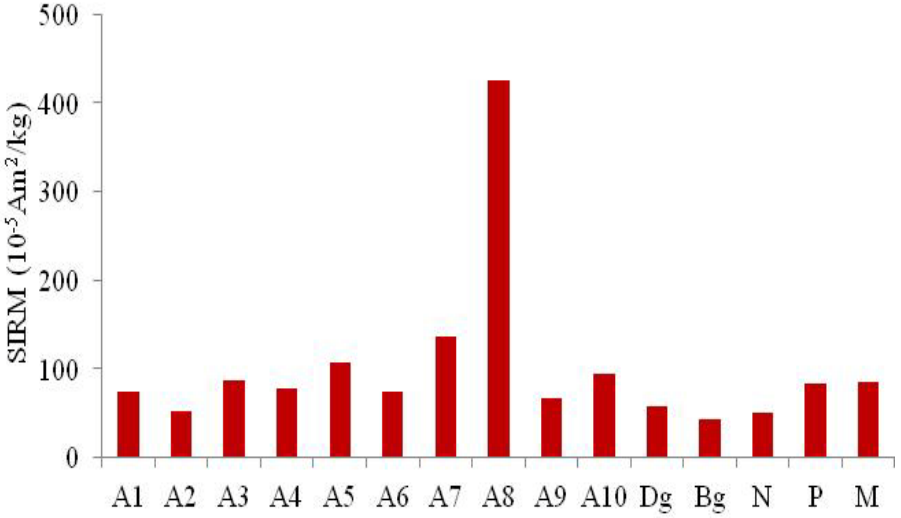
500
400
300
200
100
0
SIRM ($10^{-5}Am^2/kg$)
A1 A2 A3 A4 A5 A6 A7 A8 A9 A10 Dg Bg N P M

(b)

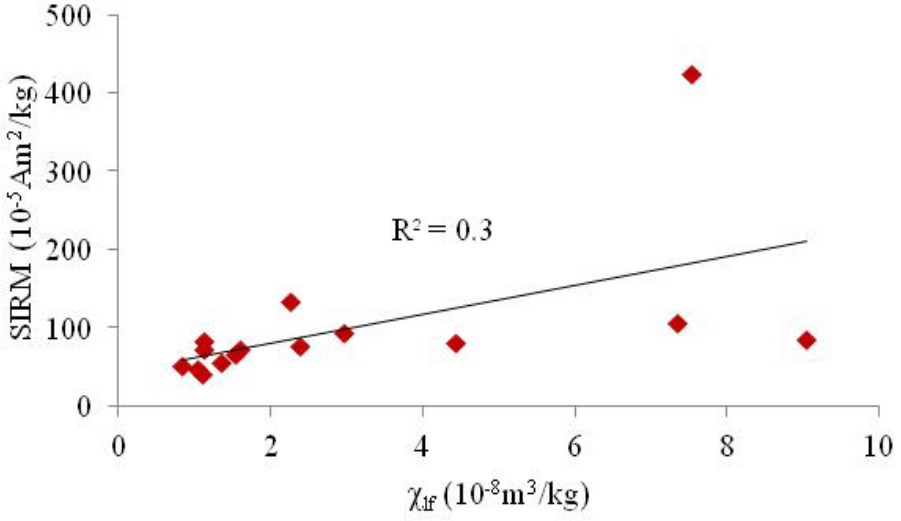
500
400
300
200
100
0
SIRM ($10^{-5}Am^2/kg$)
$R^2 = 0.3$
0 2 4 6 8 10
χ_{lf} ($10^{-8}m^3/kg$)

(c)

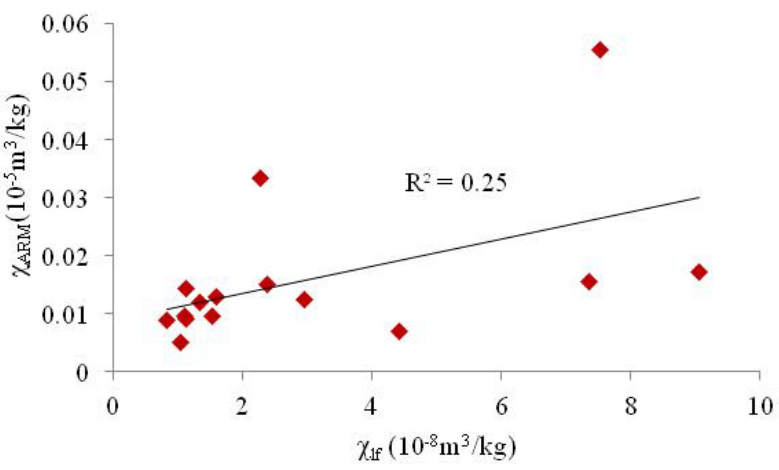

(d)

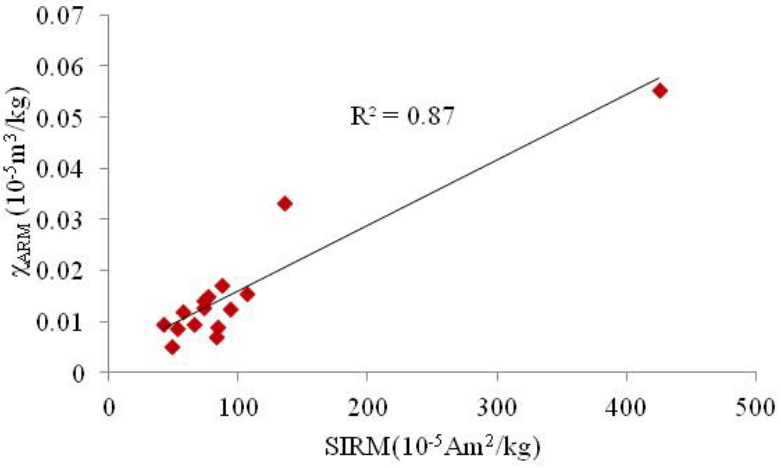

(e)

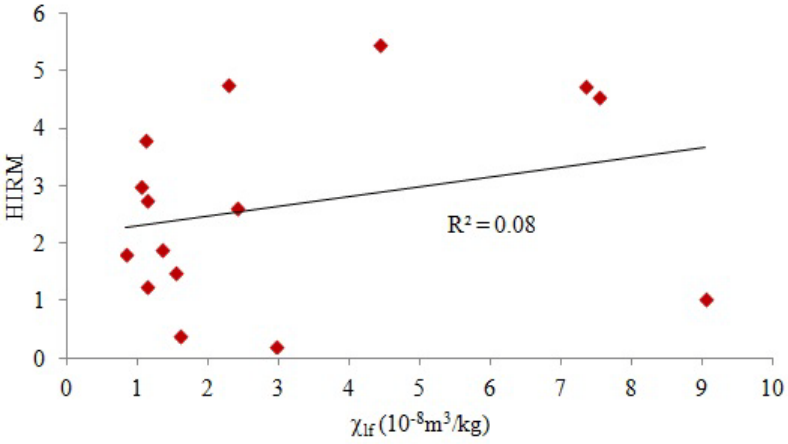

(f)

Figure 5.18 Plots of (a) downstream variation in χ_{lf} of the Alaknanda River sediments; (b) downstream variation in SIRM of the Alaknanda River sediments; (c) χ_{lf} versus SIRM; (d) χ_{lf} versus χ_{ARM}; (e) SIRM verses χ_{ARM}; (f) χ_{lf} verses HIRM

Table 5.13 Pearson correlation matrix for the mineral magnetic parameters of channel sediment samples

	χlf	**χfd**	**χ_{ARM}**	**SIRM**	**SIRM/ χlf**	**χ_{ARM}/ SIRM**	**χ_{ARM}/ χlf**	**HIRM**	**S-Ratio 300**	**$B_{(0)CR}$**
χlf	1									
χfd	-0.06	1								
χ_{ARM}	0.52	0.21	1							
SIRM	0.51	-0.03	0.93	1						
SIRM/χlf	-0.65	-0.08	0.10	0.16	1					
χ_{ARM} /SIRM	0.10	0.63	0.16	-0.17	-0.32	1				
χ_{ARM}/χlf	-0.56	0.43	0.24	0.07	0.75	0.34	1			
HIRM	0.20	-0.15	0.35	0.37	0.16	-0.15	-0.02	1		
S-Ratio 300	-0.14	-0.19	-0.35	-0.32	-0.08	-0.04	-0.24	0.64	1	
$B_{(0)CR}$	-0.40	0.30	-0.30	-0.32	0.05	0.25	0.19	0.04	0.45	1

5.4.3.3.Mineralogy Dependent Parameters

The magnetic parameters that yielded information about magnetic mineralogy include HIRM, S-ratio and SIRM/χ_{lf}. The high value of SIRM/χ_{lf} ensures minimal contribution from the paramagnetic grains (Sinha et al., 2007). Minerals with high coercivity values are termed as 'Hard' and these include anti-ferromagnetic minerals. Theoretically, the HIRM eliminates magnetic contribution from the low coercivity ferrimagnetic minerals that saturate below 300 mT (Liu et al., 2007; Xia et al., 2007). Figure 5.18(f) shows a very weak positive correlation between HIRM and χ_{lf}. The coercivity of isothermal remanent magnetization [$B_{(0)CR}$] ranged from 19-33 mT shows the dominance of ferrimagnetic single domain (SD) grains (Table 5.11) (Dunlop and Ozdemir, 1997; Sangode et al., 2007). S-ratio that quantifies the relative abundance of ferrimagnetic and antiferromagnetic minerals is given by IRM_{-100mT}/SIRM (Oldfield et al., 1985; Walden et al., 1997; Liu et al., 2007; Sinha et al., 2007). S-ratio in the Alaknanda watershed samples varied from -1 to -0.4, also indicate that the proportion of ferrimagnetic minerals contributes to the magnetic susceptibility. Thus, based on the indices such as saturation of most of the samples below 300 mT, low HIRM, negative S-ratio and $B_{(o)CR}$ values <50 mT, it can be inferred that magnetism in the Alaknanda basin is governed by ferrimagnetic grains.

5.4.3.4.Heavy Minerals and Magnetism

There is a close association between the heavy mineral assemblages and magnetic indices. To find out the influence of lithology on magnetism, mineral fraction carried by the Alaknanda

River at five locations (A1, A3, A6, A8 and A10) were identified. XRD studies showed that the dominant heavy mineral composition present in channel sediments is paramagnetic and diamagnetic. The dominant heavy minerals present in the sediments of the Alaknanda River are sillimanite, kyanite, hornblende, serpentine, and augite. The dominance of illite in the clay fraction (weathering products of the micaceous mineral) also affirms the paramagnetic nature of the Alaknanda River sediments (Section 5.3.1). The susceptibility of paramagnetic minerals is quite low typically around $5*10^{-4}$ (SI). The low value of χ_{lf} was found in all the samples. But it is generally seen that even if ferrimagnetic minerals are present in the trace amount, the paramagnetic character can be obscured. Magnetic parameters such as high value for SIRM/χ_{lf}, saturation of all samples below 300 mT and low $B_{(O)CR}$ confirm the predominance of ferrimagnetic minerals as accessory heavy minerals (low intensity peak in an XRD diffractogram) controlling the magnetic nature of the Alaknanda River.

5.4.3.5.Provenance of Channel Sediments

The Alaknanda basin is divided into upper and lower part based on the physiography and lithology of the basin (Section 3.1 and 3.3). The Higher Himalayas comprises of high grade metamorphic rocks, whereas the lower part of the basin comprises of low grade metamorphic rocks such as phyllite, quartzite, and schist of the Lesser Himalayan sequence. The presence of medium to high grade metamorphic minerals such as sillimanite, kyanite, hornblende, staurolite, garnet in the channel sediments points to the medium-high grade metamorphic and granitic-gneissic rocks as the source of the sediments (Carver, 1971). The Higher Himalayan sequence comprises of garnet-mica-schist/gneiss, quartzite, mylonitic augen gneiss, kyanite-garnet-biotite schist, sillimanite-kyanite-garnet-biotite schist with migmatite along with pegmatite veins and leucogranites (Jain et al., 2013). The presence of serpentine and augite indicates the weathering of volcanic suites of rocks that occur as intrusions in the Garhwal group. The continuous occurrence of sillimanite, kyanite, and hornblende along with a volcanic suite of minerals (serpentine and augite) points that the sediments in the Alaknanda basin owe its source from the weathering of Higher Himalayan Crystallines and Garhwal group of rocks. Similar to heavy mineral assemblages, change in magnetic susceptibility value also depicts the role of local lithology in influencing magnetic characteristics and the source of sediments.

The results are in accordance with other indices used in this study, REEs, major oxides and clay mineral assemblages. Previous studies of Galy and France-Lanord (2001); Singh (2010) and Garzanti et al. (2011) showed that the majority of sediments in the Ganga River owe their source to the Higher Himalayan Crystalline. Chakrapani et al. (2011) established that the

carbonate weathering source the dissolved load. But in this research with the employment of multiple indices in the headwater region of Ganga River (Alaknanda River basin), it can be stated that the Inner Lesser Himalayas are not only the source for the dissolved load but also a large part of the sediment load.

5.5. TOTAL ORGANIC CARBON (TOC) FLUX

5.5.1. Organic Carbon in the Alaknanda basin

DOC, POC, and COC constitute important forms of organic carbon (OC). The DOC concentration in the Alaknanda watershed varied both spatially and seasonally. During the pre-monsoon and monsoon season of the year 2014, DOC varied from 0.60-1.10 mg/l and 0.97-1.61 mg/l respectively (Table 5.14 and Fig. 5.19a). The concentration of DOC in the Alaknanda basin is far less than the global range of 1-20 mg/l (Meybeck, 1982). The absence of POC and the low amount of COC was evident in all the samples (Fig. 5.19b). Generally, it is found that POC in the river sediment is inversely related to TSS (Meybeck, 1982; Bird et al., 1991; Moreira-Turcq et al., 2003; Galy et al., 2007b; 2008).

The TSS concentration in the Alaknanda basin varied widely during different seasons. During the high flow (monsoon season), TSS concentration increases in the Alaknanda River (Fig. 5.1 and 5.2). Slopes in the Alaknanda catchment are quite unstable and a small disturbance can lead to landslides resulting in increase the sediment load in the Alaknanda River (Valdiya, 1980; Sati et al., 2011; Shukla et al., 2014; Roy et al., 2014). Figure 5.1 shows the seasonal variation and high amount of TSS during August, 2014. Figure 5.20(a) shows a moderately positive correlation between average monthly discharge (Qmean) and TSS. Permafrost is also an important source of sediment; near the proglacial source Alaknanda River carried 2.16 g/l of TSS (Hasnain and Chauhan, 1993). In Chamoli district, landslides and glaciers supply $2.75*10^5$ ton/year and $8.0*10^3$-$1.14*10^5$ ton/year of sediments respectively (Wasson, 2003). Thus, it can be considered that allochthonous input from the erosional activities (landslides and thawing of permafrost) add tons of sediments to the river system and act as the biggest source of OC carried by the river Alaknanda.

During the time of our sampling in August, 2014, TSS in the Alaknanda basin varied from 0.6 to 3.5 g/l respectively (Fig. 5.1a). The high TSS and turbulence in high flows result in reduced light penetration in the river and along with high current velocity affects the biogeochemical processes restraining the production of autochthonous organic matter and resulting in dilution of allochthonous OC (Ittekkot et al., 1985; Galy et al., 2007b; Bird et al., 1991; Moreira-Turcq et al., 2003). A moderately good correlation between TSS and DOC

suggests that as the concentration of TSS increased, dilution effect predominated resulting in high DOC concentrations (Fig. 5.20b). The high river energy during monsoon season favors the dissolution of OC resulting in high DOC concentration as shown by the positive correlation between discharge and DOC (Fig. 5.10c). The UCC normalized SiO_2 >1 and a low amount of Al_2O_3, P_2O_5, CaO in the channel sediments also suggest that dilution process predominated during the transportation of sediments in the Alaknanda River (Section 5.3.2, 5.4.1 and Fig. 5.13).

Table 5.14 Seasonal and spatial variability of DOC and COC flux

	Pre-Monsoon			Monsoon		
Sample	**DOC (mg/l)**	**COC (g/kg)**	**DOC Flux (kg/hr)**	**DOC (mg/l)**	**COC (g/kg)**	**DOC Flux (kg/hr)**
A1	0.95	1.25	0.48	1.06	0.62	19.46
A2	0.97	0.00	2.19	1.04	0.00	26.54
A3	0.86	5.39	-	1.03	2.51	-
A4	0.71	0.39	2.21	1.16	0.52	42.60
A5	0.70	2.00	3.87	1.01	0.38	53.80
A6	0.97	0.64	5.48	1.20	0.16	85.57
A7	1.10	0.39	-	1.61	0.98	-
A8	0.86	0.00	6.47	1.10	0.00	106.07
A9	0.60	1.03	-	0.97	0.00	-
A10	0.60	0.56	-	1.29	0.00	94.09
Dg	0.89	0.71	0.75	1.04	2.28	10.34
N	0.85	1.81	2.65	1.48	0.70	5.08
P	0.64	2.24	0.23	0.98	0.00	3.40
M	0.91	0.00	0.93	1.19	0.00	12.62
B	0.68	0.98	4.52	1.13	0.39	50.40
G1	0.98	0.51	-	1.21	0.00	142.22
G2	1.00	0.04	-	1.19	0.45	-

Thus, due to high energy environment prevailing in the Alaknanda catchment (because of steep terrain and high discharge), fresh and labile POC is consumed quickly and locally without significant transport downstream and hence, the Alaknanda River carried OC dominantly in the form of DOC. Figure 5.20(a-b) shows the increase in DOC and decrease in COC during the monsoon season. Thurman (1983) observed that POC has more residence time than DOC, but in the steep terrains, the residence time of POC and COC are controlled by the high river power and physiography of the basin. As 80% of the suspended flux is carried during the monsoon season and allochthonous sediments are the biggest source of OC, it is concluded that extrinsic

parameters such as physical erosion of the basin and seasonal erosivity controlled the DOC transport in the mountainous terrain of the Ganga basin.

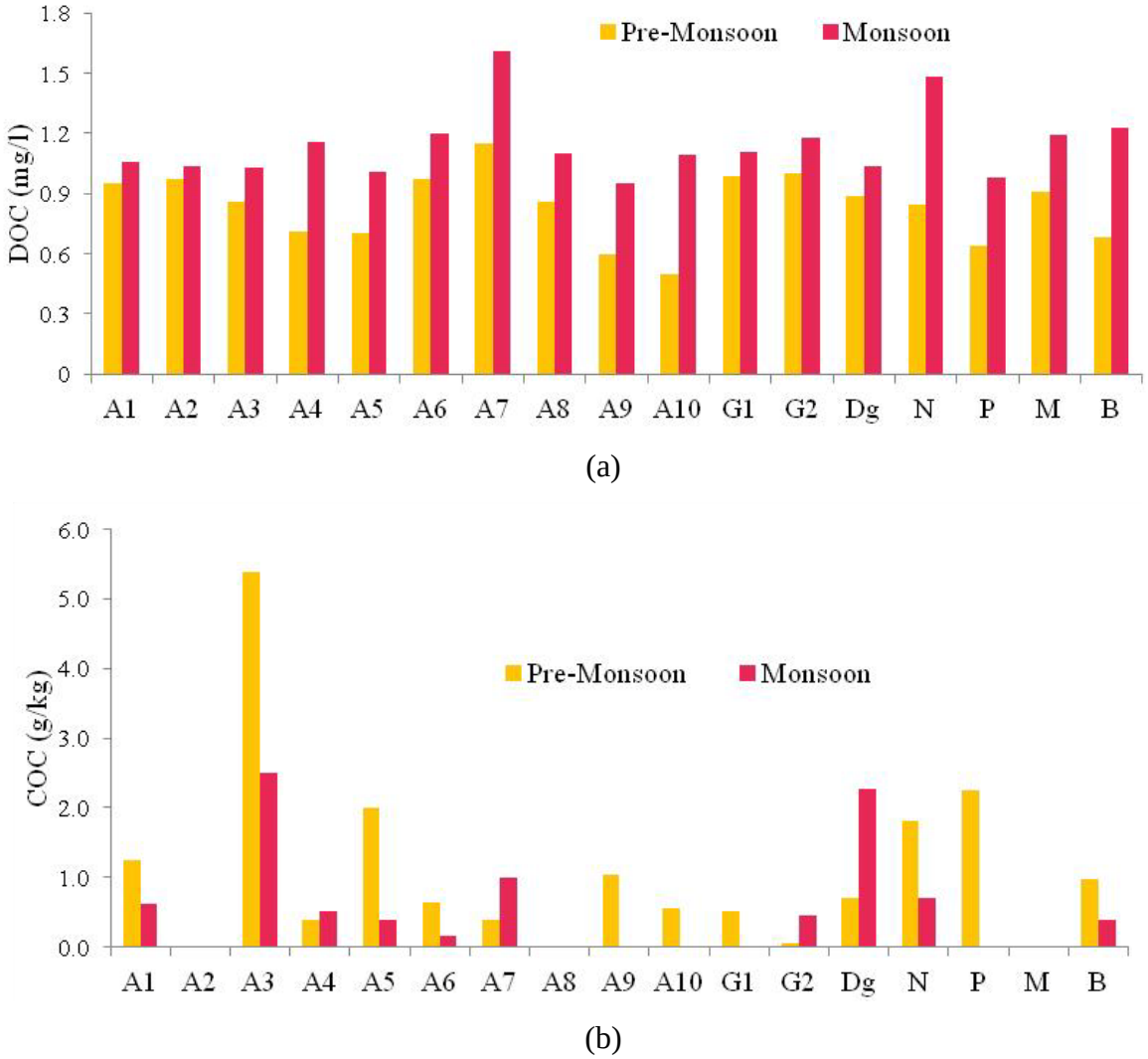

Figure 5.19 Variability of (a) DOC during pre-monsoon and monsoon season; (b) COC during pre-monsoon and monsoon season

5.5.2. Organic Carbon Flux

Using a long time series data, Singh and Hasnain (1998), Chakrapani and Saini (2009) and Chakrapani et al. (2009) established that at Devprayag, the Alaknanda River is a major contributor of the dissolved load to the Ganga River, more than its companion river Bhagirathi. Using the monthly flow data of AHEC (2011), DOC flux was estimated for the pre-monsoon and monsoon season (Table 5.14). The highest DOC flux ~106.1 kg/h was reported at Srinagar. At Devprayag, Alaknanda River added a DOC flux of ~94.1 kg/hr to the Ganga River which accounted for ~66% of the total DOC flux at Devprayag.

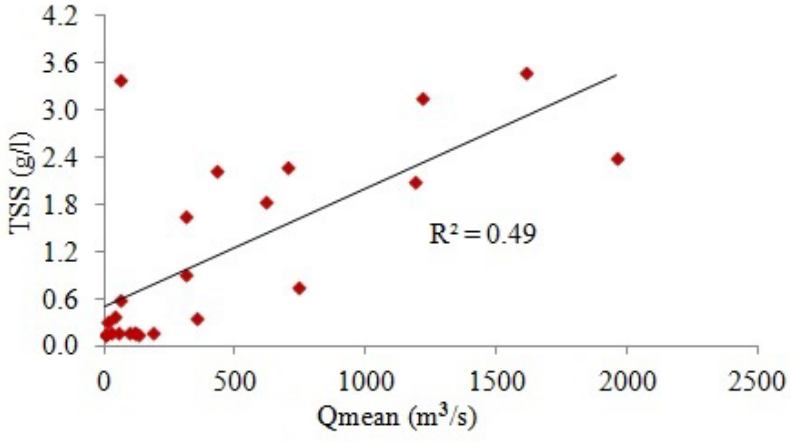

(a)

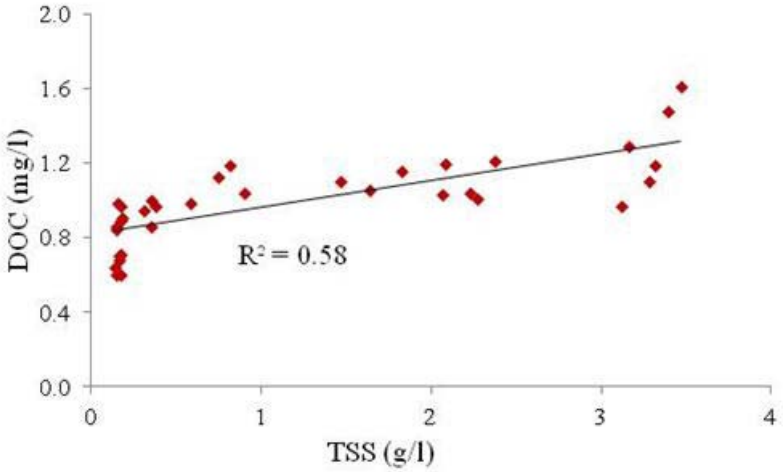

(b)

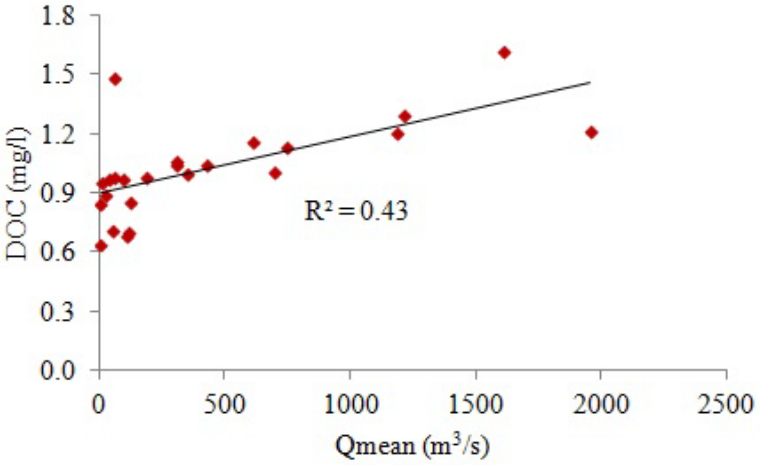

(c)

Figure 5.20 Correlations between (a) monthly discharge (Qmean) and TSS; (b) TSS and DOC; (c) monthly discharge (Qmean) and DOC (monthly discharge data mentioned in AHEC, 2011 was used)

5.5.3. Source of Organic Carbon

Raymond et al. (2007); Evans et al. (2007) and Butman et al. (2015) observed that DOC in river water is mostly of recent origin assimilated by plants and old carbon (fossilized) comprises only ~3-9% of the total DOC carried by the global rivers. Forests cover >60% of the total watershed area in the Alaknanda basin (Section 3.4, Fig. 3.6 and Table 3.5). On steep slopes, during monsoon, well-drained soils are more readily swept away by access water flowing down the streams. The $\delta^{13}C_{org}$ studies of the Bengal fan sediments by Aucour et al. (2006) and Galy et al. (2007b) established that Himalayan Rivers transport 70-85% of recent organic carbon. In the future, δ^{13}Corg and δ^{14}C measurement can further be used to study the different sources of organic carbon in the Alaknanda watershed. Both C_3 and C_4 vegetation are present in the UGB (Chakrapani and Veizer, 2005).

However, the observation in this study that OC in the Upper Ganga is significantly low in the channel sediment and absent in the suspended sediments helped in understanding the differences in the physiochemical conditions influencing TOC transport in the headwater region and the Ganga plains. The average slope of the Alaknanda River basin at Rudraprayag is 24 m/km, whereas the average slope of the Ganga plains down the Himalayan foothills is 9.5 cm/km (Shrivastava et al., 1999; AHEC, 2011). The high CIA values indicated an increase in loss of labile minerals and elements (McLennan, 1993). The Ganga plains have a CIA value of 65.9, and the Alaknanda basin has a value of ~56 (Section 5.3.2). Due to the gentle slope and high rate of chemical weathering, deposition of sediments in the Ganga plains takes place that favors the degradation of organic matter supported by the microbial growth (Galy et al., 2007b; 2008).

The integration of the data generated in this study with high OC content reported by Galy et al. (2008) in the surface suspended sediments downstream of Varanasi till the Bengal fan (Ganga Plains) points that recent OC present in the Ganga River sediments is added from the Ganga flood plains or contributed from downstream tributaries. Similar to Alaknanda River, Narayani-Gandak and Kosi rivers (Trans-Himalayan tributaries of the Ganga River, joining down the plains) also carries low OC in the particulate form (Galy et al., 2008). This comparison clearly indicates that due to continuous flushing, the upstream region of the Ganga basin acts as a supplier of sediment depleted in OC and hence, the high OC content in the Ganga sediments are due to the addition of organic matter from the Ganga plains. The Ganga plains are dominated by agricultural activities and human settlements and both C_3 and C_4 vegetation are dominantly present in the region.

CHAPTER 6

CONCLUSIONS AND FUTURE SCOPE

6.1. Conclusions

6.2. Future Scope

6.1. CONCLUSIONS

The major conclusions derived from the present studies are:

- At Devprayag, Alaknanda River delivered four times higher than the sediment load delivered by the Bhagirathi River to the River Ganga. The sediment yield during the non-monsoon and monsoon season of the year 2014 at Srinagar and Devprayag varied from 0.61 to 55.19 ton/km^2/day and 0.52 to 38.06 ton/km^2/day respectively. The seasonal sampling of suspended and channel sediment showed that there is no downstream trend in the sediment load and the grain size distribution of the sediments. Major factors that influence the sediment load in the UGB include precipitation and lithology of the basin. The long term discharge and TSS data of Rudraprayag and Lambagad highlight the existence of three distinct regimes in the UGB: low discharge-low TSS, high discharge-high TSS and the discharge peakedness that does not correspond to sediment peakedness. This indicated the effective sediment discharge of the river is not during the highest flow. Due to a high energy environment prevailing in the UGB (because of steep terrain and high discharge), fresh and labile TSS was consumed quickly and locally without significant transport downstream and restricted sediment peakedness during the precipitation and discharge peakedness (Ppk and Qpk) events.
- Grain size distribution seemed to be influenced by factors such as the climate, topography, contribution from tributaries, lithology and anthropogenic control of flow through dams and reservoirs. The study showed that more than the stream power, it is the sediment supply that controls the bedrock incision. The mean grain size (Ms) of the TSS in the Alaknanda basin is dominantly coarse silt. During both the post-monsoon and monsoon season, suspended sediments displayed poorly sorted, symmetrical to fine skewed and mesokurtic distribution. Channel sediments were mostly medium to coarse sand in all the three seasons and showed poor to moderately sorted and fine to symmetrically skewed distribution. Similar to the suspended sediments, unimodal grain size distribution was also common in the channel sediments. Bimodal grain size distribution in the samples A2, A6, B and G2 indicate the influence of tributaries, dams, and anthropogenic activities. Grain size distribution of channel sediments downstream of the Srinagar dam indicated the significant influence of man-made interventions in the Alaknanda River channel. During the low flow, enrichment of coarser channel sediments was witnessed.

- The clay mineral analysis showed that illite followed by kaolinite and chlorites are the most common clay minerals present in the Alaknanda River and its tributaries. During both the pre-monsoon and monsoon season, physical weathering (characterized by the presence of illite and chlorite) dominated the chemical weathering reactions (shown by the abundance of kaolinite). The low value of kaolinite/illite ratio, illite crystallinity index and illite chemistry index revealed the absence of hydrolysis processes and prevalence of weak chemical weathering reactions in the Alaknanda basin.

- Major oxide composition was used for quantifying the extent of silicate weathering in the basin and for the provenance determination of the sediments. The major oxide composition of channel sediments showed SiO_2 dominantly forms ~60% of the chemical composition, followed by Al_2O_3, CaO, MgO, Fe_2O_3, and K_2O. The values of Chemical Index of Alteration (CIA) and Weathering Index of Parker (WIP) and similar clay mineral assemblages in all the three seasons (pre-monsoon, monsoon and post-monsoon) indicated that due to rapid flushing of the sediments downstream, the high physical weathering during the monsoon season does not correspond to high chemical weathering in the Alaknanda basin. The average CIA value in the Alaknanda river basin is ~56, which is far less than the global average of 72.1 and the average CIA value of Asian rivers (~66) and the Yamuna River basin (a sub-basin of the Ganga River) having an average value of ~59.

- The provenance of suspended and channel sediment was determined by applying the multiple indices. The source of suspended sediment was determined by employing REEs as a fingerprinting tracer. Unlike most world rivers such as the Amazon, Mississippi, Huanghe and Indus, the sediments of Alaknanda River are enriched in HREE and LREE/HREE ratio varied from 0.44-0.70. The enrichment of HREE, the positive Eu anomaly and negative Ce anomaly in some of the samples confirmed that along with the K-feldspar (present in Higher Himalayan Crystallines), weathering of carbonates (limestone, dolomite, and magnesite of Garhwal Group) also source the suspended sediments carried by the Alaknanda River. Like previous studies, suspended sediments of the Alaknanda and the Ganga River at Devprayag and Rishikesh (sample A10, G1, and G2) showed high LREEs and the negative Eu anomaly and it was inferred that the Alaknanda River is a major contributor of the suspended load to the Ganga, more than the companion River Bhagirathi.

- The source of channel sediment was determined by applying the major oxide composition and mineral magnetism techniques along with the heavy mineral assemblages. The ratio of K_2O/Na_2O >1 signified the enrichment of K-feldspar rocks in the terrain. Principal component analysis (PCA) was performed to find out the geochemical affinity among the major oxide of the channel sediments. Three principal components extracted explained ~88% of the total variance. The three principal components represented three weathering reactions according to the geochemical affinity and the source bedrock. The results showed that the weathering of K-feldspar, carbonate and mafic rocks dominantly contribute channel sediments to the Alaknanda River.

- Similar to grain sizes, there seemed no downstream trend in the magnetic susceptibility values. Values of magnetic parameters χ_{lf}, SIRM, low HIRM, negative S-ratio and low $B_{(0)CR}$ point that magnetic mineralogy in the Alaknanda basin is governed by ferrimagnetic grains. The $\chi_{fd\%}$ of <2% and the low value of χ_{ARM}/SIRM confirmed the absence of superparamagnetic grains and χ_{ARM}/χ_{lf} indicated the presence of coarse magnetic particles in the sediment. Heavy mineral assemblages enriched in sillimanite, kyanite, hornblende, augite and serpentine prove the dominance of paramagnetic, diamagnetic and ferrimagnetic minerals in the channel sediments. The combined study of heavy mineral assemblages and magnetic parameters proved that the Higher Himalayan Crystallines and the Garhwal group of rocks source the sediments carried by the Alaknanda River.

- The results of REEs, major oxides, clay mineral assemblages, environmental magnetic parameters and heavy mineral assemblages were all in accordance with each other and revealed that Inner Lesser Himalayas does not only source dissolved load (as previously thought) but also a large part of the sediment load carried by the Alaknanda River.

- Due to dilution effects, the Alaknanda River and its tributaries carry organic carbon (OC) dominantly in the form of dissolved load (as dissolved organic carbon, DOC). Low amount of Al_2O_3, P_2O_5, CaO present in the channel sediments also suggested that process of dilution predominates during the transportation of sediments in the Alaknanda River. At Devprayag, Alaknanda River contributes 94.1 kg/hr of the DOC flux that accounts ~66% of the total DOC flux carried by the Ganga River. The residence time of the particulate organic carbon (POC) and channel organic

carbon (COC) in the basin is checked by the physiography of the basin and the seasonal erosivity. The integration of present data with high OC reported by Galy et al. (2008) in the surface suspended sediments of Ganga plains pointed that the Upper Ganga Basin exports organic carbon dominantly as DOC and the degradation of organic matter in the Ganga plains act as a major source of organic carbon carried by the Ganga River.

6.2. FUTURE SCOPE

The work done in this thesis, in the future can further be extended to study the erosion processes, sediment transportation and anthropogenic changes in the Alaknanda Basin.

- The Alaknanda basin has several gauging sites, the effect of climate and discharge on the sediment load carried by the river can be evaluated by considering the real time long term data. Sediment characteristics can be used to understand the effect of dams and reservoirs in the downstream area. Long term discharge, sediment load and grain size distribution data upstream and downstream of Lambagad and Srinagar dam can help in highlighting the significant effects of dams on the channel morphology.
- The present study highlighted the role of lithology in influencing the spatial variation in the amount of sediment load. The effect of lithology can be studied by considering a large number of detrital and bedrock sample collection and comparison of mineral and chemical phases of sediment with the bedrock lithology.
- Since anthropogenic activities are increasing in the Alaknanda basin. The anthropogenic changes influencing the erosion process in the basin can be studied on a large scale, by integrating the changes in LULC data, soil erosion, and sediment load carried by the river. The erosion models such as universal soil loss equation (USLE) or soil and water assessment tool (SWAT) can be applied on a temporal scale to understand the erosion enhancement or reduction with an increase in anthropogenic activities.
- In this study, rare earth elements (REEs), major oxides, magnetic parameters and heavy minerals prove that both the Inner Lesser Himalayas and Higher Himalayan Crystallines are the dominant supplier of sediments. However, a more detailed sampling strategy in the Alaknanda and similar studies in the adjoining Bhagirathi basin are still needed to develop a mixing model for the

Upper Ganga River basin. The contribution of tributaries (on the sub-basin scale) can also be marked using geochemistry as a tool.

- The denudation rate in the Alaknanda basin is a result of the interplay between the tectonics, climate, and physiography. The measurement of cosmogenic nuclide present in fluvial sediment can be used to estimate the denudation rate of the basin.
- A long term study related to dissolved organic carbon (DOC) flux carried by the Ganga River at Rishikesh and more sampling points in the Ganga alluvial plains can help in understanding the role of topography in controlling the carbon transportation. The δ^{13}Corg and δ^{14}C measurement in the Upper Ganga basin can further be used to understand the role of recent (vegetation) and fossilized source of the organic carbon.

BIBLIOGRAPHY

AHEC. Study on assessment of cumulative impact of hydropower projects in Alaknanda and Bhagirathi basins up to Devprayag. Ministry of Environment and Forest, New Delhi, India, chapter 7, pp. 134. 2011

Ali, K.F., de-Boer, D.H. Factors controlling specific sediment yield in the upper Indus River basin, northern Pakistan. Hydrological Processes 22:3102-3114. 2008

Allen, P.A. From landscapes into geological history. Nature, Reprinted from Vol. 451, no. 7176 (Supplement), pp. 274-276. 2008

Aller, R.C., Heilbrun, C. Panzeca, Z.B. Zhu, Baltzer, F. Coupling between sedimentary dynamics, early diagenetic processes, and biogeochemical cycling in the Amazon-Guianas mobile mud belt: Coastal French Guiana. Marine Geology 208:331-360. 2004

Andermann, C., Crave, A., Gloaguen, R., Davy, P., Bonnet, S. Connecting source and transport: Suspended sediments in the Nepal Himalayas. Earth and Planetary Science Letters 351:158-170. (2012a)

Andermann, C., Longuevergne, L., Bonnet, S., Crave, A., Davy, P., Gloaguen, R. Impact of transient groundwater storage on the discharge of Himalayan rivers. Nature Geoscience 5(2):127-132. (2012b)

Aucour, A.M., France-Lanord, C., Pedoja, K., Pierson-Wickmann, A.C., Sheppard, S.M.F. Fluxes and sources of particulate organic carbon in the Ganga-Brahmaputra river system. Global Biogeochemical Cycles 20:2004-2034. 2006

Aucour, A.M., Tao, F.X., Moreira-Turcq, P., Seyler, P., Sheppard, S.M.F., Benedetti, M.F. The Amazon River: Behaviour of metals (Fe, Al, Mn) and dissolved organic matter in the initial mixing zone at the Rio Negro/Solimoes confluence. Chemical Geology 197:271-285. 2003

Bagnold, R.A. Bed load transport by natural rivers. Water Resources Research 132:303-312. 1977

Bagnold, R.A. Sediment discharge and stream power: a preliminary announcement. US Geological Survey Circular 421:1-23. 1960

Bainbridge, Z.T., Wolanski, E., Alvarez-Romero, J.G., Lewis, S.E., Brodie, J.E. Fine sediment and nutrient dynamics related to particle size and floc formation in a Burdekin River flood plume, Australia. Marine Pollution Bulletin 65:236-248. 2012

Barnard, P.L., Owen, L.A., Sharma, M.C., Finkel, R.C. Natural and human-induced landsliding in the Garhwal Himalaya of Northern India. Geomorphology 40(1):21-35. 2001

Battin, T.J. Biophysical controls on organic carbon fluxes in fluvial networks. Nature Geoscience 1:95-100. 2008

Berner, E.K. Berner, R.A. The Global Water Cycle: Geochemistry and Environment. Prentice-Hall, Englewood cliffs, N.J., pp. 397. 1987

Berner, R.A., Berner, E.K. Global Environment: Water, Air, and Geochemical Cycles. Prentice-Hall, Englewood Cliffs, N.J., pp. 376. 1996

Bhandari, N., Shukla P.N., Azmi, R.J. Positive europium anomaly at the permotriassic boundary, Spiti, India. Geophysical Research Letters 19:1531-1534. 1992

Bhat, M., Claesson, S., Dubey, A.K., Pande, K. Sm-Nd age of the Garhwal-Bhowali volcanics, western Himalayas: vestiges of the Late Archaean Rampur flood basalt province of the northern Indian Craton. Precambrian Research 87:217-231. 1998

Bickle, M.J., Bunbury, J.M., Chapman, H.J., Harris, N.B.W., Fairchild, I.J., Ahmad, T. Fluxes of Sr into headwaters of the Ganges. Geochimica et Cosmochimica Acta 67:2567-2584. 2003

Bickle, M.J., Chapman, H.J., Bunbury, J., Harris, N.B., Fairchild, I.J., Ahmad, T., Pomies, C. Relative contributions of silicate and carbonate rocks to riverine Sr fluxes in the headwaters of the Ganges. Geochimica et Cosmochimica Acta 69(9):2221-2240. 2005

Bird, M.I., Chivas, A.R., Fyfe, W.S. Carbon ratios in the Amazon. Nature 354:271-272. 1991

Biscaye, P.E. Mineralogy and sedimentation of recent deep-sea clay in the Atlantic Ocean and adjacent seas and oceans. Geological Society of America Bulletin 76:803-831. 1965

Boggs, S. Principles of sedimentology and stratigraphy. Upper Saddle River, Prentice Hall. N.J., pp. 685. 2010

Booth, C.A., Walden, T.J., Neal, A., Smith, J.P. Use of mineral magnetic concentration data as a particle size proxy: a case study using marine, estuarine and fluvial sediments in the Carmarthen Bay area, South Wales, U.K. Science of the Total Environment 347:241-253. 2005

Borges, J., Huh, Y. Petrography and chemistry of the bed sediments of the Red River in China and Vietnam: provenance and chemical weathering. Sedimentary Geology 194:155-168. 2007

Bouchez, J., Gaillardet, J., France-Lanord, C., Maurice, L., Dutra-Maia, P. Grain size control of river suspended sediment geochemistry: clues from Amazon River depth profiles. Geochemistry, Geophysics, Geosystems 12(3):Q03008. 2011

Bravard, J.P., Goichot, M., Tronchere, H. An assessment of sediment-transport processes in the Lower Mekong River based on deposit grain sizes, the CM technique and flow-energy data. Geomorphology 207:174-189. 2014

Burdige D.J. Burial of terrestrial organic matter in marine sediments: a re-assessment. Global Biogeochemical Cycles 19:GB4011. 2005

Butman, D.E., Wilson, H.F., Barnes, R.T., Xenopoulos, M.A., Raymond, P.A. Increased mobilization of aged carbon to rivers by human disturbance. Nature Geoscience 8:112-116. 2015

Byrne, R.H., Kim, K.H. Rare earth element scavenging in sea water. Geochimica et Cosmochimica Acta 54:2645-2656. 1990

Caitcheon, G.G. The application of environmental magnetism to sediment source tracing: a new approach. Tracers in Hydrology (Proceedings of the Yokohama Symposium, July 1993), IAHS Publ. no. 215:285-292. 1993

Caitcheon, G.G. The application of environmental magnetism to sediment source tracing: a new approach. CSIRO Land and Water Technical Report No. 21/98, pp. 133. 1998

Carver, R.W. Procedures in sedimentary petrology. John Wiles, New York, pp. 458. 1971

Chakrapani, G.J. Major and trace element geochemistry in upper Ganga river in the Himalayas, India. Environmental Geology 48(2):189-201. 2005

Chakrapani, G.J., Saini, R.K. Temporal and spatial variations in water discharge and sediment load in the Alaknanda and Bhagirathi Rivers in Himalaya, India. Journal of Asian Earth Sciences 35(6):545-553. 2009

Chakrapani, G.J., Saini, R.K., Yadav, S.K. Chemical weathering rates in the Alaknanda-Bhagirathi river basins in Himalayas, India. Journal of Asian Earth Sciences 34:347-362. 2009

Chakrapani, G.J., Subramanian, V. Factors controlling sediment discharge in the Mahanadi river basin, India. Journal of Hydrology 117:169-185. 1990

Chakrapani, G.J., Veizer, J. Dissolved inorganic carbon isotopic compositions in the upstream Ganga river in the Himalayas. Current Science 89(3):553-556. 2005

Chakrapani, G.J., Veizer, J. Source of dissolved sulphate in the Alaknanda-Bhagirathi rivers in the Himalayas. Current Science 90(4):500-503. 2006

Chamley, H. Clay Sedimentology. Springer, New York, pp. 623. 1989

Choudhary, P., Routh, J., Chakrapani, G.J. An environmental record of changes in sedimentary organic matter from Lake Sattal in Kumaun Himalayas, India. Science of the Total Environment 407(8):2783-2795. 2009a

Choudhary, P., Routh, J., Chakrapani, G.J. Comparison of bulk organic matter characteristics in sediments of three Kumaun Himalayan lakes. Current Science 97(4):572-575. 2009b

Church, M.A., Kellerhals, R. On the statistics of grain size variation along a gravel river. Canadian Journal of Earth Sciences 15(7):1151-1160. 1978

Cole, J.J., Prairie, Y.T., Caraco, N.F., McDowell, W.H., Tranvik, L.J., Striegl, R.G., Duarte, C.M., Kortelainen, P., Downing, J.A., Middelburg, J.J., Melack, J. Plumbing the global carbon cycle: integrating inland waters into the terrestrial carbon budget. Ecosystems 10:172-185. 2007

Collins, A.L., Walling, D.E., Leeks, G.J.L. Use of composite fingerprints to determine the provenance of the contemporary suspended sediment load transported by rivers. Earth Surface Processes and Landforms 23(1):31-52. 1998

CWC. Report of working group to advise WQAA on the minimum flows in the rivers. Central Water Commission, Ministry of Water Resources, New Delhi, India. 2007

Dahm, C.N., Greogory, S.V., Park, P.K. Organic carbon transport in the Columbia River. Estuarine Coastal and Shelf Science 13:645-658. 1981

Dalai, T.K., Rengarajan, R., Patel, P.P. Sediment geochemistry of the Yamuna river system in the Himalaya: implications to weathering and transport. Geochemical Journal 38:441-453. 2004

Das, B.K., AL-Mikhlafi, A.S., Kaur, P. Geochemistry of Mansar Lake sediments, Jammu, India: implication for source area weathering, provenance, and tectonic setting. Journal of Asian Earth Sciences 26(6):649-668. 2006

Das, B.K., Gaye, B., Kaur, P. Geochemistry of Renuka lake and wetland sediments, Lesser Himalaya India: implication of source area. Environmental Geology 54:147-163. 2008

Das, B.K., Haake, B.G. Geochemistry of Rewalsar Lake sediment, Lesser Himalaya, India: implications for source-area weathering, provenance and tectonic setting. Geosciences Journal 74:299-312. 2003

Datta, D.K., Subramanian, V. Texture and mineralogy of sediments from the Ganges-Brahmaputra-Meghna river system in the Bengal Basin, Bangladesh and their environmental implications. Environmental Geology 30:181-188. 1997

Davis, C.M., Asce, M., Fox, J.F., Asce, M. Sediment fingerprinting: review of the method and future improvements for allocating nonpoint source pollution. Journal of Environmental Engineering 135:490-504. 2009

Dearing, J.A., Hay, K.L., Baban, S.M.J., Huddleston, A.S., Wellington, E.M.H., Loveland, P.J. Magnetic susceptibility of soil: an evaluation of conflicting theories using a national data set. Geophysical Journal International 127:728-734. 1996

Deasy, C., Quinton, J.N. Use of rare earth oxides as tracers to identify sediment source areas for agricultural hillslopes. Solid Earth Discussions 2:195-212. 2010

Dekkers, M.J. Environmental Magnetism: an introduction. Geologie en Mijnbouw 76:163-182. 1997

Demlie, M., Wohnlich, S. Soil and groundwater pollution of an urban catchment by trace metals: case study of the Addis Ababa region, Central Ethiopia. Environmental Geology 51(3):421-431. 2006

Diplas, P., Parker, G. Deposition and removal of fines in gravel-bed streams. Dynamics of gravel bed rivers, Chichester: Wiley, pp. 313-329. 1992

Dosseto, A., Vigier, N., Joannes-Boyau, R., Moffat, I., Singh, T., Srivastava, P. Rapid response of silicate weathering rates to climate change in the Himalaya. Geochemical Perspectives Letter 1:10-19. 2015

Draut, A.E., Logan, J.B., Mastin, M.C. Channel evolution on the dammed Elwha River, Washington, USA. Geomorphology 127:71-87. 2011

Dunlop, D.J. Ozdemir, O. Rock magnetism: fundamentals and frontiers. Cambridge University Press, Cambridge, pp. 565. 1997

Dupre, B., Gaillardet, J., Rousseau, D., Allegre, C.J. Major and trace elements of river-borne materials: the Congo Basin. Geochimica et Cosmochimica Acta 60:1301-1321. 1996

Duzgoren-Aydin, N.S., Aydin, A. Indices for scaling and predicting weathering-induced changes in rock properties. Environmental and Engineering Geosciences 2:121-135. 2002

Ehrmann, W. Implications of late Eocene to early Miocene clay mineral assemblages in McMurdo Sound (Ross Sea, Antarctica) on paleoclimate and ice dynamics. Palaeogeography, Palaeoclimatology, Palaeoecology 139:213-231. 1998

Evan, M.E., Heller, F. Environmental magnetism principles and applications of enviromagnetics. Academic Press, an imprint of Elsevier Science, California, USA, pp. 293. 2003

Evans, C.D., Freeman, C., Cork, L.G., Thomas, D.N., Reynold, B., Billett, M.F., Garnett, M.H., Norris, D. Evidence against recent climate-induced destabilisation of soil carbon from ^{14}C analysis of riverine dissolved organic matter. Geophysical Research Letters 34:L07407. 2007

Feng, J.L., Hu, Z.G., Ju, J.T., Zhu, L.P. Variations in trace element (including rare earth element) concentrations with grain sizes in loess and their implications for tracing the provenance of eolian deposits. Quaternary International 236:116-126. 2011

Fletcher, W.K., Loh, C.H. Transport equivalence of cassiterite and its application to stream sediment surveys for heavy minerals. Journal of Geochemical Exploration 56:47-57. 1996

Folk, R.L., Ward, W.C. Brazos river bar: a study in the significance of grain size parameters. Journal of Sedimentary Petrology 27(I):3-26. 1957

France-lanord, C., Derry, L., Micharda, A. Evolution of the Himalaya since Miocene time: isotopic and sedimentologic evidence from the Bengal Fan. In Himalayan Tectonics (ed. P.J. TRELOAR and M. SEARLE). Geological Society of London 74:603-621. 1993

France-Lanord, C., Derry, L.A. Organic carbon burial forcing of the carbon cycle from Himalayan erosion. Nature 390:65-67. 1997

Franke, C., Kissel, C., Robin, E., Bonte, P., Lagroix, P. Magnetic particle characterization in the Seine river system: implications for the determination of natural versus anthropogenic input. Geochemistry Geophysics Geosystems 10(8):Q08Z05. 2009

Franzinelli, E., Potter, P.E. Petrology, chemistry, and texture of modern river sands, Amazon River system. Journal of Geology 91:23-39. 1983

Frings, P.J., Clymans, W., Fontorbe, G., Gray, W., Chakrapani, G., Conley, D.J., De La Rocha, C. Silicate weathering in the Ganges alluvial plain. Earth and Planetary Science Letters 427:136-148. 2015

Gaillardet J., Dupre B., Allegre C.J. A global geochemical mass budget applied to the Congo Basin rivers: erosion rates and continental crust composition. Geochimica et Cosmochimica Acta 59(17):3469-3485. 1995

Gaillardet, J., Dupre, B., Allegre, C.J. Geochemistry of large river suspended sediments: silicate weathering or recycling tracer? Geochimica et Cosmochimica Acta 63(23):4037-4051. 1999

Galy, A., France-Lanord, C. Higher erosion rates in the Himalaya: geochemical constraints on riverine fluxes. Geology 29(1):23-26. 2001

Galy, V., Bouchez, J., France-Lanord, C. Determination of total organic carbon content and $d^{13}C$ in carbonate rich detrital sediments. Geostandards and Geoanalytical Research 31:199-207. 2007a

Galy, V., France-Lanord, C., Beyssac, O., Faure, P., Kudrass, H., Palhol, F. Efficient organic carbon burial in the Bengal fan sustained by the Himalayan erosional system. Nature 450:407-410. 2007b

Galy, V., France-Lanord, C., Lartiges, B. Loading and fate of particulate organic carbon from the Himalaya to the Ganga-Brahmaputra delta. Geochimica et Cosmochimica Acta 72:1767-1787. 2008

Gansser, A. Geology of the Himalayas. Interscience Publishers, John Wiley & Sons Ltd., London, pp. 289. 1964

Garzanti, E., Ando, S., France-lanord, C., Censi, P., Vignola, P., Galy, V., Lupker, M. Mineralogical and chemical variability of fluvial sediments 2. Suspended-load silt (Ganga-Brahmaputra, Bangladesh). Earth and Planetary Science Letters 302:107-120. 2011

Gibbs, R.J. The geochemistry of the Amazon River system: Part I. The factors that control the salinity and the composition and concentration of the suspended solids. Geological Society of America Bulletin 78:1203-1232. 1967

Girmay, E., Ayenew, T., Kebede, S., Alene, M., Wohnlich, S., Wisotzky, F. Conceptual groundwater flow model of the Mekelle Paleozoic-Mesozoic sedimentary outlier and surroundings (northern Ethiopia) using environmental isotopes and dissolved ions. Hydrogeology Journal 23(4):649-672. 2015

Goldich, S.S. A study in rock weathering. Journal of Geology 46:17-58. 1938

Goldstein, S.J., Jacobson, S.B. Rare earth elements in river waters. Earth and Planetary Science Letters 89:35-47. 1988

Goni, M.A, Monacci, N., Gisewhitem, R., Ogston, A., Crockett, J., Nittrouer, C. Distribution and sources of particulate organic matter in the water column and sediments of the Fly River Delta, Gulf of Papua Papua New Guinea. Estuarine, Coastal and Shelf Science 69:225-245. 2006

Griffin, J.J., Windom, H. L., Goldberg, E.D. The distribution of clay minerals in the world ocean. Deep-Sea Research 15:433-459. 1968

Gudadhe, S.S., Sangode, S.J., Patil, S.K., Chate, D.M., Meshram, D.C., Badekar, A.G. Pre-and post-monsoon variations in the magnetic susceptibilities of soils of Mumbai metropolitan region: implications to surface redistribution of urban soils loaded with anthropogenic particulates. Environmental Earth Sciences 67(3):813-831. 2012

Gupta, S., Banerjee, R., Ramesh Babu, P.V., Parihar, P.S., Maithani, P.B. Geochemistry of uraniferous Banganapalle sediments in the western part of Palnad sub-basin, Andhra Pradesh: implications on provenance and paleo-weathering. Gondwana Geological Magazine 13:1-14. 2012

Gururajan, N.S. Choudhuri, B.K. Ductile thrusting, metamorphism and normal faulting in Dhauliganga Valley, Garhwal Himalaya. Himalayan Geology 20(2):19-29. 1999

Guyot, J.L., Jouanneau, J.M., Soares, L., Boaventura, G.R., Maillet, N., Lagane, C. Clay mineral composition of river sediments in the Amazon Basin. Catena 71:340-356. 2007

Hall, F.R., Busch, W.H., King, J.W. The relationship between variations in rock magnetic properties and grain size of sediments from ODP Hole 645C. Proceedings of the Ocean Drilling Program, Scientific Results 105:837-841. 1989

Hamdan, J., Burnham, C.P. The contribution of nutrients from parent material in three deeply weathering soils of Peninsular Malaysia. Sedimentary Geology 55:319-322. 1996

Hannigan, R., Dorval, E., Jones, C. The rare earth element chemistry of estuarine surface sediments in the Chesapeake Bay. Chemical Geology 272:20-30. 2010

Hasnain, S.I., Chauhan, D.S. Sediment transfer in the glaciofluvial environment-a Himalayan perspective. Environmental Geology 22:205-211. 1993

Hatfield, R.G., Maher, B.A. Fingerprinting upland sediment sources: particle size-specific magnetic linkages between soils, lake sediments and suspended sediments. Earth Surface Processes and Landforms 34(10):1359-1373. 2009

Hayes, J.M., Strauss, H., Kaufman, A.J. The abundance of ^{13}C in marine organic matter and isotopic fractionation in the global biogeochemical cycle of carbon during the past 800 Ma. Chemical Geology 161:103-125. 1999

He, M., Zheng, H., Huang, X., Jia, J., Li, L. Yangtze River sediments from source to sink traced with clay mineralogy. Journal of Asian Earth Sciences 69:60-69. 2013

Heim, A., Gansser, A. Central Himalaya-Geological Observation of Swiss Expedition 1936. Mem. Soc. Helv. Sci. Nat. 73:1-245. 1939

Hemming, S.R., Biscaye, P.E., Broecker, W.S., Hemming, N.G., Klas, M., Hajdas, I. Provenance change coupled with increased clay flux during deglacial times in the equatorial Atlantic. Palaeogeography, Palaeoclimatology, Palaeoecology 142:217-230. 1998

Hillier, S. Erosion, sedimentation and sedimentary origin of clays. In Origin and Mineralogies of Clays (Ed. by B.Velde), Springer-Verlag, Berlin, pp. 162-219. 1995

Horng, C.S. Huh, C.A. Magnetic properties as tracers for source-to-sink dispersal of sediments: a case study in the Taiwan Strait. Earth and Planetary Science Letters 309:141-152. 2011

Horowitz, A., Elrick, K. The relation of stream sediment surface area, grain size, and composition to trace element chemistry. Applied Geochemistry 2:437-451. 1987

Horowitz, A.J. A primer on sediment trace element chemistry, 2nd edn, Lewis Publishers, Inc.: Chelsea, MI, pp. 136. 1991

Horowitz, A.J., Stephens, V.C., Elrick, K.A., Smith, J.J. Concentrations and annual fluxes of sediment-associated chemical constituents from conterminous US coastal rivers using bed sediment data. Hydrological Processes 26(7):1090-1114. 2012

Hounslow, M.W., Morton, A.C. Evaluation of sediment provenance using magnetic mineral inclusions in clastic silicates: comparison with heavy mineral analysis. Sedimentary Geology 171(1):13-36. 2004

Hren, M.T., Hilley, G.E., Chamberlain, C.P. The relationship between tectonic uplift and chemical weathering rates in the Washington Cascades: field measurements and model predictions. American Journal of Science 307:1041-1063. 2007

Hung, L.Q., Batelaan, O., DeSmedt, F. Lineament extraction and analysis, comparison of LANDSAT ETM and ASTER imagery. Case study: Suoimuoi tropical karst catchment, Vietnam. Remote Sensing. International Society for Optics and Photonics, Proceedings of SPIE: 598359830T-1. 2005.

Huyghe, P., Guilbaud, R., Bernet, M., Galy, A., Gajurel, A.P. Significance of the clay mineral distribution in fluvial sediments of the Neogene to Recent Himalayan foreland basin (West-Central Nepal). Basin Research 23(3):332-345. 2011

Irion, G. Clay mineralogy of the suspended load of the Amazon and of rivers in the Papua-New Guinea mainland. Mitteilungen Geologie und Palaontologie Institut Universitat Hamburg 55:483-504. 1983

Ittekkot, V., Safiullah, S., Mycke, B., Seifert, R. Seasonal variability and geochemical significance of organic matter in the River Ganges, Bangladesh. Nature 317:800-802. 1985

Jain, A.K., Seth, P., Shreshtha, M., Mukherjee, P.K., Singh, K. Structurally controlled melt accumulation: Himalayan migmatites and related deformation-Dhauli Ganga valley, Garhwal Himalaya. Journal of the Geological Society of India 82(4):313-318. 2013

Jenkins, P.A., Duck, R.W., Rowan, J.S., Walden, J. Fingerprinting of bed sediment in the Tay Estuary, Scotland: an environmental magnetism approach. Hydrological Earth System Sciences 6(6):1007-1016. 2002

Johnsson, M.J., Meade, R.H. Chemical weathering of fluvial sediments during alluvial storage: the Macuapanim island point bar, Solimoes River, Brazil. Journal of Sedimentary Petrology 60:827-842. 1990

Juyal, N., Sundriyal, Y., Rana, N., Chaudhary Singhvi, A.K. Late Quaternary fluvial aggradation and incision in the monsoon-dominated Alaknanda valley, Central Himalaya, Uttarakhand, India. Journal of Quaternary Science 25(8):1293-1304. 2010

Kamaruzzaman, Y., Siti, W.A., Ong, M.C., Joseph, B. Spatial distribution of lead and copper in the bottom sediments of Pahang river estuary, Pahang, Malaysia. Sains Malaysiana 39:543-547. 2010

Keil, R.G., Mayer, L.M., Quay, P.D., Richey, P.D., Richey, J.E., Hedges, J.I. Loss of organic matter from riverine particles in deltas. Geochimica et Cosmochimica Acta 61:1507-1511. 1997

Khanna, P.P., Saini, N.K., Mukherjee, P.K., Purohit, K.K. An appraisal of ICP-MS technique for determination of REEs: long term QC assessment of silicate rock analysis. Himalayan Geology 30(1):95-99.2009

Krishnaswami, S., Singh, S.K. Chemical weathering in the river basins of the Himalaya, India. Current Science 89(5):841-849. 2005

Krumm, S., Buggisch, W. Sample preparation effects on illite crystallinity measurements: grain size gradation and particle orientation. Journal of Metamorphic Geology 9:671-677. 1991

Kulkarni, Y.R., Sangode, S.J., Meshram, D.C., Patil, S.K., Dutt, Y. Mineral magnetic characterization of the Godavari River Sediments: implications to Deccan Basalt weathering. Journal of Geological Society of India 83:376-384. 2014

Kumar, G. Geology and sulphide mineralization in the Pokheri area Chamoli District, Uttar Pradesh. Geological Survey of India (Miscellaneous Publication) 16:92-12. 1971

Kumar, G. Geology of Uttar Pradesh and Uttaranchal. Geological Society of India, Bangalore, pp. 383. 2005

Legleiter, C.J., Roberts, D.A., Marcus, W.A., Fonstad, M.A. Passive optical remote sensing of river channel morphology and in-stream habitat: physical basis and feasibility. Remote Sensing of Environment 93(4):493-510. 2004

Lenzi, M.A., Mao, L., Comiti, F. Effective discharge for sediment transport in a mountain river: computational approaches and geomorphic effectiveness. Journal of Hydrology 326(1):257-276. 2006

Li, C., Yang, S.Y. Is chemical index of alteration a reliable proxy for chemical weathering in global drainage basins? American Journal of Science 310:111-127. 2010

Li, C.S., Shi, X.F., Kao, S.J., Liu, Y.G., Lyu, H.H., Zou, J.J., Liu, S.F., Qiao, S.Q. Rare earth elements in fine-grained sediments of major rivers from the high-standing island of Taiwan. Journal of Asian Earth Sciences 69:39-47. 2013

Limmer, D.R., Boning, P., Giosan, L., Ponton, C., Kohler, C.M., Cooper, M.J., Tabrez, A.R., Clift, P.D. Geochemical record of Holocene to Recent sedimentation on the Western Indus continental shelf, Arabian Sea. Geochemisty, Geophysics and Geosystems 13:Q01008. 2012

Lin, S., Hsieh, I.J., Huang, K.M., Wang, C.H. Influence of the Yangtze River and grain size on the spatial variations of heavy metals and organic carbon in the East China Sea continental shelf sediments. Chemical Geology 182(2):377-394. 2002

Lindholm, R.A. Practical Approach to Sedimentology. Allen & Unwin, London, pp. 278. 1987

Liu, J., Saito, Y., Kong, X.H., Wang, H., Zhao, L. Geochemical characteristics of sediment as indicators of post-glacial environmental changes off the Shandong Peninsula in the Yellow Sea. Continental Shelf Research 29:846-855. 2009

Liu, S., Zhang, W., He, Q., Li, D., Liu, H., Yu, L. Magnetic properties of East China Sea shelf sediments off the Yangtze Estuary: influence of provenance and particle size. Geomorphology 119:212-220. 2010

Liu, W.X., Li, X.D., Shen, Z.G., Wang, D.C., Wai, O.W.H., Li, Y.S. Multivariate statistical study of heavy metal enrichment in sediments of the Pearl River Estuary. Environmental Pollution 121(3):377-388. 2003

Liu, X., Rolph, T., Bloemendal, J., Shaw, J. Liu, T. Quantitative estimates of palaeoprecipitation at Xifeng in the Loess Plateau of China. Palaeogeography, Palaeoclimatology, Palaeoecology 113:243-248. 1995

Liu, Z., Colin, C., Huang, W., Phon Le, K., Tong, S., Chen, Z., Trentesaux, A. Climatic and tectonic controls on weathering in south China and Indochina Peninsula: clay mineralogical and geochemical investigations from the Pearl, Red, and Mekong drainage basins. Geochemistry, Geophysics, Geosystems 8(5):1-18. 2007

Lunetta, R.S., Ediriwickrema, J., Johnson, D.M., Lyon, J.G., McKerrow, A. Impacts of vegetation dynamics on the identification of land-cover change in a biologically complex community in North Carolina, USA. Remote sensing of Environment 82(2):258-270. 2002

Lupker, M., Blard, P.H., Lave, J., France-Lanord, C., Leanni, L., Puchol, N., Charreau, C., Bourles, D. ^{10}Be-derived Himalayan denudation rates and sediment budgets in the Ganga basin. Earth and Planetary Science Letters 333:146-156. (2012a)

Lupker, M., France-Lanord, C., Galy, V., Lave, J., Gaillardet, J., Gajurel, A.P., Guilmette, C., Rahman, M., Singh, S.K., Sinha, R. Predominant floodplain over mountain weathering of Himalayan sediments (Ganga basin). Geochimica et Cosmochimica Acta 84(C):410-432. (2012b)

Lupker, M., France-Lanord, C., Lave, J., Bouchez, J., Galy, V., Metivier, F., Gaillardet, G., Lartiges, B., Mugnier, J.L. A Rouse-based method to integrate the chemical composition of river sediments: Application to the Ganga basin. Journal of Geophysical Research 116(F4):F04012. (2011)

Machiwal, D., Srivastava, S.K., Jain, S. Estimation of sediment yield and selection of suitable sites for soil conservation measures in Ahar river basin of Udaipur, Rajasthan using RS and GIS techniques. Journal of the Indian Society of Remote Sensing 38(4):696-707. 2010

Maher, B.A., Alekseev, A., Alekseeva, T. Variation of soil magnetism across the Russian steppe: its significance for use of soil magnetism as a palaeorainfall proxy. Quaternary Science Reviews 21(14):1571-1576. 2002

Maher, B.A., Thompson, R. Quaternary Climates, Environments and Magnetism. Cambridge University Press, pp. 383. 1999

Maher, B.A., Thompson, R., Zhou, L.P. Spatial and temporal reconstructions of changes in the Asian palaeomonsoon: a new mineral magnetic approach. Earth and Planetary Science Letters 125(1):461-471. 1994

Marques, W.S., Sial, A.N., de Albuquerque Menor, E., Ferreira, V.P., Freire, G.S.S., de Albuquerque Medeiros Lima, E., do Amaral Vaz Manso, V. Principal component analysis (PCA) and mineral associations of litoraneous facies of continental shelf carbonates from North Eastern Brazil. Continental Shelf Research 28(20):2709-2717. 2008

Martin, J.M., Maybeck, M. Elemental mass-balance of material carried by major world rivers. Marine Chemistry 7:173-206. 1979

Martinelli, L., Victoria, R.L., Dematte, J.L.I., Richey, J.E., Devol, A.H. Chemical and mineralogical composition of Amazon River floodplain sediments, Brazil. Applied Geochemistry 8:391-402. 1993

McLennan, S.M. Relationships between the trace element composition of sedimentary rocks and upper continental crust. Geochemistry Geophysics Geosystems 2:4. 2001

McLennan, S.M. Weathering and global denudation. The Journal of Geology 101:295-303. 1993

Meade, R.H., Dunne, T., Richey, J.E. Santos, U.D.M., Salati, E. Storage and remobilization of suspended matter in the lower Amazonas River of Brazil. Science 228:488-490. 1985

Meybeck, M. Carbon, nitrogen and phosphorus transport by World Rivers. American Journal of Science 282:401-450. 1982

Meybeck, M. Global chemical weathering from surficial rocks estimated from river dissolved loads. American Journal of Science 287:401-428. 1987

Meyers, P.A. Eadie B.J. Sources, degradation and recycling of organic matter associated with sinking particles in Lake Michigan. Organic Geochemistry 20(1):47-56. 1993

Milliman, J.D., Farnsworth, F.L. River discharge to the coastal ocean: a global synthesis. Cambridge University Press, New York, pp. 382. 2011

Milliman, J.D., Meade, R.H. Worldwide delivery of river sediment to the oceans. Journal of Geology 91(1):1-21. 1983

Milliman, J.D., Syvitski, J.M.P. Geomorphic/tectonic control of sediment discharge to the ocean: the importance of small mountainous rivers. Journal of Geology 100:525-544. 1992

Moreira-Turcq, P., Seyler, P., Guyot, J.L., Etcheber, H. Exportation of organic carbon from the Amazon River and its main tributaries. Hydrological Processes 17:1329-1344. 2003

Morin, G.P., Vigier, N., Verney-Carron, A. Enhanced dissolution of basaltic glass in brackish waters: impact on biogeochemical cycles. Earth and Planetary Science Letters 417:1-8. 2015

Morton, A.C., Davies, J.R., Waters, R.A. Heavy minerals as a guide to the turbidite provences in the Lower Palaeozoic Southern Welsh Basin: a pilot study. Geological Magazine 129(5):573-580. 1992

Morton, A.C., Hallsworth, C. Identifying provenance-specific features of detrital heavy mineral assemblages in sandstones. Sedimentary Geology 90:241-256. 1994

Morton, A.C., Hallsworth, C. Processes controlling the composition of heavy mineral assemblages in sandstones. Sedimentary Geology 124:3-29. 1999

Mukherjee, P.K., Purohit, K.K., Saini, N.K., Khanna, P.P., Rathi, M.S., Grosz, A.E. A stream sediment geochemical survey of the Ganga River headwaters in the Garhwal Himalaya. Geochemical Journal 41:83-95. 2007

Muller, G. Sedimentary petrology. In: methods in sedimentary petrology (translated by H.U. Schmincke). Hafuer Publishing, New York, pp. 283. 1967

Nagarajan, R., Madhavaraju, J., Armstrong-Altrin, J.S., Nagendra, R. Geochemistry of Neoproterozoic limestones of the Shahabad Formation, Bhima Basin, Karnataka, southern India. Geosciences Journal 15(1):9-25. 2011

Nesbitt, H.W., Markovics, G., Price, R.C. Chemical processes affecting alkalis and alkaline earths during continental weathering. Geochimica et Cosmochimica Acta 44:1659-1666. 1980

Nesbitt, H.W., Wilson, R.E. Recent chemical weathering of basalts. American Journal of Science 292(10):740-777. 1992

Nesbitt, H.W., Young, G.M. Early Proterozoic climates and plate motions inferred from major element chemistry of lutites. Nature 199:715-717. 1982

Nesbitt, H.W., Young, G.M. Formation and diagenesis of weathering profiles. Journal of Geology 97:129-147. 1989

Nesbitt, H.W., Young, G.M. Petrogenesis of sediments in the absence of chemical weathering: effects of abrasion and sorting on bulk composition and mineralogy. Sedimentology 42:341-358. 1996

Nesbitt, H.W., Young, G.M. Prediction of some weathering trends of plutonic and volcanic rocks based on thermodynamic and kinetic considerations. Geochimica Cosmochimica Acta 48:1523-1534. 1984

Ni, H.G., Lu, F.H., Luo, X.L., Tain, H.Y., Zeng, E.Y. Riverine inputs of total organic carbon and suspended particulate matter from the Pearl River Delta to the coastal. China Marine Pollution Bulletin 56:1150-1157. 2008

Nigel Harris, N., Mike Bickle, M., Hazel Chapman, H., Ian Fairchild, I., Bunbury, J. The significance of Himalayan Rivers for silicate weathering rates: evidence from the Bhote Kosi tributary. Chemical Geology 144:205-220. 1998

Oldfield, F., Brown, A. Thompson, R. The effect of microtopography and vegetation on the catchment of airborne particles measured by remanent magnetism. Quaternary Research 12:326-332. 1979

Oldfield, F., Maher, B.A., Donaghue, J., Pierce, J. Particle-size related magnetic source sediment linkages in the Rhode River catchment, Maryland, USA. Journal of Geological Society of London 142:1035-1046. 1985

Palmer, M.R. Rare earth elements in foraminifera tests. Earth and Planetary Science Letters 73:285-298. 1985

Pande, K., Sarin, M.M., Trivedi, J.R., Krishnaswami, S., Sharma, K.K. The Indus river system (India-Pakistan): major-ion chemistry, uranium and strontium isotopes. Chemical Geology 116(3):245-259. 1994

Pandey, S.K., Singh, A.K., Hasnain, S.I. Grain-size distribution, morphoscopy and elemental chemistry of suspended sediments of Pindari Glacier, Kumaon Himalaya, India. Hydrological Science Journal 472:213-226. 2002

Pandey, S.K., Singh, A.K., Hasnain, S.I. Weathering and geochemical processes controlling solute acquisition in Ganga headwater-Bhagirathi river, Garhwal Himalaya, India. Aquatic Geochemistry 5(4):357-379. 1999

Pant, R.K., Juyal, N., Rautela, P., Yadav, M.G., Sangode, S.J. Climate instability during last glacial stage: evidence from varve deposits at Gonting, district Chamoli, Garhwal Himalayas, India. Current Science 75(8):850-855.1998

Panwar, S., Khan, M.Y.A., Chakrapani, G.J. Grain size characteristics and provenance determination of sediment and dissolved load of Alaknanda River, Garhwal Himalayas, India. Environmental Earth Sciences 75:91. 2016

Parker, A. An index of weathering for silicate rocks. Geological Magazine 107:501-504. 1970

Passega, R. Significance of CM diagram of sediments deposited by suspensions. Sedimentology 24:723-733. 1977

Peart, M.R. Walling, D.E. Fingerprinting sediment source: the example of a drainage basin in Devon, U.K. In Drainage Basin Sediment Delivery, IAHS Publ. no. 159. IAHS: Wallingford. 1986

Petschick, R., Kuhn, G., Gingele, F. Clay mineral distribution in surface sediments of the South Atlantic: sources, transport, and relation to oceanography. Marine Geology 130:203-229. 1996

Phillips, J.M, Walling, D.E. The particle size characteristics of fine-grained channel deposits in the River Exe Basin, Devon, UK. Hydrological Processes 13:1-19. 1999

Porate, S., Sangode, S.J., Meshram, D.C., Kulkarni, Y., Patil, S.K., Dhongle, D.S. Mineral magnetic approach of sediment source mixing in Godavari and Kaddam Rivers, Adilabad district, Andhra Pradesh. Gondwana Geological Magazine 27(1):17-30. 2012

Pourret, O., Davranche, M., Gruau, G., Dia, A. New insights into cerium anomalies in organic-rich alkaline waters. Chemical Geology 251:120-127. 2008

Price, J.R., Velbel, M.A. Chemical weathering indices applied to weathering profiles developed on heterogeneous felsic metamorphic parent rocks. Chemical Geology 202:397-416. 2003

Purohit, K.K., Islam, R., Thakur, V.C. Metamorphism of Psammo-Pelitic rock, Bhagirathi valley, Garhwal Himalayas. Journal Himalayan Geology 1(2):167-174. 1990

Ramesh, R., Ramanathan, A.L., Arthur James, R., Subramanian, V., Jacobsen, S.B., Holland, H.D. Rare earth elements and heavy metal distribution in estuarine sediments of east coast of India. Hydrobiologia 57:1-11. 1999

Ramesh, R., Ramanathan, A.L., Ramesh, S., Purvaja, R., Subramanian, V. Distribution of rare earth elements and heavy metals in the surficial sediments of the Himalayan river system. Geochemical Journal 34(4):295-319. 2000

Rana, N., Singh, S., Sundriyal, Y.P., Juyal, N. Recent and past floods in the Alaknanda valley: causes and consequences. Current Science 105(9):1209-1212. 2013

Rao, P.J, Razia Sulthana, S.K., Srivastava, S.K., Samyuktha, N., Venugopalanaidu, C.H. Role of drainage characteristics on silt deposition in Meghadrigedda reservoir, Visakhapatnam-a spatial technology approach. International Journal of Earth Sciences and Engineering 4(8):46-55. 2011

Raymo, M.E., Ruddiman, W.F. Froelich, P.N. Influence of late Cenozoic mountain building on ocean geochemical cycles. Geology 16:649-653. 1988

Raymo, M.E., Ruddiman, W.F. Tectonic forcing of Late Cenozoic climate. Nature 359:117-122. 1992

Raymond, P.A., McClelland, J.W., Holmes, R.M., Zhulidov, A.V., Mull, K., Peterson, B.J., Striegl, R.G., Aiken, G.R., Gurtovaya, T.Y. Flux and age of dissolved organic carbon exported to the Arctic Ocean: a carbon isotopic study of the five largest arctic rivers. Global Biogeochemical Cycles 21:GB4011. 2007

Reid, M.K., Spencer, K.L. Use of principal components analysis (PCA) on estuarine sediment datasets: the effect of data pre-treatment. Environmental Pollution 157:2275-2281. 2009

Rengarajan, R., Sarin, M.M. Distribution of rare earth elements in the Yamuna and the Chambal rivers, India. Geochemical Journal 38(6):551-569. 2004

Restrepo, J.D., Kjerfve, B., Hermelin, M., Restrepo, J.C. Factors controlling sediment yield in a major South American drainage basin: the Magdalena River, Colombia. Journal of Hydrology 316:213-232. 2006

Rice, S., Church, M. Grain size along two gravel-bed rivers: statistical variation, spatial pattern and sedimentary links. Earth Surface Processes and Landforms 23(4):345-363. 1998

Rietveld, H.M. A profile refinement method for nuclear and magnetic structures. Journal of Applied Crystallography 2:65-71. 1969

Robertson, D.J., Taylor, K.G., Hoon., S.R. Geochemical and mineral magnetic characterisation of urban sediment particulates, Manchester, UK. Applied Geochemistry 18:269-282. 2003

Roy, P., Martha, T.R., Kumar, K.V. Sediment influx in the Mandakini catchment due to landslides triggered by the June 2013 extreme rainfall event in Uttarakhand. ISRS Proceedings, ISPRS Technical Commission VIII Mid-Term Symposium, Hyderabad, 2014

Russell, R.D. Mineral composition of Mississippi River sands. Geological Society of America Bulletin 48:1307-1348. 1937

Sachse, A., Henrion, R., Gelbrecht, J., Steinberg, C.E.W. Classification of dissolved organic carbon (DOC) in river systems: influence of catchment characteristics and autochthonous processes. Organic Geochemistry 36(6):923-935. 2005

Safiullah, S., Chowdhury, M.I., Mafizuddin, M., Iqbal Ali, S.M., Karim, M. Monitoring of the Padma (Ganga), the Jamuna (Brahmaputra) and the Baral in Bangladesh, Mitt. Geol. Palaeontol. Inst. Univ. Hamburg 58:519-524. 1985

Sahoo, P.K., Tripathy, S., Equeenuddin, Sk.Md., Panigrahi, M.K. Geochemical characteristics of coal mine discharge vis-a-vis behavior of rare earth elements at Jaintia Hills Coalfield, Northeastern India. Journal of Geochemical Exploration 112:235-243. 2012

Sahoo, P.K., Tripathy, S., Panigrahi, M.K., Equeenuddin, S.M. Geochemical characterization of coal and waste rocks from a high sulfur bearing coalfield, India: implication for acid and metal generation. Journal of Geochemical Exploration 145:135-147. 2014

Saini, N.K., Mukherjee, P.K., Rathi, M.S., Khanna, P.P. Evaluation of energy dispersive X-ray fluorescence spectrometry in the rapid analysis of silicate rocks using pressed powder pellets. X-Ray Spectrometry 29:166-172. 2000

Sangode, S.J., Sinha, R., phartiyal, B., Chauhan, O.S., Mazari, R.K., Bagati, T.N., Suresh, N., Mishra, S., Kumar, R., Bhattacharjee, P. Environmental magnetic studies on some Quaternary sediments of varied depositional settings in the Indian sub-continent. Quaternary International 159:102-118. 2007

Sangode, S.J., Suresh, N., Bagati, T.N. Godavari source in the Bengal fan sediments: results from magnetic susceptibility dispersal pattern. Current Science 80(5):660-664. 2001

Sarin, M.M., Krishnaswami, S. Major ion geochemistry of the Ganges-Brahmaputra river system, India. Nature 312:538-41. 1984

Sarin, M.M., Krishnaswami, S., Trivedi, J.R., Sharma, K.K. Major ion chemistry of the Ganga source waters: weathering in the high altitude Himalaya. Proceedings of the Indian Academy of Sciences-Earth and Planetary Sciences 101:89-98. 1992

Sati, S.P., Rana, N., Dangwal, S. Recent landslides in Uttarakhand: nature's fury or human folly. Current Science 100(11):1617-1620. 2011

Sati, S.P., Sundriyal, Y.P., Rawat, G.S. Geomorphic indicators of neotectonic activity around Srinagar (Alaknanda basin), Uttarakhand. Current Science 92(6):824-829. 2007

Sati, V.P. A Final Report On “The Alaknanda Basin (Uttarakhand Himalaya): a study on enhancing and diversifying livelihood options in an ecologically fragile mountain terrain” Submitted to Indian Council of Social Science Research, ICSSR. Enhancing and Diversifying Livelihood Options. 2009

Shao, J., Yang, S. Does chemical index of alteration (CIA) reflect silicate weathering and monsoonal climate in the Changjiang River basin? Chinese Science Bulletin 57:1178-1187. 2012

Shao, J., Yang, S., Li, C. Chemical indices (CIA and WIP) as proxies for integrated chemical weathering in China: inferences from analysis of fluvial sediments. Sedimentary Geology 265-266:110-120. 2012

Sherriff, S.C. Environmental magnetism: sediment source tracing. Geomorphological Techniques, British Society for Geomorphology, chapter 1, pp. 1-12. 2014

Sholkovitz, E.R. Chemical evolution of rare earth elements: fractionation between colloidal and solution phases of filtered river water. Earth and Planetary Science Letters 114:77-84. 1992

Shouye, Y., Congxian, L., Lee, C.B., Na, T.K. REE geochemistry of suspended sediments from the rivers around the Yellow Sea and provenance indicators. Chinese Science Bulletin 48(11):1135-1139. 2003

Shrivastava, V.K. Commercial activities and development in the Ganga Basin. Concept Publishing Company, New Delhi, pp. 58. 1999

Shukla, D., Dubey, C., Ningreichon, A., Singh, R., Mishra, B., Singh, S. GIS-based morphotectonic studies of Alaknanda river basin: a precursor for hazard zonation. Natural Hazards 71(3):1433-1452. 2014

Singh, A.K., Hasnain, S.I. Major ion chemistry and weathering control in a high altitude basin: Alaknanda River, Garhwal Himalaya, India. Hydrological Sciences Journal 436:825-843. 1998

Singh, A.K., Hasnain, S.I., Banerjee, D.K. Grain size and geochemical partitioning of heavy metals in sediments of the Damodar River-a tributary of the lower Ganga, India. Environmental Geology 39(1):90-98. 1999

Singh, P. Geochemistry and provenance of stream sediments of the Ganga River and its major tributaries in the Himalayan region, India. Chemical Geology 269(3):220-236. 2010

Singh, P. Major, trace and REE geochemistry of the Ganga River sediments: influence of provenance and sedimentary processes. Chemical Geology 266(3):242-255. 2009

Singh, P., Rajamani, V. REE geochemistry of recent clastic sediments from the Kaveri floodplains, southern India: implication to source area weathering and sedimentary processes. Geochimica et Cosmochimica Acta 6518:3093-3108. 2001

Singh, S.K., Kumar, A., France-Lanord, C. Sr and $^{87}Sr/^{86}Sr$ in waters and sediments of the Brahmaputra river system: silicate weathering, CO_2 consumption and Sr flux. Chemical Geology 234(3):308-320. 2006

Singh, S.K., Rai, S.K., Krishnaswami, S. Sr and Nd isotopes in river sediments from the Ganga Basin: sediment provenance and spatial variability in physical erosion. Journal of Geophysical Research 113:F03006. 2008

Singh, S.K., Trivedi, J.R., Pande, K., Ramesh, R., Krishnaswami, S. Chemical and strontium, oxygen, and carbon isotopic compositions of carbonates from the Lesser Himalaya: implications to the strontium isotope composition of the source waters of the Ganga, Ghaghara, and the Indus rivers. Geochimica et Cosmochimica Acta 62(5):743-755. 1998

Singh, V., Devrani, R., Ansari, Z. Estimation of the rate of erosion of valley fill deposits in a part of the NW Lesser Himalaya. Episodes 35(3):445-452. 2012

Sinha, R., Bhattacharjee, P.S., Sangode, S.J., Gibling, M.R., Tandon, S.K., Jain, M., Godfrey-Smith, D. Valley and interfluve sediments in the Southern Ganga plains, India: Exploring facies and magnetic signatures. Sedimentary Geology 201:386-411. 2007

Sklar, L.S., Dietrich, W.E. Sediment and rock strength controls on river incision into bedrock. Geology 29:1087-1090. 2001

Slattery, M.C., Burt, T.P. Particle size characteristics of suspended sediment in hillslope runoff and stream flow. Earth Surface Processes and Landforms 22:705-719. 1997

Stanley, J.D., Wingerath, J.G. Nile sediment dispersal altered by the Aswan High Dam: the kaolinite trace. Marine Geology 133:1-9. 1996

Subramanian, V. Mineralogical input of suspended matter by Indian rivers into the adjacent areas of the Indian Ocean. Marine Geology 36(3):M29-M34. 1980

Syvitski, J.P., Peckham, S.D., Hilberman, R., Mulder, T. Predicting the terrestrial flux of sediment to the global ocean: a planetary perspective. Sedimentary Geology 162(1):5-24. 2003

Tamooh, F., Meersche, K.V., Meysman, F., Marwick, T.R., Borges, A.V., Merckx, R., Dehairs, F., Schmidt, S., Nyunja, J., Bouillon, S. Distribution and origin of suspended matter and organic carbon pools in the Tana River Basin, Kenya. Biogeosciences 9:2905-2920. 2012

Taylor, S.R., McLennan, S.M. The Continental Crust: its composition and evolution. Blackwell Scientific Publications Oxford, pp. 312. 1985

Thill, A., Moustier, S., Garnier, J.M., Estournel, C., Naudin, J.J., Bottero, J.Y. Evolution of particle size and concentration in the Rhone river mixing zone: influence of salt flocculation. Continental Shelf Research 21(18):2127-2140. 2001

Thompson, R., Oldfield, R. Environmental Magnetism: New York (Allen and Unwin), pp. 227. 1986

Thurman, M.E. Suspended Sediment: transport and chemistry of organic carbon. Proceeding of advanced seminar on sedimentation, Denver, Colorado. US Geological Survey Circular 953:29-30. 1983

Tripathi, J.K., Ghazanfari, P., Rajamani, V., Tandon, S.K. Geochemistry of sediments of the Ganges alluvial plains: evidence of large-scale sediment recycling. Quaternary International 159:119-130. 2007

Tripathi, J.K., Rajamani, V. Geochemistry of the loessic sediments on Delhi ridge, eastern Thar Desert, Rajasthan: implication for exogenic processes. Chemical Geology 155:265-278. 1999

Tripathy, G.R., Singh, S.K. Chemical erosion rates of river basins of the Ganga system in the Himalaya: reanalysis based on inversion of dissolved major ions, Sr, and $^{87}Sr/^{86}Sr$. Geochemistry, Geophysics, Geosystems 11(3):Q03013. 2010

United States Environmental Protection Agency (USEPA) Office of Water. “National water Quality Inventory,” Report to Congress 2002 Reporting Cycle, EPA 841-R-07-001, Washington, D.C. 2007

Valdiya, K.S. Damming rivers in the tectonically resurgent Uttarakhand Himalaya. Current Science 106(12):1658-1688. 2014

Valdiya, K.S. Geology of Kumaun Lesser Himalaya. WIHG Dehradun, pp. 291. 1980

Veerasingam, S., Venkatachalapathy, R., Basavaiah, N., Ramkumar, T., Venkatramanan, S., Deenadayalan, K. Identification and characterization of tsunami deposits off southeast coast of India from the 2004 Indian Ocean tsunami: Rock Magnetic and Geochemical Approach. Journal of Earth System Science 123(4):905-921. 2014

Venkatachalapathy, R., Veerasingam, S., Basavaiah, N., Ramkumar, T., Deenadayalan, K. Environmental magnetic and geochemical characteristics of Chennai coastal sediments, Bay of Bengal, India. Journal of Earth System Science 120(5):885-895. 2011

Verma, M., Singh, B.P., Srivastava, A., Mishra, M. Chemical behavior of suspended sediments in a small river draining out of the Himalaya, Tawi River, northern India: implications on provenance and weathering. Himalayan Geology 33:1-14. 2012

Vital, H., Stattegger, K. Major and trace elements of stream sediments from the lowermost Amazon River. Chemical Geology 168:151-168. 2000

Walden, J., Slattery M.C., Burt, T.P. Use of mineral magnetic measurements to fingerprint suspended sediment sources: approaches and techniques for data analysis. Journal of Hydrology 202:353-372. 1997

Walling, D.E. Suspended sediment transport by rivers: a geomorphological and hydrological perspective. Archiv fuer Hydrobiologie 47:1-27. 1996

Walling, D.E. Tracing suspended sediment sources in catchments and river systems. Science of the Total Environment 344(1):159-184. 2005

Walling, D.E., Golosov, V., Olley, J. Introduction to the special issue 'Tracer Applications in Sediment Research'. Hydrological Processes 27(6):775-780. 2013

Walling, D.E., Moorehead, P.W. The particle size characteristics of fluvial suspended sediment: an overview. In Sediment/Water Interactions. Springer Netherlands, pp. 125-149. 1989

Walling, D.E., Owens, P.E., Leeks, G.J.L. The role of channel and floodplain storage in the suspended sediment budget of the River Ouse, Yorkshire, UK. Geomorphology 22:225-242. 1998

Walling, D.E., Owens, P.N., Leeks, G.J. Fingerprinting suspended sediment sources in the catchment of the River Ouse, Yorkshire, U.K. Hydrological Processes 13(7):955-975. 1999

Walling, D.E., Owens, P.N., Waterfall, B.D., Leeks, G.J., Wass, P.D. The particle size characteristics of fluvial suspended sediment in the Humber and Tweed catchments, UK. Science of the Total Environment 251:205-222. 2000

Walling, D.E., Peart, M.R., Oldfield, F., Thompson, R. Suspended sediment sources identified by magnetic measurements. Nature 281:110-113. 1979

Walling, D.E., Woodward, J.C. Tracing sources of suspended sediment in river basins: a case study of the River Culm, Devon, UK. Marine and Freshwater Research 46(1):327-336. 1995

Warren, N., Allan, I.J., Carter, J.E., House, W.A., Parker, A. Pesticides and other micro-organic contaminants in freshwater sedimentary environments-a review. Applied Geochemistry 18:159-94. 2003

Wasson, R.J. A sediment budget for the Ganga-Brahmaputra catchment. Current Science 84(8):1041-1047. 2003

Waznah, A.S., Kamaruzzaman, B.Y., Ong, M.C., Rina, S.Z., Mohd Zahir, S. Spatial and temporal bottom sediment characteristics of Pahang River-Estuary, Pahang, Malaysia. Oriental Journal of Chemistry 26:39-44. 2010

Webster, J.R., Kight, R.P., Winburn, R.S., Cool, C.A. Heavy mineral analysis of sandstones by rietveld analysis. JCPDS-International Centre for Diffraction Data, Advances in X-ray Analysis, 46:198-203. 2003

Wei, W., Chen, L.D., Fu, B.J., Lu, Y.H., Gong, J. Responses of water erosion to rainfall extremes and vegetation types in a loess semiarid hilly area, NW China. Hydrological Processes 23:1780-1791. 2009

Weiguo, Z., Lizhong, Y.U. Magnetic properties of tidal flat sediments of the Yangtze Estuary and its relationship with particle size. Science China (Ser. D) 46(9):954-966. 2003

Weltje, G.J., von Eynatten, H. Quantitative provenance analysis of sediments: review and outlook. Sedimentary Geology 171:1-11. 2004

Wheatcroft, R.A., Hatten, J.A., Pasternack, G.B., Warrick, J.A. The role of effective discharge in the ocean delivery of particulate organic carbon by small, mountainous river systems. Limnology and Oceanography 55(1):161-171. 2010

Whipple, K.X., Hancock, G.S., Anderson R.S. River incision into bedrock: mechanics and relative efficacy of plucking, abrasion, and cavitation. Geological Society of America Bulletin 112:490-50. 2000

Whipple, K.X., Meade, B.J. Controls on the strength of coupling among climate, erosion, and deformation in two-sided, frictional orogenic wedges at steady state. Journal of Geophysical Research: Earth Surface 109:F01011. 2004

White, A.F., Blum, A.E. Effects of climate on chemical weathering in watersheds. Geochimica et Cosmochimica Acta 59:1729-1747. 1995

Wiggering, H., Beukes, N.J. Petrography and Geochemistry of a 2000-2200?Ma?Old Hematitic Paleo? Alteration Profile on Ongeluk Basalt of the Transvaal Supergroup, Griqualand West, South Africa. Precambrian Research 46:241-258. 1990

Wohl, E., Bledsoe, B.P., Jacobson, R.B., Poff, N.L., Rathburn, S.L., Walters, D.M., Wilcox, A.C. The natural sediment regime in rivers: broadening the foundation for ecosystem management. BioScience 65(4):358-371. 2015

Wu, W., Zheng, H., Xu, S., Yang, J., Yin, H. Geochemistry and provenance of bed sediments of the large rivers in the Tibetan Plateau and Himalayan region. International Journal of Earth Sciences Geologische Rundschau 101:1357-1370. 2012

Wu, Y., Zhang, J., Liu, S.M., Zhang, Z.F., Yao, Q.Z., Hong, G.H., Cooper, L. Sources and distribution of carbon within the Yangtze River system. Estuarine Coastal and Shelf Science 71:13-25. 2007

Xia, J., Ming, Liu, X., Chen, F., Ma, J., Zhao, H., Wang, X., Wei, H. A preliminary study on the magnetic signatures of modern soil in Central Asia. Frontiers of Earth Sciences in China 1(3):275-283. 2007

Xu, J. Grain-size characteristics of suspended sediment in the Yellow River, China. Catena 38:243-263. 1999

Xu, J. Implication of relationships among suspended sediment size, water discharge and suspended sediment concentration: the Yellow River basin, China. Catena 49:289-307. 2002

Xu, J. Trends in suspended sediment grain size in the upper Yangtze River and its tributaries, as influenced by human activities. Hydrological Sciences-Journal-des Sciences Hydrologiques 52(4):37-41. 2007

Xu, J.X. Complex behaviour of suspended sediment grain size downstream from a reservoir: an example from the Hanjiang River, China. Hydrological Sciences Journal 41(6):837-849. 1996

Xu, Y., Song, J., Duan, L., Li, X., Yuan, H., Li, N., Zhang, P., Zhang, Y., Xu, S., Zhang, M., Wu, X., Yin, X. Fraction characteristics of rare earth elements in the surface sediment of Bohai Bay, North China. Environmental and Monitoring Assessment 184:7275-7292. 2012

Xu, Z., Lim, D., Choi, J., Yang, S., Jung, H. Rare earth elements in bottom sediments of major rivers around the Yellow Sea: implications for sediment provenance. Geo-Marine Letters 29(5):291-300. 2009

Yadav, S.K., Chakrapani, G.J. Geochemistry, dissolved elemental flux rates, and dissolution kinetics of lithologies of Alaknanda and Bhagirathi rivers in Himalayas, India. Environmental Earth Sciences 62:593-610. 2011

Yan, B., Fang, N.F., Zhang, P.C., Shi, Z.H. Impacts of land use change on watershed stream flow and sediment yield: an assessment using hydrologic modelling and partial least squares regression. Journal of Hydrology 484:26-37. 2013

Yan, B., Yan, W., Miao, L., Huang, W., Chen, Z. Geochemical characteristics and provenance implication of rare earth elements in surface sediments from bays along Guangdong Coast, Southeast China. Environmental Earth Sciences 65(7):2195-2205. 2012

Yang, S., Jung, H.S., Li, C. Two unique weathering regimes in the Changjiang and Huanghe drainage basins: geochemical evidence from river sediments. Sedimentary Geology 164:19-34. 2004

Yang, S., Youn, J.S. Geochemical compositions and provenance discrimination of the central south Yellow Sea sediments. Marine Geology 243:229-241. 2007

Yang, S.Y., Jung, H.S., Choi, M.S., Li, C.X. The rare earth element compositions of the Changjiang (Yangtze) and Huanghe (Yellow) river sediments. Earth and Planetary Science Letters 201(2):407-419. 2002

Zhang, C., Wang, L., Zhang, S., Li, X. Geochemistry of rare earth elements in the mainstream of the Yangtze River, China. Applied Geochemistry 13:451-462. 1998

Zhang, Q., Xu, C., Becker, S., Jiang, T. Sediment and runoff changes in the Yangtze River basin during past 50 years. Journal of Hydrology 331(3-4):511-523. 2006